UNIVERSITÀ DEGLI STUDI DI CATANIA
DOTTORATO IN SISTEMI COMPLESSI PER LE SCIENZE FISICHE,
SOCIO-ECONOMICHE E DELLA VITA

Letizia Stella Di Mauro

The Cooperation vs Competition dilemma in economic and ecological applications

PHD THESIS

Supervisor:
Prof. Alessandro Pluchino
Prof. Alessio Emanuele Biondo
Prof. Christian Mulder

ANNO ACCADEMICO 2019/2020

The only thing that will redeem mankind is cooperation.

Bertrand A. W. Russell

Contents

Introduction

During my PhD I studied cooperation and competition, two opposing manifestations that an entity of any nature can present when it interacts with another one. I used the term "entity" because these two behavioral tendencies can manifest themselves in various subjects and at different levels. Our cells cooperate to allow the functioning of body, cancer cells instead, growing selfishly, tend to damage it. Cooperation can take place between individuals of a group such as, for example, colleagues who work for the same company; in turn companies are entities that compete in their marketing sector. In the case of empires, civilizations and nations throughout history, they struggled and fought each other, or have joined forces to fight a common enemy. Each of us, in everyday life, chooses whether to cooperate with other members the society we all are a part of, or to pursue their own selfish interests. Building our philosophy on these choices we usually decide, for example whether to recycle, keep public places clean or help a child or an old man to cross the street, or not. The topic is therefore of crucial importance: understanding the basic concepts of cooperation and competition is fundamental to improve social behavior of humans and animals, to explain historical events and even to better understand the functioning of our body.

The first chapter is devoted to the discussion of mathematical models for the study of cooperation and competition. From the mathematical point of view the topic of cooperation as opposed to competition was the main object of Game Theory. Indeed this branch of mathematics studies and analyzes individual choices in situations of conflict or strategic interaction between individuals in order to maximize one's payoff. For this reason, section 1.1 is dedicated to a brief discussion on game theory and the famous prisoner's dilemma which represents the conflict between individual and collective interests. The prisoner's dilemma, which consists of a strategy game between just two individuals, can be extended to a collective action dilemma between several people and, as said before, any choice we face during our daily life can be traced back to a problem of this kind. I discuss the dilemmas of collective action in section 1.2. Section 1.3 is dedicated to Martin Nowak who has dealt in depth with the theme of cooperation. All ecological communities in nature are characterized by pervasive competition that constitutes the

main way through which is realized Darwinian evolution. Nowak with his studies highlighted the role of cooperation in evolution showing how the first shapes the latter. In section 1.4 a brief review of the equations describing the dynamics of the populations present in an ecosystem is made: on the one hand the logistic equation which describes intra-specific competition in presence of limited resources and, on the other hand, the well-known Lotka-Volterra model which describes the phenomenon of predation, the main modality through which inter-specific competition operates. Finally, in section 1.5 a general discussion on dynamic systems is made.

Without claiming to explain the deep mechanisms underlying the phenomena of cooperation and competition, during my PhD I explored two somewhat different areas in which cooperation and competition play a massive role. The systems I dealt with in these two studies are very different in nature, but their study still falls within the framework of complex systems. The second chapter is therefore dedicated to complex networks. In particular, section 2.1 deals with graph theory through which it is possible to analyze the properties and topology of complex networks, while section 2.2 is dedicated to an in-depth analysis of trophic networks, which constitutes the topic of the second study.

In the first study I address the issue of tax evasion, an age-old phenomenon that clearly is related to cooperation and competition. Think about a selfish citizen who uses public goods and services without properly contributing to the related costs. The main effect of this behavior is a severe damage to the socio-economical environment that deprives governments of their fiscal resources and plays an important role in reducing well-being of societies. In the third chapter I present an agent-based model of a simple economic system where the personal satisfaction gained from public services and the perceived opinion of neighbors are shown to drive the individual decision on tax compliance. Results of simulations, consistent with existing literature on the topic, suggest a peculiar approach to face the plague of tax evasion.

In the second study, exposed in the fourth chapter, using data collected in the Netherlands, I investigate ecosystems of soil invertebrates through the knowledge of their characteristic trophic web. In the first part, I focus on a single ecosystem and I create a model whose dynamics is dictated by an extension of the Lotka-Volterra equations. In particular, I combine the Lotka-Volterra model with the logistic equation in order to take into account intra-specific and inter-specific competition. Subsequently, through simulations, I study what may be the consequences of artificial perturbations induced to the system. Results are interesting because they give an idea of the vulnerability of soil ecosystems if subjected to the use of herbicides or pesticides typical of intensive agriculture.
In the second part, I apply the same model to other two ecosystems different from

the first for the type of human activity to which they are subject. I compare their structure and their response to external disturbances. The final analysis on their robustness clearly shows that the ecosystem less subject to anthropogenic disturbances has a structure that makes it more resistent against perturbations. In this second study, competitiveness is not only found at the level of the trophic web (in the search for resources and in the fight for survival between prey and predator), but, at a different level, comes into play competitiveness between ecosystem organisms and human action that tends to contaminate natural habitats. Human cooperation in this case would consist of seeking eco-sustainable solutions rather than intensive farming methods.

Chapter 1

Mathematical Models of Cooperation and Competition

1.1 Game Theory

Cooperation and competition are topic vastly treated in scientific literature and particularly addressed by Game Theory, a branch of mathematics. As we will see, most of the studies about this phenomenon are based on the famous Prisoner's Dilemma, that shows why two rational individuals might not cooperate, even if appears that it is in their best interest to do so. The eminent mathematician John von Neumann can be considered the founder of modern game theory. The term "game" was used by von Neumann to indicate a generic conflict situation between individuals whose purpose is to achieve the optimal result for them. In these situations of rivalry a player must make decisions taking into account also the possible strategies implemented by the opponent. Von Neumann realized that these conflicting situations are present not only in board games, such as poker and chess, but manifest themselves in a variety of forms in everyday life, in economics, politics and war. The theory tries to find the most correct strategy to follow in a competitive situation and to give a concrete explanation to the behavior of rival individuals. But beware, game theory cannot be considered a branch of psychology: assuming that the players are perfectly rational in their thinking, game theory admits that it is possible to carry out a precise analysis of the situation, which therefore makes it a branch of mathematics. One of the fundamental questions about game theory to which von Neumann tried to answer was if there is always a rational way to solve a game. With his Minimax Theorem, von Neumann proved mathematically that there is always an optimal way to play a game of two players whose interests are completely opposed. He proved the minimax theorem in his 1928 article *Zur Theorie der Gesellschaftsspiele* (Theory of Parlor Games) that

can be considered the seminal paper of game theory (von Neumann, 1928). In the book *Theory of Games and Economic Behavior* written with the economist Oskar Morgenstern in 1944, the pioneering intent of approaching the economy through game theory was clearly announced by the authors who stated: "*We hope to establish satisfactorily...that the typical problems of economic behavior become strictly identical with the mathematical notions of suitable games of strategy*" (von Neumann and Morgenstern, 1944). Von Neumann's desire was to extend his result even to games with more than two players whose interests could partly overlap, only in this way could game theory have dealt with any type of existing human conflict. After the publication of *Theory of Games and Economics Behavior*, game theory became extremely popular especially in the RAND Corporation (of which Von Neumann was a member along with other prominent scientists), founded by the Air Force after the Second World War with the intent to carry out strategy studies on nuclear war.

1.1.1 Minimax Theorem

The Minimax theorem applies to "zero-sum game", ie those games in which the total winnings are fixed so that the loss of one player equals the winnings of the other, and therefore the interests of the players are completly opposed. It is also assumed that the two players participating in the game are both rational and both willing to win the game, choosing a particular strategy only for their own personal benefit. With strategy we mean the set of choices made during the game by a player in all situations that arise during the course of the game and therefore a complete description of a player's game mode. Let A and B be the two players. Suppose that player A has different m strategies and player B has n. We will indicate with $i = 1, ..., m$ the strategy chosen by A and with $j = 1, ..., n$ the one chosen by B. For each pair of strategies chosen by A and B we can consider the quantity a_{ij} which indicates the payoff of player A (being a zero-sum game, we will also have unequivocally the payoff of player B given by $-a_{ij}$). We can therefore associate a $m \times n$ matrix to a given game, whose elements are the quantities a_{ij} (Figure 1.1). We then ask: what is the best strategy that A can adopt? For a given strategy i chosen by A, player B will choose a strategy j such that the payoff of A is the minimum, $\alpha_{ij} = min_j a_{ij}$. So, in the hope of getting a better win, A will choose the strategy that has the highest value of α_{ij}, $\alpha = max_i \alpha_{ij} = max_i min_j a_{ij}$. This is the value called maximin of the game. Similarly, player B will look for the number $\beta = min_j max_i a_{ij}$, where β is the minimax value of the game from which the theorem takes its name. When the maximin and the minimax are identical, that outcome is called a saddle point and this is the rational solution of the game. Von Neumann showed that in a 2-person, zero sum game, the optimal strategies of each player would always end in a stable solution, a saddle point for which

	B_1	B_2	...	B_n
A_1	$a_{1,1}$	$a_{1,2}$	...	$a_{1,n}$
A_2	$a_{2,1}$	$a_{2,2}$	...	$a_{2,n}$
:	:	:	$\ddots$	:
A_m	$a_{m,1}$	$a_{m,2}$	...	$a_{m,n}$

Figure 1.1: Payoff matrix of a game

$minimax = maximin$. More specifically, the minimax theorem states that in every finite zero sum game with 2 rational players, there is always a rational solution in the form of a pure or mixed strategy. Von Neumann believed that his result could also extend to games with more than two players even though the analysis of these games increases exponentially with the number of the players. N-person game can be seen as cooperative game in which the players can create coalitions between them. For example, a game with three people A, B and C in which A and B join together, can be seen as a two-player game, the A-B coalition and player C. Similarly, any n-person game can be traced back to the analysis of a two-player game, whose solution is guaranteed by the Minimax Theorem.

1.1.2 The Nash Equilibrium

Another renowned member of the RAND corporation was the mathematician John Nash. Von Neumann's analysis was limited to the treatment of non-cooperative two-player zero-sum games and cooperative n-person zero-sum games. Nash extended Von Neumann's studies to include non-zero-sum games for two players (whose interests are therefore not completely opposite) and non cooperative n-person games in which each partecipant acts indipendently and no coalitions occur (Nash, 1951).
The equilibrium points of a game are the outcome where the players, given the other players' strategies, have no interest in changing their game strategy. Consider a game with N players each with a set of strategy S_i. All players have an utility function U_i consisting of the payoff to be maximized by playing, that will depend on the strategies $\alpha_i \in S_i$ adopted. The set of all the strategies adopted by all the players $\alpha = (\alpha_1, ..., \alpha_N)$ is a Nash equilibrium if

$$\begin{gathered} U_i(\alpha_1, ..., \alpha_{i-1}, \alpha_i, \alpha_{i+1}, ..., \alpha_N) \geq U_i(\alpha_1, ..., \alpha_{i-1}, \beta, \alpha_{i+1}, ..., \alpha_N) \\ \forall \beta \in S_i, \qquad \forall i = 1, ..., N \end{gathered} \tag{1.1}$$

That is, keeping the strategies of the other players fixed, none of them will be interested in changing their own.
The minimax solutions are equilibrium point of zero-sum games, but Nash proved that any finite non-cooperative game has at least one equilibrium point. In many games equilibrium point corresponds to the most reasonable and rational solution, but as we shall see, there are cases in which the Nash equilibrium turns out to be a completely irrational choice in a collective perspective.

1.1.3 The Flood-Dresher Experiment

Two other mathematicians belonging to the RAND corporation were Merril Flood and Melvin Dresher. With an experiment (Flood, 1952) they wanted to test the concept of Nash equilibrium to understand if real people spontaneously converged to the equilibrium strategy when playing a game. It was a two-player non-zero-sum game, with the payoff table in Figure 1.2. Each of the two players was required to

		Player 1	
		Strategy 1 [defect]	Strategy 2 [cooperate]
Player 2	Strategy 1 [cooperate]	-1 , 2	1/2 , 1
	Strategy 2 [defect]	0 , 1/2	1 , -1

Figure 1.2: Payoff matrix of Flood and Dresh experiment

choose their strategy at every turn without knowing the opponent's choice. Player 1 is better off choosing his strategy 1, while player 2 choosing his strategy 2. But if both choose their best strategy, both have a lower gain than if they both choose their worst strategies. Considering Figure 1.2, Nash's theory suggests that the rational outcome is the lower left cell in which both players defect. But if both players played as the upper right cell, both would earn more. This strategy can be considered as a desire for cooperation by the two players. The two persons who participated in the game played for 100 rounds. The results show that the cooperation between the two players was the most frequent choice (sixty times out of a hundred)(Flood, 1952). There was therefore no evidence of a natural tendency towards Nash equilibrium.

1.1.4 Prisoner's Dilemma

In the attempt to test with an experiment the concept of the Nash equilibrium, Flood and Dresher discovered what was later known as the Prisoner's dilemma thanks to the most know version devised by Albert Tucker. In Tucker's anecdote there are two members of a criminal gang that are arrested and imprisoned in solitary confinement. The police don't have enough evidence to convict the pair on the principal charge, so they plan to sentence both to a year in prison on a lesser charge. But the police offer each prisoner a bargain: if he testifies against his partner, he will go free while the partner will get three years in prison on the main charge. But if both prisoners testify against each other, both will be sentenced to two years in jail. Each of them is informed that the other prisoner is being offered the same deal, but they cannot know what the other has decided. The payoffs are show in the matrix represented in Figure 1.3.

The argument of one prisoner can contemplate that testifying take a year off his

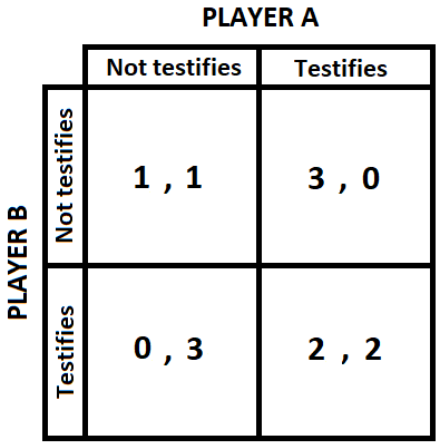

Figure 1.3: Payoff matrix of prisoner's dilemma. The years of prison to which players are forced, based on their decision, are indicated.

sentence, no matter what the partner does. So the rational move is to testify. The trouble is that the other prisoner can come to the same conclusion. Therefore if both parties are rational, both will testify and both will get two year in jail. But if only they had both refused to testify, they would have got just a year each. In prisoner's dilemma rationality prevents a deal beneficial to both parties because testifying undermines the common good. In a prisoner's dilemma, the equilibrium point strategy is called defection; a player is always better off defecting no matter what the other does. The other strategy, which lead to the best collective outcome, is called cooperation. How should one act in a prisoner's dilemma is still an unanswered question. There are many forms of the prisoner's dilemma, it is only

required that the reward payoff for mutual cooperation is greater than the average of the payoff if only you defect and the payoff if only the other player defect. Prisoner's dilemma present a conflict between individual and collective interest that we all experience in our everyday life, in this sense it represent an universal problem (for example in Poundstone (1993) the insight of game theory, and in particular of the prisoner's dilemma, are related to real-world conflict).

1.2 Collective Action Dilemma

The dilemma of collective action can be considered an extension of the prisoner's dilemma generalized from two people to a group of any size and for this reason it is also called many-person prisoner's dilemma. This dilemma occurs whenever there is a group whose members can decide whether or not to participate in a certain activity. Joining this activity brings an individual disadvantage but, at the same time, a benefit to the whole group, so that the members of the group are better off if most of the other members participate without their contribution. In social life the dilemma of collective action is a frequent problem that occurs in many forms. For example, one of the most actual issues of our society, namely climate change and environmental sustainability, is exactly what is called a collective action dilemma. Making ecological choices in everyday life has a cost from the individual point of view, whether it is eating less meat, being careful to use less plastic or having to comply with public transport timetables. Making these eco-sustainable choices, however, is in the interest of the whole society, to preserve the conditions of our planet for future generations.
The philosopher and sociologist Jon Elster treats this issue in his book *Nuts and bolts for the social sciences* (Elster, 1989), in which he shows the simplest case of the many-person prisoner's dilemma as represented in Figure 1.4. The two heavy lines show how the expected benefits, for the cooperators and for the free riders, vary with the number of cooperators (the altruists). The line representing reward to free riders is constantly above the other, this means that noncooperation is individually rational in terms of selfish benefits. At the same time, it is better for all if everyone cooperate than if none do, indeed B is above 0. The free riders get the largest benefit C, whereas the worst outcome A is reserved for the cooperators. If there are at least D cooperators their benefits become positive. The thin line shows how the average benefits for the collectivity varies with the number of cooperators (by definition, it must begin at 0 and end at B). The distance between the two heavy lines represents the cost (per altruist) of cooperation. In Figure 1.4 the cost doesn't vary with the number of cooperators, but in general it may increase or decrease as more people cooperate. For example, in Figure 1.5 is represented a circumstance in which the first and the last cooperators that join the activity,

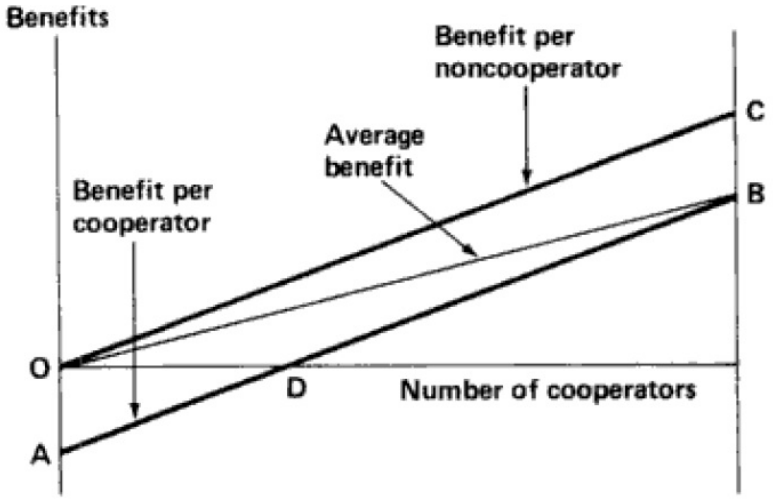

Figure 1.4: Many-person prisoner's dilemma as represented in Elster (1989). Expected benefits as a function of the number of cooperators for the collective group, for the cooperators and for the free riders.

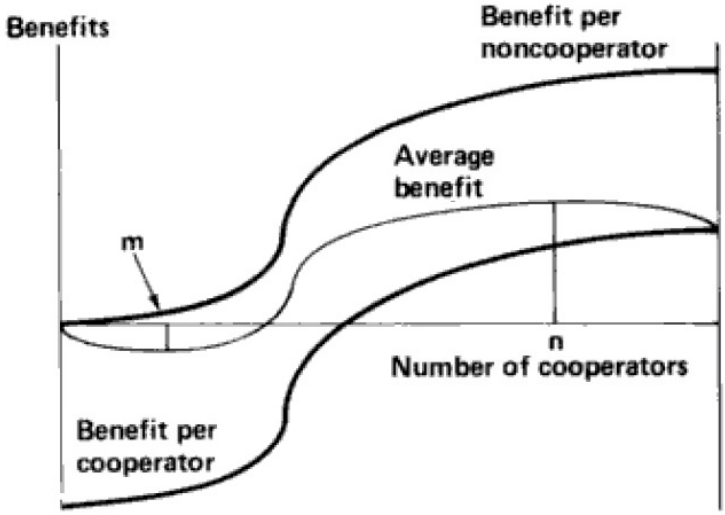

Figure 1.5: Many-person prisoner's dilemma as represented in Elster (1989). Expected benefits as a function of the number of cooperators for the collective group, for the cooperators and for the free riders. The cost of cooperation vary with the number of the altruists.

add a little amount to everybody's welfare, whereas those coming in the middle are more efficacious. In this situation the cost of cooperation is very high when there are few cooperators, so the first altruists make the average situation worse, in the sense that the harm they do to themselves exceeds the benefit they do to everybody else. As the number of altruists raises the cost of cooperation decrease, so, beyond m, average benefits rapidly increase. It can also happen that when the number of cooperators is very high, the cost of cooperation begin to increase and after n, average benefits return to decrease.
Elster classifies individuals into three categories based on the motivations that lead them to cooperate. The Kantians are the ones who decide to cooperate because this would be the best for the society if only everyone did it. Utilitarians are those who want to promote the collective good, so they participate in the activity only if their collaboration leads to an increase in the average benefit. The last category is made up of those who apply the norm of fairness, that is, those who collaborate only if the majority of the community already does it, each with different thresholds. Generally there are few Kantians in society, but their presence is fundamental because, if they reach the threshold m in Figure 1.5, they constitute a trigger for utilitarians, who in turn, increasing in number, will constitute a catalyst for people who are motivated by the norm of fairness.
Let me take the case of intensive meat farms as an example. Intensive farms are harmful to the environment for several reasons: they are one of the main sources of greenhouse gases released into the atmosphere and indirect cause of deforestation and exorbitant water consumption, for the cultivation of the feed necessary to make the bred animals survive. For these ecological reasons same people have decided not to eat meat from intensive farms anymore. Finding non-intensive breeding meat is not easy, almost impossible at times. You pay a cost not to eat meat, both in terms of health because the omnivorous diet involves the consumption of meat (albeit little), and simply in the pleasure of enjoying a good slice of meat cooked with barbeque. If this action is carried out by very few individuals, the cost they pay is much greater than the benefit the society derives from it. The farmers will not even perceive the effects of this little-attended boycott. But if these Kantian people succeeded in reaching the adequate number so that the demand for meat in the market suffered a significant decline, intensive farming would decrease. Consequently there would be an improvement in environmental conditions, that exceeds the cost paid by the cooperators, for the benefit of the community. At this point even the utilitarians would begin to come into play and if this action is carried out by many people the demand for meat from intensive farms can drop drastically. Maybe a situation would be reached in which intensive farming would give way to organic ones. I just wanted to do this example because I am very sensitive to this issue and, as a perfect Kantian, are now 7 years that I

do not eat meat from intensive farming in the hope that even utilitarians will join my cause.

1.3 The Evolution of Cooperation

As we saw in the previous chapter the prisoner's dilemma can be seen as the mathematical representation of a central struggle in life, the one between individual interest and the greater good, between competition and cooperation. Darwinian evolution underlines the fundamental role of competition: every living being is the protagonist of a struggle for survival that aims to increase one's own fitness, that is to say, one's reproductive success. In Darwinian evolution there is no room for cooperation: if I help others, my fitness will decrease and their fitness will increase. Making an analogy with the Elster theory discussed in the previous paragraph, we know that cooperators will always have a lower fitness than that of defectors and therefore less chances of survival. Yet a population formed entirely by cooperators will have a higher average fitness than a population made up entirely of defectors. According to this reasoning it would seem that natural selection is opposed to what is the best for the entire population. In the book *SuperCooperators* the mathematician and biologist Martin Nowak hypothesizes mechanisms that would lead to the development of cooperation in biological populations, showing how natural evolution is not opposed to cooperation (Nowak, 2011). Using computer models, mathematics and experiments, Nowak has identified five mechanisms that explain how cooperation may have prospered in a ruthless Darwinian world.
The first mechanism for the evolution of cooperation is, according to Nowak, the kin selection, also called nepotism. The key entities for the functioning of this mechanism are the genes. An individual can propagate his genes either by increasing his fitness (direct fitness) or by increasing that of relatives who carry his own gene (indirect fitness) (Haldane, 1955). Thus the concept of inclusive fitness, given by the sum of direct and indirect fitness (Hamilton, 1964). The greater the degree of kinship between an individual and his relative, i.e. how many more genes are shared, the greater the inclusive fitness of the individual. Kin selection is an evolutionarily stable strategy since the genes that codify altruism towards relatives will be those that, thanks to the kin selection, will have more probabilities of propagating. This mechanism could be the explanation of the phenomenon of eusociality shown by some species of social insects and other animals that have the aptitude to treat offspring in a cooperative manner.
The second mechanism is that of direct reciprocity, known as "tit for tat". This is the simple principle of the exchange. In order for direct reciprocity to work it is necessary that two same individuals have repeated contacts so that they can have the opportunity to repay any acts of courtesy. The experiment of Flood and

Dresher suggests precisely this: if the prisoner's dilemma is iterated it leads in most cases to cooperation. According to the evolutionary biologist Robert Trivers, some human emotions, such as gratitude, empathy, guilt and sympathy, have sprung up from the logic of direct reciprocity (Trivers, 1971). Also in animal populations there are numerous phenomena of direct reciprocity, such as grooming, that is the mutual cleaning of the coat and skin exhibited by numerous mammals.
The third mechanism for the development of cooperation is that of indirect reciprocity. The difference with respect to the second mechanism is that, in the interaction with another individual, one does not only take into account own past experience with him, but also the experience that others people have had with the same individual. This interaction mechanism works through the reputation that each individual has within the society. In a prisoner's dilemma played with a badly reputed adversary I will be less inclined to cooperate since I know that his favorite strategy is defection. On the contrary, if I am faced with a reputable player, I will be more inclined to cooperate. Following this way of thinking, it will be more advantageous for the individual to make a good reputation and therefore to collaborate most of the times, in this way cooperation can thrive. The moral principle underlying this way of acting is the famous golden rule present in all cultures and religions, quoting Confucius: "*don't do unto others what you don't want done unto you*". On this principle is based the optimistic thought that every good deed you do to someone, in the future will come back to you even if not by the same person. It is important to emphasize that this third mechanism of action can be present only in evolved societies like the human one, since it presupposes a certain social intelligence necessary to recognize the reputation of the others. For indirect reciprocity to work it is necessary to have a way to communicate between us and even Nowak hypothesizes that the demand for social cooperation through indirect reciprocity has been one of the decisive factors for the evolution of human language.
According to Nowak, the fourth mechanism for the evolution of cooperation is network reciprocity that take into account the spatial structures present in living societies. In a prisoner's spatial dilemma we must be taken into consideration random encounters between two individuals in a heterogeneous population with a certain structure. In his models, Nowak set rules similar to those of cellular automata: at each turn, every cell changes its state according to rules that depend not only on its game's strategy but also on the strategy of neighboring cells. Nowak thus demonstrated that patches of cooperation coexist with patches of defection in ever-changing complex forms which he called "dynamic fractals". In particular, he found that groups of cooperators are able to prevail even if surrounded by defectors. Cellular automata and Nowak's simulations show how complex structures can be generated from simple rules, so much that it is supposed that this fourth

mechanism for cooperation has been fundamental for the origin of life on Earth.
The fifth and last mechanism, that results in the development of altruism, is group selection. All of us, someone more and someone less, have an innate instinct that leads them to help people in need. In most cases, some charitable acts could fall into the case of indirect reciprocity: unconsciously we help someone to increase our good reputation in society. But in history there are also cases of heroism in which the benefactor puts his own life at risk to save another person even if unknown. These events are hardly attributable to indirect reciprocity: reputation is useless if you are dead! These extreme cases can be explained only by taking group selection into consideration. The altruist acting against his own selfish interest gives an advantage to his group. Thus groups formed by altruistic individuals are more advantaged than groups formed by selfish individuals. Belonging to a cooperative group guarantees you a greater chance of survival: this is another mechanism for developing cooperation. It so happens that a soldier sacrifices himself for his own country and perhaps that is why we are more willing to sacrifice our lives for a child than for an old man, the child can still reproduce and therefore carry on our species. Group selection occurs in humans and animals and also acts on multiple levels, including the cellular and molecular one (a single individual can be considered as a group formed by a large number of cells that cooperate with each other). This is why group selection is also called multi-level selection. It is a fundamental mechanism that permeates the entire evolution, from the emergence of the first cells to the social behavior of man.
With its five mechanisms for the evolution of altruism, Nowak demonstrates how, after all, altruism is not an irrational choice as the prisoner's dilemma suggests. Nowak goes further, showing how essential cooperation was to several major transitions of evolution, from the origin of life to the evolution of social insects until human domination of the planet. Nowak emphasizes how important it is to maintain and expand the range of cooperation for civilization to survive overcoming the tragedies of the commons and making us what he calls supercooperators.

1.4 Intra-specific and inter-specific competition in population ecology

An ecological community is a set of living organisms belonging to at least two different species that interact with each other, directly or indirectly, within a certain geographical area. The ecological interactions can be classified as intra-specific, if these occur between organisms of the same species, and inter-specific, if these involve organisms belonging to two different species.
Living organisms increase their fitness by exploiting the resources of the environ-

ment in which they live (food, space, light). When these resources are not enough, there is a competition between the species to get hold of them. The intra-specific competition for resources is stronger than the inter-specific one, since the organisms belonging to the same species have all the resources they need in common. As we will see, as long as the resources are sufficient for the whole community, there is no competition and the abundance of the species increases exponentially. When resources start to run low, intra-specific competition begins to act as a regulator of population growth and a sigmoidal shaped growth of the population is observed. Inter-specific competition, on the other hand, mostly concerns the phenomenon of predation in which a predatory species feeds on another prey species. The density of predatory species regulates the growth of prey species and vice versa.
In the next paragraphs, the mathematical equations describing the growth of populations in situations of intra-specific and inter-specific competitiveness are shown.

1.4.1 Exponentially Growth Model

In the simplest mathematical model of population growth (Neal, 2019), the rate of population increase is proportional to the size of population at any time, in the assumption of unlimited resources. Let us denote by $N(t)$ the population at the time t and by k a positive constant. Then

$$\frac{dN}{dt} = kN \tag{1.2}$$

which gives by integration

$$N(t) = N_0 exp(kt) \tag{1.3}$$

where N_0 denotes the population at the time $t = 0$. This law is called the Malthusian growth model and predicts an exponential growth in the population with time (Figure 1.6).

A more realistic model considers

$$\frac{dN}{dt} = (b - d)N = rN \tag{1.4}$$

where b and d denote, respectively, the birth rate and death rate per individual and $r = b - d$ is known as the intrinsecal rate of natural increase, or the Malthusian parameter. The exponential law corresponds to the case $b = k$ and $d = 0$ ($r > 0$). For $b < d$ ($r < 0$) population decreases exponentially and for $b = d$ ($r = 0$) population dimension do not change.

1.4.2 Logistic Growth Model

In the real world, resources are not unlimited, and their demand tends to increase with the growth of the population. The consequent reduction of the resources

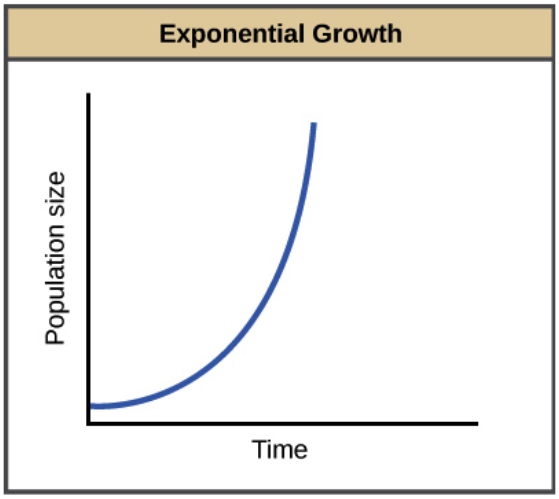

Figure 1.6: Exponential growth of a population with time.

produces, in turn, an increase of the mortality rate and a decrease of the natality rate. The variation of the birth rate b and of the death rate d in function of the abundance N of the population can be assumed as linear:

$$b = b_0 - aN$$

$$d = d_0 + cN$$

where b_0 and d_0 are the values respectively of the birth rate and of the death rate when N is close to 0. Parameters a and c are, respectively, the slopes of the straight lines that describe the variation of the birth rate and of the mortality rate as a function of the population size N. Equation (1.4) thus becomes:

$$\frac{dN}{dt} = [(b_0 - aN) - (d_0 + cN)]N \tag{1.5}$$

that describes intra-specific regulation of the population.

When $b > d$ population increases with a slower growth rate for increasing value of N. When $b < d$ the growth becames negative and population decreases. When $b = d$ the abundance of the population reaches a stationary state corresponding to its maximum sustenaible value, also called carrying capacity K of the system. This value can be obtained by putting $dN/dt = 0$ in equation (1.5), which gives:

$$K = \frac{b_0 - d_0}{a + c} \tag{1.6}$$

Using the carrying capacity, equation (1.5) takes the well-known form of the logistic equation (Verhulst, 1838), that describes the sigmoidal growth of the population

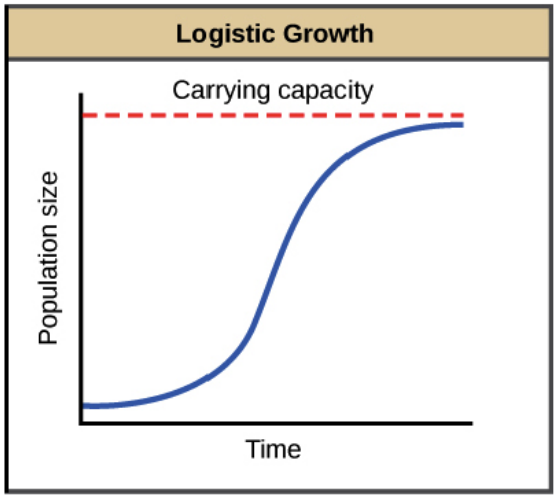

Figure 1.7: Logistic growth of a population with time.

when resources are limited:

$$\frac{dN}{dt} = rN\left(1 - \frac{N}{K}\right) \tag{1.7}$$

with $r = b_0 - d_0$. Equation (1.7) has two component: an exponential term (rN) which is important for small N values, and a second one ($1 - \frac{N}{K}$) that reduces population growth when approaching the environmental-driven carrying capacity (Figure 1.7).

1.4.3 Lotka-Volterra equations

The chemist and statistician Alfred J. Lotka (Lotka, 1920) and the mathematician Vito Volterra (Volterra, 1926 and 1939) produced independently the non-linear coupled differential equations for the study of the ecological problem of predation, the main modality through which inter-specific regulation occurs. The simplest Lotka-Volterra model involves only two species. One of them feeds on the other, which in turn feeds on a third available source of food. The assumptions about the environment and the evolution of the predator and prey populations are:

- The prey population have an unlimited food supply.
- In the absence of predators, the population X_1 of the prey would grow proportionally to its size,

$$\frac{dX_1}{dt} = A_1 X_1 \tag{1.8}$$

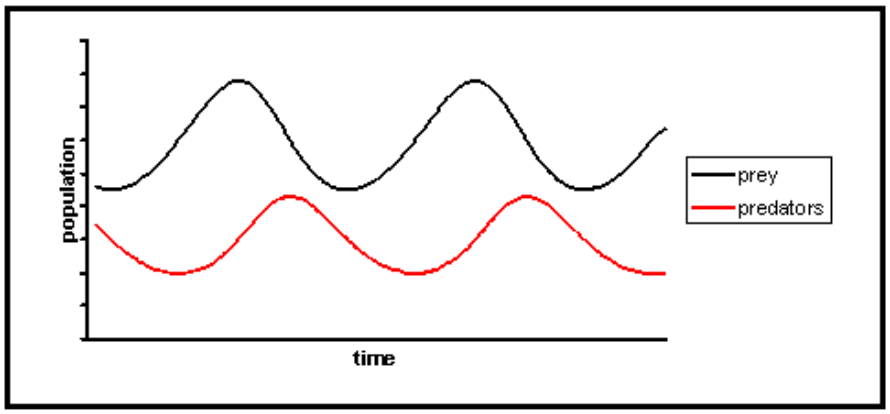

Figure 1.8: Periodic fluctuations of prey and predator populations, according to the dynamics of the Lotka-Volterra equations.

being $A_1 > 0$ the growth rate of the prey. So, in this case, a Malthusian growth of the prey occurs.

- In the absence of prey, the population X_2 of the predator would decline proportionally to its size,

$$\frac{dX_2}{dt} = A_2 X_2 \tag{1.9}$$

being $A_2 < 0$ the predators' death rate, meaning extinction of that population.

- When both predator and prey are present, to the previous terms is added a quantity representing the effect of the predation that is a decrease in the prey population and a growth in the predator population:

$$\frac{dX_1}{dt} = A_1 X_1 + A_{12} X_2 X_1, \qquad \frac{dX_2}{dt} = A_2 X_2 + A_{21} X_1 X_2 \tag{1.10}$$

being $A_{12} < 0$ and $A_{21} > 0$, respectively, the negative and the positive growth rate for prey and predator.

The Lotka-Volterra equations connect the two populations each of which acts as a regulator of the density of the other species. Predators act as a cause of mortality for the prey and prey control the natality rate of the predators. In this way periodic fluctuations of the two populations occur with the predator population always following the prey (Figure 1.8).

1.4.4 Multiple Prey-Predator Model

When in an ecosystem there are more then one prey and one predator species, Lotka-Volterra equations can be extended as in Hodzic et al.(2016):

$$\frac{dX_i}{dt} = X_i \left[A_i + \sum_j A_{ij} X_j \right] \tag{1.11}$$

where $i, j = 1, 2, ..., n$, being n the total number of species in the ecosystem. Coefficient A_i is the intrinsic growth rate of the i-th species, while coefficients A_{ij} in the summation take into account the effect of the predation. We can therefore build a community matrix $\mathbf{A}$, relative to the ecosystem, whose elements weigh the effect of predation between pairs of species:

$$\mathbf{A} = \begin{bmatrix} A_{11} & A_{12} & \dots & A_{1j} & \dots A_{1n} \\ A_{21} & A_{22} & \dots & A_{2j} & \dots A_{2n} \\ \dots & \dots & \dots & \dots & \dots \\ A_{i1} & A_{i2} & \dots & A_{ij} & \dots A_{in} \\ \dots & \dots & \dots & \dots & \dots \\ A_{n1} & A_{n2} & \dots & A_{nj} & \dots A_{nn} \end{bmatrix}$$

Here $A_{ij} \neq 0$ when species i and j are linked by predation phenomena (in particular, $A_{ij} > 0$ when species i preys species j and $A_{ij} < 0$ when species j preys species j) and $A_{ij} = 0$ when species i and j do not have any predation connection. Non-zero diagonal elements A_{ii} represent the phenomenon of cannibalism when an individual of species i preys on another individual of the same species.

1.5 Dynamic Systems Theory

A dynamic system can be defined as a set of elements in mutual interaction that change over time and it is specified by a set of equations that determine its evolution. There is a class of dynamical systems whose evolution is described by a set of n first-order differential equations

$$\dot{X}_i = f_i(X_1, X_2, ..., X_n) \, \forall i = 1, 2, ...n. \tag{1.12}$$

in which n is the number of degrees of freedom of the system that is, the number of independent variables necessary to describe the dynamical state of the system. The state of the system at any instant of time is specified by its location in state space and its evolution over time is represented by a trajectory in state space described by the time evolution equations. State space dimensionality is determined

by the number of degrees of freedom of the system. The behavior of the trajectories within the state space is strongly limited by the No-Intersection Theorem according to which, two distinct state space trajectories cannot intersect nor can a single trajectory cross itself at a later time. The No-Intersection Theorem derives mathematically from the Existence and Uniqueness Theorem for the solution: if the functions f_i in equations 1.12 are continuous, only one solution can pass at a given point in the state space.
To play a crucial role in the dynamics of these systems are the attractors, subspaces of dimensionality inferior to that of the state space, which have the property of attracting the trajectories. The dynamic systems characterized by the presence of an attractor are called dissipative systems. Generally we can speak of "zones"in the state space for which the variables that describe the system do not change. To find these subspaces it will therefore be sufficient to set the time derivatives of the state variables equal to zero.

1.5.1 One-Dimensional State Space

Let us first consider the case of a one-dimensional dissipative system described by a single state variable X. The equation that regulates the dynamics of the system is

$$\dot{X} = f(X) \tag{1.13}$$

In this case, since the system has dimensionality 1, the attractor can only have dimensionality 0, so it is a fixed point. As we have already said, the fixed points are stationary solutions of the system and can be found by setting the first derivative of the state variable equal to zero:

$$\dot{X} = 0 \tag{1.14}$$

Let's call this solution X_0.
For a one-dimensional state space there are three types of fixed point:

- Nodes: fixed points that attract nearby trajectories.
- Repellors: fixed points that repel nearby trajectories.
- Saddle points: fixed points that attract the trajectories on one side and on the other reject them.

To know the nature of the fixed point X_0, we need to understand what happens in the points near it. To do this we can evaluate a Taylor series expansion of the function $f(X)$ in the neighborhood of the fixed point X_0:

$$f(X) = f(X_0) + (X - X_0)\frac{df}{dX} + \frac{1}{2}(X - X_0)^2\frac{d^2f}{dX^2} + \frac{1}{6}(X - X_0)^3\frac{d^3f}{dX^3} + ... \tag{1.15}$$

in which all derivatives are calculated for $X = X_0$. Considering that, for the definition of fixed point, the first term on the right-hand side is zero and neglecting the terms of order higher than the first because these are very small, we can write the previous equation as

$$f(X) = (X - X_0)\frac{df}{dX} \tag{1.16}$$

which, by introducing the variable $x = X - X_0$, becomes

$$\dot{x} = \left.\frac{df}{dX}\right|_{x=0} x = \lambda x \tag{1.17}$$

whose solution is

$$x(t) = x(0)e^{\lambda t} \tag{1.18}$$

The term λ, defined as

$$\lambda \equiv \left.\frac{df(X)}{dX}\right|_{X_0} \tag{1.19}$$

is the characteristic value of the fixed point, also called the Lyapunov exponent. It is precisely this term that determines the nature of the fixed point, in fact, for equation (1.18), if $\lambda < 0$ the trajectory approaches the fixed point, while if $\lambda > 0$ the trajectory is repelled from the fixed point. So to establish the nature of a fixed point we need to calculate the derivative of the function $f(X)$ with respect to X evaluated in $X = X_0$. If the derivative is negative the fixed point is a node, if the derivative is positive the fixed point is a repellor. Finally, in the case in which the derivative is zero, it will be necessary to calculate the second derivative with respect to X and most likely the fixed point will be a saddle point, otherwise it is a node or a repellor that attract or repel the trajectory slowly. The possible fixed points in the one-dimensional case are summarized in Figure 1.9.

Once we have calculated the fixed points of a dynamic system and established their nature, we know what happens in their proximity and therefore we know the local behavior of the system. Knowing the nature of all the fixed points it is also possible to construct a global phase portrait and to imagine the trend of the trajectory in the state space, considering that the continuity of the function f constitutes a constraint.

The logistic equation, described in the previous paragraph, is an example of a one-dimensional dynamic system: by putting in equation 1.7 the carrying capacity K of the system equal to 1, we obtain

$$\dot{N}(t) = rN(1 - N) \tag{1.20}$$

in which the only degree of freedom is the abundance of the population N. By putting the first derivative equal to zero it is easily found that the two fixed points

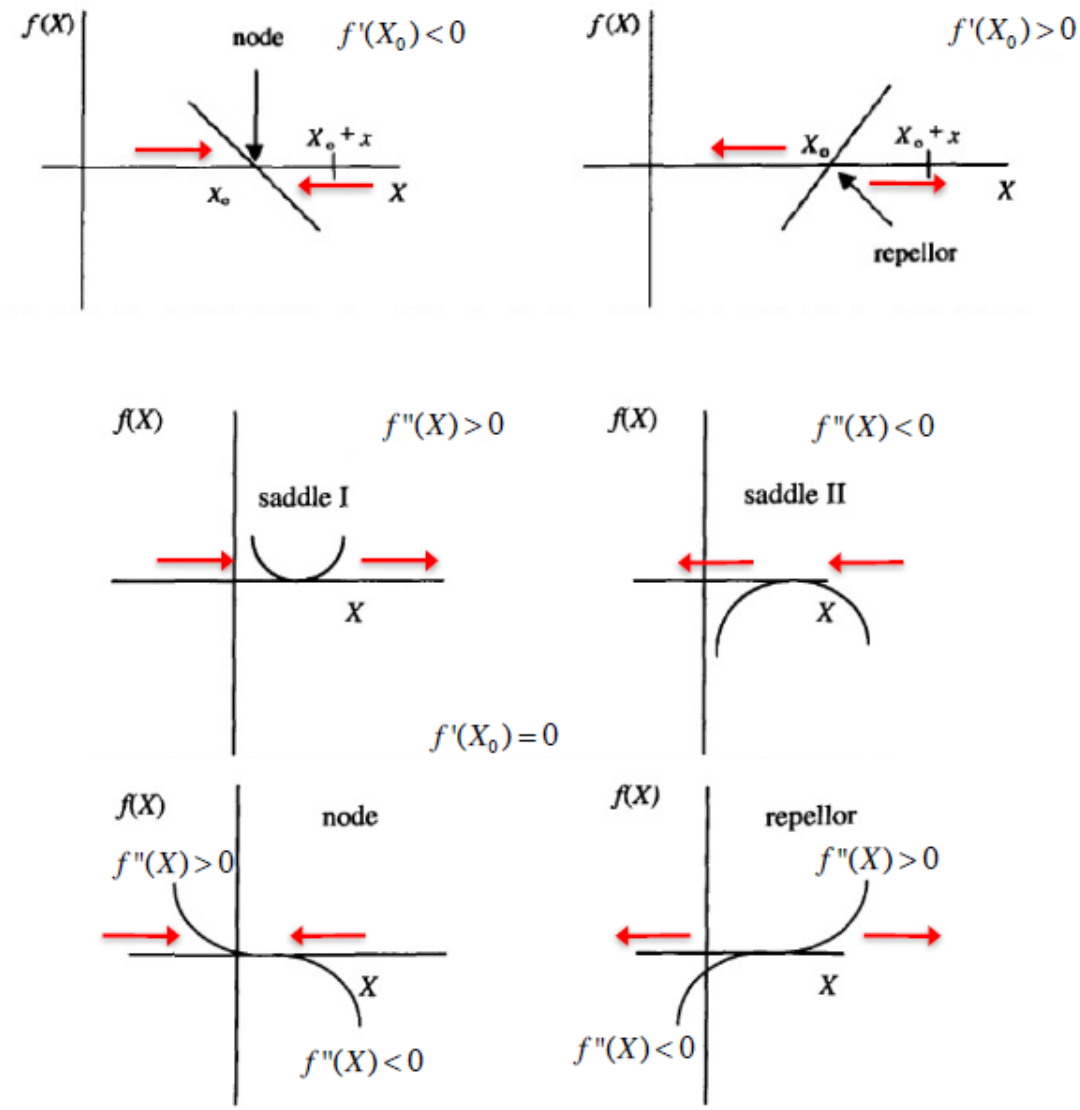

Figure 1.9: Possible types of fixed point in one-dimensional dynamic system.

of the system are $N_1 = 0$ and $N_2 = 1$. Furthermore

$$f(N) = rN - rN^2 \tag{1.21}$$

which is the equation of a parabola, and

$$\lambda = \frac{df(N)}{dN} = r - 2rN \tag{1.22}$$

Then we can evaluate the nature of the fixed points:

$$\lambda(N_1) = r > 0 \tag{1.23}$$

therefore $N_1 = 0$ is a repellor.

$$\lambda(N_2) = r - 2r = -r < 0 \tag{1.24}$$

so $N_2 = 1$ is a node. We can conclude that the trajectory in the state space is a parabola that starts from the point $N = 0$ and arrives at the point $N = 1$, as shown in (Figure 1.10). Plotting N as a function of time we observe a sigmoid

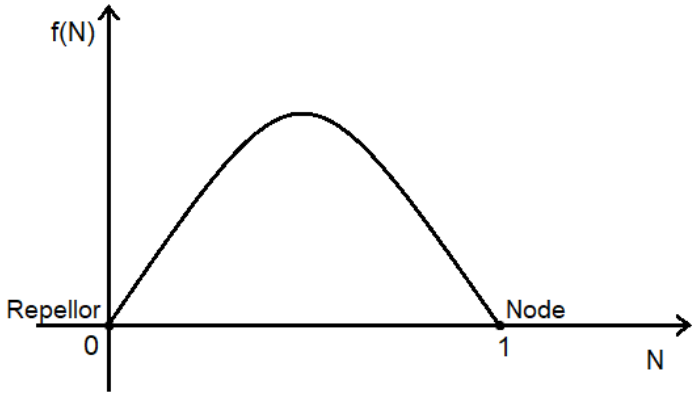

Figure 1.10: Trajectory in state space for a system described by a logistic differential equation.

behavior as in Figure 1.7, in which the population grows until it reaches the value of the carrying capacity, which in this case is equal to 1.

1.5.2 Two-Dimensional State Space

Now consider the case of a dynamic system described by two independent state variables X_1 and X_2. The time evolution equations are

$$\begin{aligned} \dot{X}_1 &= f_1(X_1, X_2) \\ \dot{X}_2 &= f_2(X_1, X_2) \end{aligned} \tag{1.25}$$

The evolution of the system will be plotted in a two-dimensional state space $X_1 - X_2$. Similarly to the previous case, fixed points are those points X_{10} and X_{20} satisfying

$$\begin{aligned} \dot{X}_1 &= f_1(X_1, X_2) = 0 \\ \dot{X}_2 &= f_2(X_1, X_2) = 0 \end{aligned} \tag{1.26}$$

A simple way to calculate the Lyapunov exponents, for knowing the type of fixed points, is through the Jacobian method. We construct the Jacobian matrix, whose elements are given by the partial derivatives of the functions f_1 and f_2 with respect to the variables $x_1 = X_1 - X_{10}$ and $x_2 = X_2 - X_{20}$ evaluated at the fixed point:

$$J = \begin{pmatrix} f_{11} & f_{12} \\ f_{21} & f_{22} \end{pmatrix} \tag{1.27}$$

with

$$f_{ij} = \frac{\partial f_i}{\partial x_j} \tag{1.28}$$

We then derive the eigenvalue equation by subtracting λ from the elements of the principal diagonal and setting the determinant of this matrix equal to zero:

$$\begin{vmatrix} f_{11} - \lambda & f_{12} \\ f_{21} & f_{22} - \lambda \end{vmatrix} = 0 \tag{1.29}$$

Performing the determinant, we obtain the characteristic equation of the Jacobian:

$$\lambda^2 - (f_{11} + f_{22})\lambda + (f_{11}f_{22} - f_{12}f_{21}) = 0 \tag{1.30}$$

which has the solutions

$$\lambda_{\pm} = \frac{f_{11} + f_{22} \pm \sqrt{(f_{11} + f_{22})^2 - 4(f_{11}f_{22} - f_{12}f_{21})}}{2} \tag{1.31}$$

Observing that the trace and the determinant of the Jacobian matrix in equation 1.27 are given respectively by

$$TrJ = f_{11} + f_{22} \tag{1.32}$$

and

$$\Delta = f_{11}f_{22} - f_{12}f_{21} \tag{1.33}$$

it is possible to write Lyapunov exponents as

$$\lambda_{\pm} = \frac{TrJ \pm \sqrt{(TrJ)^2 - 4\Delta}}{2} \tag{1.34}$$

It should be noted that in this case the Lyapunov exponents are complex numbers consisting of a real part and an imaginary part:

$$\lambda_{\pm} = R \pm i\Omega \tag{1.35}$$

with

$$R = \frac{1}{2}TrJ \tag{1.36}$$

and

$$\Omega = \frac{1}{2}\sqrt{(TrJ)^2 - 4\Delta} \tag{1.37}$$

The variables x_1 and x_2 can be written as

$$\begin{aligned} x_1(t) &= C_1 e^{\lambda_+ t} + D_1 e^{\lambda_- t} = e^{Rt}[C_1 e^{i\Omega t} + D_1 e^{-i\Omega t}] = F_1 e^{Rt} sin(\Omega t) \\ x_2(t) &= C_2 e^{\lambda_+ t} + D_2 e^{\lambda_- t} = e^{Rt}[C_2 e^{i\Omega t} + D_2 e^{-i\Omega t}] = F_2 e^{Rt} sin(\Omega t) \end{aligned} \tag{1.38}$$

These are oscillating solutions: in the case in which the Lyapunov exponents are complex, the variables x_1 and x_2 (which are distances from the fixed point) oscillate and the trajectories in the state space are spirals around the fixed points. Whether or not the spirals approach the central point depends on the amplitude and therefore on the sign of the real part R of the Lyapunov exponent. In the event that the Lyapunov exponents are real, if both are negative we have an attractive node, if both are positive we have a repellor and if these have opposite signs we have a saddle point. The possible fixed points in the two-dimensional case are summarized in Figure 1.11.

As an example of a two-dimensional dynamic system we can consider the Lotka-Volterra model in the case of competition between only two species. In particular, consider the case of a population of rabbits $x(t)$ and a population of sheep $y(t)$ that compete for the same grassy resource whose availability is limited. We ignore further complications such as the presence of other animal species and predators. We assume that each of the two species follows a logistic growth to its carrying capacity in absence of the other. As seen in section 1.4, the term b which describes the intrinsic growth rate of the population, takes into account both the birth rate b_0 and an intra-specific competition term that depends on the abundance of the population:

$$\begin{aligned} \dot{x} &= x b_{rabbit} = x(b_{0rabbit} - a_{rabbit} x) \\ \dot{y} &= y b_{sheep} = y(b_{0sheep} - a_{sheep} y) \end{aligned} \tag{1.39}$$

In presence of the other species it will be necessary to consider a further subtractive term, which describes inter-specific competition, that depends on the abundance of the other species:

$$\begin{aligned} \dot{x} &= x(b_{0rabbit} - a_{rabbit} x - c_{rabbit} y) \\ \dot{y} &= y(b_{0sheep} - a_{sheep} y - c_{sheep} x) \end{aligned} \tag{1.40}$$

We can assign arbitrary values to the coefficients present in equations 1.40. Since rabbits reproduce faster than sheep, we can assume $b_{0rabbit} = 3$ and $b_{0sheep} = 2$. We also assume that animals consume grass in proportion to their size and that sheep

λ_1 and λ_2 are real numbers:

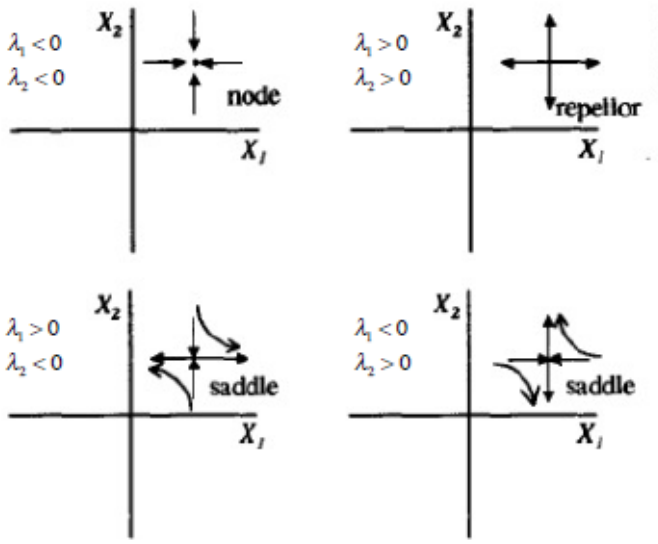

λ_1 and λ_2 are complex conjugate numbers:

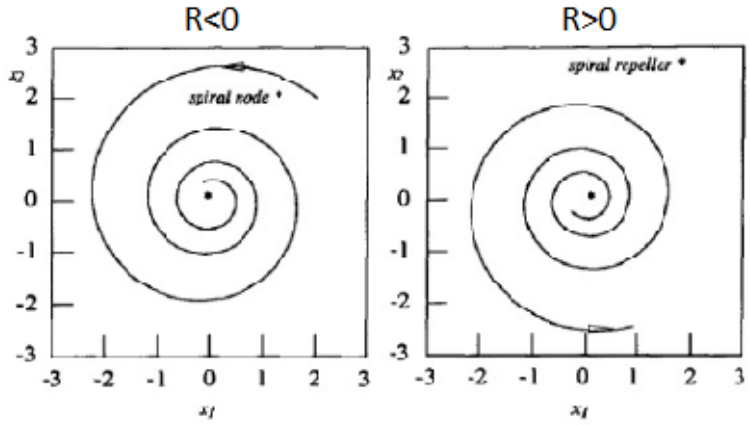

Figure 1.11: Possible types of fixed points in two-dimensional dynamic system.

are twice as large as rabbits, we will therefore have $a_{rabbit} = a_{sheep} = 1$, $c_{rabbit} = 2$ and $c_{sheep} = 1$. Equations 1.40 thus become:

$$\begin{aligned} \dot{x} &= x(3 - x - 2y) \\ \dot{y} &= y(2 - x - y) \end{aligned} \tag{1.41}$$

To find the fixed points of the system it is necessary to solve simultaneously $\dot{x} = 0$ and $\dot{y} = 0$. In this way four fixed points are obtained: $(0, 0)$, $(0, 2)$, $(3, 0)$ and $(1, 1)$. The nature of these fixed points can be inferred calculating the Jacobian for each of them:

$$J = \begin{pmatrix} 3 - 2x - 2y & -2x \\ -y & 2 - x - 2y \end{pmatrix} \tag{1.42}$$

- Fixed point $(0, 0)$:

$$J = \begin{pmatrix} 3 & 0 \\ 0 & 2 \end{pmatrix} \tag{1.43}$$

  The eigenvalues are $\lambda = 3, 2$ so the origin $(0, 0)$ is a repellor. This means that if we are close to this point, that is we are in a situation with few rabbits and few sheep, both species will tend to thrive. The departure from the origin takes place along the tangent to the direction given by the eigenvector relatives to the lower eigenvalue, i.e. $\mathbf{v} = (0, 1)$.

- Fixed point $(0, 2)$:

$$J = \begin{pmatrix} -1 & 0 \\ -2 & -2 \end{pmatrix} \tag{1.44}$$

  The eigenvalues are $\lambda = -1, -2$ so $(0, 2)$ is a stable node. This means that if we are close to this point, that is we are in a situation with more sheep than rabbits, sheep will tend to thrive and rabbits will become extinct. The approach to this point occurs along the direction $\mathbf{v} = (1, -2)$ associated with the eigenvalue $\lambda = -1$.

- Fixed point $(3, 0)$:

$$J = \begin{pmatrix} -3 & -6 \\ 0 & -1 \end{pmatrix} \tag{1.45}$$

  The eigenvalues are $\lambda = -3, -1$ so $(3, 0)$ is a stable node. This means that if we are close to this point, that is we are in a situation with more rabbits than sheep, rabbits will tend to thrive and sheep will become extinct. The approach to this point occurs along the direction $\mathbf{v} = (3, -1)$ associated with the eigenvalue $\lambda = -1$.

- Fixed point $(1, 1)$:

$$J = \begin{pmatrix} -1 & -2 \\ -1 & -1 \end{pmatrix} \tag{1.46}$$

  The eigenvalues are $\lambda = -1 \pm \sqrt{2}$ so $(1, 1)$ is a saddle point.

By putting together the previous information, we can build a global phase portrait (Figure 1.12) that shows the dynamics of the system depending to the initial conditions in which it is found. Figure 1.12 shows that the in-set of the saddle

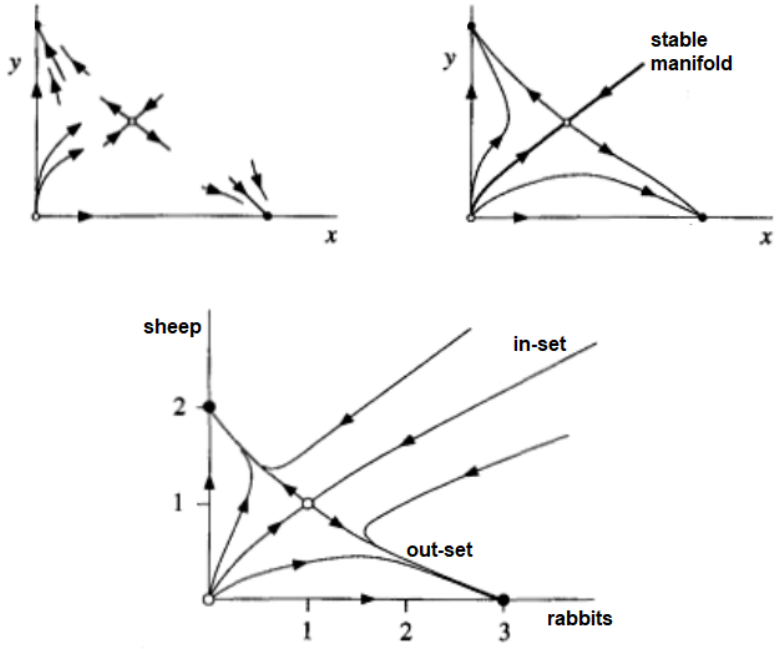

Figure 1.12: Global phase portrait for the dynamical system rabbits vs. sheep.

point, also called stable manifold, divides the plane into two parts. The area below the in-set constitutes a basin of attraction for the point (3.0) in which rabbits thrive and sheep become extinct. The area above the in-set constitutes a basin of attraction for the point (0.2) in which the sheep thrive and the rabbits become extinct. Only if the dynamics takes place along the direction established by the in-set, the system will be attracted by the point (1,1), which is the only one that allows the coexistence of both species. But even small deviations downwards or upwards the in-set will lead to the predominance of one species over the other which will become extinct. This phase portrait has an interesting biological interpretation that resides in the principle of competitive exclusion: two species that compete for the same limited resource typically fail to coexist.

Chapter 2

Complex Networks

Over the past three years, many people I have met have asked me what I was doing in my job. The reaction to my answer, "I am doing a Ph.D in Complex Systems", has always been the same: perplexity. For non-experts, the idea of a complex system easily refers to the concept of something complicated to understand or something with which only scientists have to deal. They do not know that complex does not mean complicated and they do not know that complex systems surround us and each of us interacts with them or is a part of them ... let alone the reaction when I tell them that they themselves are a complex system. The first question to answer is therefore: what is a complex system? There is no univocal definition of a complex system, but with it we can indicate those systems that are made up of a multiplicity of elements that interact with each other usually in a non-linear way. Any complicated technological machinery cannot be considered a complex system because the relationships between its parts are designed to be predictable and linear, in the sense that the effects are proportional to the cause. Think, for example, of a car in which a double or triple brake pressure corresponds to a double or triple braking. In a complex phenomenon, however, the individual parts interact in a non-linear way giving rise to unpredictable behavior. The knowledge of the individual components is not enough to derive the collective behavior of the system. We also need to understand how these parts interact with each other. For this reason, behind each complex system there is a network that encodes all the interactions between the components. And thus every living being is a complex system whose working mechanism can only be understood starting from the cellular network that encodes the interactions between genes, proteins and metabolites. The brain itself is a complex system that works through the neural network. The society in which we live is a complex system that can be studied through the social network of which we are part as components. The transportation network, the power grid, the communications network and so on are all complex systems. Therefore, complex systems constitute an interdisciplinary field whose

study has a major scientific and social impact for the study of ecosystems, financial markets, terrorist networks and the spread of pathogenic viruses, just to give a few examples. Given the fundamental role that complex systems play in our daily life, in science and economics, we agree that it is necessary to understand them in order to be able to predict or control their behavior. Network science is a new discipline that developed only in the 21st century thanks to the digital revolution that made it possible to collect, store and analyze large amounts of data and which allows to reproduce the behavior of systems made up of an ever-increasing number of elements in mutual interaction through simulations. Despite the diversity that distinguishes the various complex systems, due to the different nature of its components and their interactions, the structure and the evolution of the networks behind them are governed by common fundamental laws.

2.1 Graph Theory

From the mathematical point of view, the study of complex networks is carried out through graph theory. A graph is the mathematical counterpart of empirical real networks: it is made up of nodes or vertices that represent the elements of the network and connections between them, called links or edges, which reflect the interactions between the components. It follows that the basic parameters of a graph are the number of nodes N, which determines the size of the network, and the number of links L. A network or graph is said to be direct if all its links are direct and therefore with a specific direction, otherwise the graph is indirect.
Each node of the graph is characterized by a degree, that is the total number of links it has with other nodes. If k_i is the degree of the i-th node of an indirect network, we have that

$$L = \frac{1}{2}\sum_{i=1}^{N} k_i \tag{2.1}$$

And the average degree is

$$\langle k \rangle = \frac{1}{N}\sum_{i=1}^{N} k_i = \frac{2L}{N} \tag{2.2}$$

For a direct graph it is necessary to distinguish between the incoming degree k_i^{in}, given by the number of links entering the node, and the outgoing degree k_i^{out}, which represents the number of links leaving the node. The total degree of a node is therefore given by

$$k_i = k_i^{in} + k_i^{out} \tag{2.3}$$

The total number of links L and the average degree $\langle k \rangle$ for a direct network are respectively given by

$$L = \sum_{i=1}^{N} k_i^{in} = \sum_{i=1}^{N} k_i^{out} \tag{2.4}$$

$$\langle k^{in} \rangle = \frac{1}{N} \sum_{i=1}^{N} k_i^{in} = \langle k^{out} \rangle = \frac{1}{N} \sum_{i=1}^{N} k_i^{out} = \frac{L}{N} \tag{2.5}$$

A very important property of a graph is its degree distribution p_k, which gives the probability that any node of the graph has degree k. This probability is given by the fraction of nodes with degree k with respect to the total number of nodes

$$p_k = \frac{N_k}{N} \tag{2.6}$$

For normalization we have

$$\sum_{i=1}^{\infty} p_k = 1 \tag{2.7}$$

A network can be encoded through its $N \times N$ adjacency matrix whose elements are:

- $A_{ij} = 1$ if there is a link from node j to node i;
- $A_{ij} = 0$ if node j and node i are not connected to each other.

The adjacency matrix of an indirect network is symmetric and so $A_{ij} = A_{ji}$.
In weighted graphs, to each link is assigned a weight w_{ij} that represents the extent of the connection between the nodes i and j. For these types of graphs, the non-null elements of the adjacency matrix are given by these weights:

$$A_{ij} = w_{ij} \tag{2.8}$$

Considered two nodes i and j of a network, we can have different routes that, following the links, connect the two nodes. The shortest of these paths, that is, the one that is made up of the least number of links, is called distance d_{ij} between nodes i and j. In an indirect network $d_{ij} = d_{ji}$, on the contrary in a direct network generally $d_{ij} \neq d_{ji}$. To characterize a network we can consider the average path length $\langle d \rangle$ given by the average distances between all pairs of nodes in the network. For a direct network this quantity is given by

$$\langle d \rangle = \frac{1}{N(N-1)} \sum_{\substack{i,j=1,N \\ i \neq j}} d_{ij} \tag{2.9}$$

Another important property to characterize a network is the average clustering coefficient $\langle C \rangle$ which gives an idea of how strong the aggregation between the nodes is. For a single node i with degree k_i, the local clustering coefficient is given by

$$C_i = \frac{2L_i}{k_i(k_i - 1)} \tag{2.10}$$

where L_i represents the number of links that connect the k_i neighbor nodes of node i. Basically, C_i gives the probability that two neighbors of a node are in turn connected and it is a quantity between 0 and 1. The degree of clustering of the entire network is determined by the average clustering coefficient

$$\langle C \rangle = \frac{1}{N} \sum_{i=1}^{N} C_i \tag{2.11}$$

2.1.1 Network Topology

The topology of a network is determined by the two aforementioned characteristic quantities: the average path length $\langle d \rangle$ and the average clustering coefficient $\langle C \rangle$. In the middle of the last century only two types of graphs were known: the regular graph (figure 2.1 (a)), in which each node is connected, for example, only to its first four neighbors and the random graph (figure 2.1 (c)) in which the links between the nodes are randomly distributed. Looking at figure 2.1, it is easy to understand that the regular graph has a strong aggregation, that is a high average clustering coefficient, and a high average path length, in fact if we consider two nodes placed at the antipodes it takes many steps to get from one to the other. On the contrary, in random graphs the average path length and the average clustering coefficient are both low.
One of the goals of graph theory is to reproduce the properties of real networks. The social network, that is, the network of our friendships and acquaintances, was one of the first real networks to be studied. In the late 1960s a Harvard psychologist, Stanley Milgram, carried out an experiment to understand how many degrees of separation exist on average between any two people within the United States social network. Milgram chose a sample of 160 people taken at random in Omaha, Nebraska, and asked them if they knew a specific person, a stockbroker who lived in Boston. He asked them to send a letter to the stockbroker if they knew him or otherwise to send a letter to one of his acquaintances, the one they thought was most likely to know him. Sooner or later the letters would arrive at destination and Milgram's goal was to calculate the degrees of separation on the basis of the number of stamps present in each letter. Considering that, at that time, the United States social network counted almost 200 million people, Milgram

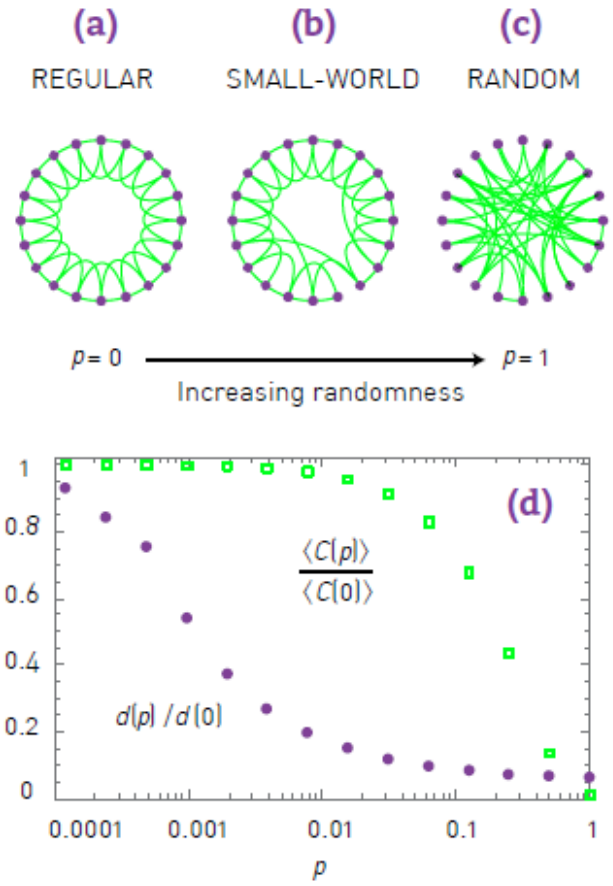

Figure 2.1: Network Topology. (a) Regular graph. (b) Small world network. (c) Random graph. (d) The small world network of the Watts and Strogatz model have an intermediate randomness with respect to that of regular and random graphs. It is characterized by a high average clustering coefficient and a low average path length (Barabasi (2016)).

expected to find hundreds of stamps on the letters. Instead he was stunned to find that on average the stamps in the letters were only six. This experiment makes us understand an important property of the US social network: it is a small world in which the average distance between nodes is small. Subsequently it was found that all social networks share this feature. Another property of social networks is given by the presence of communities or aggregations of nodes connected in a dense way by friendship or kinship links. This means that two people who are our friends are often friends with each other. From a mathematical point of view this property translates into a high average clustering coefficient. Social networks therefore have a low average path length (the small world property) and a high clustering coefficient, properties that are not reflected neither with the regular graph nor with the random graph. Only in 1998 two mathematicians from Cornell University, Duncan Watts and Steven Strogatz, proposed a type of graph halfway between the regular and the random one (Wattz and Strogatz, 1998). It is a graph that can be built from a regular graph by replacing some of its links with random links (figure 2.1 (b)). The Watts and Strogatz model allows to create a graph that presents both the small world property and a high average clustering coefficient and which therefore reproduces the structure of many real networks, including the social ones.
The small world networks of the Watts and Strogatz model are egalitarian networks in which all nodes have about the same number of links. Examples of egalitarian networks are neuronal networks whose nodes are neurons and whose links are axons and synapses or electrical networks that distribute energy from power plants. This type of graphs have a Poisson degree distribution which defines a typical scale given by the average degree of the nodes in the network (figure 2.2 (a)). However, many real small world networks (indeed most of them) do not follow a Poisson degree distribution and are aristocratic consisting of most nodes with few links and a minority of hyper-connected nodes, called hubs. Examples of real networks of this type are the World Wide Web (Albert et al. 1999), the Internet (Faloutsos et al. 1999), the network of scientific collaborations (Newman, 2001), the network of sexual contacts (Liljeros et al. 2001), the protein networks (Jeong et al. 2001) or the metabolic networks (Jeong et al. 2000). Since they do not have a typical scale, they are called scale-free networks. Their degree distribution follows a power law (figure 2.2 (b)):

$$p_k \sim k^{-\gamma} \tag{2.12}$$

The different nature of the systems which, if described in terms of complex networks, show the scale-free property make it an almost universal feature. One might wonder why there are so many networks in nature that have the scale-free property. It is due to a spontaneous mechanism known as the "Matthew effect", due to

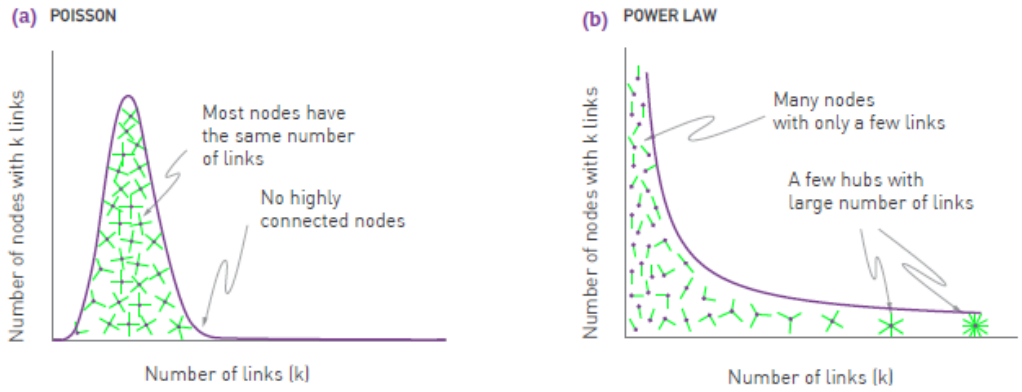

Figure 2.2: Poisson distribution of an egalitarian network (a) and power law distribution of an aristocratic network (b) (Barabasi (2016)). The main difference between the two types of distribution is the presence of the fat tail in the power law distribution due to the presence of the hubs.

a passage from the Gospel according to Matthew in which, in verse 25-29, we read: "*For to every one who has will more be given, and he will have abundance; but from him who has not, even what he has will be taken away*". The phenomenon is also known with the expression "rich get richer": it is easy to understand that those who are richer have more chances of becoming richer, just as those who have many friends are more likely to meet new people and so on. Exploiting the Matthew effect it is possible to create scale-free networks, through the mechanism of preferential attachment (Barabasi and Albert, 1999): starting from some nodes whose links are chosen arbitrarily, so that each of them has at least one link, the network evolves by adding new nodes one after the other and attaching them to the existing ones with a probability $\Pi(k_i)$ proportional to the degree k_i of the latter:

$$\Pi(k_i) = \frac{k_i}{\sum_j k_j} \tag{2.13}$$

Through this procedure the hyper-connected nodes will tend to receive more and more connections, while the little connected nodes will remain peripheral. If there are no load limits or costs related to the addition of new nodes in the network, a scale-free network is created with a power law distribution of the links. If, on the contrary, there are costs or load limits, as in the case of adding new power plants or new neurons to the existing networks, the formation of hyper-connected hubs will be hindered and egalitarian small-world networks will be created with a Gaussian distribution of the links.

2.1.2 Network Robustness

Some natural and social systems show a great capacity in maintaining basic functions despite the failure or lack of some of its components. Understanding the reasons for the robustness of complex networks is of fundamental importance in various fields: in biology and medicine to understand in which cases mutations can lead to diseases, in sociology and economics to study the stability of human communities and institutions, in ecology for the study of the environmental risks to which ecosystems are subject due to anthropic activity, in epidemiology for the study of the spread of pandemics or for the fight against terrorist attacks. Once again what needs to be studied is the network that underlies the system, whatever its nature.
The percolation theory studies the robustness of networks by assessing the impact of removing nodes or, alternatively, links. Robustness is inferred from the percentage of nodes that must be removed to completely break up the system. The percolation theory considers as a network a square lattice whose intersections can be considered as nodes. A fraction f of nodes are randomly selected and removed. To get an idea of the degree of disintegration of the system we can consider the measure of the largest component of the network, which is given by the probability P_∞ that a randomly selected node belongs to it. If f is small, the lack of a few nodes does not affect the integrity of the network. As the fraction f increases, groups of nodes begin to come off from the giant component which therefore decreases in size. Finally, for sufficiently high values of f the giant component, and therefore the whole network, breaks down into many small components that are no longer connected to each other. In this phase, the system represented by the network stops working. However, this fragmentation process is not gradual, but it is characterized by a critical threshold f_c. For $f < f_c$ the giant component continues to exist, but as soon as f exceeds f_c, it vanishes (Figure 2.3).
The percolation theory refers to regular lattices where all nodes have the same degree k. It also fits well with random graphs whose nodes have comparable degrees. Contrariwise, in scale-free graphs node degree is very variable, being there many nodes with a low degree and very few nodes with a high degree, according to a power law distribution. The topology of the graph, and in particular the presence of hubs in scale-free networks, strongly influences its resistance to external attacks, determining the robustness of the system.
The Molloy-Reed criterion (Molloy and Reed, 1995) establishes that the condition for a random network to have a giant component is

$$\kappa = \frac{\langle k^2 \rangle}{\langle k \rangle} > 2 \tag{2.14}$$

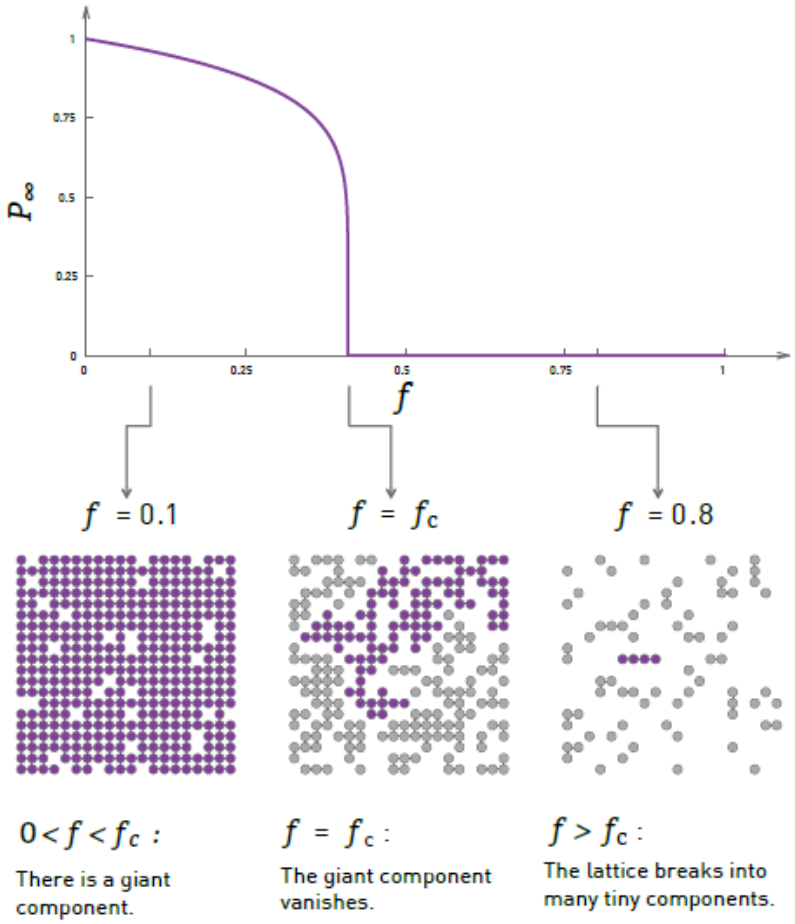

Figure 2.3: Fragmentation process is not gradual and it is characterized by a critical threshold f_c: P_∞ is nonzero under f_c, but it drops to zero as we approach f_c (Barabasi, 2016).

This criterion is valid for an arbitrary degree distribution. From the Molloy-Reed criterion it follows that the critical threshold f_c for the existence of the giant component is given by (Barabasi, 2016):

$$f_c = 1 - \frac{1}{\frac{\langle k^2 \rangle}{\langle k \rangle} - 1} \tag{2.15}$$

In the case of a random network, using $\langle k^2 \rangle = \langle k \rangle (1 + \langle k \rangle)$, we get

$$f_c = 1 - \frac{1}{\langle k \rangle} \tag{2.16}$$

Therefore, the denser the network, the higher the f_c. In any case, f_c is a finite quantity: after the removal of a finite fraction of nodes random network disintegrates. It can be shown (Barabasi, 2016) that in the case of scale-free networks with degree exponent $\gamma < 3$, the second moment $\langle k^2 \rangle$ diverges in the $N \to \infty$ limit and therefore we have $f_c = 1$. This means that in order to fragment a scale-free network it is necessary to remove almost all its nodes. In the case where $\gamma > 3$ the scale-free network behaves like the random one, that is, it disintegrates after the removal of a finite number of nodes. The greater robustness of scale-free networks compared to random ones, in response to the random removals of links, is due to the presence of hubs. Being random, removals will be much more likely to involve nodes that have a low degree because these are much more numerous than hubs. On the contrary, hubs will be removed with an extremely lower probability and this is what allows the network to remain intact. In general, for a network that is not infinite we have that the larger the network the more the critical threshold approaches $f_c = 1$. It can be said that a network shows good robustness if its critical threshold exceeds that of a random graph of the same size.
The question is different in the case of targeted attacks on the system rather than random removals. Assuming to know in detail the topology of the network, attacks aimed at removing nodes with a high degree can be perpetrated. The removal of even a small fraction of hubs is sufficient to disrupt a scale-free network. The systems with a scale-free networks are therefore very tolerant of random errors or failures, but very vulnerable to targeted attacks, for example think of terrorist attacks that target the hubs of our social, economic or computer networks.
The removal or failure of one node is not independent of the others because the activity of each node depends on the activity of its neighboring nodes. Therefore, cascade failures could be observed in which the failure of a node induces the failure of the nodes connected to it, as in the domino effect in which a local variation propagates throughout the whole system. We will have a demonstration of such a phenomenon in the fourth chapter which concerns the study of a trophic network. As we will see in fact, the forced removal of a species, which simulates a primary extinction within the ecosystem, sometimes causes secondary extinctions.

2.1.3 Degree Correlation

Degree correlation is a property of graphs that regard the tendency of nodes to connect with other nodes of similar or completely different degrees. Based on this characteristic, three types of networks are distinguished. In neutral networks nodes link to each other randomly, so the number of links between the hubs coincides with what predected by chance. In assortative networks nodes with comparable degree tend to link each other: small-degree nodes to small-degree nodes and hubs to hubs. Finally, in disassortative networks the hubs avoid each other, linking instead to small-degree nodes.
In neutral networks nodes are randomly connected and the probability that nodes with degrees k and k' link to each other is

$$p_{k,k'} = \frac{kk'}{2L} \tag{2.17}$$

A network displays degree correlation if the number of links between the high- and the low-degree nodes is systematically different from what is expected by chance, deviating from equation (2.17). But the calculation of this probability is not always easy and this method does not allow to have information on the magnitude of the correlation.
A simpler way to quantify degree correlation makes use of the degree correlation function (Barabasi, 2016). For each node i we can measure the average degree of its neighbors:

$$k_{nn}(k_i) = \frac{1}{k_i} \sum_{j=1}^{N} A_{ij} k_j \tag{2.18}$$

The degree correlation function calculates equation (2.18) for all nodes with degree k:

$$k_{nn}(k) = \sum_{k'} k' P(k'|k) \tag{2.19}$$

where $P(k'|k)$ is the conditional probability that by following a link of a degree-k node, we reach a degree-k' node. Therefore, $k_{nn}(k)$ is the average degree of the neighbors of all degree-k nodes. In a neutral network the average degree of a node's neighbors is independent of the node's degree k. So plotting $k_{nn}(k)$ as a function of k we have a horizontal line, as observed for the power grid (figure 2.4 (b)). In assortative networks the higer is the degree k of a node, the higer is the average degree of its nearest neighbors. Consequently, $k_{nn}(k)$ increases with k, as observed for scientific collaboration networks (figure 2.4 (a)). In disassortative networks hubs prefer to link to low-degree nodes. Consequently, $k_{nn}(k)$ decreases with k, as observed for the metabolic network (figure 2.4 (c)). If we approximate the degree

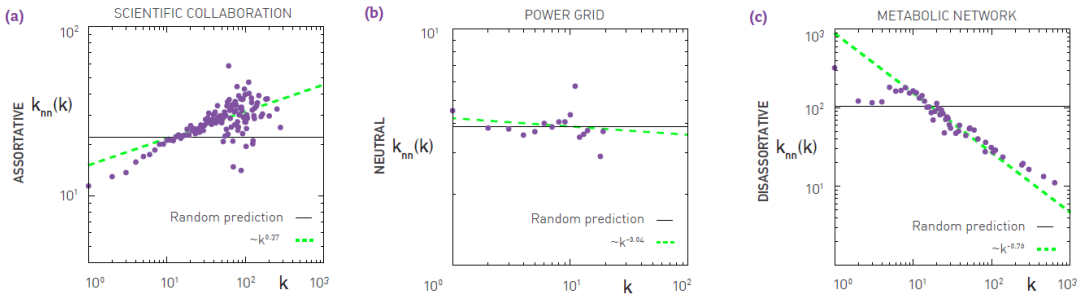

Figure 2.4: The degree correlation function $k_{nn}(k)$ on a log-log plot, for three real networks. (a) Scientific Collaboration Network (assortative), (b) Power Grid (neutral) and (c) Metabolic Network (disassortative) (Barabasi, 2016).

correlation function with

$$k_{nn}(k) = ak^{\mu} \tag{2.20}$$

the nature of the degree correlation is determined by the sign of the correlation exponent μ: positive for assoratative neworks, negative for disassotative networks and almost zero for neutral networks. Examples of assortative networks are the Internet, Social Networks and the citation network. Instead the email network, biological networks (protein interaction and the metabolic network) and the WWW have a disassortativity nature (Barabasi, 2016).
In scale-free networks there are few hubs and many more low-degree nodes. It is therefore very likely that the hubs are connected with low-degree nodes rather than with other hubs. This is the reason why the scale-free property can induce disassortativity. But there are also networks, like the citation one, which, despite their scale-free structure, are assortative. This suggests that networks degree correlation could derive from evolutionary adaptations. There are many studies investigating the properties of networks that derive from their degree correlation, among which Murakami et al. (2017), D'Agostino et al. (2012), Tanizawa (2012) and Thedchanamoorthy et al. (2014). According to these studies, assortative networks have the capacity to be more robust against targeted attacks, while disassotative networks have greater efficiency in the transport of informations. This would explain why communication-oriented networks, i.e. networks whose primary function is the exchange of information, have evolved a disassortative structure. In assortative networks, hub removal in targeted attack causes less damage because the hubs form a core group, hence many of them are redundant. Hub removal is more damaging in disassortative networks, as in these the hubs connect to many small-degree nodes, which fall off the network once a hub is deleted. Real world networks display assortative hubs in some instances, particularly when high robustness to targeted attacks is a necessity (Thedchanamoorthy et al., 2014).

2.2 The complex structure of trophic networks

The first descriptions of trophic networks among living species of an ecosystem date back to the late 1800s and were compiled by the American entomologist and naturalist Stephen Alfred Forbes, who was recognized by the National Academy of Sciences as the "*founder of the science of ecology in the United States*". However, it was the English biologist and ecologist Charles Elton that in 1927 coined the term "food chains" for these type of food relationships and denoted with "food cycles" the sets of food chains present in a community, what we now call "food webs": complex networks of trophic interaction between the species that coexist in the same ecosystem.
The most recent research on the structure of food networks are based on Graph Theory. Indeed food web can be seen as graph whose nodes represent the species present in the ecosystem and whose links symbolize their food relationships. Each node/species is distinguished by a degree which indicates the number of links that connect it to other nodes. Graphs describing food webs are direct because trophic relations are represented by oriented links that connect the predator/consumer with the prey/resource it feeds on. Thanks to the progress in the study of complex systems through graph theory, which also occurred in other fields of science, and to the qualitative and quantitative growth of empirical documentation on trophic networks, in the last decades the study of food webs has recognized a considerable attention and development in the field of ecology.
The study of trophic networks is of fundamental importance from an ecological point of view, as they feature the structure of the ecosystems and determine their properties, including their resistance to environmental disturbances of various kinds.

2.2.1 Complexity and stability in food webs

In the case of trophic networks, the number of nodes and therefore of species, defines the biodiversity S of the ecosystem. By calling L the number of trophic links between the species, each graph is distinguished by the value of the connectance C, which gives the ratio between the number of connections actually present on the possible ones. Therefore we have $C = L/S^2$ in the event that loops (i.e. connections of a node with itself) are taken into consideration, that, in the case of food webs, is equivalent to consider the phenomenon of cannibalism. Otherwise, if we do not consider the presence of loops, we have $C = L/S(S-1)$. Thereby connectance gives a measure of the probability that two species interact with each other within a graph. The complexity c of a network, and in particular in this case of an ecosystem, is closely connected to the concept of connectance. Complexity is in fact defined as the product of the connectance C for the biodiversity S of the

ecosystem and corresponds to the linkage density L/S of the web: $c = CS = L/S$.
One of the most controversial debates in the context of food networks is the relationship between stability and complexity of an ecological system. The stability of an ecosystem is connected to the resistance it opposes to its disintegration when subject to various kinds of perturbations. In particular, the stability is considered as a measure of the reaction of the system to an external perturbation that makes it move away from its state of equilibrium, given by the densities of the populations of each species involved: a system is more stable the more quickly it returns to its state of initial equilibrium or how much closer it returns to it after the disturbance.
Until the seventies, the predominant idea among ecologists was that the stability of ecological communities would increase with their complexity (Elton, 1958; MacArthur, 1955). In this regard, Charles Elton stated that: *"simple communities are more easily upset than richer ones; that is, more subject to destructive oscillations in populations, and more vulnerable to invasions"* (Elton, 1958). Indeed, simpler communities would be more easily disturbed by changes than more complex ones, whose multiplicity in the number of prey and predators would tend to eliminate the risk of dramatic changes if one of the species decreased in density. This belief was questioned by the theoretical ecologist Robert May (May, 1973) who used methods related to dynamic models. May created community models in which the connections between the elements are established in a random way. Through a local stability analysis, he observed a transition from stable to unstable behavior with increasing complexity, thus coming to the conclusion that the stability of an ecosystem decreases with increasing number of species and interactions. Considering weighted graphs with an interaction force i between the nodes, May formulated the criterion according to which ecological communities tend to be stable when

$$i(SC)^{\frac{1}{2}} < 1 \tag{2.21}$$

that is, when there are low values of S, C or i. May's result contradicts the empirical observations of experimental ecologists and seems inconsistent with the existence of extremely complex ecosystems, rich in biodiversity such as rain forests and coral reefs. Thus was born the "paradox of May". May's analysis was therefore subject to criticism that highlighted its limitations, including the most obvious one of considering random interactions between species. In fact, within an ecosystem, trophic relationships are not random (for example, most animals prey on species smaller than their own) and these interactions significantly affect the dynamics of the system.

2.2.2 Scale invariance and the Cascade Model

If we consider the interaction force i as constant, May's criterion suggests that a community remains stable if a decrease in connectance C is accompanied by an increase in diversity S, so that $SC = L/S$ remains a constant quantity. Many studies, among which Cohen and Newman (1985) and Cohen et al. (1986), at first seemed to corroborate May's hypothesis: the connectance C seemed to decreas with the diversity S and the ratio L/S seemed to assume approximately constant values between 1 and 2. In particular, they found that $L/S \simeq 2$ and called this scale invariance link-species scaling law (Figure 2.5). This was not the only scale invariance found. Other studies reported constant proportions between species without predators above the food chain (top species T), intermediate species (I) having both prey and predators and basal species (B)that have no prey. This regularity was called species scaling law. The proportion in the links between species T, I and B also appeared to be constant, a regularity which was called link scaling law (Briand and Cohen, 1984).

Cohen et al. tried to explain the regularities observed in empirical studies through a simple Cascade Model. In this model, species and food links are distributed stochastically and are subject to only two constraints: species are located in a one-dimensional food hierarchy and can predate only species that are lower than them in the hierarchy. This procedure for the construction of the trophic network automatically excludes the presence of loops and therefore does not take into consideration the phenomenon of cannibalism. The model is based on two parameters: the number of species S and the link density L/S. Assuming the constancy of the L/S ratio and setting for this quantity the average value found in the experimental analysis, Cohen et al. found that their model correctly reproduced the regularities empirically observed: the species scaling law and the link scaling law (Cohen and Newman, 1985, Cohen et al., 1986). It therefore seemed that a simple stochastic model, analytically treatable, could successfully generate network topologies and regularities similar to those empirically observed.

2.2.3 Improvement of data and new evidences

Many criticisms were made of the studies that supported the evidence of the aforementioned regularities and of the cascade model that sought to reproduce these scale invariance. In particular, many studies, including Martinez (1991), highlighted the limitedness of the data accompanied by a poor resolution so that many species within the food chains were poorly represented, even absent or even aggregated into similar but different species. Instead the cascade model was reproached for the stochastic method through which networks are built and for the exclusion of the cannibalism phenomenon. New research, based on more detailed empirical

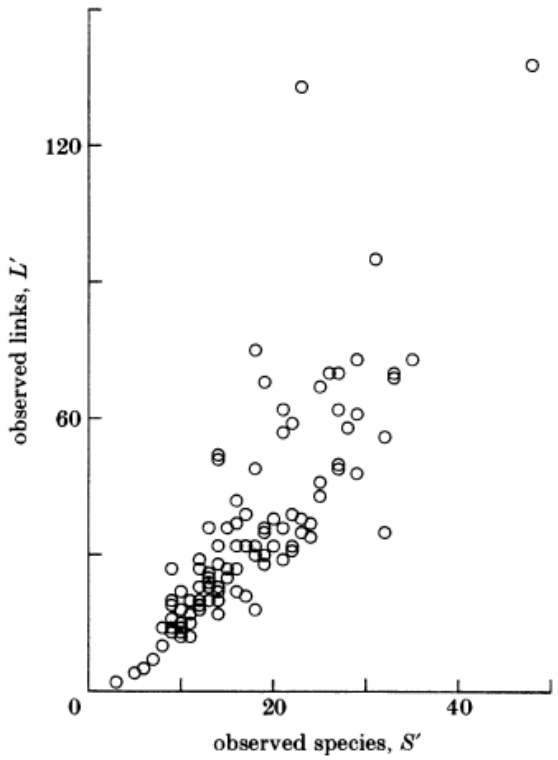

Figure 2.5: A graph showing one of the results found by Cohen and Newman in Cohen et al. (1986). The number of links L as a function of the number of species S for 113 experimental trophic chains. The slope of the regression curve gives $L/S \simeq 2$.

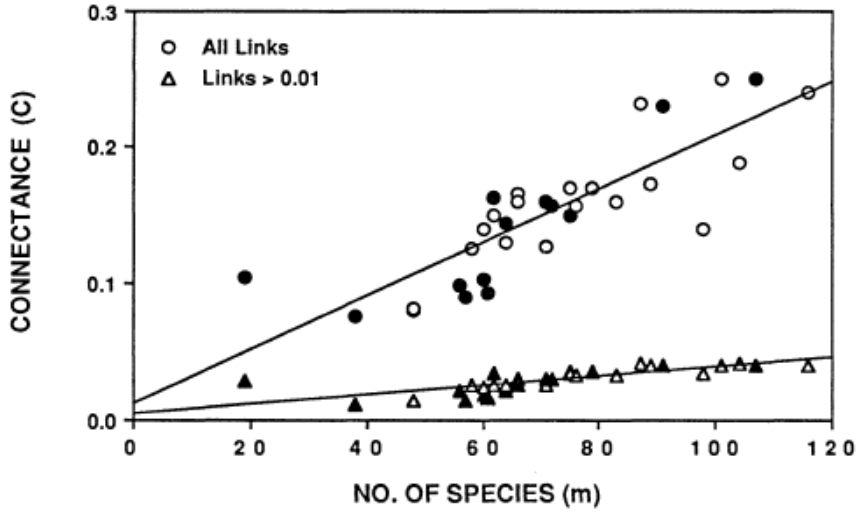

Figure 2.6: A graph showing the result found in Sugihara et al. (1989). The connectance C is positively related to the number of species.

data which also included cannibalism, was done. In his research, Martinez found a value of the L/S ratio much higher (close to 10) than that obtained by Cohen and Newman and therefore a higher degree of interaction between species. Other studies improved sampling accuracy by also including information related to the volumetric fraction of each prey in the diet of each predator. In this way weighted graphs are created, in which the extent of the interaction between two species is represented by the weight of the link that connects them. Using data structured in this way, which also include the weakest connections, Sugihara et al. (1989) obtained a positive relationship between C and S contrary to what predicted by the May criterion (Figure 2.6). These new studies seem not to support the hypothesis of the constancy of the L/S ratio and therefore of the decrease of C with the increase of S. Rather Martinez (1992) proposes a new hypothesis on the constancy of the connectance $C = L/S^2$, so that instead of being constant, L/S would grow with S in a fixed proportion. According to this hypothesis predators consume an approximately constant fraction of the prey available, so that as diversity increases, the number of interactions between species increases.

2.2.4 The Niche Model and the Generalized Analytical Model

The cascade model had been developed on the basis of poorly resolved data and did not pass the tests with new more detailed data. Moreover, in this model link distribution, besides being random, requires the constancy of the L/S ratio. Williams and Martinez (2000) proposed the Niche Model, in the attempt to repro-

duce real food webs by overcoming the limitations found in the cascade model. In this model the two parameters to be set as input are the number of species S and the connectance C, that determines the links between species. Unlike the cascade model, this one makes no assumption about the constancy of the L/S ratio. Also in the niche model species are ordered along a single dimension: each species is assigned a random niche value which determines its position along a line. For link distribution, each species is assigned a feeding range whose midpoint is a random number less than the niche value. All the species that fall within this range constitute the prey of the species considered. The length of the feeding range is randomly selected from a beta distribution so that the connectance value of the simulated network is close to that observed in the empirical network. With this model cannibalism is taken into consideration and the trophic overlap is higher than that obtained with a purely stochastic link distribution and therefore more similar to that observed in real food webs. Williams and Martinez in the same study tested their model: through numerical simulations they statistically compared the results obtained with the niche model with those obtained with the cascade model and with a purely random model. They used S and C as input parameters, so that the three models differed only in the link distribution. The niche model turned out to be the best providing a good fit of the experimental data. Other models were created in the attempt to further improve the match with experimental data (including the Nested Hierarchy Model described in Cattin et al., 2004), but none exceeded the quality of the results found with the niche model.
Stouffer et al. (2005) found that models must meet two conditions to well reproduce the central properties of real food webs:

- Niche values for species must form an ordered set;
- Each species has a specific probability of predating other species with a lower niche value and this probability must be derived from an approximately exponential distribution.

This theory is referred to as the Generalized Analytical Model. Stouffer et al. tested their hypothesis on the centrality of these two conditions by modifying the cascade model so that it also observed the second condition. This modified version led to good results reproducing features of real food webs and so corroborating their hypothesis.

2.2.5 Topology and universal patterns

As already mentioned, the topology of a network is strongly determined by three quantities: the average path length, the average clustering coefficient and the degree distribution of the nodes. Most real networks have a small world structure

and appear to be scale-free, showing a power law degree distribution with many low-degree nodes and a few highly interconnected nodes.
Many studies questioned the structure presented by trophic networks. In particular, Montoya and Solé (2002) compared the properties of real food webs with those obtained for random networks with the same number of links and found that the average path length is very similar and very short, but the clustering coefficient is much greater for real food webs compared to random ones (Figure 2.7). This, as we have seen, is a characteristic aspect of small-world behavior. In addition, they obtained a strongly non-Poissonian link distribution $P(k)$ which seems to follow a power law (Figure 2.8).

Camacho et al. (2002) contradicted these results by stating that the clustering coefficient of real food chains is lower than that observed in small-world networks and therefore more similar to that of a random network. Furthermore, according to them, link distribution does not appear to be scale-free. However, they found that, when link distribution is normalized for link density L/S, it shows a universal functional shape given by an exponential decay instead of by a power law one (Figure 2.9). Also the clustering coefficient and the average path length seem, according to Camacho et al. (2002), to follow a universal functional form that scales with the density of the links.

Milo et al. (2002) studied the presence, within food webs, of recurrent and significant interconnection patterns, defined by them as motifs. They used a statistical approach through an algorithm that identifies and counts all possible configurations of subgraphs with three or four nodes. Then they compared the frequency of these subgraphs in empirical networks and in comparable random networks. By applying this method to some empirical food webs, Milo et al. found that a particular subgraph consisting of four species (a chain with two species sharing both a predator and a prey) constitutes a universal pattern. The presence of this pattern in food webs seems to be independent of network size, but their frequency increases linearly with S.

2.2.6 Robustness of trophic networks

Research on trophic networks concerns topics of great ecological interest since the robustness of an ecosystem in response to external perturbations depends on its structure. Solé and Montoya (2001) studied the response of some food chains by simulating the loss of nodes, i.e. the disappearance of species within the ecosystem, and looking at the level of consequent secondary extinctions. Indeed, if the primary extinction causes a species to lose all its resources, this will in turn become extinct. They came to the conclusion that the removal of highly connected species causes a very high rate of secondary extinctions compared to a random removal of species (Figure 2.10). It would therefore seem that food webs are more vulnerable to

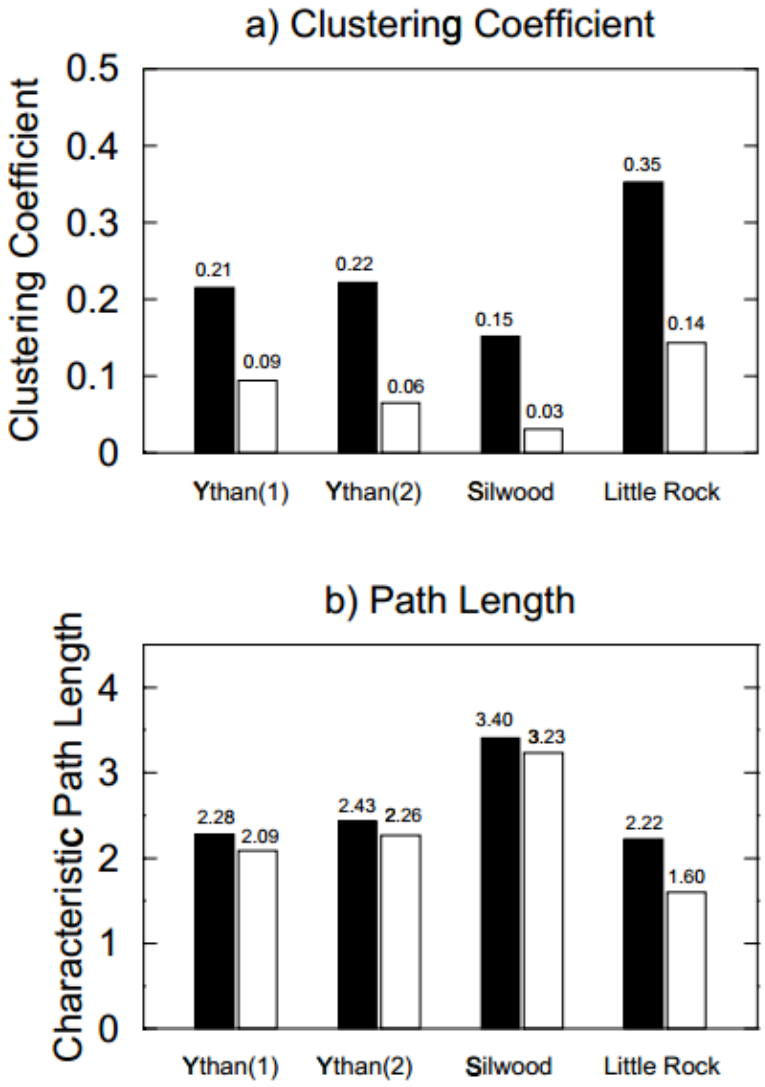

Figure 2.7: (a) The Clustering coefficient for four food webs. The black columns represent the real networks and the white columns the average results obtained from over 200 randomly generated networks with the same average number of links per species. Real clustering is greater than the random counterparts. (b) Average distance between two nodes: excluding the case of Little Rock the difference between the random and the real case is very small (Montoya and Solé, 2002).

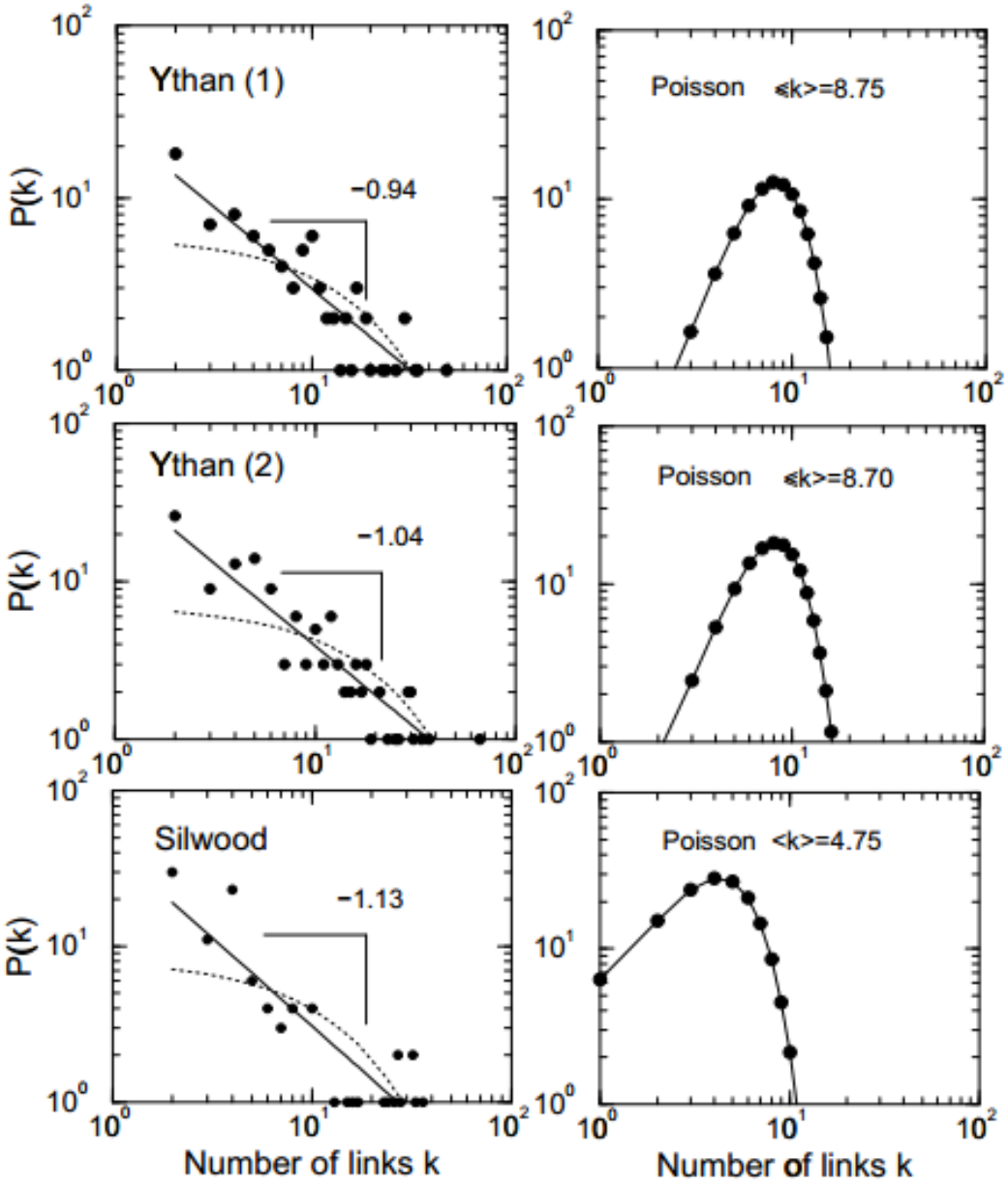

Figure 2.8: Link distribution $P(k)$ for the networks analyzed. Left column: the data obtained in the case of Ythan and Silwood approximate a power law (pointed line in the figure). Right column: distributions predicted using a random graph. Poissonian behavior cannot be compared to the results obtained for real food webs (Montoya and Solé, 2002).

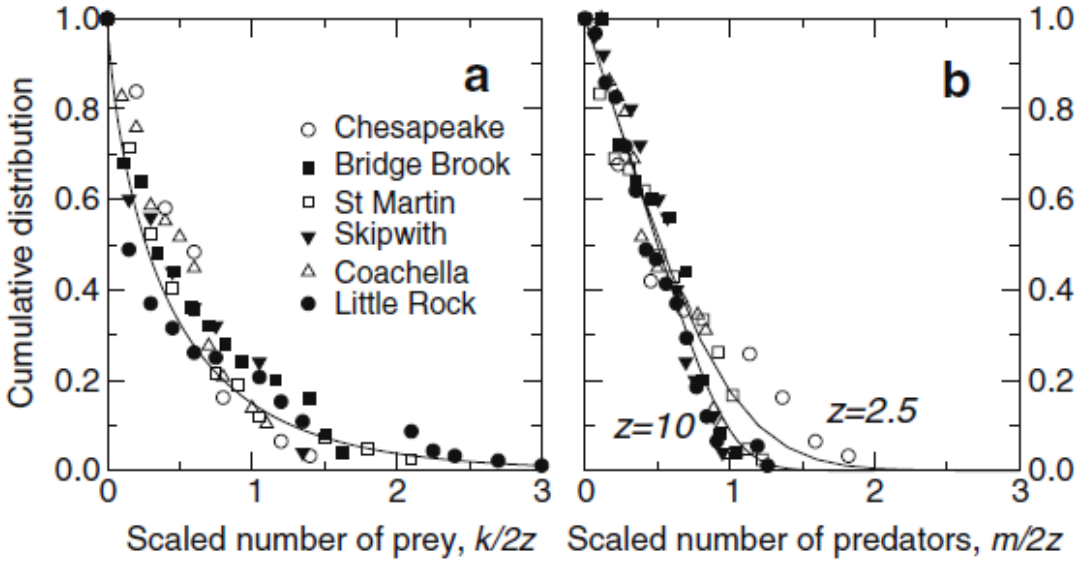

Figure 2.9: The distributions of the number of prey and predators scaled with the link density follow the same pattern (an exponential decay) for all the food webs (Camacho et al. (2002)).

targeted attacks to hubs than to random attacks, characteristic generally found in scale-free networks. According to Solé and Montoya (2001), this would be the proof that even trophic networks, like most real networks, have a scale-free structure with a power law degree distribution.

As mentioned previously, however, trophic networks do not seem to have a scale-free structure. According to Dunne et al. (2002), the degree distribution still being fat tailed, even if not properly with a power law slope, alters the response to targeted and random removals so that the first modality is more effective than the second, similarly to what happens in scale-free networks. Dunne et al. also found that the robustness of the food webs, defined as the fraction of primary species removed which induces a total loss of at least 50 % of the species (primary and secondary extinctions), increases with increasing connectance $C = L/S^2$ and this result applies both for targeted removals of hyper-connected species and for random removals of nodes (Figure 2.11).

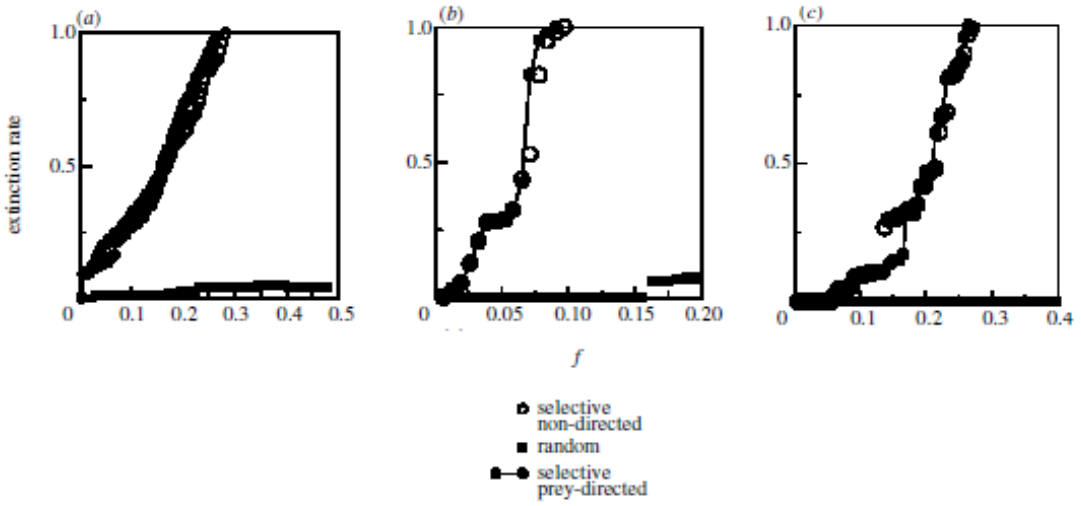

Figure 2.10: Extinction rate (fraction of secondary extinctions) in relation to the fraction of species removed f for three different empirical food webs (Solé and Montoya, 2001).

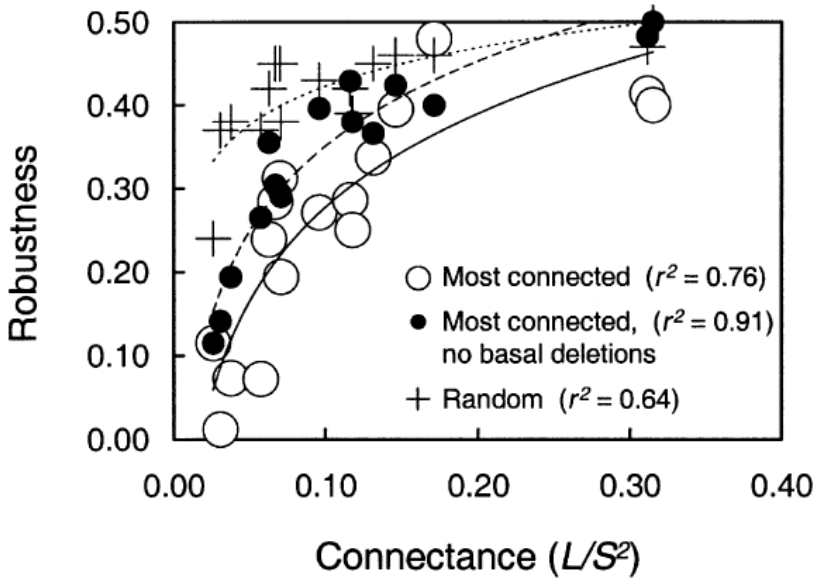

Figure 2.11: Network robustness, as defined by Dunne et al., as a function of connectance for 16 empirical trophic webs subjected to three different types of node removal (Dunne et al., 2002).

Chapter 3

First case study: Tax Evasion as a contagion game

Tax evasion is the "*illegal and intentional actions taken by individuals to reduce their legally due tax obligations*" (Alm 2012, p.55). Its main effect is a severe damage to the socio-economical environment that deprives governments of their fiscal resources and plays an important role in reducing well-being of societies. It is quite an age-old phenomenon that has been studied for decades, both theoretically and empirically. The well-known free rider problem rises when a selfish citizen consumes public goods and services without properly contributing to related costs (Baumol 1952). This causes inefficiency and bad allocations of governments expenditures for healthcare, education, defence, social security, transportation, infrastructure, science and technology, as widely documented in a vast literature, among which Andreoni et al. (1998), Slemrod and Yitzhaki (2002), Torgler (2002), Kirchler (2007), Slemrod (2007). Tax evasion and the so-called black economy are, also, related to social inequality, as underlined by part of the literature, among which, Alstadsaeter et al. (2017), Bertotti and Modanese (2014, 2016), dealing with the differentiation of the propensity to evade with respect to income and with redistributive aspects. Finally, it matters in terms of social justice, since it specially afflicts poorer people, who do not have the possibility to substitute public services with private ones with higher prices.
In his *An Essay on the Nature and Significance of Economic Science*, Lionel Robbins (1932, p.15) wrote that "*economics is the science which studies human behavior as a relationship between ends and scarce means which have alternative uses*". Thus, human decision on public goods can be interpreted as a behavioral choice in terms of cooperation vs. competition in the society. The model here presented aims to show the collective relevance of such behavioral elements in driving the decision of each citizen, which reflects also the perceived quality of the public good and the relational feedback received by her surrounding social environment.

The initial stages of the formal analysis of tax evasion can be dated back to the Seventies, with contributions by Allingham and Sandmo (1972) and Srinivasan (1973). Despite many similarities, such contributions, which are a propagation of an earlier approach advanced by Becker (1968), differ from each other with respect to optimization procedures, taxpayer's risk attitudes (which affect second order conditions of chosen objective functions), decision variables, audit probabilities, tax tariffs, and fine functions. In particular, Allingham and Sandmo (1972), find that income understatement is decreasing in audit probabilities or in the fine, whereas the dependence on tax rate is more controversial, reflecting income and substitution effects. Yitzhaki (1974) obtained a conter-intuitive result by modelling fines computed on the basis of evaded taxes (instead of the understated income): as the tax rate increases, the evasion decreases, differently from the empirical evidence shown in Clotfelter (1983), Crane and Nourzad (1987), Poterba (1987). Many other studies have been done in the attempt to find a positive relatioship between tax rate and evasion (see for example, among others, Yitzhaki 1987, Panades 2004, Dalamagas 2011, Yaniv 2013).

Such a standard theoretical framework inspired several contributions in related literature, concerning tax evasion and related issues, such as the shadow economy, as in Buehn and Schneider (2012), psychological perception and society (social norms and moral sentiments like guilt or shame), as in Myles and Naylor (1996), Traxler (2006), Fortin et al. (2007), Kirchler (2007) and many others. Also literature from statistical physics and network science is deeply connected to such topics, as shown in recent reviews by Perc and Szolnoki (2010), Perc et al. (2013, 2017), Capraro and Perc (2018).

More generally, a growing stream of literature presenting agent-based models dealing with tax evasion exists. A survey of such papers could be gained by the joint reading of Bloomquist (2006), Alm (2012), Hokamp (2013), Pickhardt and Prinz (2014), Oates (2015), Bazart et al. (2016). The advantage of agent-based models is that they are prone to describe the complexity of aggregate contexts, as documented in previous studies of socio-economic analysis, Pluchino et al. (2010, 2011, 2018), Biondo et al. (2013a, 2013b, 2013c, 2014, 2015, 2017). Simulative models (as in Lima and Zaklan, 2008) can help investigating relevant questions, as the correspondence between the provision of the public good and tax evasion, as in Hokamp (2013), the importance of social norms and auditing, as in Hokamp and Pickhardt (2010), and the effect of social networks on the tax compliance, as in Vale (2015). Such aspects, like many others, can be explained in terms of behavioral attributes, seeking for the roots of decisions in the evolution of personal traits, influenced by the surrounding environment.

As reported by the IRS (2016), given the extent of the tax evasion, the expenditures paid by governmental authorities to induce virtuous behaviors are significant.

Nonetheless, in many cases, free riders remain unpunished. Honest citizens considering the participation to social costs as a moral imperative are the sole fully compliant taxpayers. We rephrase the provoking question asked by Alm et al. (1992): why should people pay taxes? Different reasons can be reported: first of all, because of altruism, as recalled, for just some examples, in Stevens (2018), Epstein (1993), and Zappalà et al. (2014); secondly, because of imitation, as in Callen and Shapero (1974), in Elsenbroich and Gilbert (2014) and McDonald and Crandall (2015); finally, because of an assessment of the quality of the public good, as in Nicolaides (2014), La Porta et al. (1999), Feld and Frey (2007) and Torgler and Schneider (2009).

The main motivation of this study is to combine the agent-based approach to the prisoner's dilemma perspective of the standard *public goods game*, in order to show a very simple way in which the conflict between individual and collective rationality (Rapoport 1974) can be enriched by imitation coming from the social interaction. Such a social dilemma motivated a vast amount of literature, regarding the production of public goods, as in Heckathorn (1996), the emergence of social norms and social interaction, as in Hardin (1995), and Voss (2001), the reasons behind cooperative behavior, as in Nowak (2006), the social preference models, as in Fehr and Schmidt (1999), Bolton and Ockenfels (2000), Charness and Rabin (2002), Capraro (2013) and with specific reference to moral preferences in Capraro and Rand (2018) and Tappin and Capraro (2018). The effect of the observation within social structures can be determinant to drive individual decisions, as shown in previous contributions, among which, Granovetter (1978) and Mäs and Opp (2016). This model contributes to the stream of literature dealing with collective behavior (both in terms of triggering threshold and spreading) in the dynamic perspective of a public good game, in the case in which players are aware of the behavior of their neighbors within a realistic social network. A very recent contribution on the same line is Liu *et al.* (2019).

The study presented here, developed in collaboration with Prof. Alessandro Pluchino and Prof. Alessio E. Biondo, has been published by the European Physical Journal (Di Mauro et al., 2019). The model describes a community in which agents decide whether to pay taxes or not, according to their personal satisfaction and to the imitation of neighbors' behavior. In Section 3.1, is presented the simplest setting of the model, showing that it is able to reproduce results obtained by Elster (1989) in terms of multi-person prisoner's dilemma; then, is highlighted the role of taxpayers in contrast with that of evaders for the dynamics of the system; in Section 3.2 is introduced the dynamic decisional rule based on personal satisfaction and imitation; in Section 3.3, is studied the effect of three policy parameters regulating the tax rate, the fine, and the audit probability; finally in Section 3.4 are presented some conclusive insights.

3.1 Tax Evasion Model

Consider a community of N citizens (players), $\{P_i\}_{i=1,2,\ldots,N}$, who have to pay their personal contributes $d_{i,t}$ to produce a public good, e.g. a public service, assumed to be perfectly non-excludable and only partly non-rival. We assume that time $t = 0, 1, 2, \ldots, T$ is measured by a discrete variable indexing simulative steps (i.e., turns of the game). At each turn, a randomly number of citizens are assumed to consume the public good/service, from which they receive a utility in terms of units of a dimensionless reward, which we shall denominate $G_{i,t}$. Of course, the total available amount of the public good is limited to the cumulated contributes paid by tax-payers, i.e. $\sum_{i,t} G_{i,t} = \sum_{i,t} d_{i,t}$, $\forall t$. Initially, at $t = 0$, all community members are endowed with the same initial amount of capital $C_{i,0}$, which will be increased at each time step, by $\Delta C_{i,t} = \Delta C = 1$ unit, $\forall i$. Thus, the monetary value of individual utility is $U_{i,t} = C_{i,t} + G_{i,t}$. In the simplest setting, the topological configuration of the social network is irrelevant because each player is assumed to decide independently of other players' decisions. Later we will remove such an initial simplification and specify how people is reciprocally linked to each other.

3.1.1 The basic setting

At each turn, each player P_i chooses how to behave from the following two alternative strategies:

- **strategy A**: to pay $d_{i,t}$ units of capital to contribute to the public good production;
- **strategy B**: to evade the tax and possibly incur in the fine, equal to $h_{i,t}$ units of capital (which will not be redistributed to other players), with probability p.

Let us consider for simplicity a lump-sum taxation/fine system only, i.e., $d_{i,t} = d$ and $h_{i,t} = h$, $\forall i$, and assume that $h > d$. As in every other prisoner's dilemma, from the individual point of view, the best choice is to play the non-cooperative strategy B, since its payoff is greater than the one associated to strategy A for every possible decision assumed by other players. Consider that the partial non-rivalry of the public good is modeled by assuming that at each time step t, a random number of players is extracted to divide among them the total amount of resources collected from tax payment of the whole community. From the standpoint of the single citizen/player, the ex-ante probability to be selected, i.e. to use the public good, and receive any amount $G_{i,t}$ is the same in both cases (equal to γ, say) and is not affected by the fact that she is a cooperator or not. For the sake of simplicity, let us assume that $\gamma G_{i,t} = \Gamma$, $\forall i$. The individual payoff associated to the strategy

A is $\pi^A_{i,t} = \Delta C + \Gamma - d$, whereas $\pi^B_{i,t} = \Delta C + \Gamma - ph$. Thus, for each player, the strategy B Nash-dominates the strategy A if $p < d/h$.

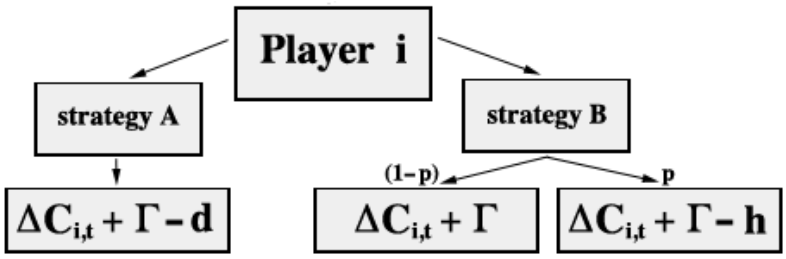

Figure 3.1: Rules of the basic setting: at each turn, after receiving $\Delta C_{i,t}$, each player decides what to do: taxpayers play only strategy A; tax evaders play only strategy B.

Figure 3.1 depicts the basic setting of the game at each time step. Agents receive the exogenous ΔC and, according to their behavior, are partitioned in two groups: taxpayers, who altruistically always play strategy A, indicated as $\{A_i\}_{i=1,2,...,N_\mathrm{a}}$; and tax evaders, who selfishly always play strategy B, indicated as $\{S_i\}_{i=1,2,...,N_\mathrm{s}}$. Of course, $N = N_\mathrm{a} + N_\mathrm{s}$. The basic settings for the first set of simulations is: $p = 0.4$ (audit probability), $d = 2$ units (tax payment), $h = 3$ units (fine) and $\Delta C = 1$ units (external gain).

3.1.2 Effects of a change of N_a

Let us investigate the asymptotic behavior of the average social capital $\bar{C}(T) = \frac{1}{N}\sum_{i=1}^{N} C_i(T)$, calculated at the end of a set of single-run simulations, with $T = 100$ turns per players, when the percentage $f = N_\mathrm{a}/N$ of taxpayers changes by steps of 1 % in $[0, 100]$. In Figure 3.2, the average final capital $\bar{C}(T)$ is reported (red line) as function of f, confronted with its two components, i.e., $\bar{C}_a(T) = \frac{1}{N_a}\sum_{i=1}^{N_a} C_i(T)$ (green line) and $\bar{C}_s(T) = \frac{1}{N_s}\sum_{i=1}^{N_s} C_i(T)$ (blue line) calculated separately for the altruistic taxpayers and selfish evaders (a horizontal black line at $\bar{C} = 0$ is also drawn for comparison). The three values of social capital have been rescaled in order to have $\bar{C}(T) = 0$ when $f = 0\%$, since – by definition – if no one pays taxes the collectivity must have zero benefits. A confirmation for a very elementary intuition, i.e., that the average capital $\bar{C}_s(T)$ of the evaders is a positive function of f. This happens because an always smaller number of evaders is surrounded by an increasing number of taxpayers. Furthermore, even the capital of taxpayers ($\bar{C}_a(T)$) is positively linked with f since, as long as the number of altruists grows, the amount of available public good increases for all citizens and, meanwhile, evaders are becoming numerically less relevant. When the fraction f of taxpayers

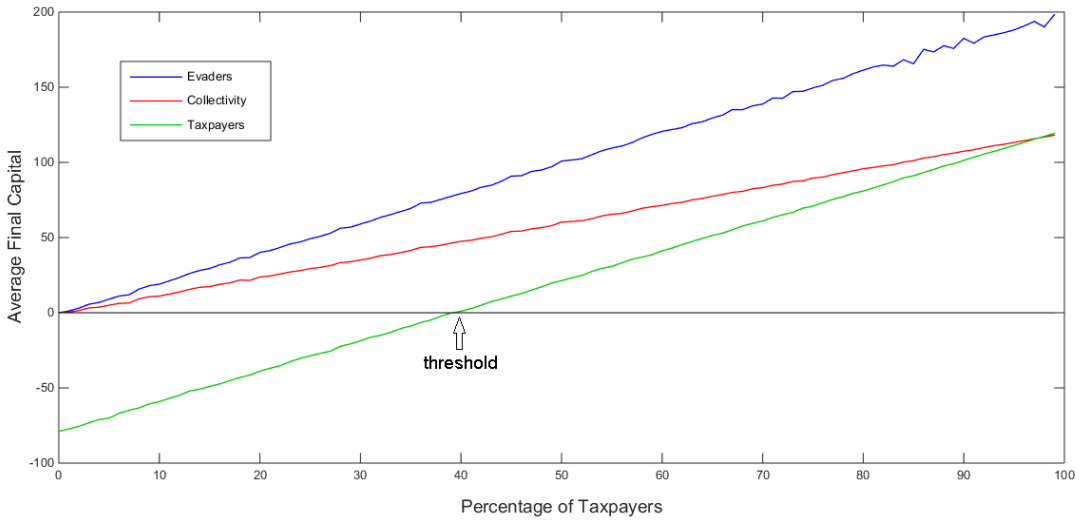

Figure 3.2: The final average social capital $\bar{C}(T)$ (red), over $T = 100$ turns, as a function of the percentage f of taxpayers. Average final capitals $\bar{C}_a(T)$ (green) and $\bar{C}_s(T)$ (blue), for taxpayers and tax evaders respectively, are also reported and compared with the first one.

goes below a threshold f_{th}, which in Figure 3.2 is almost 40% (given the chosen parameters), the average capital of taxpayers becomes negative, while the collective capital $\bar{C}(T)$ is still positive. This means that – on average – they pay more than they receive. The average social capital of taxpayers is always lower than the average social capital of evaders, i.e. $\bar{C}_a(T) < \bar{C}_s(T)\ \forall f$. This is the graphical evidence of Nash-dominance of the non-cooperative behavior and reproduces the same result described by Elster (1989) and shown in Figure 1.4. The two heavy lines in the Elster's diagram show the expected benefits, of both cooperators and free riders, as functions of the number of cooperators (altruists). The strong similitude is evident: as in our Figure 3.2, the average benefits are a positive function of the number of cooperators and the line representing the reward to free riders is constantly above the other one. It is very natural to conclude that the capital of the collectivity increases only thanks to the contribution of altruistic players. Thus, from the collective point of view, groups with more cooperators are favored compared to groups with few cooperators. Indeed, the more numerous altruists are, the smaller the cost of free riders (in both absolute and relative terms).

3.1.3 Degrees of necessity, degrees of failure...

The basic setting showed the known market failure due to the presence of free riders in action. Economic theory says that in this case the intervention of the policy maker is the only solution to create a remedy, which hopefully can represent a second best solution, since the social optimum cannot be reached by private market forces only. Despite such a result is quite definitive, we try to advance the analysis collaterally, by questioning whether the degree of importance (or the difficulty of substitution) of the public good at hand can play a role and become an endogenous mechanism to partly amend the disequilibrium. If, for example, a public good were a primary good, then the low quality caused by insufficient funds could force people (free riders included) to buy substitutes on the private market. In other words, if a public pool is always crowded or dirty is one thing; if an hospital is unable to aid people even for immediate emergency services, is another. Both cases respond to the logic of the model with free riders and the set of consequences is theoretically identical. Nonetheless, a citizen would suffer from two qualitatively different losses. In particular, for the case of the hospital, the primary need for health services pushes the citizen to buy them on the private market. This dramatically creates a strong form of social injustice, since poor people will be hit much harder than rich ones. For the sake of simplicity, we neglect such redistributive issues (being developed in a forthcoming paper, in which tax evasion is a function of personal income as well) and focus on the case of a primary public good/service. If the number of taxpayers is not big enough, tax evaders may end up with a negative final capital value, since they will have to buy on the market what has not been produced because of their evasion. Thus, when the public good is a primary good, a loss suffered by free riders emerges and the percentage of taxpayers turns out to be a fundamental ingredient for the tax evasion be a convenient strategy, as shown in Figure 3.3.
As a consequence, we can recognize no longer one but three thresholds, namely a, b, c.

1) When $f < a$, social capital is negative for all of the three groups because paid taxes cannot grant the public services for everybody. It is worth noting that this is a very bad situation, in which tax evaders damage both the community and also themselves, and tax payers suffer twice because they pay taxes and may also need to buy private substitutes of the public good.

2) When $a \leq f < b$, the number of altruists is sufficient to cover the expenses of the public good production that make, on average, tax evasion convenient for tax evaders (the break-even point is reached in point a). The average capital of tax payers and that of the whole society remain negative.

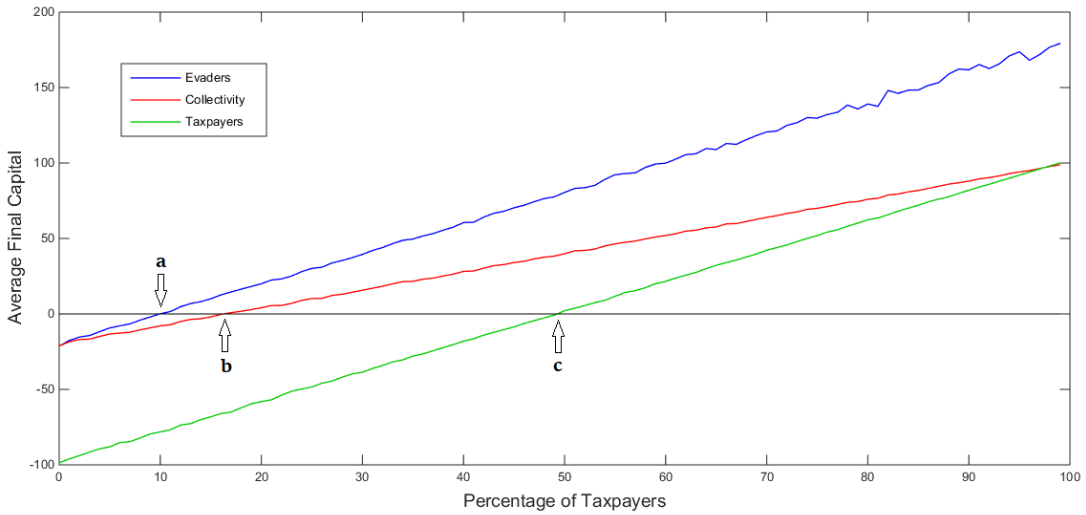

Figure 3.3: When the public good is a primary good, the loss suffered by free riders matters. Average final capital functions presented in Figure 3.2, i.e., $\bar{C}(t)$, $\bar{C}_a(t)$ and $\bar{C}_s(t)$, cannot be rescaled and the percentage of taxpayers turns out to be a fundamental ingredient for the tax evasion be a convenient strategy. Two new thresholds appear: see text for details.

3) When $b \leq f < c$, the negative average capital of tax payers is more than compensated, at the social level, by the gain of evaders.

4) When $f \geq c$, average capital for taxpayers becomes finally positive and public services are sufficient for the community (even if the collected resources are less than they should be). Tax evaders are still present in the community (unless $f = 100\%$) and continue to be better off than altruists. In particular, the reduction of tax evaders would improve the life conditions of the community either by increasing (if possible) the quality/quantity of the public good, or by reducing the tax pressure.

The behavioral characterization of each citizen i, can be described by adapting an interesting diagram proposed by Cipolla (2011) and showed in Figure 3.4. Let us indicate on the horizontal axis the quantity/quality of the public good Γ_i and, on the vertical axis, the individual contribution C_i of i, in order to identify four types of players:

Smart: those who consume the public good and participate to its production for the whole community by their personal contribution, namely, taxpayers when $f \geq c$;

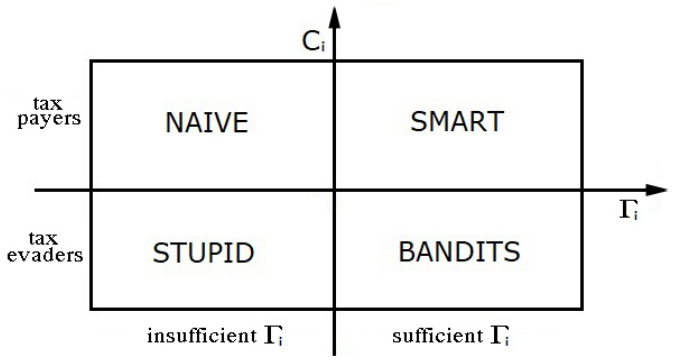

Figure 3.4: A possible taxonomy of citizens can be derived by considering how each of them combine individual contribution (C_i) to the production of the public good and consumption of it (Γ_i).

Naive: those who contribute to the public good production for the whole community even when their consumption is insufficient or absent, namely, taxpayers when $f < c$;

Stupid: those who do not contribute to the production of the public good but suffer because their consumption of it is insufficient or absent, namely, tax evaders when $f < a$;

Bandits: those who do not contribute to the production of the public good and enjoy a satisfactory consumption of it at expenses of the rest of the community, namely, tax evaders when $f \geq a$.

3.2 Satisfaction and contagion on complex network

In this section we update the set of possible behaviors that each player can choose. Differently from the basic setting, we add the possibility, at each time step, to randomly alternate (with probability 0.5) between strategy A and strategy B. As we named taxpayer players always choosing strategy A and tax evaders those ones always choosing strategy B, we label "mixed players" all citizens choosing such a third strategy, as explained in Figure 3.5. As described before, regarding the basic setting, chosen strategies now determine univocally three groups in the population.

In order to select the transition rules from a group to another, each player has been given a new variable, i.e., the "believeness" $B_{i,t} \in [0, 1]$, which measures the level of commitment in choosing and maintaining a given strategy. Values assumed by this variable change in time and affect possible transitions. Values of $B_{i,t}$ close to 1 mean that the player is a sort of zealot and that most probably she will not

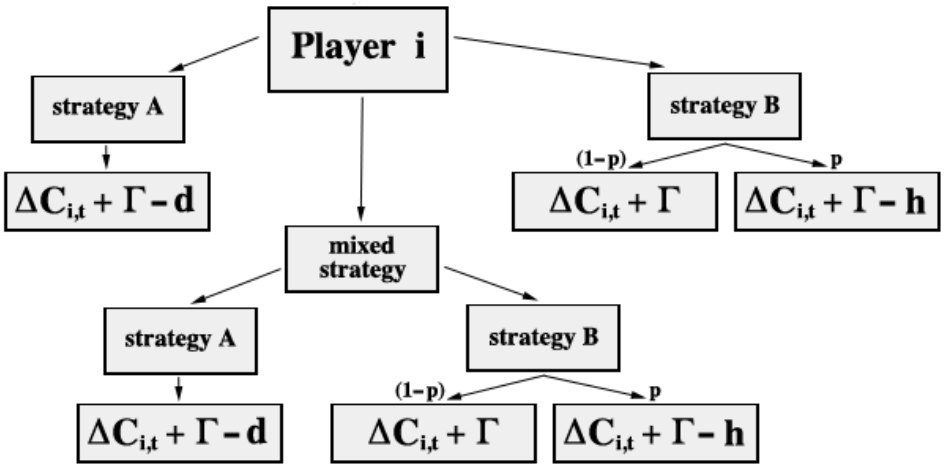

Figure 3.5: New rules for a community of N players: taxpayers play only strategy A, tax evaders play only strategy B, and mixed players randomly alternate between strategy A and strategy B.

change behavior; on the contrary, values of $B_{i,t}$ close to 0 mean that the agent is easily influenced and that her behavioral change is highly probable. For both taxpayers and tax evaders, the transition leads to become a mixed player (and the value of $B_{i,t}$ is re-set at random again). For mixed players, instead, the believeness operates as a sort of reservoir, whose level affects the successive transformation: values lower than 0.5 reveal a propensity to become an evader, if $B_i = 0.5$, the agent is and remains undecided, and values greater than 0.5 show the tendency to become taxpayers. The value of $B_{i,t}$ is based on both the imitation of neighbors and on the individual evaluation of the public good.

3.2.1 Imitation and social ties

In order to account the first point, we need to introduce a topological structure for our community. We assume a realistic social structure configured as a small-world (Watts and Strogatz 1998), where each player is a node connected with short-range ties (to mimic strong social relationships) to four neighbors, and with a small rewiring probability ($r = 0.02$) of substituting one of those ties with a long-range one (representing a weak social relationship).
In the left panel of Figure 3.6 a small-world $2D$-lattice is depicted, with taxpayers, tax evaders, and mixed players (respectively, green, blue, and yellow nodes). For taxpayers and evaders, if at a given time step the number of nearest neighbors belonging to their same group is smaller (greater) than the sum of the players of other groups, included the mixed one, the believeness value B_i decreases (increases)

of a quantity $IF \times \delta B$, where IF is the "Imitation Factor" and $\delta B = 0.01$. When $B_i \leq 0$, player i becomes a mixed player and a new value of $B_i \in [0, 1]$ is randomly assigned to her. For mixed players, if the number of nearest neighbors belonging to their same group is smaller than the sum of players of other two groups, B_i decreases of the quantity $IF \times \delta B$ if the evaders are more than taxpayers, otherwise it increases of the same quantity. Instead, if the number of mixed players is greater than (or equal to) the sum of the players belonging to the other two groups, B_i moves towards 0.5 of a quantity $IF \times \delta B$ and the agent maintains her mixed behavior. When, for a given mixed player i, $B_i \leq 0$ (respectively $B_i \geq 1$), that player becomes a tax evader (respectively, a taxpayer).

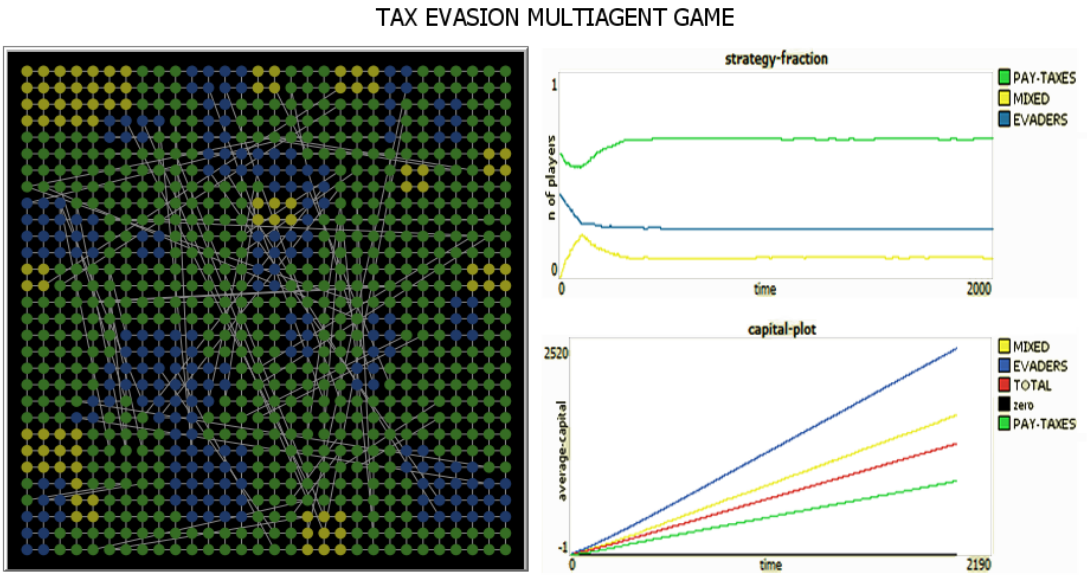

Figure 3.6: Left panel: The small-world configuration of the community, with taxpayers, tax evaders and mixed players (respectively green, blue and yellow nodes). Right panel: Dynamics of groups (top) and respective average social capital (bottom). Initial percentage of taxpayers is 60% (above the critical value for both IF and CF equal to 1).

3.2.2 Satisfaction and behavioral reactions

The second mechanism influencing behavioral transitions concerns the economic situation of the players. If the social capital of a given player is negative, the agent will be disappointed because of her experience and so more prone to change her strategy. Thus, for both evaders and taxpayers, when their capital is negative the

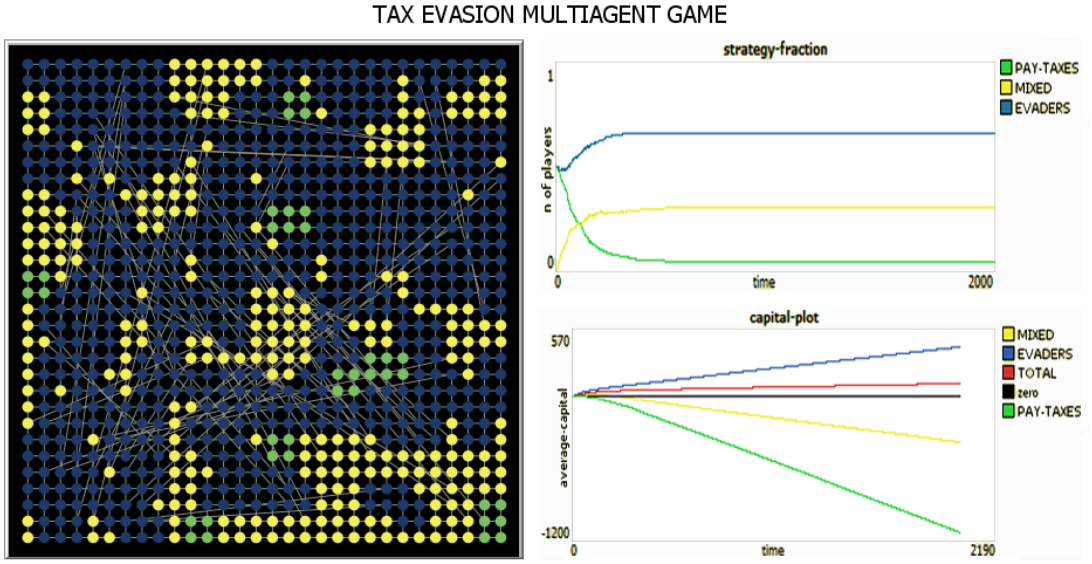

Figure 3.7: The same setting of Figure 3.6, with the same plots, but in the case of an initial percentage of taxpayers equal to 50% (below the critical value for both IF and CF equal to 1).

believeness value decreases of a quantity $CF \times \delta B$, where CF is the "Capital Factor". Instead, for mixed players, B_i varies by the quantity $CF \times \delta B$, depending on their actual state: if $B_i \geq 0.5$ it will increase, if $B_i < 0.5$ it will decrease. Setting the initial percentage of mixed players to zero, if taxpayers are more numerous than tax evaders, our simulations show that there exist a critical value for the initial percentage of taxpayers (depending on both IF and CF), below which the global situation gets always worse. Similarly, above that threshold, it gets always better. In Figure 3.6 and in Figure 3.7, results of two typical single-run simulations are reported, with $IF = CF = 1$ and two different initial percentages of taxpayers - respectively, above (60%) and below (50%) the critical value (that, for these values of IF and CF turns out to be around 55%). In the first one, the final economic condition appears to be good for all citizens and a majority of taxpayers emerges; instead, in the second case, the final economic situation is good only for tax evaders, who become the majority.
Threshold values for the initial percentage of taxpayers as a function of CF are showed in Figure 3.8 for different values of IF. As we can see, for a given value of IF, generally the critical value of the initial percentage of pay taxes rapidly increases with CF, then it tends to oscillate around a stationary asymptotic value, which decreases with IF. For $IF = 0$, i.e. without imitation, a change in strategy is due to CF only. Thus, when CF is low, i.e., when the dissatisfaction for a neg-

ative economic situation is not significant, a small initial percentage of taxpayers is enough to induce a final positive trend for the whole community; on the contrary, when CF is high, i.e., when a negative capital heavily acts on the personal disappointment, the initial percentage of taxpayers has to be more consistent in order to counterbalance the proliferation of tax evaders. Such an effect is reduced by the effect of the imitation, which on average helps: however, the initial fraction of taxpayers has to be always greater than 50%, for the altruism to spread around the community.

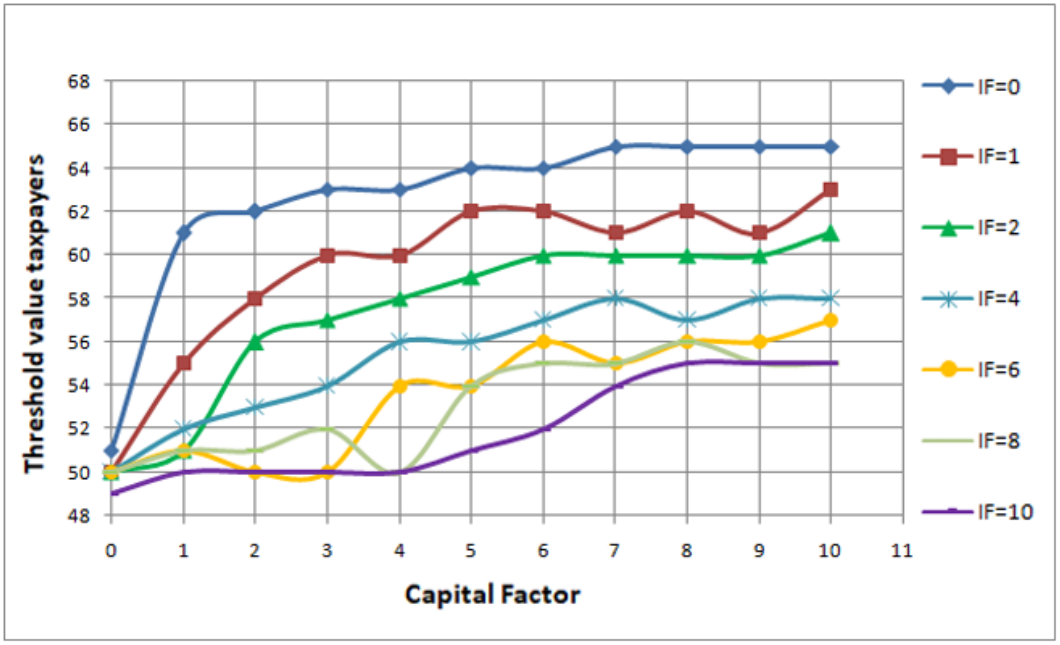

Figure 3.8: Threshold values for the initial percentage of taxpayers as a function of the capital factor CF and for different values of the imitation factor IF.

3.3 Tax rate, fines and audit probability

In this last section we present results of simulations with different values of the three main free parameters of our model, namely, the tax rate, the fine and the probability of an audit, set hitherto to: $d = 2$, $h = 3$, and $p = 0.4$. Changes in ΔC will be neglected because they would only produce a symmetric rescaling on the final capital of all groups. Values for IF and CF have been set equal to 1, and two different initial percentages of taxpayers have been used, above and below the 55% threshold (which has already been shown in Figure 3.8).
Considering a population with 60% taxpayers, 40% tax evaders, and 0% mixed

players. Figure 3.9 presents results of simulations with different tax rates after 2000 time-iterations: the final percentage of individuals (panel a) and the final average capital (panel b) are confronted with increasing values of the tax rate d. It clearly appears that for $d < 3$ units (i.e. when the tax is lower than the fine h) the final composition of the population is dominated by taxpayers, whose percentage grows above 70%. This implies a good situation for all citizens. For higher values of the tax (i.e. for $d \geq h$), the evolution of the system leads to a majority of tax evaders and this situation fits good only to evaders. This conclusion is strongly consistent with the initial setting of the model (without the mixed strategy) in which tax evasion Nash-dominates the other strategy if the probability to incur in a fine is lower than the ratio between the tax rate and the fine amount.
Figure 3.9 presents, instead, results of simulations performed increasing values of the fine h (panels c and d) and of the audit probability p (panels e and f), respectively. Looking at the average capital in panels (d) and (f), we can see that for values of the fine $h > 6$ and for the audit probability $p > 0.8$, tax evaders are worse off than taxpayers and mixed players. This does not reduce of tax evasion: while the number of mixed players increases at expenses of taxpayers, panels (c) and (e) show that the final percentage of evaders is not lower for $h > 6$ and $p > 0.8$. The reason is that in the present release of the model the behavioral update rules are constant and not adaptive with respect to the ex-post probability that a tax evader is discovered. Therefore, when required conditions occur (according to the dynamics induced by imitation and/or capital factors) group shifting happens, irrespective of the fact that simulations are running for higher values of fine and audit probability. This means that both the amount of the fine and the audit probability have an indirect effect. A higher probability and/or a more expensive fine cause more frequent fine payments and an overall stronger reduction of the capital of tax evaders. This can induce them, by means of the capital factor, to change group. It is worth to notice that, in the current setting, the number of taxpayer is sufficient to maintain the convenience to be tax evader even for high values of the audit probability and neutralize the consequent negative indirect effect on the capital. A small change in the percentage of tax payers can affect this conclusion.

Considering a population with 50% taxpayers, 50% tax evaders, and 0% mixed players. Figure 3.10 shows results of simulation with different tax rates (panels a and b), fines (panels c and d) and audit probability (panels e and f). As expected, the final capital of the taxpayers is always lower than before. Looking at the final capital of tax evaders (right panels) a conclusion similar to the previous case emerges: small values for the tax and high values for both the fine and the audit probability do induce a worse economic situation for tax evaders. Further, the final composition of the community (left panels) is always dominated by tax evaders,

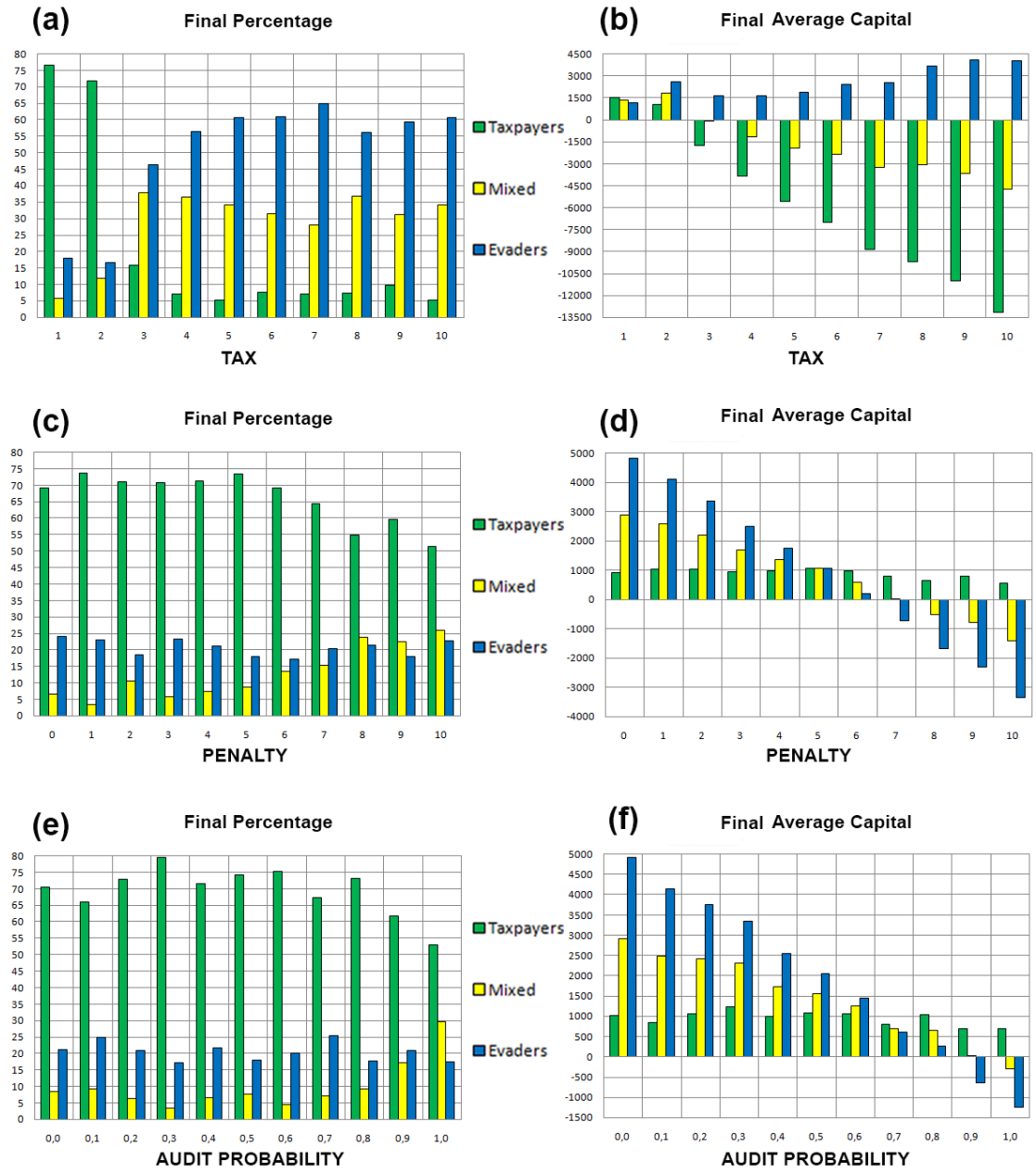

Figure 3.9: Final percentage and final average capital after 2000 turns of the three groups for increasing values of, respectively, tax (a-b), fine (c-d) and audit probability (e-f). The initial percentage of taxpayers is always equal to 60%.

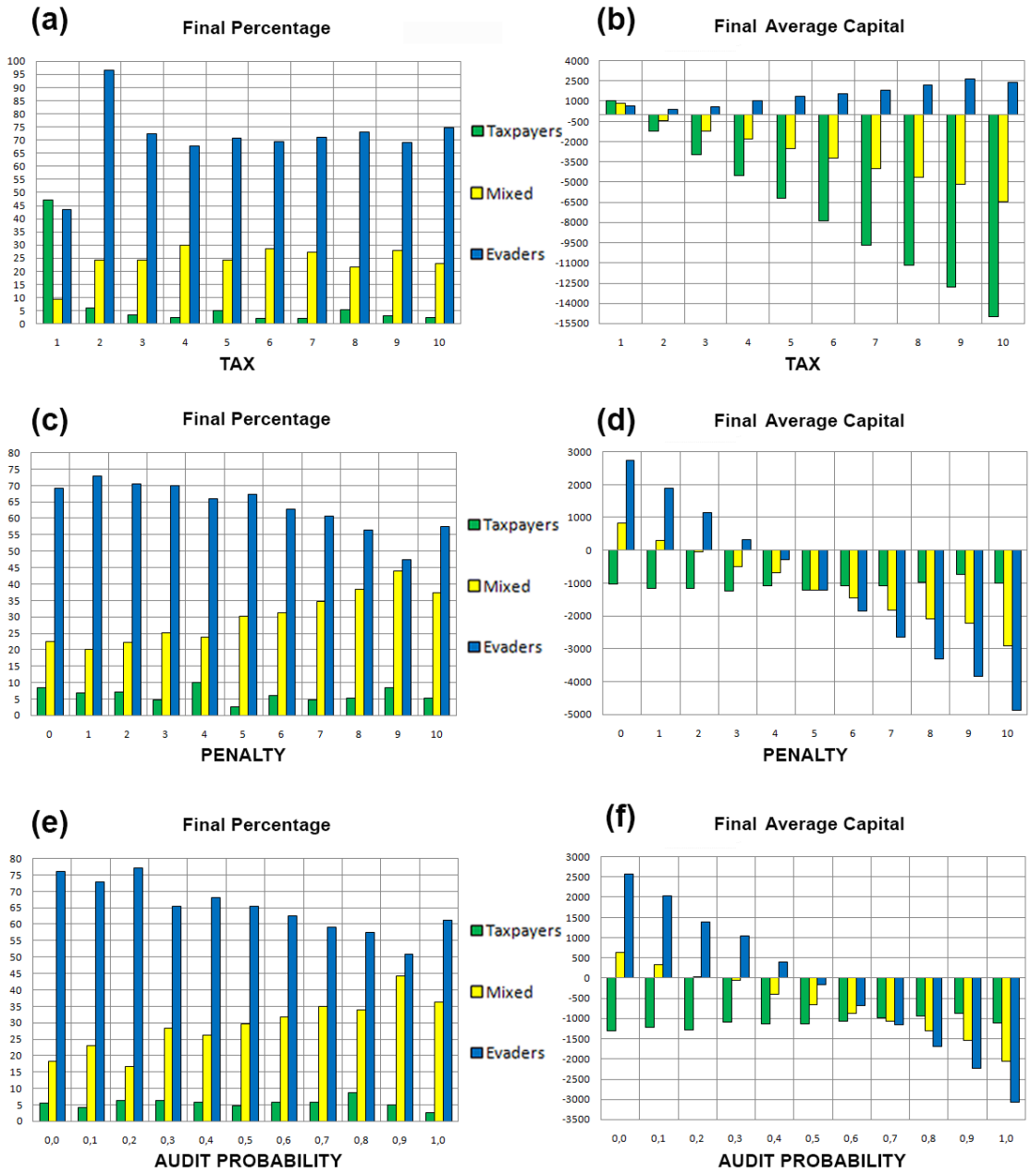

Figure 3.10: Final percentage and final average capital after 2000 turns of the three groups for increasing values of, respectively, tax (a-b), fine (c-d) and audit probability (e-f). The initial percentage of taxpayers is always equal to 50%.

with the exception of the case with $d = 1$. It is worth to notice that, differently from the previous case, an increase of either the fine or the audit probability, has now the beneficial effect of reducing the number of evaders, who tend to change strategy becoming mixed players. However, for maximum values $h = 10$ and $p = 1.0$, this trend is inverted and the percentage of evaders slightly increases.

3.4 Conclusive insights

In this study is presented a simple model of tax evasion, which augments a prisoner's dilemma framework with an agent-based design, in order to characterize some elements of collective dynamics when altruism and egoism come to play with regards to the number of taxpayer of a community.
In the first part of the study, the impact of a varying fraction of altruistic players on the final capital of a fully connected community has been shown. Results of simulations showed that, with its basic settings, the model replicated consolidated results of basilar game theory, as presented by Elster (1989). A further specification of the model, in which the public good has been designed as a primary good, identified a threshold level for the fraction of taxpayers in the community. Below such a threshold, not only do tax evaders create a damage for the collectivity (as usual), but they harm themselves as well.
In the second part of the study, the model was enriched by the introduction of some extensions: a small-world network topology for the social community (driving the imitation), and a third group of "mixed" players (playing alternatively, at random, the two possible strategies). New interesting results have been obtained, showing the presence of a threshold, in the initial percentage of taxpayers, able to ensure an average economic advantage to altruists. Such a threshold is influenced by the individual propensity of agents to imitate and by their sensitivity with respect to their personal economic situation.
Finally, a brief parametric analysis has shown how the tax rate, the fine, and the audit probability are able to influence both the final composition of the community and the final average capital of the three social groups (taxpayers, evaders and mixed players). As in real systems, the percentage of citizens paying taxes is crucial in sustaining a sufficient quality/quantity of the public good. Results of simulations show that values above such a threshold can paradoxically allow tax evaders to resist even to very high values of the audit probability.
Following such results, reasonable policy intuitions are devoted to induce a feeling of satisfaction in taxpayers, in order to reduce the temptation to evade, even when the personal economic situation is bad. Thus, if Government takes care of taxpayers more than tax evaders is better: e.g., an educational policy spreading a tax morale is expected to be more effective than a tax amnesty, because it operates in

such a way that individuals feel themselves rewarded by institutions. Education can also impact on the number of taxpayers, which has been described as a key factor in determining the average social capital. There is also evidence that the amount of the fine should be far greater than the tax pressure, in order to induce tax payment as a strong economic convenience while an increase in the probability of an audit drastically reduces the value of tax evasion.
Further research will be devoted to deepen both the analytical and the computational elements of the model, after a more detailed design of individual decision process is added. The incentive to pay taxes will be shown to descend more directly from interactions among citizens, when reputation and transparency of personal conduct are added to the model.

Chapter 4

Second case study: Ecological networks of soil invertebrates

Safeguarding natural ecosystems is one of the most relevant current issues. A new report from the Intergovernmental Science-Policy Platform on Biodiversity and Ecosystem Services (IPBES), released on May 2019, finds that due to human impact on the environment in the past half-century, the Earth's biodiversity has suffered a catastrophic decline: around 1 million animal and plant species are now threatened with extinction, many within decades, more than ever before in human history (IPBES, 2019). IPBES Chair, Sir Robert Watson said: "*The overwhelming evidence of the IPBES Global Assessment, from a wide range of different fields of knowledge, presents an ominous picture. The health of ecosystems on which we and all other species depend is deteriorating more rapidly than ever. We are eroding the very foundations of our economies, livelihoods, food security, health and quality of life worldwide.*"

Natural ecosystems are increasingly subjected to severe stress due to human action: climate change, deforestation and resource depletion as evidenced by numerous research, including Exbrayat et al. (2017), Lawrence and Vandecar (2015), Malhi et al. (2008). As a cause of this we observe on the one hand a decline in biodiversity with many species at risk of extinction (Strona and Bradshaw (2018), Barnosky et al. (2012), Barnosky et al. (2011), Ceballos et al. (2015), Jackson et al. (2001)) and on the other hand the phenomenon of alien species invasion (Simberloff et al. (2013), Anton et al. (2019)).

In the context of the exploitation of land for agricultural purposes, chemical cocktails (including fungicides or herbicides) can affect entire functional guilds, hence specific functional groups of species will be at risk. Given the rapidly increasing trend in the use of chemical agents, especially emerging contaminants (Bernhardt et al., 2017), such a functional loss due to human impact would strongly erode the health of entire ecosystems and urgently deserves our attention to safeguard our

Planet.
In the first study showed in this chapter, to investigate the structural changes of a food-web architecture, real data coming from a soil food web in an abandoned pasture with former low-pressure agriculture management are considered. The corresponding ecological network is reproduced within a multi-agent fully programmable modeling environment in order to simulate dynamically the cascading effects due to the removal of entire functional guilds. Results give an idea of the vulnerability of soil ecosystems if subjected to the use of herbicides or pesticides typical of intensive agriculture. In the second part of the chapter, the same study is carried out on two other Dutch ecosystems, that differ from the first for the type of management, in order to compare the results with those obtained for the first network. Then there is a study on the topology and robustness of the three networks, which aims to ascertain whether and how they vary due to the different anthropic disturbance to which the sites are subject.

4.1 Description of food web sites in Netherlands

The data used in this study derived from sampling and monitoring activities performed in the framework of the Dutch Soil Quality Network. Thanks to this survey, we have available data on the taxonomy, abundance, body size, and general feeding habits of soil invertebrates at 135 sites in the Netherlands. Environmental variables were collected at each site, including soil chemistry, atmospheric variables and human management practices of those sites. A total of 258 genera, families, and morpha of free-living soil nematodes, mites, insects, myriapods, enchytraeids, and earthworms, ranging in dry body mass more than 7 orders of magnitude, were identified, counted and measured for biomass estimates (Cohen and Mulder 2014). Data were collected in Pleistocene sandy soils at 135 sites in the Netherlands under seven different regimes of management (Figure 4.1). Pine plantations were kept following traditional low intensity agro-forestry. Other sites were cultivated actively. Organic farms, grasslands, and conventional farms were subjected to middle intensity management. Intensive and super-intensive farms were subjected to high-intensity management. Organic farms were certified by the Agricultural Economics Research Institute of the Netherlands (LEI) (Cohen and Mulder 2014). The numbers and main characteristics of sites in each category were on average:

- 9 Mature grasslands with a suboptimal input of N, mostly fallowed pastures;
- 20 Organic farms, using compost/farmyard manure and no biocides, averaging 1.7 livestock units per hectare;
- 19 Conventional farms, using mineral fertilizers, a much smaller amount of farmyard manure, averaging 2.4 livestock units per hectare;

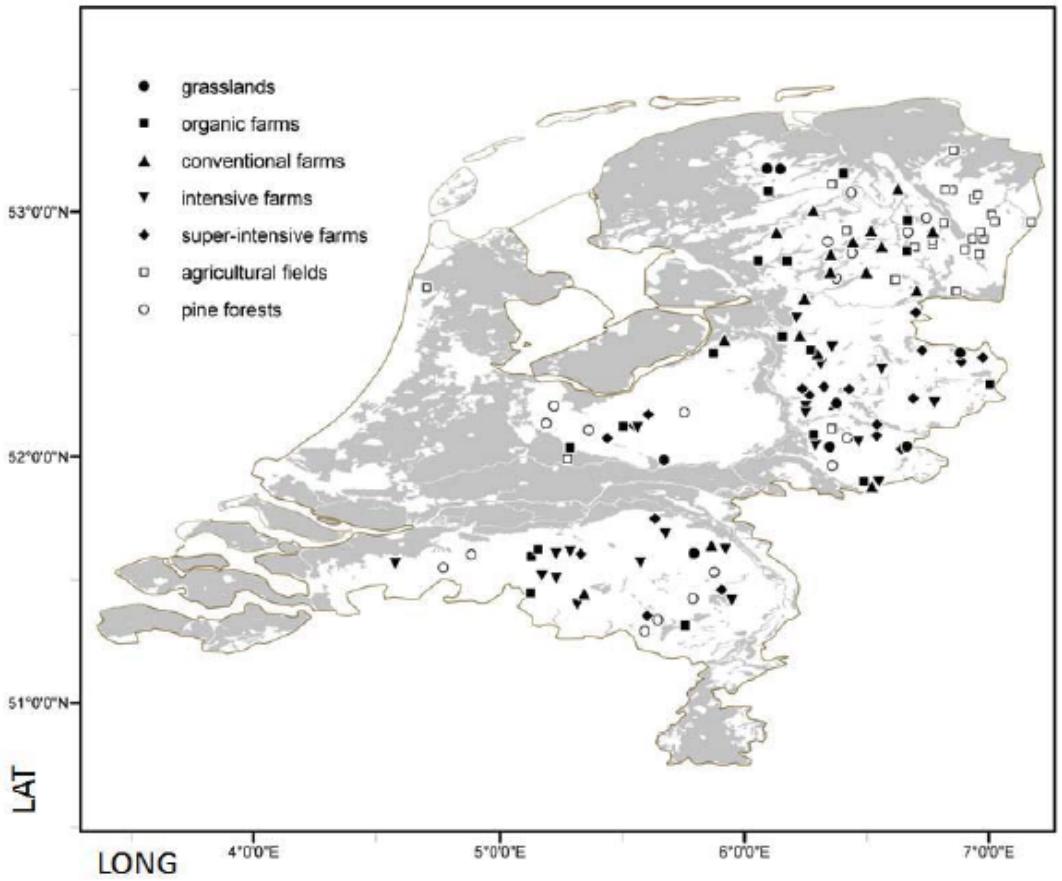

Figure 4.1: Locations of the 135 investigated sites in sandy soils of the Netherlands. Some locations were too close to each other to be plotted separately. Peaty or loamy soils are shaded in gray (Cohen and Mulder 2014).

- 21 Intensive farms, using fertilizers, averaging 3.2 livestock units, and aiming for high yield while minimizing pesticides per hectare;

- 19 Super-intensive farms, using registered biocides and fertilizers to obtain maximum yield, averaging 5.1 livestock units per hectare;

- 28 Agricultural fields, mostly a 4-year crop rotation, pesticides only for seed dressing, minimum input of mineral fertilizers; and

- 19 Scots Pine forests, often mixed with deciduous oaks or naturalized spruces.

4.2 A first exploration on a single community

Interacting species are embedded within complex food webs and according to their traits determine the architecture of the entire system (Brose et al., 2019; Potapov et al., 2019). Despite the huge amount of literature on a catastrophic species decline (IPBES, 2019), experimental evidence from the soil biota on weakened functional groups (less individuals, less species, or even missing guilds) is still lacking. The functional loss due to human impact would strongly erode the health of entire agroecosystems and urgently deserves more attention. For instance, an inverse correlation between aboveground farming intensity and the belowground functional diversity is known (Mulder et al., 2003, 2005) and makes some assumptions on constant biomass restrictive. For instance, Hunt et al. (1987) assumed that biomass inputs exactly balance biomass outputs at all times in each soil compartment of the detrital food web. But this steady-state assumption not always holds, as the biomass decreases of microorganisms, microfauna and mesofauna indicate negative effect on the soil buffer capacity (Hunt and Wall, 2002; Wall et al., 2015), for instance due to an increased pressure, or even soil exploitation, caused by intensive management practice (Mulder et al., 2008, 2011).
There is a consensus regarding the evidence that any loss of keystone species severely disrupts ecosystem functioning (IPBES, 2019), but the functional impacts of such decimations on the food-web architecture are almost unknown. Functional guilds are keystone units and can be defined as trait-driven groups of species with key roles in community architecture and therefore ecosystem functioning (Power et al., 1996; Mouquet et al., 2013). Recently, Brose et al. (2019) pointed out the importance of prey-predator relationships demonstrating that metabolic rate and functional traits of predatory species are more important in determining the interactions between the weight of the prey and that of the predator. Despite their recent meta-analysis, it seems often difficult to extrapolate to a much wider context, like behavioral ecology, ecosystem services or ecosystem functioning. Hence, such an extrapolation has to rely entirely upon undiluted mathematical evidences (Cohen, 2004; Bourne et al., 2005).
Many valuable models demonstrate the power of such an integration between computation and field ecology. For instance, it is well-known that the density of predatory species regulate the growth of prey species and vice versa. Lotka-Volterra model is possibly one of the most used classical extrapolation that relies upon maths. As the classical Lotka-Volterra model involves two species, here an extension of it is used. Big data at all biological scales became a central feature of research and discovery in the life sciences (Bourne et al., 2005).
This study was carried out in collaboration with Prof. Alessandro Pluchino and biologists Prof. Christian Mulder and Prof. Erminia Conti and has been published by the journal Ecology and Evolution (Conti et al., 2020). Our aim is to propose

a simple method to quantify how disproportionate the impact of less taxonomic and functional diversity can be, and to illustrate its application with one real soil food web. In particular, we rebuilt the considered ecological network (Mulder and Elser, 2009) within a fully programmable multi-agent environment (Wilensky, 1999) in an attempt to figure out the cascading effects by weakening the functional diversity of soil invertebrates through a simulated removal of entire guilds.

4.2.1 Data Sampling

We used a reference data set of empirically observed soil invertebrates in the sandy soils of one Dutch pasture with former low-pressure management (Mulder and Elser, 2009). Three replicate samples of about 5 m^2 from the upper 10 cm of soil for the fauna were taken. Bulk samples of 50 soil cores (diameter 2.3 cm) were used to extract the microfauna and two soil cores (diameter 5.8 cm) were used to extract the mesofauna. Extraction of free-living nematodes was performed within one week of core sampling using Oostenbrink funnels, and all the elutriated nematodes were collected; ecto-and endoparasitic nematodes were recovered with centrifugal flotation. All nematode individuals were counted, and ~ 150 randomly chosen specimens were identified and measured under a light microscope (Mulder and Vonk, 2011). Enchytraeid worms (Oligochaeta: Enchytraeidae) were sampled by wet extraction and microarthropods (Acarina and Collembola) by dry extraction (Cohen and Mulder, 2014). In both sampling protocols, the heat was increased gradually with incandescent bulbs, and the invertebrates escaped by moving downward. For enchytraeids and microarthropods, the abundances for $1\,m^2 \times 10\,cm$ depth were derived from the surface and the bulk density of the soil samples (Mulder et al., 2011).

All these organisms live in a dark and intricate world, interacting in a detrital food web and in close contact with the soil. Each organism has its own trait-driven function in soil biota, giving the soil its exclusive properties, and an interaction matrix was created based on an inventory of multitrophic interactions of soil food webs that provide all links consistent with literature-derived guilds (Mulder and Elser, 2009). Despite the observation that energetic equivalence rule is rarely supported within local communities (Morlon et al., 2009), our reference soil food web was particularly stable according to both the Eltonian rule (Elton, 1927), being the lumped dry weight of all the sampled invertebrates of the first trophic level exactly 10.28 times the lumped dry weight of all the sampled invertebrates of the second trophic level, as to the energetic equivalence rule (Mulder and Elser, 2009).

Figure 4.2: View of the study area of Soest, the Netherlands, during the field sampling in 2012. Photo credit: Christian Mulder.

4.2.2 Analysis of the food web: a modified Lotka-Volterra model

In contrast to previous studies on simulated species extinction (e.g., Ives and Cardinale, 2004), in this study we want to disentangle the cascading effects of the removal of selected functional groups (here, entire guilds of soil invertebrates). Using the data obtained from the sampling discussed in the previous paragraph, a food web consisting of $n = 62$ species of soil organisms was built (see Figure 4.4) within NetLogo, a multi-agent fully programmable modeling environment particularly suitable for the simulation of complex systems (Wilensky, 1999). For these species we know the abundance X_i, the body mass M_i, the biomass B_i (given by $B_i = X_i M_i$) and the value of the growth rate r_i in condition of mutual interaction, with $i = 0, 1, ..., n$. All identified soil invertebrates in Figure 4.4 fell into five guilds and the independent trophic links among guilds (from any resource to its consumer) were inferred from published literature. The complete inventory of multitrophic interactions consistent with literature-derived guilds is fully downloadable from Mulder and Elser (2009).
Mathematically, the species detected in the sample can be seen as nodes belonging to a trophic web. The links between the nodes represent the known food interactions existing between the species (the direction of the link follows the flow of energy that, through predation, passes from the prey to the predator). In Figure 4.3 is showed our ecological network, with the 62 numbered nodes/species placed in a circular layout, where each group of species is distinguished by a different color (as also explained in detail in Figure 4.4). The size of each node is proportional to the base-10 logarithm of the abundance of the corresponding species ($LogX$).

As multitrophic interactions between basal consumers and allochthonous resources are donor-controlled, i.e. according to Polis et al. (1997) "*consumers benefit from but do not affect resource renewal rate*", we postulated constant allochthonous resources. Our lemma is therefore that the faunal populations have an unlimited resource supply of bacteria, fungi and roots. This is because we are focusing here only on the inter-specific prey-predator interactions among soil invertebrates and not on all the resource-consumer interactions occurring in soil biota. Hence, we kept in our simulations microbial and plant biomasses constantly available for grazing by basal (specialized) species and non-basal (omnivore) species (cf. Hunt et al., 1987; Polis et al., 1997).
In order to model the dynamical behavior of the species in the food web, we adopt a set of modified Lotka-Volterra equations. Our starting point is the logistic equation (1.7), which takes into account the intra-specific regulation due to the presence of limited resources, applied here to the abundance X_i of each one of our $n = 62$ species as in Kondoh (2005):

$$\frac{dX_i}{dt} = r_i X_i \left(1 - \frac{X_i}{K_i}\right) \ (i = 1, 2, ..., n) \tag{4.1}$$

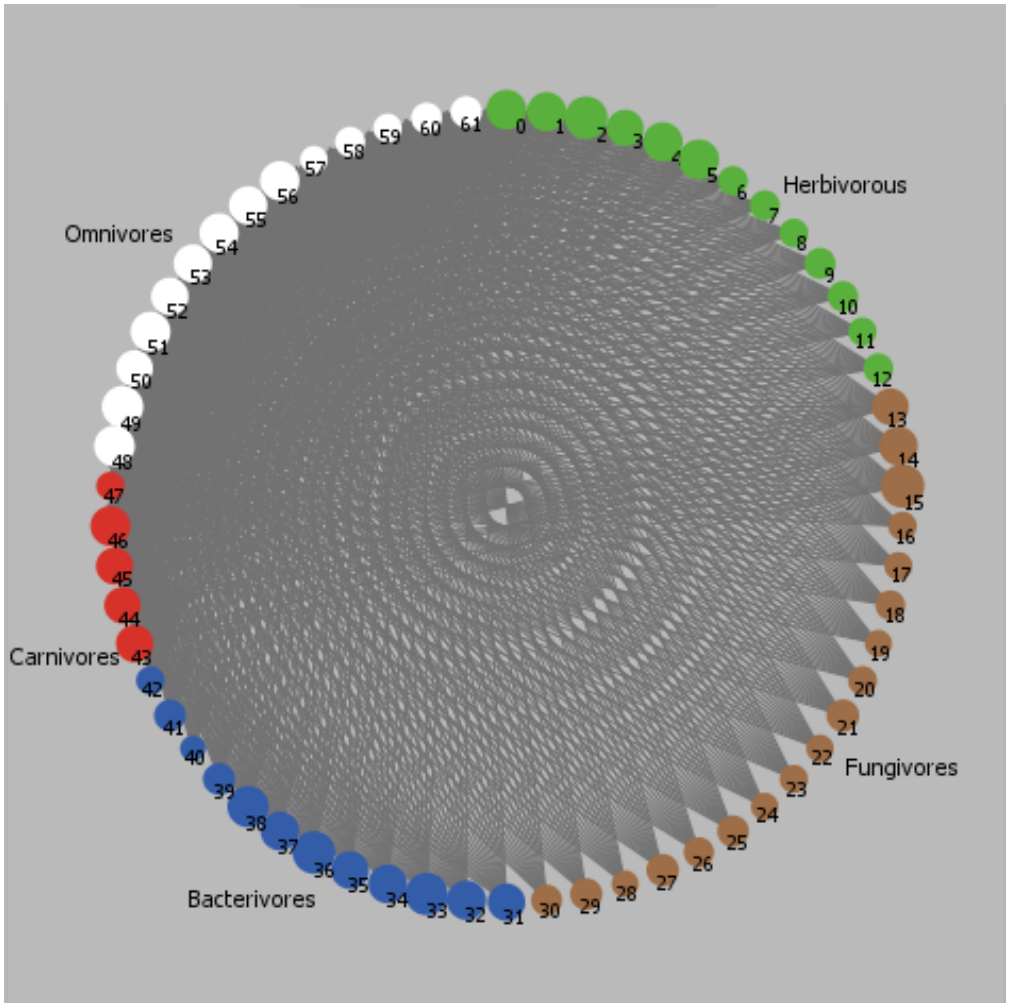

Figure 4.3: A sketch of the food web network with 62 nodes/species organized in groups of different colors (see Figure 4.4) and placed in a circular layout. Directed links, between the organisms belonging to trophic level 1 (primary consumers, being they herbivorous, fungivorous or bacterivorous invertebrates) and the organisms belonging to trophic level 2 (secondary consumers, either carnivorous or omnivorous invertebrates), represent the prey/predator connections, going from the prey node to the predator node.

NODE_ID	TROPHIC_ID	FUNCTIONAL_ID	SPECIES NAME
0	Herbivorous	Plant-feeding nematodes	Aglenchus
1	Herbivorous	Plant-feeding nematodes	Dolichodoridae
2	Herbivorous	Plant-feeding nematodes	Helicotylenchus
3	Herbivorous	Plant-feeding nematodes	Malenchus
4	Herbivorous	Plant-feeding nematodes	Pratylenchus
5	Herbivorous	Plant-feeding nematodes	Tylenchorhynchus
6	Herbivorous	Plant-feeding mites	Achipteria
7	Herbivorous	Plant-feeding mites	Galumna
8	Herbivorous	Plant-feeding mites	Platynothrus
9	Herbivorous	Plant-feeding collembolans	Sminthuridae
10	Herbivorous	Plant-feeding collembolans	Sphaeridia
11	Herbivorous	Plant-feeding collembolans	Sminthurinus
12	Herbivorous	Plant-feeding collembolans	Sminthurus
13	Fungivorous	Hyphal-feeding nematodes	Achromadora
14	Fungivorous	Hyphal-feeding nematodes	Aphelenchoides
15	Fungivorous	Hyphal-feeding nematodes	Tylenchidae
16	Fungivorous	Fungivore mites	Microppia
17	Fungivorous	Fungivore mites	Minunthozetes
18	Fungivorous	Fungivore mites	Medioppia
19	Fungivorous	Fungivore mites	Tectocepheus
20	Fungivorous	Fungivore collembolans	Friesea
21	Fungivorous	Fungivore collembolans	Parisotoma
22	Fungivorous	Fungivore collembolans	Proisotoma
23	Fungivorous	Fungivore collembolans	Folsomia
24	Fungivorous	Fungivore collembolans	Onychiurus
25	Fungivorous	Fungivore collembolans	Lepidocyrtus
26	Fungivorous	Fungivore collembolans	Isotomurus
27	Fungivorous	Fungivore collembolans	Isotoma
28	Fungivorous	Fungivore enchytraeids	Achaeta
29	Fungivorous	Fungivore enchytraeids	Cognettia
30	Fungivorous	Fungivore enchytraeids	Fridericia
31	Bacterivorous	Bacterivore nematodes	Alaimus
32	Bacterivorous	Bacterivore nematodes	Anaplectus
33	Bacterivorous	Bacterivore nematodes	Eucephalobus
34	Bacterivorous	Bacterivore nematodes	Metateratocephalus
35	Bacterivorous	Bacterivore nematodes	Panagrolaimus
36	Bacterivorous	Bacterivore nematodes	Plectus
37	Bacterivorous	Bacterivore nematodes	Prismatolaimus
38	Bacterivorous	Bacterivore nematodes	Teratocephalus
39	Bacterivorous	Bacterivore enchytraeids	Enchytraeus
40	Bacterivorous	Active substrate ingestion (Enchytraeids)	Buchholzia
41	Bacterivorous	Active substrate ingestion (Enchytraeids)	Marionina
42	Bacterivorous	Active substrate ingestion (Enchytraeids)	Henlea
43	Carnivorous	Nematodes predating nematodes	Anatonchus
44	Carnivorous	Nematodes predating nematodes	Clarkus
45	Carnivorous	Nematodes predating nematodes	Mylonchulus
46	Carnivorous	Nematodes predating nematodes	Tripyla
47	Carnivorous	Generalist predatory mites	Dendrolaelaps
48	Omnivorous	Omnivore nematodes	Aporcelaimellus
49	Omnivorous	Omnivore nematodes	Dorylaimoidea
50	Omnivorous	Omnivore nematodes	Epidorylaimus
51	Omnivorous	Omnivore nematodes	Eudorylaimus
52	Omnivorous	Omnivore nematodes	Mesodorylaimus
53	Omnivorous	Omnivore nematodes	Nordiidae
54	Omnivorous	Omnivore nematodes	Pungentus
55	Omnivorous	Omnivore nematodes	Qudsianematidae
56	Omnivorous	Omnivore nematodes	Thornematidae
57	Omnivorous	Omnivore mites	Scutacarus
58	Omnivorous	Omnivore mites	Mesostigmata
59	Omnivorous	Omnivore mites	Oribatida
60	Omnivorous	Omnivore mites	Eupodes
61	Omnivorous	Omnivore mites	Scheloribates

Figure 4.4: Trophic ID, functional ID and name of the taxa (mostly families or genera, here after called "species") corresponding to the nodes of the network shown in Figure 4.3.

where r_i and K_i are respectively the growth rate and the carriyng capacity of the i-th species. It is likely important to state that we did not assume that all species have the same carrying capacity as in other simulations (Gross and Cardinale, 2005), but species- specific K_i values. Within each guild, we derived the r_i values for the functional groups shown in Table 4.4 from Moore et al. (1993) and De Ruiter et al. (1995).
In order to adapt these equations to real data, it must be considered that, in addition to the intra-specific interaction, an inter-specific interaction also occur among species. For this reason the growth rate r_i must also consider the effect due to predation. According to the prescription of equation (1.11), we assume that, in presence of interaction, r_i is expressed as:

$$r_i = r_{i0} + \sum_j A_{ij} X_j \tag{4.2}$$

where A_{ij} are the elements of the community matrix $\mathbf{A}$ and r_{i0} is the growth rate of the i-th species in absence of interaction. By combining formulas (4.1) and (4.2) one finally gets:

$$\frac{dX_i}{dt} = \left[r_{i0} + \sum_j A_{ij} X_j \right] X_i \left(1 - \frac{X_i}{K_i} \right) \tag{4.3}$$

As we have already seen, in general the elements A_{ij} of the community matrix weigh the food interaction among pairs of species ($A_{ij} = 0$ when species i and j don't have any predation connection). In this study we decided to link these weights to the biomasses of the prey species. Such a biomass-driven perspective, in fact, focuses on groups of species and on the lumped biomass values of the populations that constitute that functional group (Moore and De Ruiter, 2012). Let us consider, for example, a generic node/species i with degree 2 which is, simultaneously, a predator for a given node/species m (therefore, an ingoing link will exist from node m towards node i) and a prey for another node/species l (in this case a directed outgoing link will exist from node i towards node l). In this case, we will define the coefficient A_{im} as the following ratio:

$$A_{im} = \frac{B_m}{\sum_k B_k} \tag{4.4}$$

where at the numerator there is the biomass B_m of the prey species m and at the denominator the summation of the biomasses of all the prey species of node i (included B_m): the coefficient is positive because the flux of energy goes from m to i, therefore, after an encounter, species i will have an increase in abundance. Similarly, the coefficient A_{il} will be defined as:

$$A_{il} = -\frac{B_i}{\sum_h B_h} \tag{4.5}$$

where at the numerator there is the biomass B_i of the prey species i and at the denominator the summation of the biomasses of all the prey species of node l (included B_i): in this case the coefficient is negative because the flux of energy goes from i to l, consequently, after an encounter, species i will have a decrease in abundance. The rationale behind these definitions (which, of course, can be applied to node/species with any degree) is that, when a predator has a diet based on a few prey species, he will consume a greater quantity of each of them depending on their single biomass in relation to the total biomass of its prey species. If, on the contrary, the same predator preys many species, it will consume a smaller quantity of each of them in relation to their biomass compared to the total.
In order to proceed with the calculation of the abundances through equation (4.3), we should know the term r_{i0} which can be inferred from real data by making the following assumption. At the time of sampling, the system was, according to Eltonian rules, in a state of stability in which the abundance of each species, in presence of interactions with all the other ones, had reached its carrying capacity, thus $X_i = K_i$. Therefore according to the formula (4.2), it is possible to obtain the value of the net growth rate without interaction r_{i0} starting from that one measured when there is interaction r_i, considering all the species in their stationary state K_i:

$$r_{i0} = r_i - \alpha \sum_j A_{ij} K_j \tag{4.6}$$

The parameter α is a coupling coefficient that can be considered as a measure of the interaction strength of a given species within the rest of the food web and it is chosen so that the carnivores and part of the omnivores (species 57, 58, 59, 60 and 61 of Table 4.4) have a negative r_{i0}. In fact, in the absence of interaction between species, and therefore without possibility of predation, carnivores must have a negative growth rate. The same can be said for omnivores whose diet is composed of animal rather than plant.
Considering our lemma (we kept bacteria, fungi and roots constantly available to soil invertebrates) and under the further plausible assumption that, in absence of interaction among species, the carriyng capacity of each species, say K_{i0}, would be greater than the same one in presence of interaction, i.e. K_i, we postulate that:

$$K_{i0} = K_i + \frac{K_i}{2} \tag{4.7}$$

Notice that, despite this prescription, in absence of interaction, species with $r_{i0} < 0$ will tend to extinction as expected.
Summarizing, we can effectively rewrite our dynamical equations (4.3) as:

$$\frac{dX_i}{dt} = \left[r_{i0} + \beta\alpha \sum_j A_{ij} X_j \right] X_i \left(1 - \frac{X_i}{K_i + (1-\beta)\frac{K_i}{2}} \right) \tag{4.8}$$

with $\beta = 0$ in the case in which there is no interaction and $\beta = 1$ in the case in which there is interaction, of strength α, between the species.
Equation (4.8), applied to each node of our ecological network, allows us to simulate the dynamical evolution of the system in several representative scenarios, where different kind of perturbations will be realized in order to study the reaction of the species. All the simulations were done by choosing the initial abundance of the species in the interval:

$$X_i(0) \in \left[K_i - \frac{K_i}{2}; K_i\right] \tag{4.9}$$

so that they cannot exceed their carriyng capacity. For each scenario, starting from the initial conditions (4.9), at each time step the populations $X_i(t)$ of all species are updated by numerically integrating equation (4.8) until the system has reached a condition of stability. Notice that a variation of $X_i(t)$ for a given species does imply a variation of its biomass $B_i(t) = M_i X_i(t)$. Then, depending on the chosen scenario, the forced removal of a certain number of species was carried out in the following way: after 100 time steps, which has been verified to be enough for the system to have reached a stationary state, i.e. for the populations of all the species to have reached their initial carrying capacity K_i, the abundances of the species we have chosen to remove are decreased exponentially over time. In turn, this can induce cascading effects on some of the other species, according to the following rules. When the abundances of carnivores or omnivores, for some reason, start to decrease in time, it is reasonable to assume that a corresponding increase in the carrying capacity K_i of their prey will occur. The latter can be obtained starting from the potential variation of the biomass of the i-th prey at time t, that is calculated as the product of its own current biomass $B_i(t)$ times the ratio between the total biomass of dead predators and the total biomass of all their prey, i.e.:

$$\Delta B_i(t) = B_i(t) \frac{tot\_biomass\_dead\_predators}{tot\_biomass\_prey} \tag{4.10}$$

This quantity can be translated into a consequent potential increase of the prey's abundance, allowed by the decrease of its predators,

$$\Delta X_i(t) = \frac{\Delta B_i(t)}{M_i} \tag{4.11}$$

and this increase can therefore be added to its carrying capacity, so that:

$$K_i(t+1) = K_i(t) + 10 \times \Delta X_i(t) \tag{4.12}$$

for herbivores, fungivores and bacterivores (trophic level 1), and

$$K_i(t+1) = K_i(t) + \Delta X_i(t) \tag{4.13}$$

for carnivores and omnivores (trophic level 2). The multiplicative factor 10 in equation (4.12) was inserted according to the Eltonian rule across adjacent trophic levels (Elton, 1927). The new value for $K_i(t+1)$ will be inserted in the equation (4.8) thus influencing the further dynamical evolution of the system. The same rule does not need to be applied if the decrease concerns the abundances of herbivores, fungivores and bacterivores since these grazing species are, according to the lemma, only prey, therefore they cannot induce variations in the carrying capacity of other species.
In order to quantify structural changes and to compare one single simulation to others, i.e.the results of the simulations carried out by removing either guilds or species, we introduce an *Alteration Index (AI)*, defined as:

$$AI = \sum_k \frac{|X_{sk} - X_{fk}|}{X_{sk}} = \sum_k \frac{|\Delta X_k|}{X_{sk}} \tag{4.14}$$

where X_{sk} and X_{fk} are, respectively, the abundance of species k-th calculated after 100 time steps, i.e. in the steady state, and the abundance of the same species calculated at the end of the simulation. In other words, AI considers the sum of the absolute variations in abundance that the species undergo due to the forced removal of some other species, normalized with respect to their abundance in the steady state. It is therefore a measure of the alteration of the ecosystem due to the introduced perturbation. Note that the summation includes only the guilds/species for which forced removal does not occur, since we are interested in quantifying only the effects of the perturbation (without including the perturbation itself). Our AI is of particular interest as the stability of depaupered food webs remaining after deleting functional groups has not been examined systematically by Hunt and Wall (2002). These authors state that such a new food-web stability maybe critically important to ecosystem function.

4.2.3 Computational results

In the simulation shown in Figure 4.6 we set $\beta = 0$ in order to test the behavior of the system in the (unrealistic) scenario in which there were no interactions among species. As expected, species with $r_{i0} < 0$, i.e. carnivores and omnivores 57, 58, 59, 60 and 61, become extinct. The other species, instead, rapidly reach their own carrying capacity. On the other hand, in the simulation shown in Figure 4.7, we set $\beta = 1$ i.e. we consider the standard scenario in which there is interaction between species, but the system is not disturbed. In this case, all species reach

their carrying capacity and the system goes rapidly in balance. This is the condition with which we have to compare all the next scenarios, in which we always set $\beta = 1$ but the system is perturbed by the removal of several species.
Let's now discuss in detail the results of the simulations performed in eleven different scenarios. In the first nine of these we remove separately the five guilds or four combinations of them, even an entire trophic level in the case of the removal of all omnivores and carnivores to forecast an evolution of such an artificially depleted food web. We are not aware of any study where a combination of functional guilds was removed, although independent cascading effects due to the loss of a single guild has been addressed by Hunt and Wall (2002). In the last two scenarios we want to verify the importance of the abundance of the species by removing the first two or the first three most abundant species.
Removal of either all the herbivorous species ($AI = 3.39 \times 10^{-7}$) or all the bacterivorous species ($AI = 1.08 \times 10^{-4}$). The soil system does not seem to be affected by one of these disturbances and all other species settle at their carrying capacity (Figure 4.8 and Figure 4.9) and the alterations of the food-web architecture, as computed by equation (4.14), are in both scenarios statistically undistinguishable from 0. Such comparable results for so different scenarios are rather surprising, as the lumped biomass of the bacterivores is 1.58 times larger than the lumped biomass of the herbivores ($10^{5.62}$ vs. $10^{5.42}$ log[$\mu g\ m^{-2}$ dry weight], respectively), although the removal of all the fungivorous species (with a much higher lumped biomass of $10^{6.19}$ log[$\mu g\ m^{-2}$ dry weight]) influences the numerical abundances of other species (see next scenario). A possible biological explanation is on one hand the specialization of grazing invertebrates, as herbivores and bacterivores have evident morphological adaptations to attack plant roots and ingest bacterial cells (Yeates et al., 1993), in contrast to larger consumers like fungivore oribatids which can handle many more different resources than smaller consumers like bacterivore nematodes. On the other hand, the relative energetic contribution in terms of flux is on average the highest for herbivorous microarthropods and bacterivorous enchytraeids (Mulder et al., 2008) and therefore we would have expected stronger cascading effects.
Removal of all the fungivorous species ($AI = 0.94$). In this case, being the fungivorous Tylenchidae (node 15) the most abundant species of the entire system, its removal causes a slight decline of the second most abundant species of the system, the herbivorous Helicotylenchus (node 2) which decreases from $10^{5.9}$ to $10^{5.82}$. A possible explanation of this unexpected correlation between a fungivorous nematode and herbivorous nematode could be due to an indirect cascading effect where the removal of the most abundant species forces a shift in the prey-predator relationships. Consequently, after about 400 time steps with respect to the diminishing herbivorous 2, a minimal decrease of the abundance of carnivorous

Anatonchus (node 43 of Table 4.4) from $10^{4.6}$ to $10^{4.56}$ is observed (Figure 4.10), as resources do not seem to be sufficient. This is surprising, as Anatonchusis is well known to be a stress-resistant nematode, capable to survive and dominate in hostile environments (Neher et al., 2005; Fiscus and Neher, 2002).

Removal of all the herbivorous and fungivorous species together (AI = 1.82). The abundance of the carnivorous nematode Anatonchus (node 43 of Table 4.4) decreases from $10^{4.6}$ to $10^{4.48}$ and, as a consequence, a slight increase is also observed in some species of bacterivorous nematodes and enchytraeid worms (Figure 4.11) and the AI is correspondingly low (AI = 1.82). Being Anatonchus the most abundant predatory nematode, the lack of herbivorous and fungivorous prey not only affects this predatory species but also enhances the occurrence of bacterivorous prey at a lower trophic level.

Removal of all the herbivorous and bacterivorous species together (AI = 11.53). The carnivorous mite Dendrolaelaps (node 47 of Table 4.4) and the truely omnivorous mites (nodes 57-61, those with $r_{i0} < 0$) become extinct. Carnivores 43-46 succeed in adapting their population size to the much fewer resources available. There is also a slight increase in fungivores and in the remaining omnivores (Figure 4.12). At the end, this simulation is resulting in a strong re-assemblage of the food web with an AI equal to 11.53 and the fluctuations in the numerical abundances of so many species were rather unexpected given the lack of response of the food web to the removal of herbivores alone (Figure 4.8) or bacterivores alone (Figure 4.9). In short, the sum of the effects due to the removal of both guilds was highly relevant even if the separate removal of these two guilds did not influence our web.

Removal of all the fungivorous and bacterivorous species (AI = 12.97). Carnivores 44, 45 and 46 become extinct but even the abundance of second most abundant species, the herbivorous Helicotylenchus (node 2) decreases. There is still a slight increase in herbivorous and omnivorous species (Figure 4.13), in fact AI reaches 12.97. Only the carnivores 43 and 47 seem to succeed in adapting their number to the fewer resources available. As aforementioned, Anatonchus (node 43) is well known as stress-resistant (Neher et al., 2005; Fiscus and Neher, 2002), and therefore its successful performance is expected. The same holds for the mite Dendrolaelaps (node 47), because as generalist its trophic niche will be much larger than that of other more specialized carnivores. As in the previous scenario, the effect due to the removal of two guilds at the same time was really relevant, although it should be mentioned that these effects are likely due to the removal of fungivores (Figure 4.10) more than the removal of bacterivores (Figure 4.9). In any case, the trophic effects due to the combined removal of microbivores in Figure 4.13 were opposite for the first trophic level (mostly increase of herbivorous species: primary consumers) and the second level (mostly decrease of carnivorous

species: secondary consumers).

Removal of either all the omnivorous species ($AI = 195.75$) or all the carnivorous species ($AI = 29.41$). Omnivores are known to have the capability to modify their feeding behavior based on the resource profitability, either by switching prey species (Holt and Polis, 1997) or by adjusting the relative proportion of each prey across different guilds (for instance, preying on the most abundant basal species, like in our case fungivorous 15, herbivorous 2 and bacterivorous 33). Therefore omnivores and food-web architecture are closely linked to each other and a high degree of omnivory mostly stabilizes the web structure (Holt and Polis, 1997, and Kratina et al., 2012, respectively). However, our Figure 4.14 clearly shows the reduced exploitation of the soil system by the omnivores once the entire functional guild has been removed. This destabilizing system is assessed by a remarkably high food-web architecture alteration (AI = 195.75), the highest alteration due to a sole deleted guild. In contrast, Figure 4.15) shows that the removal of only the carnivorous species causes only a disproportionally small impact on the food-web architecture (AI = 29.41).

Removal of all the invertebrates at trophic level 2 (omnivorous and carnivorous species) ($AI = 261.41$). Omnivores and carnivores ate the producers in proportion to their biomass, with omnivores sharing no evident random preference. As expected, species losses are very unlikely when predators were removed and an increase in the abundance of all other species at trophic level 1 is observed, showing the response of the system to the lack of top-down control (Figure 4.16). This scenario is the one with the highest alteration value despite it does not lead to the secondary extinction of any species because the entire upper trophic level was removed. In fact, the removal of omnivores and carnivores causes a significant increase of their preys according to the formula 4.12 and the total alteration due to the removal of omnivores and carnivores together is much more than the sum of the single alterations due to the removal of either the omnivores or the carnivores ($261.41 > 195.75 + 29.41 = 225.16$). With an additional alteration of 16 % of the food-web architecture, we can only conclude that omnivory strongly enhances the flux of nutrients between the soil invertebrates belonging to the first trophic level and those belonging to the second trophic level.

Power et al. (1996) distinguished keystone species from dominant species. Two and three dominant species were chosen according to their numerical abundances.

Removal of the two most abundant species in the ecosystem: fungivorous 15 and herbivorous 2 ($AI = 2.76$). The abundances of all carnivorous species decrease but surprisingly it is just the generalist Dendrolaelaps that becomes extinct. There is also a slight increase in other species (Figure 4.17).

Removal of the three most abundant species in the ecosystem: fungivorous 15, herbivorous 2 and bacterivorous 33 ($AI = 15.21$). The abundance

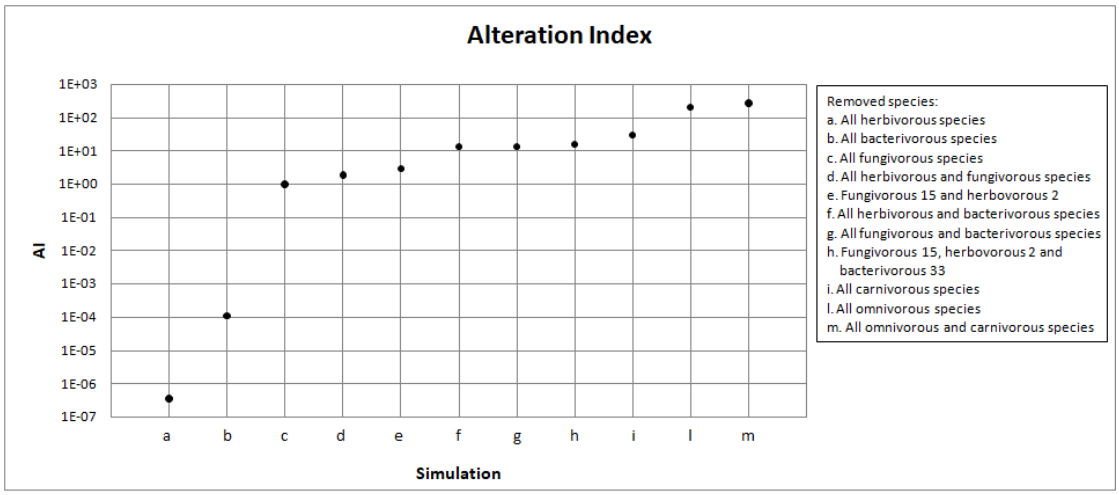

Figure 4.5: Alteration Index for the simulations performed, sorted in ascending order from left to right.

of all carnivorous species decrease. Again the generalist mite Dendrolaelaps and all omnivore mites but Scheloribates (node 61) become extinct. There is also a slight increase in other species (Figure 4.18). According to Power et al. (1996), these three species are dominant but given the disproportionately large impact on the other species by the removal of the bacterivorous nematode (node 33), the latter might even be a foundation species.
In Figure 4.5 are reported, in ascending order and in logarithmic scale, the AI-values calculated for each considered scenario. Comparing the results obtained in the simulations with the values of the alteration index, one realizes that the latter is very close to zero when spontaneous extinctions do not take place and there are no variations of abundance in the species not removed (scenarios a and b). On the other hand, the AI index takes relatively low values (between 1 and 10) when a slight variation in the abundance of some species is observed (scenarios c and d) or when there are also few spontaneous extinctions (scenario e), while takes values greater than 10 in the scenarios (f, g, h, i, l and m) in which many spontaneous extinctions occur. Finally, note that the last scenario (m) is the one with the highest AI value despite it does not lead to the secondary extinction of any species because the entire upper trophic level was removed (Figure 4.16). In fact, the removal of omnivores and carnivores causes a significant increase of their preys according to the formula (4.12). The results obtained for the Alteration Index show its high sensitivity to altered food-web architectures.

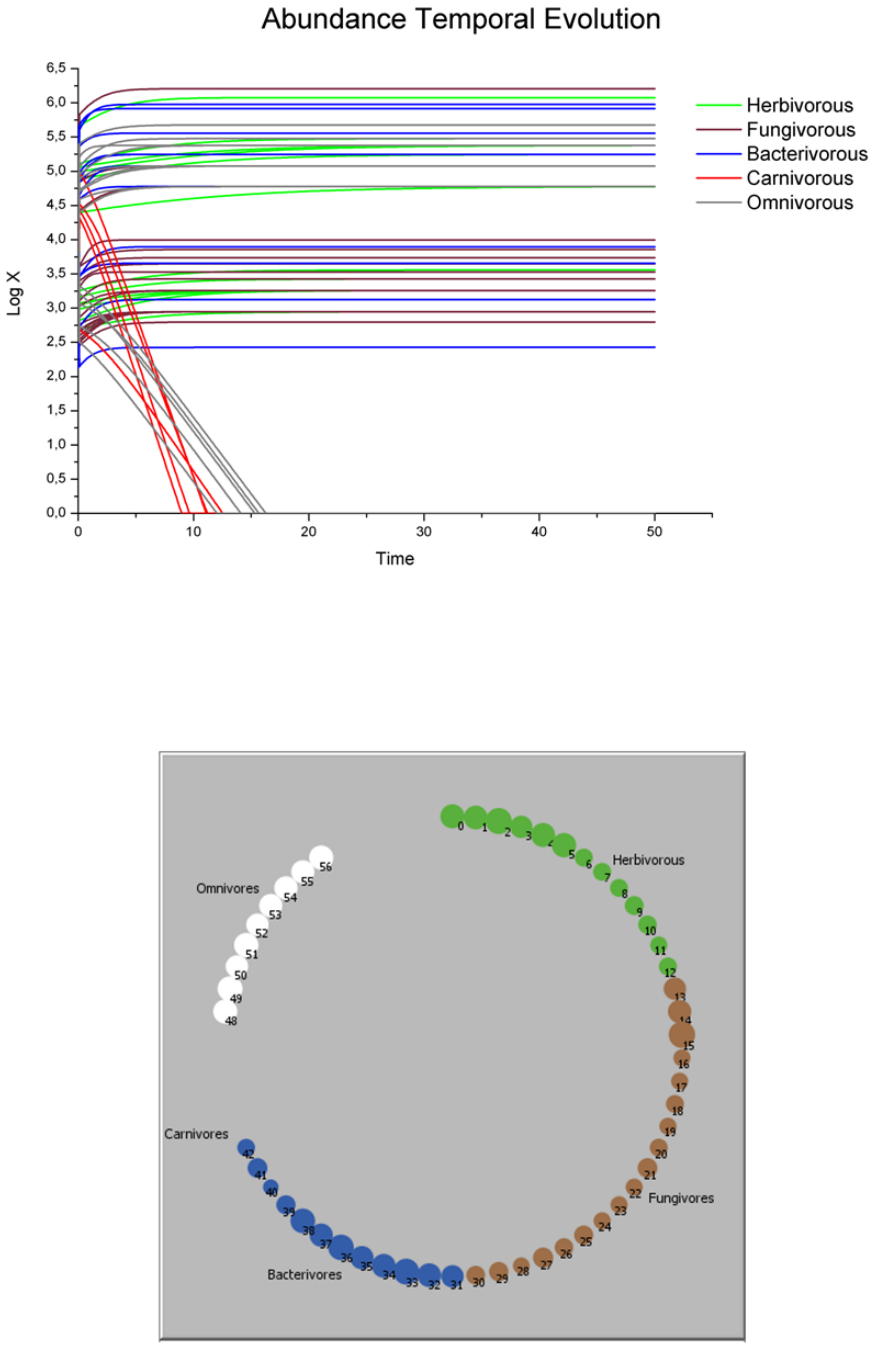

Figure 4.6: Graphic representation of the simulation results without interaction ($\beta = 0$).Above the temporal evolutions of species abundances and below the representations of the trophic web at the end of the simulation.

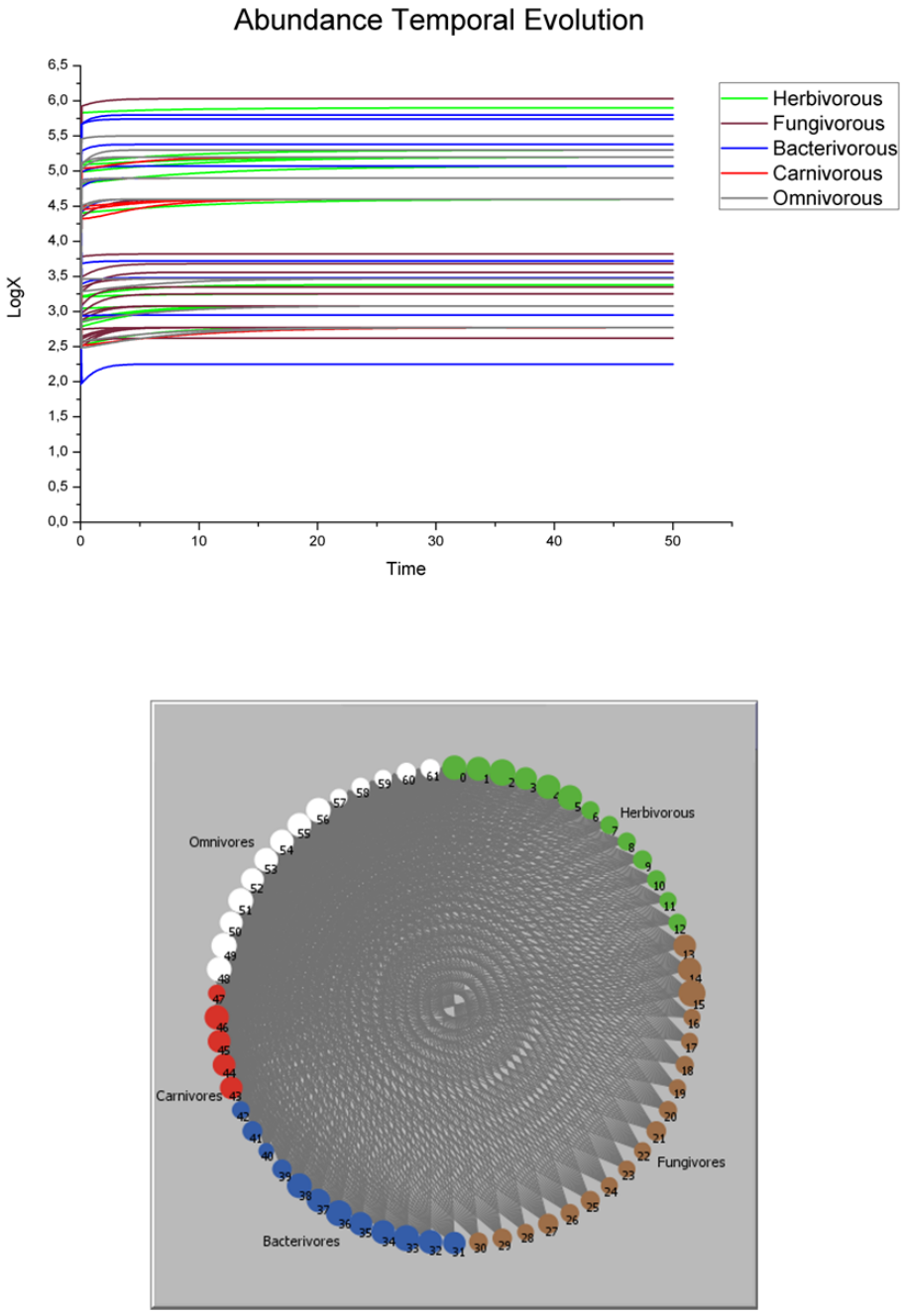

Figure 4.7: Graphic representation of the simulation results with interaction ($\beta = 1$). Above the temporal evolutions of species abundances and below the representations of the trophic web at the end of the simulation.

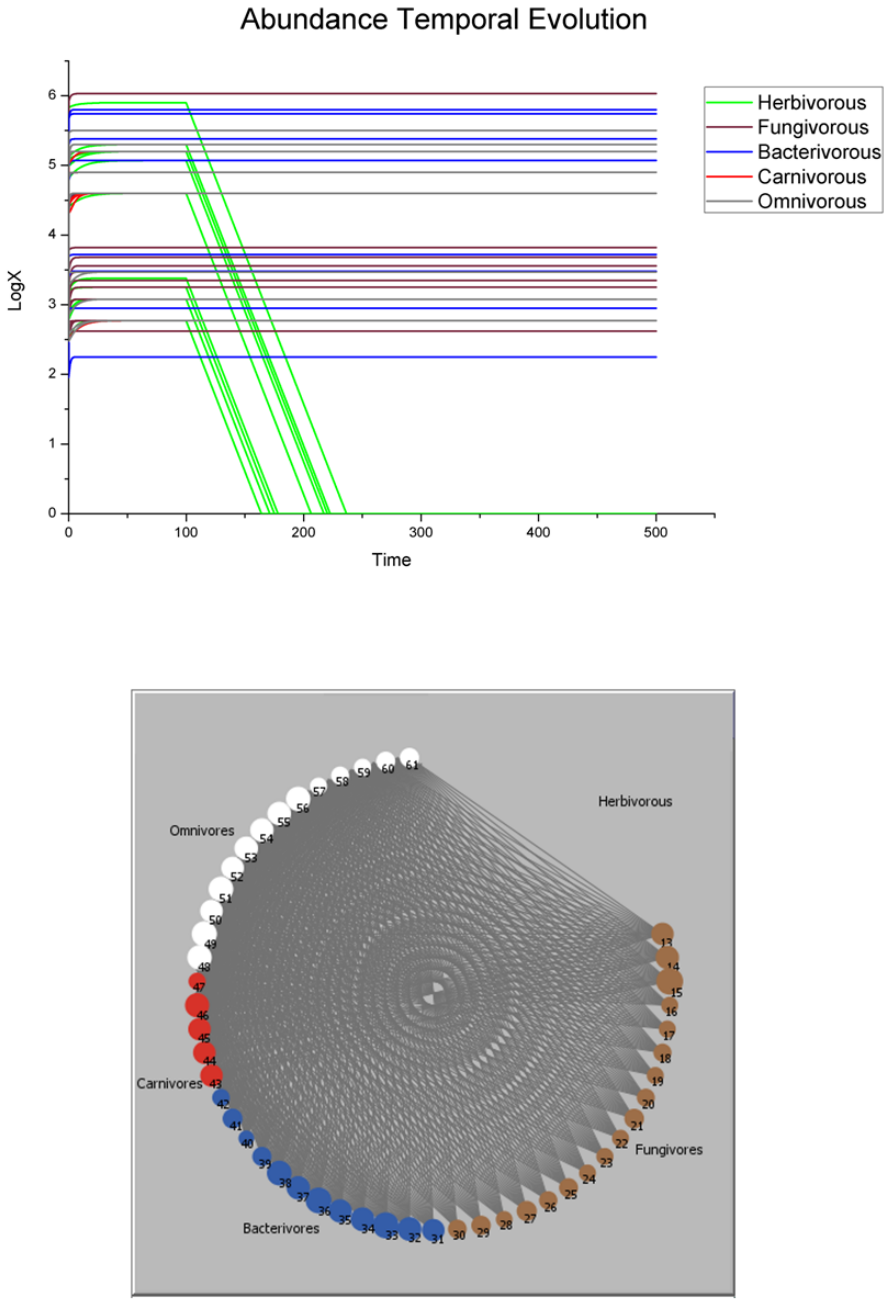

Figure 4.8: Graphic representation of the simulation results in the case all herbivores are removed from the ecosystem. Above the temporal evolutions of species abundances and below the representations of the trophic web at the end of the simulation.

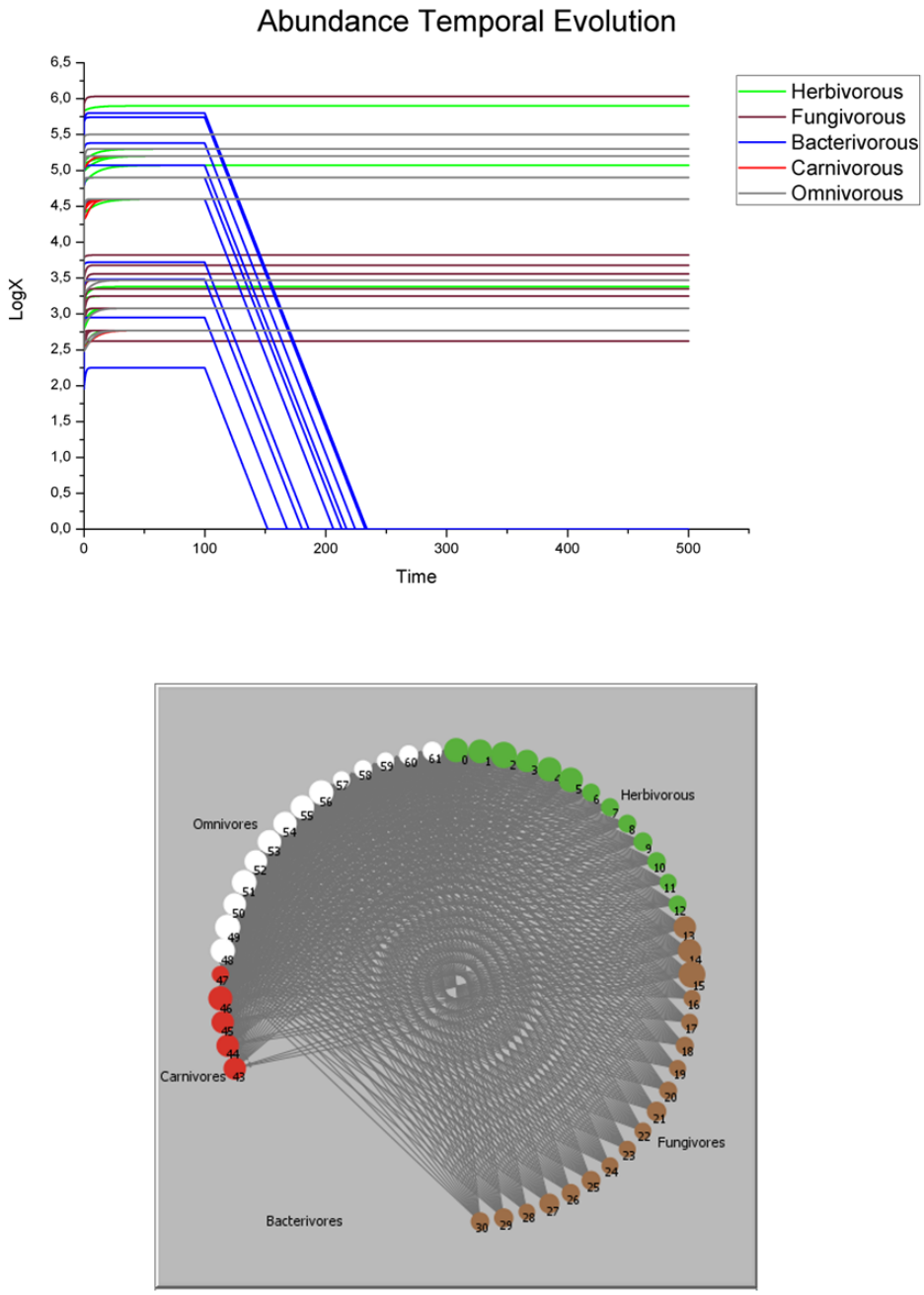

Figure 4.9: Graphic representation of the simulation results in the case all bacterivores are removed from the ecosystem. Above the temporal evolutions of species abundances and below the representations of the trophic web at the end of the simulation.

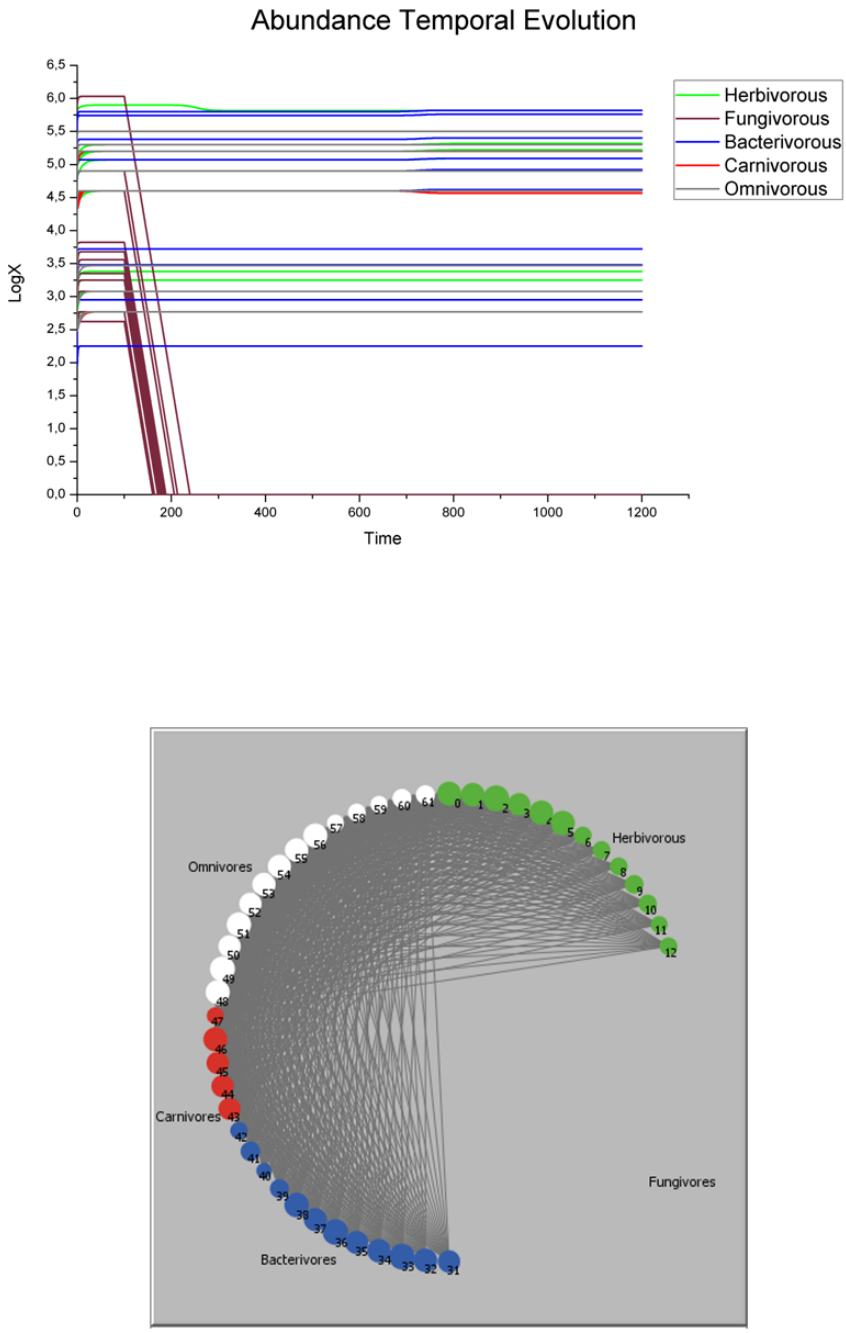

Figure 4.10: Graphic representation of the simulation results in the case all fungivores are removed from the ecosystem. Above the temporal evolutions of species abundances and below the representations of the trophic web at the end of the simulation.

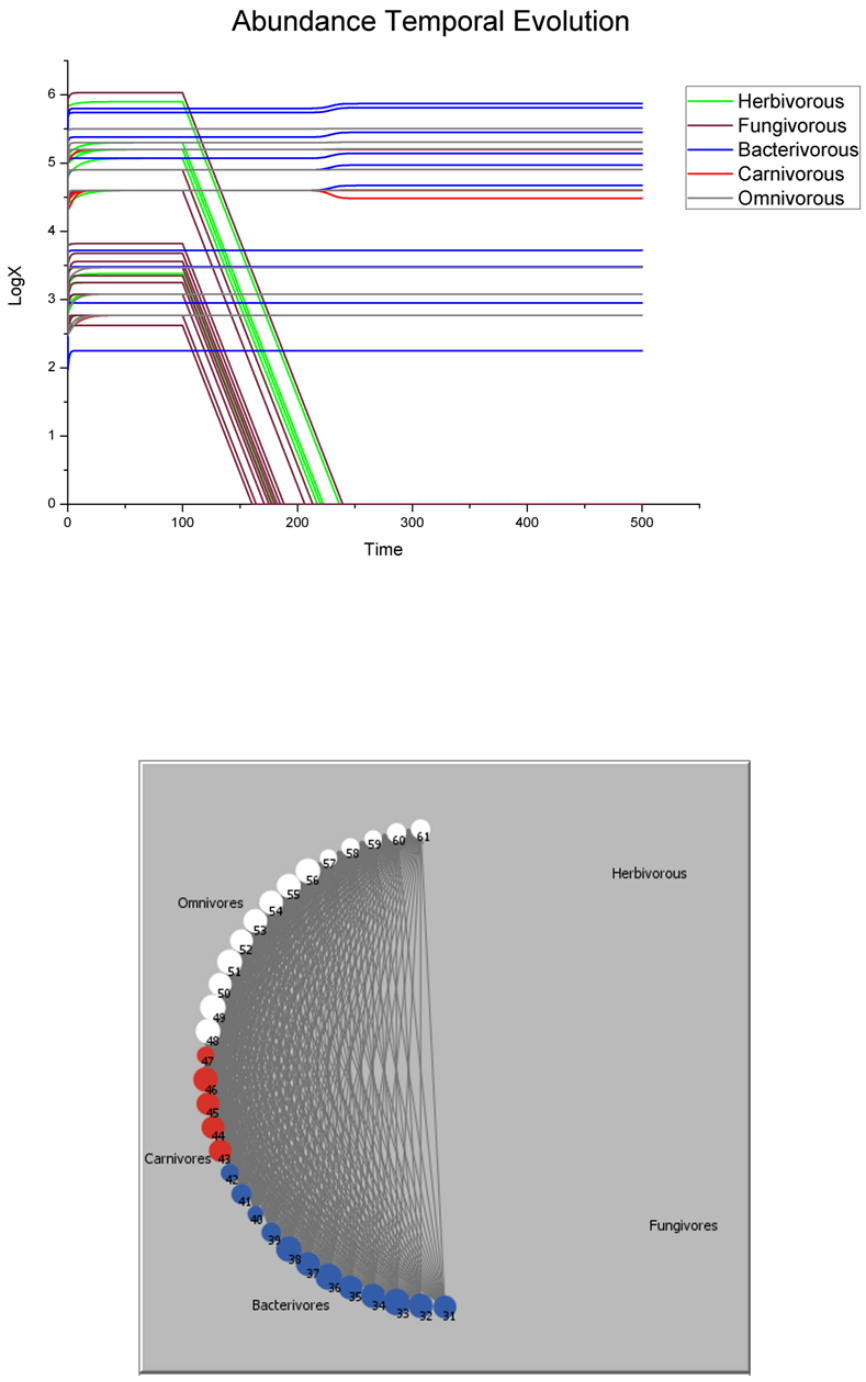

Figure 4.11: Graphic representations of the simulation results in the case all herbivores and fungivores are removed from the ecosystem. Above the temporal evolutions of species abundances and below the representations of the trophic web at the end of the simulation.

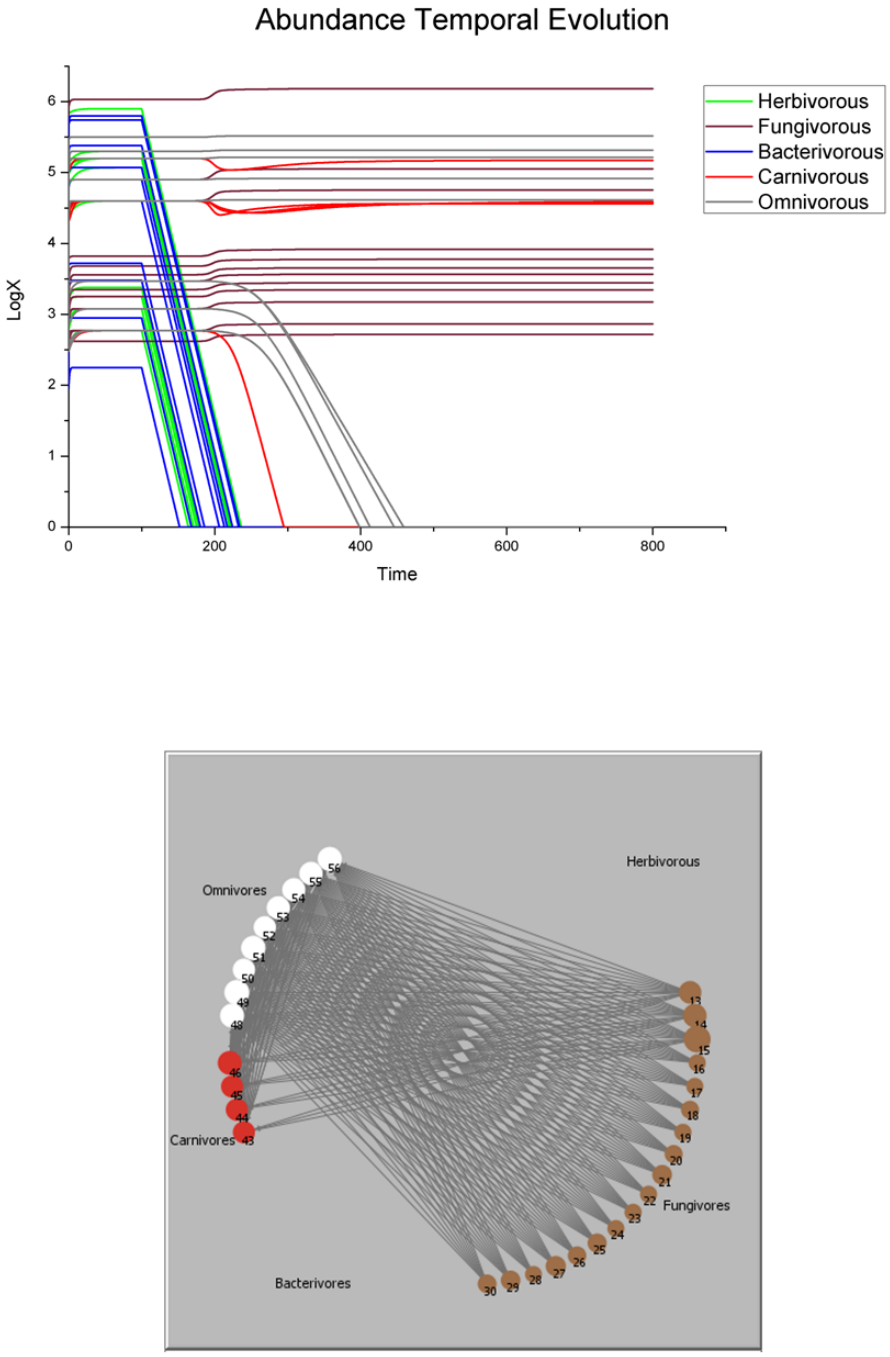

Figure 4.12: Graphic representations of the simulation results in the case all herbivores and bacterivores are removed from the ecosystem. Above the temporal evolutions of species abundances and below the representations of the trophic web at the end of the simulation.

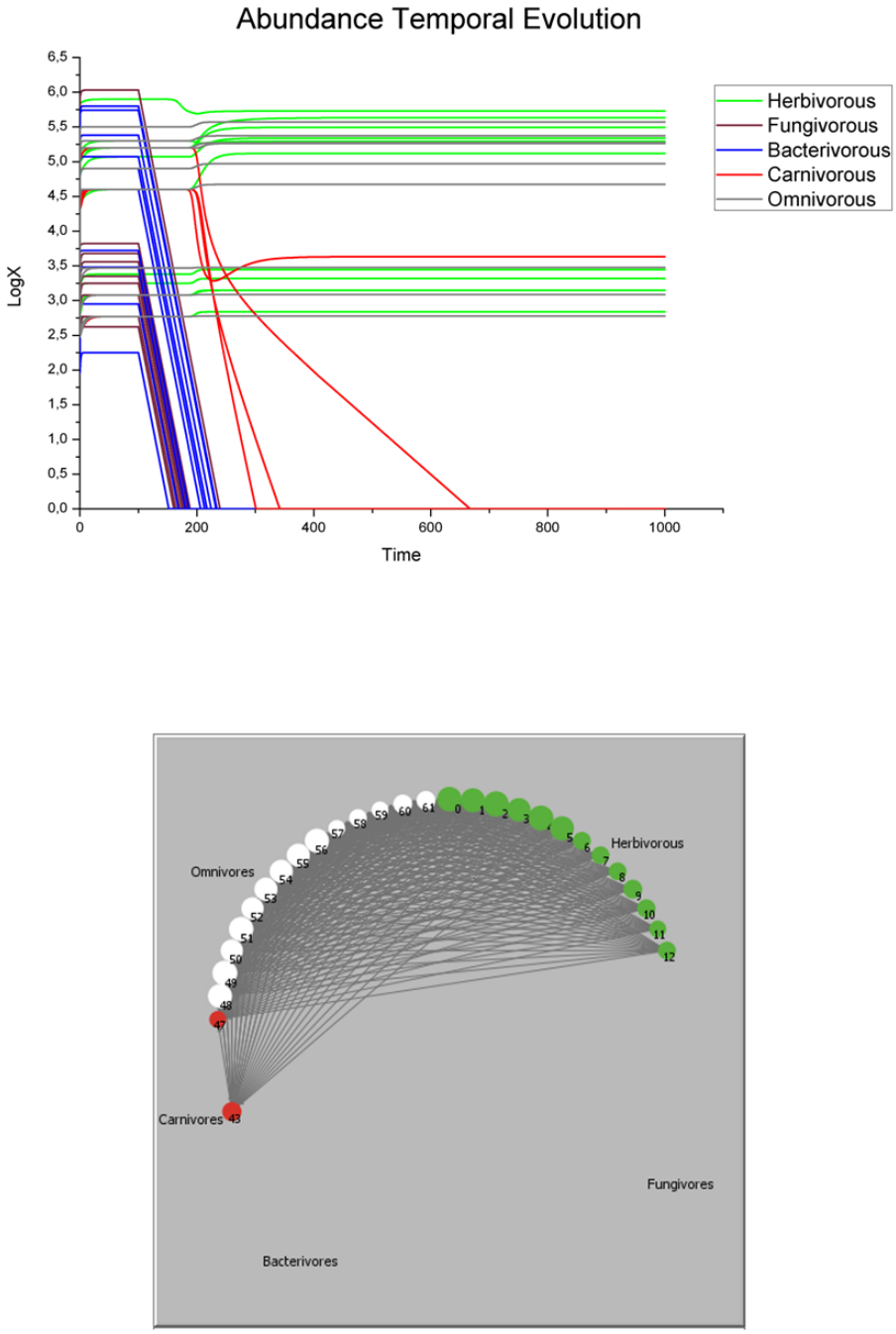

Figure 4.13: Graphic representations of the simulation results in the case all fungivores and bacterivores are removed from the ecosystem. Above the temporal evolutions of species abundances and below the representations of the trophic web at the end of the simulation.

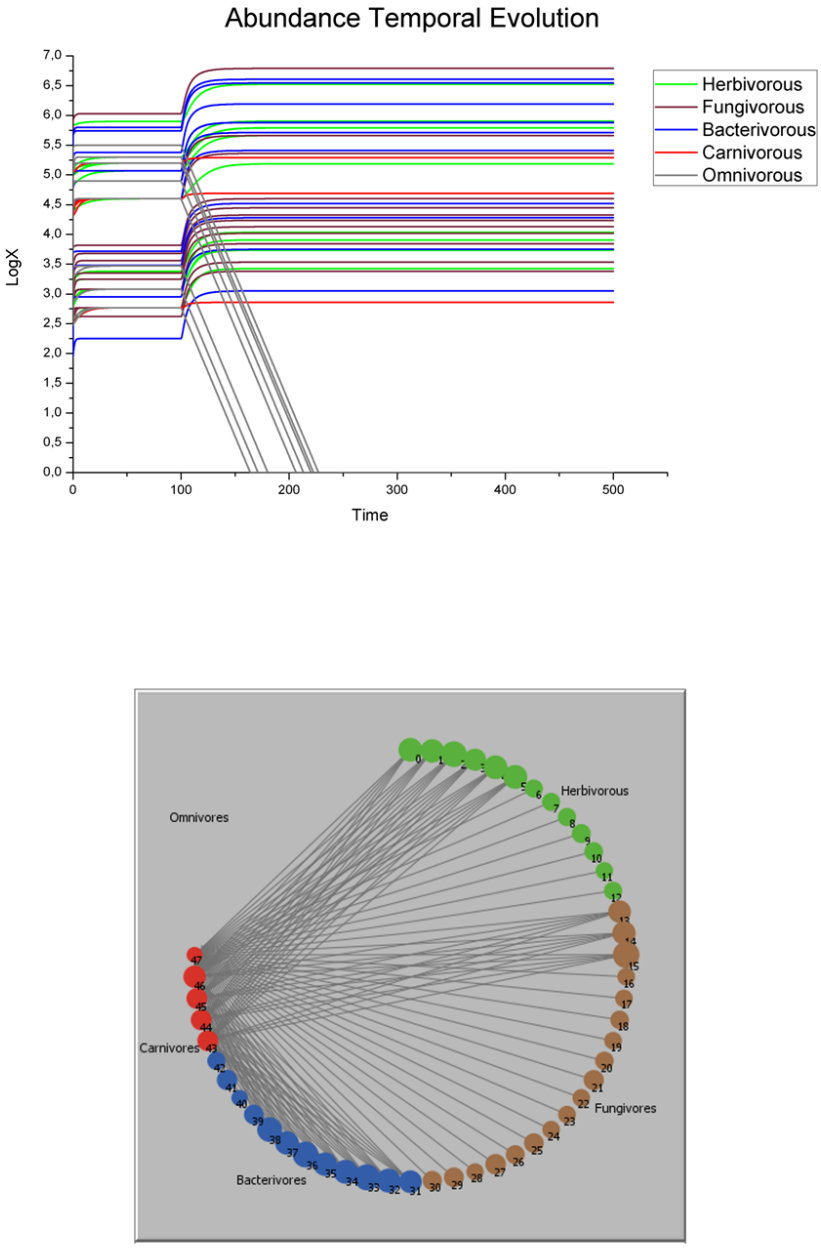

Figure 4.14: Graphic representation of the simulation results in the case all omnivores are removed from the ecosystem. Above the temporal evolutions of species abundances and below the representations of the trophic web at the end of the simulation.This temporal simulation of a real food-web assemblage confirms the theoretical scenario by Borrvall et al. (2000), when they stated that "*the probability of further species losses is almost zero when a top predator is removed*".

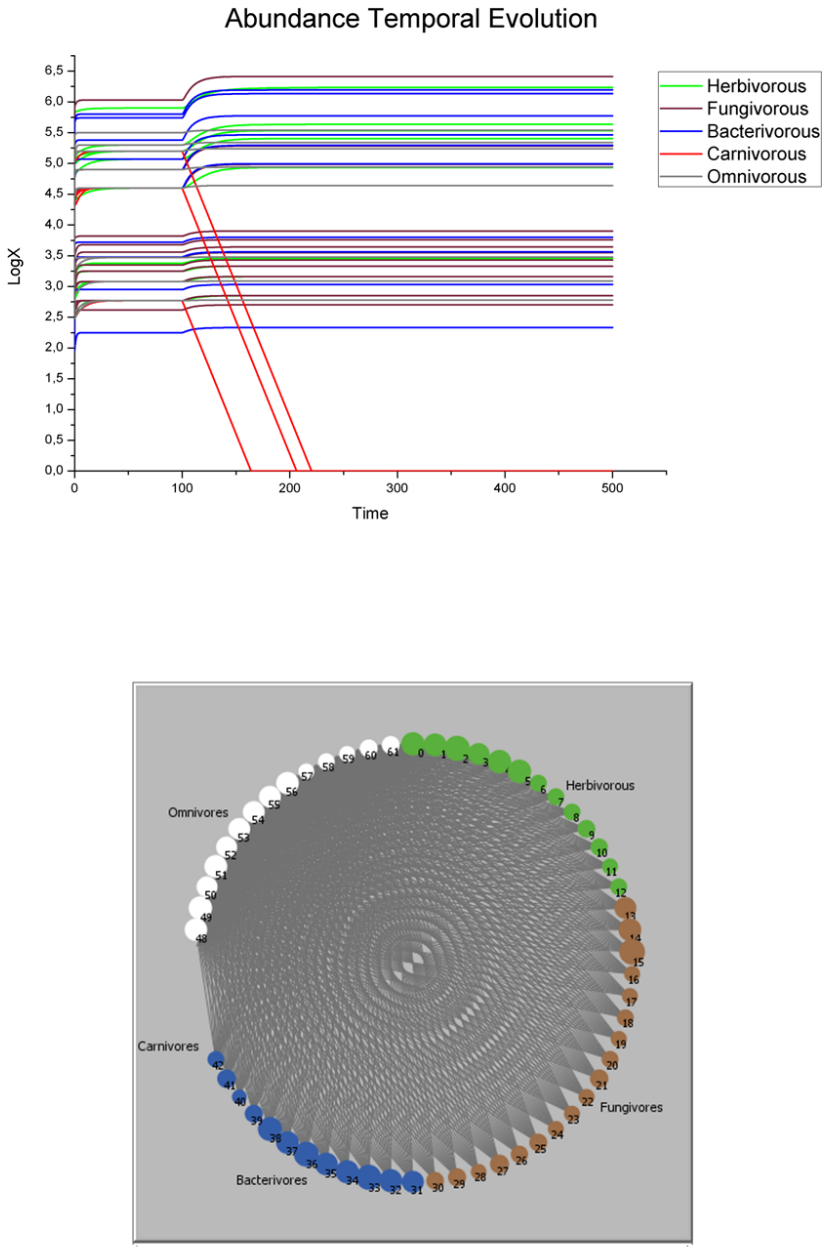

Figure 4.15: Graphic representation of the simulation results in the case all carnivores are removed from the ecosystem. Above the temporal evolutions of species abundances and below the representations of the trophic web at the end of the simulation. This temporal simulation of a real food-web assemblage confirms the theoretical scenario by Borrvall et al. (2000), when they stated that "*the probability of further species losses is almost zero when a top predator is removed*".

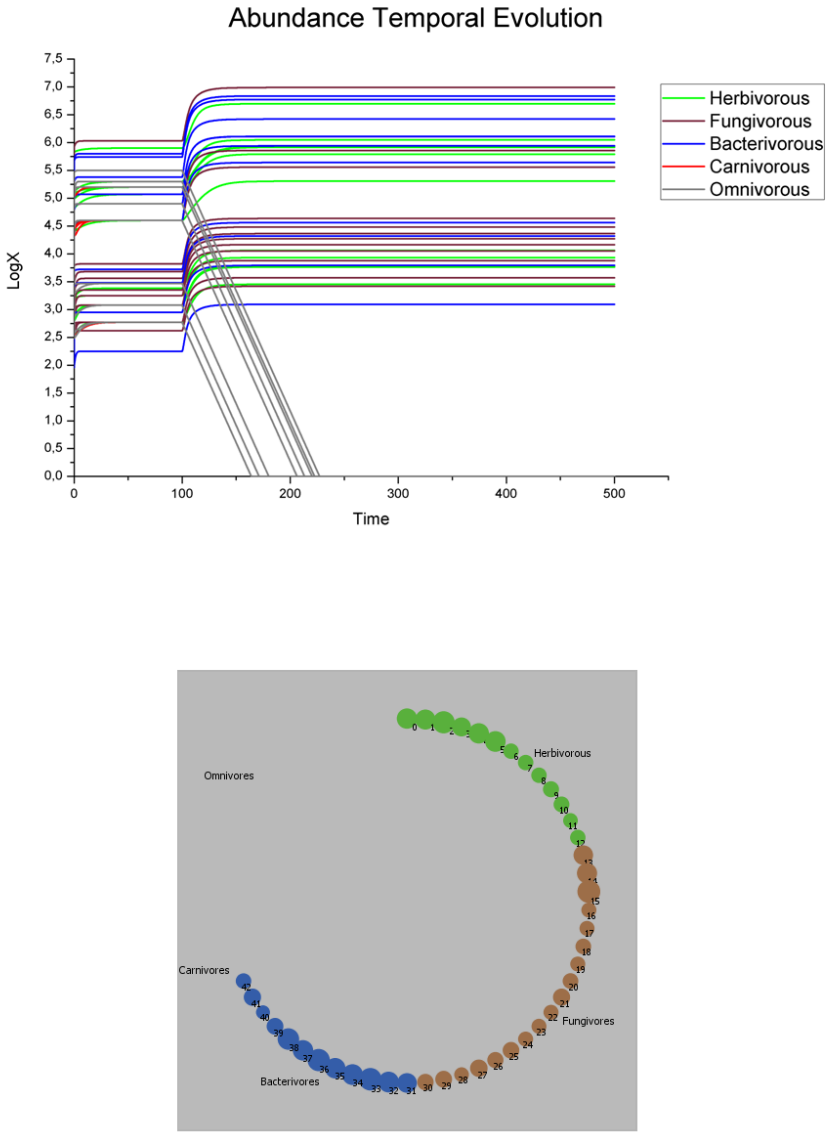

Figure 4.16: Graphic representation of the simulation results in the case all omnivores and carnivores are removed from the ecosystem. Above the temporal evolutions of species abundances and below the representations of the trophic web at the end of the simulation. This temporal simulation of a real food-web assemblage confirms the theoretical scenario by Borrvall et al. (2000), when they stated that "*the probability of further species losses is almost zero when a top predator is removed*".

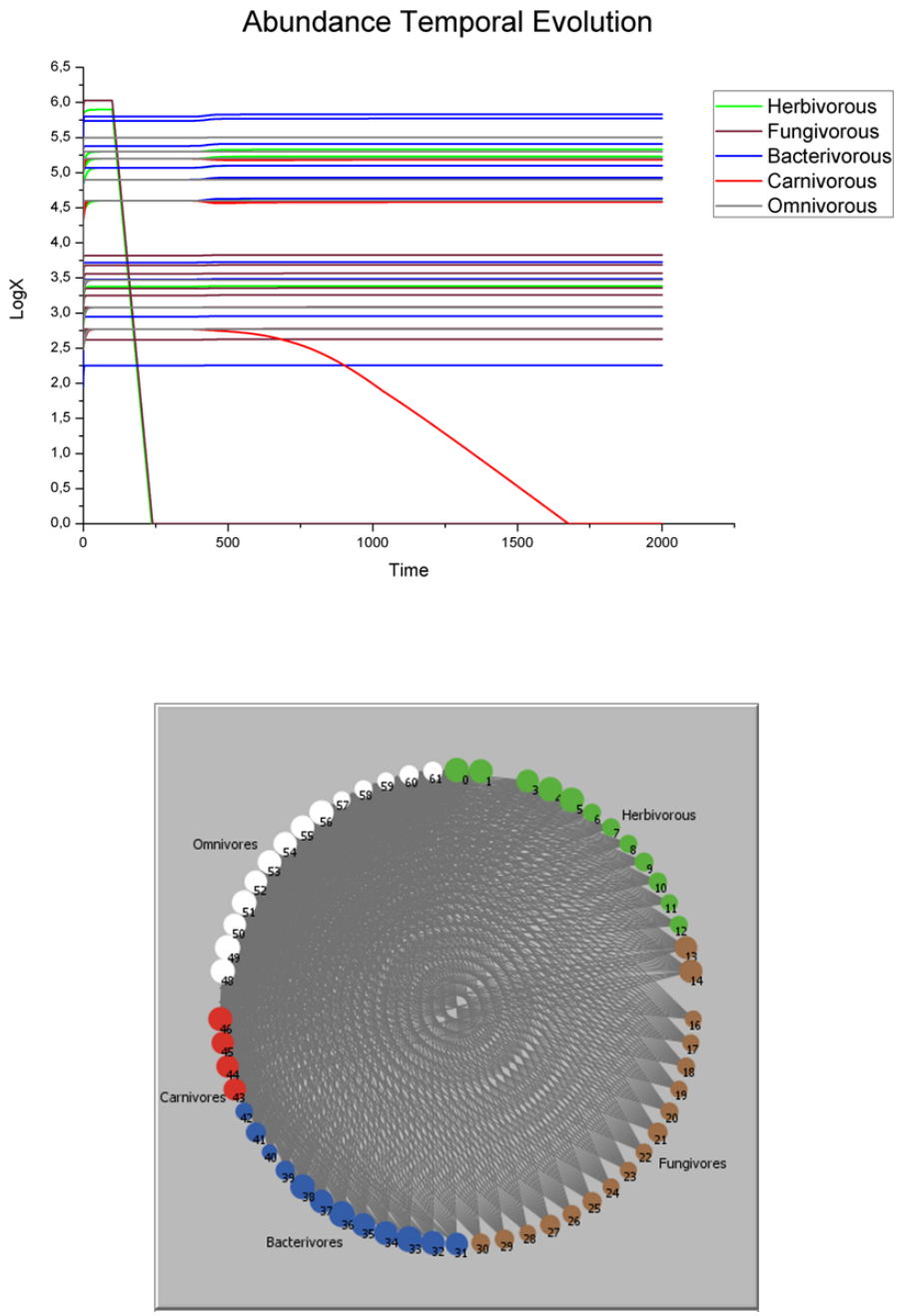

Figure 4.17: Graphic representation of the simulation results in the case only herbivores 2 and fungivores 15 are removed from the ecosystem (see the text for the explanation of these choices). Above the temporal evolutions of species abundances and below the representations of the trophic web at the end of the simulation.

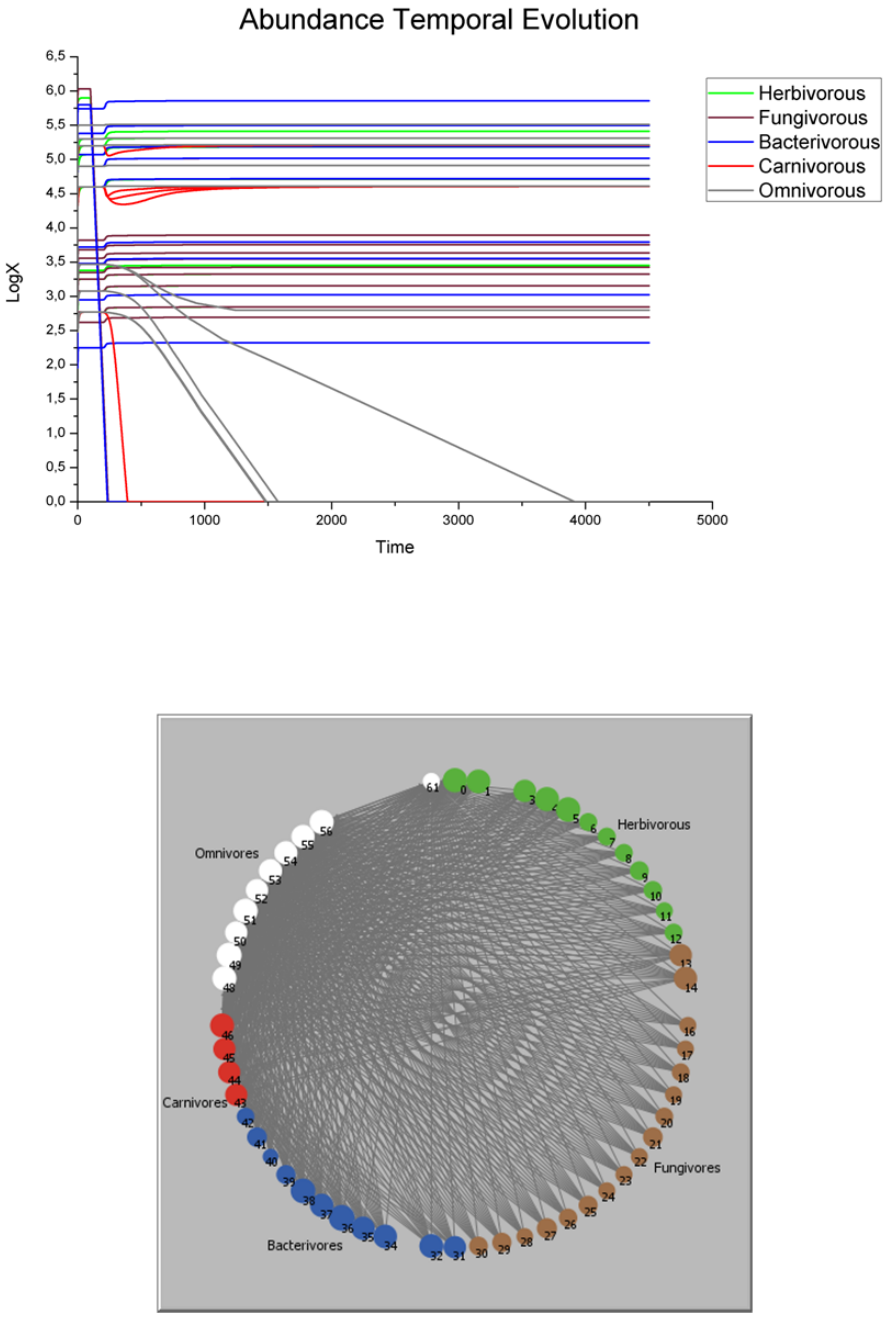

Figure 4.18: Graphic representation of the simulation results in the case only herbivores 2, fungivores 15 and bacterivores 33 are removed from the ecosystem (see the text for the explanation of these choices). Above the temporal evolutions of species abundances and below the representations of the trophic web at the end of the simulation.

4.2.4 Conclusive insights

Natural ecosystems are increasingly subjected to severe stress events due to global warming, deforestation and resource depletion, as evidenced by numerous studies, e.g. Hunt and Wall (2002), Malhi et al. (2008), Barnosky et al. (2011, 2012), Ceballos et al. (2015), but the contribution of particular species to the compensation and the community resistance after the extinction of other co-occurring species is uncertain (Ives and Cardinale, 2004). Therefore, the study of food webs is of fundamental ecological importance, as webs define the structure of the ecosystem and determine its properties, including its stability respect to environmental disturbances. Any ecosystem is stable if the system opposes to its disintegration when subject to various types of disturbances that can cause the extinction of species. Following a numerical approach able to combine both dynamical and topological aspects of the problem, in this study we quantified the reaction of a real density-driven ecological network of soil invertebrates to different perturbative scenarios by means of extended simulations realized within a fully programmable agent-based environment. If we consider the average number of species per guild as functional redundancy, the removal of all fungivorous and bacterivorous species lessens 60% of redundancy of our food web in time. On the other hand, even the removal of the three most abundant species belonging to the primary consumers (one herbivore, one fungivore and one bacterivore) clearly shows evident bottom-up cascading effects among the secondary consumers, and lessens the biodiversity of carnivores of 20% and the biodiversity of omnivores of 29%. Assuming like Borrvall et al. (2000) and Katrin et al. (2012) that a major effect of omnivory is to lessen the risk of species extinctions following the loss of a herbivore, it is surprising that so many omnivores belonging to such a resilient guild got extinct. However, missing top-down control by secondary consumers in general, and by omnivores in particular, independently increased the numerical abundances of all the primary consumers and confirm a recent meta-analysis (Mancinelli and Mulder, 2015). These authors concluded in fact that omnivores, either alone or with predators, exerted a much stronger negative effect than predators in terrestrial systems. Seen that the probability of species loss in other food webs can be assessed when key species or guilds disappear, this simple computational method visualizes alterations in the food-web architecture and can identify possible tools in environmental assessment and ecological conservation.

4.3 Comparison between different communities

The aim of the study here described is to analyze the topology and the robustness of three trophic networks corresponding to soil ecosystems under different regimes of management, highlighting similarities and differences. Unlike previous studies, that are based on a purely topological network-structure analysis, this study derives the robustness of the food webs through a dynamical analysis through the use of the model previously described (Conti et al., 2020). This represents an upgrade considering that the structure of a given network has a strong impact on the outcomes of dynamics, as highlighted in Pimm and Lawton (1978), McCann and Hastings (1997), Hastings (1996) and Jordan et al. (2002). In this regard, Dunne (2006) stated that "*the dynamics of species in complex ecosystems are more tightly connected than conventionally thought, which has profound implications for the impact and spread of perturbations*".
Several studies have investigated the different structural characteristics shown by food webs representative of different types of habitats and environments (Briand (1983), Briand and Cohen (1987), Chase (2000), Cohen (1994), Link (2002), Dunne et al. (2004)). Similarly, the present study is useful in highlighting structural differences between food networks representative of agricultural fields subject to different types of management, differences that may affect the dynamics and robustness of these networks. Land-management practices and environmental changes affect belowground communities, influencing the overall stability and productivity of the food webs (Wall et al. (2015), Clay (2004), Powell (2007)). In this respect this study aims also to suggest a possible link between agricultural practices and the robustness of ecosystems subject to these types of management. Understand if and how anthropogenic action affects soil ecosystems can be helpful in establishing the eco-sustainability of certain agricultural methods, promoting the ecological complexity and robustness of soil biodiversity.
This study is the subject of a paper (Di Mauro et al., 2020) currently in phase of submission to the journal Food Webs. It focused on three sampling sites, among those described at the beginning of the chapter, and can be considered as a preliminary study for further analysis to be carried out on the remaining available sites. The first ecosystem considered is the one studied in the previous paragraph (site 247), that is fallowed pastures with low pressure management. As mentioned above this ecosystem turns out to be particularly stable according to both the Eltonian rule (Elton, 1927) and the energetic equivalence rule (Mulder and Elser, 2009). Consequently, we can consider this ecosystem as a reference network subject to low anthropic disturbance.
The other two analyzed ecosystems (sites 225 and 230) are organic farms certified by the Agricultural Economics Research Institute of the Netherlands (LEI). These meet all the legal requirements for this type of agriculture (using com-

ELEMENT	DESCRIPTION	CONCENTRATION	
		SITE 225	SITE 230
Manure-N	Mean Nitrogen (kg N_{TOT} ha^{-1} yr^{-1}) excreted by cows, calves, pigs and poultry	357	298
Soil-Hg	Mercury (mg/kg dry soil) measured by Atomic Absorption after pyrolysis	0.04	0.08
Soil-Pb	Lead (mg/kg dry soil) measured by Inductively Coupled Plasma (ICP) Mass Spectrometry after sample digestion	20.5	43.0

Figure 4.19: Concentration values of nitrogen from manure, mercury and lead in the soil of sites 225 and 230.

post/farmyard manure and no biocides, averaging 1.7 livestock units per hectare) and are periodically monitored (Cohen and Mulder (2014)). Despite this, being fields dedicated to agriculture, albeit organic, are subject to middle intensity management and this is the main feature that distinguishes these sites from ecosystem 247.
Furthermore, the two organic farms differ from each other in the concentration of some elements present in their soil. The first of these two ecosystems (site 225) is a field with high concentrations of nitrogen from manure and this suggests that it is an area subject to grazing (organic farming also includes the possibility of pasture). The second ecosystem (site 230) was instead selected for its high concentrations of heavy metals such as lead and mercury which might suggest the presence of a nearby factory functioning at present or in the past. The concentration values of these significant elements in the two sites are shown in table 4.19. Unfortunately we are not aware of the concentration of these elements in site 247, because for natural lands this type of chemical analysis has not been carried out.
Data sampling for sites 225 and 230 was carried out in the same ways and with the same procedures described in the previous paragraph for site 247. In Figures 4.20 and 4.21, the list of the n species found in sampling sites 225 and 230 is shown. For these species we know the abundance X_i, the body mass M_i, the biomass B_i and the value of the growth rates r_i, with $i = 0, 1, ..., n$. Even for these two soil ecosystems, using the data obtained from the sampling, we have built two direct and unweighted food webs. Figure 4.22 shows the representative networks (the species present and how these are connected to each other) of ecosystems 225 and 230.

NODE_ID	TROPHIC_ID	FUNCTIONAL_ID	SPECIES NAME
0	Herbivorous	Plant-feeding nematode	Coslenchus
1	Herbivorous	Plant-feeding nematode	Dolichodoridae
2	Herbivorous	Plant-feeding nematode	Helicotylenchus
3	Herbivorous	Plant-feeding nematode	Heterodera
4	Herbivorous	Plant-feeding nematode	Malenchus
5	Herbivorous	Plant-feeding nematode	Meloidogyne
6	Herbivorous	Plant-feeding nematode	Paratylenchus
7	Herbivorous	Plant-feeding nematode	Pratylenchus
8	Herbivorous	Plant-feeding nematode	Tylenchorhynchus
9	Herbivorous	Macrophytophage and panphytophage mites	Tydeidae
10	Herbivorous	Plant-feeding collembolans and symphylids	Sminthuridae
11	Herbivorous	Plant-feeding collembolans and symphylids	Sminthurinus
12	Herbivorous	Plant-feeding collembolans and symphylids	Sminthurus
13	Herbivorous	Plant-feeding collembolans and symphylids	Sphaeridia
14	Fungivorous	Fungivore nematode	Aphelenchoides
15	Fungivorous	Fungivore nematode	Tylenchidae
16	Fungivorous	Microphytophage mite (feeding on fungi)	Oppiella
17	Fungivorous	Microphytophage mite (feeding on fungi)	Pygmephorus
18	Fungivorous	Fungivore insects and pauropods	Brachystomella
19	Fungivorous	Fungivore insects and pauropods	Friesea
20	Fungivorous	Fungivore insects and pauropods	Isotoma
21	Fungivorous	Fungivore insects and pauropods	Isotomiella
22	Fungivorous	Fungivore insects and pauropods	Isotomurus
23	Fungivorous	Fungivore insects and pauropods	Lepidocyrtus
24	Fungivorous	Fungivore insects and pauropods	Mesaphorura
25	Fungivorous	Fungivore insects and pauropods	Parisotoma
26	Fungivorous	Fungivore insects and pauropods	Pauropoda
27	Fungivorous	Fungivore insects and pauropods	Proisotoma
28	Fungivorous	Fungivore enchytraeids	Fridericia
29	Bacterivorous	Bacterivore nematode	Acrobeloides
30	Bacterivorous	Bacterivore nematode	Cephalobidae
31	Bacterivorous	Bacterivore nematode	Eucephalobus
32	Bacterivorous	Bacterivore nematode	Panagrolaimus
33	Bacterivorous	Bacterivore nematode	Plectus
34	Bacterivorous	Bacterivore nematode	Rhabditidae
35	Bacterivorous	Bacterivore mite	Histiostoma
36	Bacterivorous	Bacterivore enchytraeids	Enchytraeus
37	Bacterivorous	Passive, substrate-related nematode	Dauerlarvae stage
38	Bacterivorous	Substrate-inhabiting enchytraeids	Buchholzia
39	Bacterivorous	Substrate-inhabiting enchytraeids	Henlea
40	Bacterivorous	Substrate-inhabiting enchytraeids	Marionina
41	Carnivorous	Predating nematode (consuming nematodes)	Mononchidae
42	Carnivorous	Predating nematode (consuming nematodes)	Mylonchulus
43	Carnivorous	Predatory mite (attacking nematodes)	Alliphis
44	Carnivorous	Generalist mite	Arctoseius
45	Carnivorous	Generalist mite	Dendrolaelaps
46	Carnivorous	Generalist mite	Lysigamasus
47	Carnivorous	Generalist mite	Macrocheles
48	Carnivorous	Generalist mite	Parasitus
49	Carnivorous	Generalist mite	Uropoda
50	Omnivorous	Omnivore nematode	Dorylaimoidea
51	Omnivorous	Omnivore nematode	Qudsianematidae
52	Omnivorous	Omnivore mite	Eupodes
53	Omnivorous	Omnivore mite	Mesostigmata (juveniles)
54	Omnivorous	Omnivore mite	Scutacarus

Figure 4.20: Trophic ID, functional ID and name of the taxa (mostly families or genera, here after called "species") corresponding to the nodes of the network shown in Figure 4.22 (a) (site 225).

NODE_ID	TROPHIC_ID	FUNCTIONAL_ID	SPECIES NAME
0	Herbivorous	Plant-feeding nematode	Aglenchus
1	Herbivorous	Plant-feeding nematode	Dolichodoridae
2	Herbivorous	Plant-feeding nematode	Helicotylenchus
3	Herbivorous	Plant-feeding nematode	Heterodera
4	Herbivorous	Plant-feeding nematode	Hoplolaimidae
5	Herbivorous	Plant-feeding nematode	Malenchus
6	Herbivorous	Plant-feeding nematode	Meloidogyne
7	Herbivorous	Plant-feeding nematode	Paratylenchus
8	Herbivorous	Plant-feeding nematode	Pratylenchus
9	Herbivorous	Plant-feeding nematode	Rotylenchus
10	Herbivorous	Plant-feeding nematode	Trichodorus
11	Herbivorous	Macrophytophage and panphytophage mites	Pachygnatidae
12	Herbivorous	Macrophytophage and panphytophage mites	Rhizoglyphus
13	Herbivorous	Macrophytophage and panphytophage mites	Tydeidae
14	Herbivorous	Plant-feeding collembolans and symphylids	Sminthuridae
15	Herbivorous	Plant-feeding collembolans and symphylids	Sminthurides
16	Herbivorous	Plant-feeding collembolans and symphylids	Sminthurinus
17	Herbivorous	Plant-feeding collembolans and symphylids	Sminthurus
18	Fungivorous	Fungivore nematode	Aphelenchoides
19	Fungivorous	Fungivore nematode	Tylenchidae
20	Fungivorous	Microphytophage mite (feeding on fungi)	Microppia
21	Fungivorous	Microphytophage mite (feeding on fungi)	Oppiella
22	Fungivorous	Microphytophage mite (feeding on fungi)	Pygmephorus
23	Fungivorous	Microphytophage mite (feeding on fungi)	Schwiebea
24	Fungivorous	Microphytophage mite (feeding on fungi)	Speleorchestes
25	Fungivorous	Fungivore insects and pauropods	Ceratophysella
26	Fungivorous	Fungivore insects and pauropods	Folsomia
27	Fungivorous	Fungivore insects and pauropods	Friesea
28	Fungivorous	Fungivore insects and pauropods	Isotoma
29	Fungivorous	Fungivore insects and pauropods	Isotomurus
30	Fungivorous	Fungivore insects and pauropods	Lepidocyrtus
31	Fungivorous	Fungivore insects and pauropods	Parisotoma
32	Fungivorous	Fungivore insects and pauropods	Proisotoma
33	Fungivorous	Fungivore enchytraeids	Achaeta
34	Fungivorous	Fungivore enchytraeids	Fridericia
35	Bacterivorous	Bacterivore nematode	Acrobeloides
36	Bacterivorous	Bacterivore nematode	Alaimus
37	Bacterivorous	Bacterivore nematode	Anaplectus
38	Bacterivorous	Bacterivore nematode	Eucephalobus
39	Bacterivorous	Bacterivore nematode	Panagrolaimus
40	Bacterivorous	Bacterivore nematode	Plectus
41	Bacterivorous	Bacterivore nematode	Prismatolaimus
42	Bacterivorous	Bacterivore nematode	Rhabditidae
43	Bacterivorous	Bacterivore mite	Histiostoma
44	Bacterivorous	Bacterivore enchytraeids	Enchytraeus
45	Bacterivorous	Passive, substrate-related nematode	Dauerlarvae stage
46	Bacterivorous	Substrate-inhabiting enchytraeids	Marionina
47	Carnivorous	Predating nematode (consuming nematodes)	Tripyla
48	Carnivorous	Predatory mite (attacking nematodes)	Alliphis
49	Carnivorous	Generalist mite	Arctoseius
50	Carnivorous	Generalist mite	Cheiroseius (Sejus)
51	Carnivorous	Generalist mite	Dendrolaelaps
52	Carnivorous	Generalist mite	Hypoaspis
53	Carnivorous	Generalist mite	Lysigamasus
54	Carnivorous	Generalist mite	Pachylaelaps
55	Carnivorous	Generalist mite	Parasitus
56	Carnivorous	Generalist mite	Pergamasus
57	Carnivorous	Generalist mite	Rhodacarellus
58	Omnivorous	Omnivore nematode	Dorylaimoidea
59	Omnivorous	Omnivore nematode	Qudsianematidae
60	Omnivorous	Omnivore mite	Eupodes
61	Omnivorous	Omnivore mite	Mesostigmata (juveniles)
62	Omnivorous	Omnivore mite	Scutacarus
63	Omnivorous	Omnivore mite	Stigmaeidae
64	Omnivorous	Omnivore mite	Tarsonemus
65	Omnivorous	Parasitizing mite (hosts are mites or nematodes)	Pyemotes

Figure 4.21: Trophic ID, functional ID and name of the taxa (mostly families or genera, here after called "species") corresponding to the nodes of the network shown in Figure 4.22 (b) (site 230).

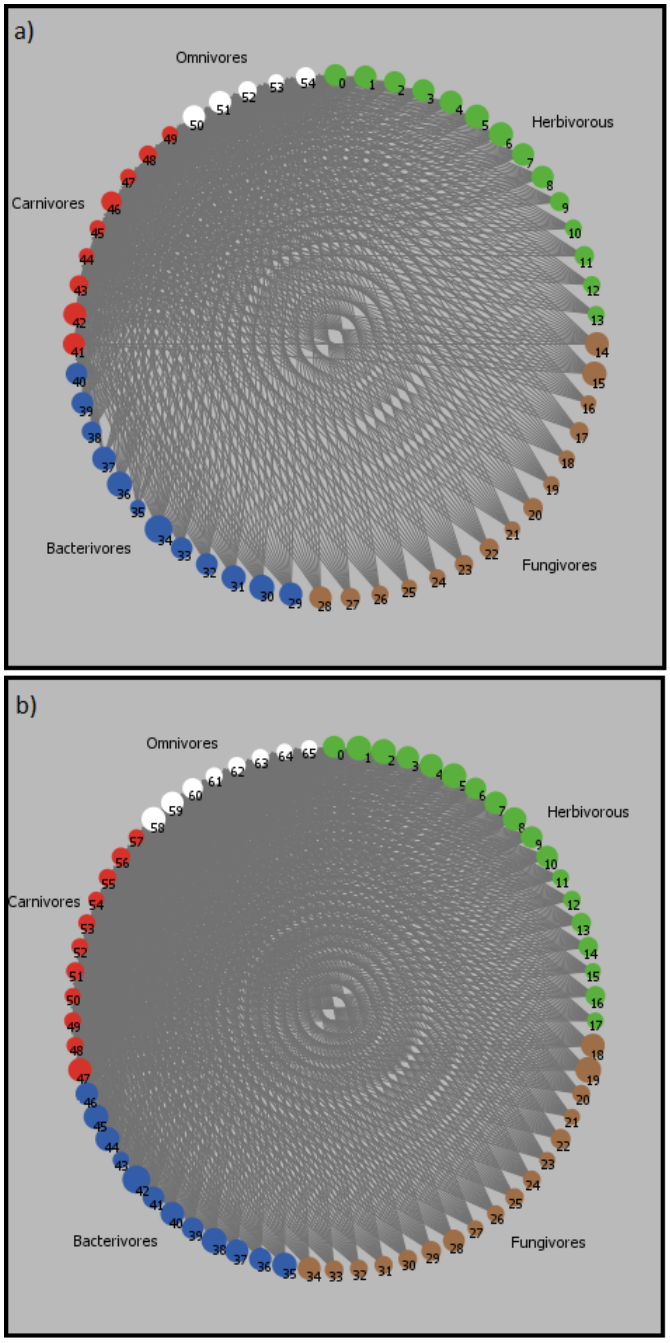

Figure 4.22: A sketch of the food web networks for site 225 (a) and for site 230 (b). Nodes/species are organized in groups of different colors (see Figures 4.20 and 4.21) and placed in a circular layout. Directed links represent the prey/predator connections, going from the prey node to the predator node. The size of each node is proportional to the base-10 logarithm of the abundance of the corresponding species ($LogX$)

4.3.1 Response of the three ecosystems to the different perturbative scenarios

In the first analysis carried out, it was applied the same model created for network 247 to these two new food webs by simulating the same scenarios. The results of the simulations for networks 225 and 230 are reported in the appendix. It is quite evident that the results obtained are very similar for networks 225 and 230, while these deviate quite from the results obtained for network 247.
The alteration index has proved to be a good parameter for the comparison of the different simulation scenarios within the same network and its values can allows to highlight the differences in the response of the three systems to the applied perturbations. In Figure 4.5 the alteration indices for the different scenarios in the three networks are shown.

We immediately notice that both networks 225 and 230 show a greater alteration in the simulations in which the bacterivores species are removed. It can be deduced that these webs are extremely sensitive to the removal of the bacterivores species rather than to the removal of the species in the second trophic level (omnivores and carnivores), a completely different response from that shown by network 247. The explanation of this behavior would seem to be the strong presence, within the two ecosystems, of the bacterivorous Rhabditidae (node 34 of network 225 and node 42 of network 230), with abundances of $10^{5.74}$ and $10^{5.61}$ respectively in networks 225 and 230, not present in network 247. Just think that the number of individuals of this species alone is almost half of all the living organisms sampled in network 225, and a third of all those sampled in network 230. The removal of such an abundant species is sufficient to create a great alteration within these ecosystems, especially if combined with the removal of other species in the first trophic level.
Considering the values assumed by the alteration index in the same network, we observe that in networks 225 and 230 there are lower values in the scenarios that concern the removal of species in the second trophic level. On the contrary, in network 247 the scenarios concerning the removal of carnivores and, specially, omnivores are characterized by a much higher alteration than in the other scenarios. A possible explanation could be that within network 247 there is a greater number of omnivorous species with high betweenness and closeness centrality (these are the omnivores with $r_i > 0$, see next paragraph) compared to that one present in the other two networks. As we will see, the species that have high values of these two quantities are those which, if disturbed, cause greater disturbance and therefore alteration within the system.
Finally, also in these networks, the phenomenon for which the alteration due to the removal of two groups of species together is greater than the sum of the alterations due to the individual removals of the two groups, is observed, with the

Alteration Index

	Network 227	Network 225	Network 230
Scenario 1	3.39 E-7	8.59 E-8	1.22 E-6
Scenario 2	0.94	2.38 E-4	2.08 E-4
Scenario 3	1.08 E-4	18.21	20.72
Scenario 4	1.82	8.59 E-8	1.22 E-6
Scenario 5	11.53	15.17	18.86
Scenario 6	12.97	104.38	71.03
Scenario 7	1.08 E-4	20.04	19.83
Scenario 8	2.76	17.88	19.76
Scenario 9	15.21	17.73	19.69
Scenario 10	29.41	3.72	3.59
Scenario 11	195.8	1.11	2.73
Scenario 12	261.41	4.62	6.22

Simulation scenarios:

1. Removal of all the herbivorous species
2. Removal of all the fungivorous species
3. Removal of all the bacterivorous species
4. Removal of all the herbivorous and fungivorous species
5. Removal of all the herbivorous and bacterivorous species
6. Removal of all the fungivorous and bacterivorous species
7. Removal of the first most abundant species in the system (fungivorous 15 in network 247, bacterivorous 34 in network 225 and bacterivorous 42 in network 230).
8. Removal of the two most abundant species in the system (fungivorous 15 and herbivorous 2 in network 247, bacterivores 34 and 36 in network 225 and bacterivorous 42 and fungivorous 19 in network 230).
9. Removal of the three most abundant species in the system (fungivorous 15, herbivorous 2 and bacterivorous 33 in network 247, bacterivores 34, 36 and 30 in network 225 and bacterivorous 42, fungivorous 19 and bacterivorous 38 in network 230).
10. Removal of all the carnivorous species
11. Removal of all the omnivorous species
12. Removal of all the omnivorous and carnivorous species

Figure 4.23: Alteration Index for the simulation scenarios performed for the three networks.

only exception of the scenarios involving the removal of the species in the second trophic level where these two quantities assume almost the same values.

4.3.2 Topology of the three food webs

The three sites studied differ in the type of management and are subject to different anthropic disturbances, as can be deduced from the concentration of certain elements present in the soil. Therefore I found very interesting to analyze the topology of the three networks in order to observe whether these differences we are aware of are reflected in the structure of the three ecosystems. As already mentioned, the structure of the network that underlies a complex system determines many of its features and emerging behaviors. The topological study of the three networks could allow us to make considerations on some properties such as efficiency in the exchange of information, degree of competition of the species and robustness of the ecosystem.
To check if the three food networks have a small world structure I calculate their average path length and their average clustering coefficient and I compare these results with the average values of the same quantities obtained from 10 random networks with the same number of nodes and the same average number of links. Since the considered direct networks are disconnected, for the calculation of the average path length it was preferred to take into account the corresponding indirect graph. Results are shown in Figure 4.24. The average clustering coefficient of real networks is much greater than that obtained for random networks. Instead the average path length assumes a value similar, if not equal, to that of the random counterpart. These results are in line with those obtained by Montoya and Solé (2002) for other types of food webs. The low values of the average path length and the great difference between the average clustering coefficient of real and random networks can be considered a confirmation of the small world nature of the three networks analyzed.
By comparing the values of the average clustering coefficient of the three real networks, we observe that networks 225 and 230, both organic farms, have very similar and, evidently, lower clustering coefficients than network 247, an uncultivated land. A higher clustering coefficient could indicate a greater robustness of the system, since the presence of clusters within the network, and therefore of "triangles", guarantees the presence of alternative routes in the event of disappearance of nodes.
For all three networks the value of the connectance, given by $C = L/S(S-1)$ (as the phenomenon of cannibalism was not taken into consideration), was calculated. The connectance values are 0.27, 0.21 and 0.24 respectively for networks 247, 225 and 230. According to Dunne et al. (2002), low connectance values may reveal a lower robustness of the network. Thus, also in this respect, network 247 seems to

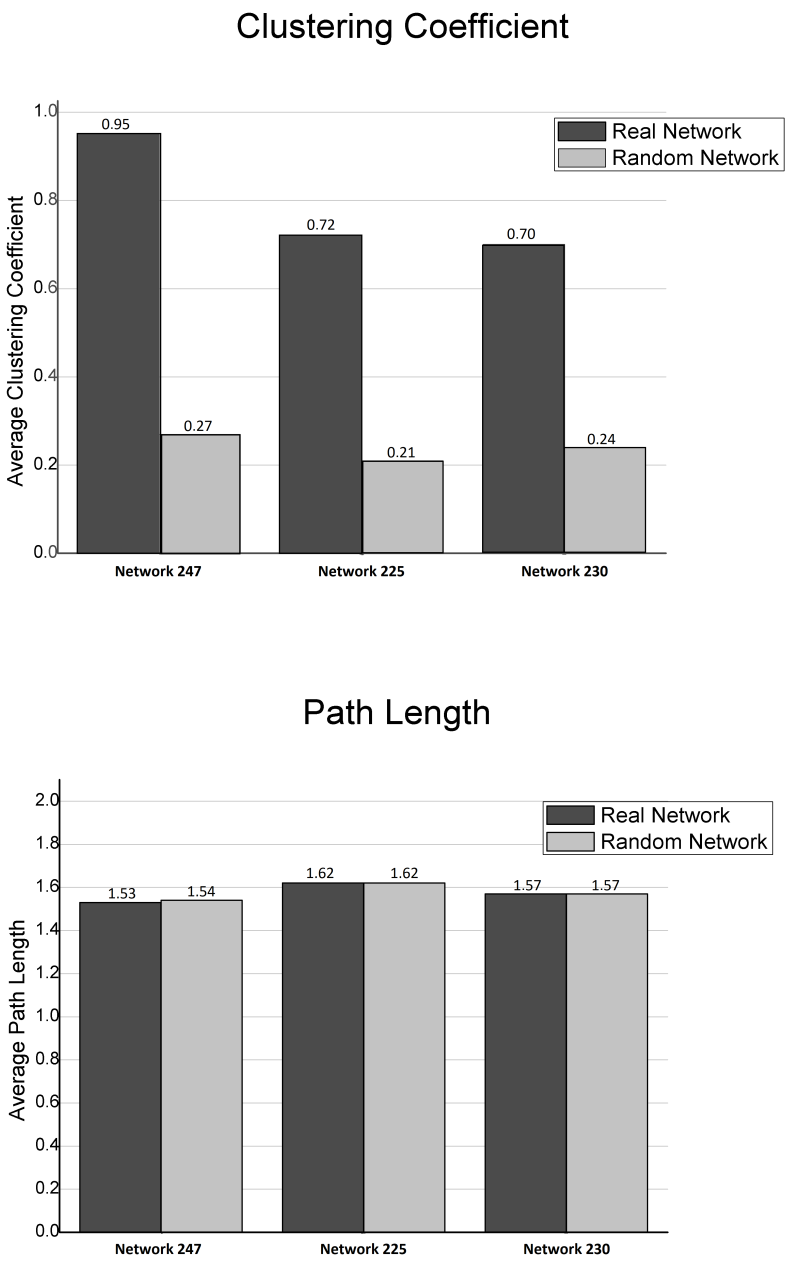

Figure 4.24: Average Clustering Coefficient and Average Path Length. The dark grey columns represented the real networks and the light grey columns the average results for 10 comparable random networks.

be the most robust.
The study of the degree distribution of the links did not show particular trends in any of the three networks. So it cannot be said that they have a scale-free structure. On the other hand, all three networks have a disassortative nature, as expected for food networks (Newman (2002, 2003); Stouffer et al.(2005)): nodes with many links are mostly connected with nodes with a low number of links. In this calculation, the total number of links, given by the sum of the incoming and outgoing links, was considered for each node. The results are shown in Figure 4.25 in which is plotted the node degree vs. the average degree of neighbor nodes for the three networks. The assortativity values are deduced from the slope of the lines that fitted the data in the log-log plot. All three networks have similar and negative assortativity values: -0.387 ± 0.011, -0.388 ± 0.057 and -0.390 ± 0.064 for networks 247, 225 and 230 respectively. According to some research (Murakami et al. (2017), D'Agostino et al. (2012), Tanizawa (2012) and Thedchanamoorthy et al. (2014)), this property confers them a greater efficiency in the transport of information and could explain their weakness towards targeted attacks to the most interconnected nodes, more than their degree distribution.

4.3.3 Generalist species, vulnerable species and competition in the three ecosystems

In the case of trophic networks, high in-degree value is characteristic of species that show generalist trophic habits. As can be expected, in all three networks the species that have highest in-degree values are omnivores and, secondly, carnivores. On the contrary, species that have high out-degree value are vulnerable species, i.e. species undergoing high predatory pressure (Rocchi et al. 2017). In the three considered networks, these species are herbivores, fungivores, bacterivores and those omnivores that have $r_i > 0$ (see Figure 4.26).
Given the structure of a network, some nodes can be topologically more important than others. Mainly there are two quantities that allow you to calculate the centrality and therefore the importance of each node within the network. The first of these is the betweenness centrality: to calculate this value for a node, you take every other possible pairs of nodes and, for each pair, you calculate the proportion of shortest paths between members of the pair that passes through the considered node. The betweenness centrality of a node is the sum of these. It measures how central a given node is in terms of being included in many shortest paths in the network, thus describing how crucial a species is in mediating the diffusion of indirect effects throughout the whole food web (Rocchi et al., 2017). The second measure is the closeness centrality of a node, defined as the inverse of the average of its distances to all other nodes. It measures how close a node is to

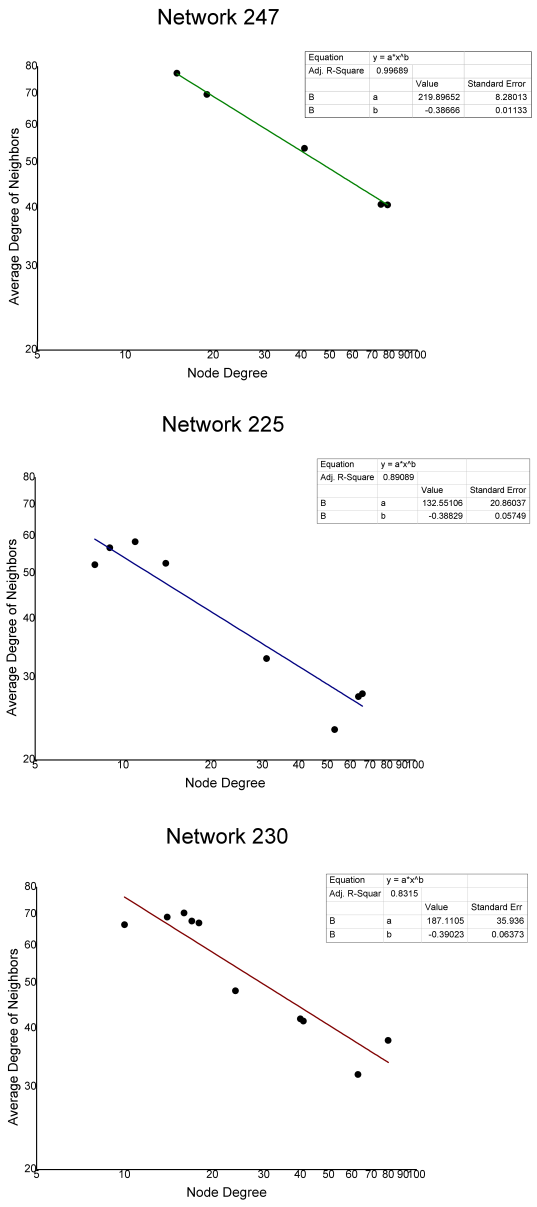

Figure 4.25: Node degree vs the average degree of neighbor nodes in a log-log plot for the three networks. The slope of the line that fits the data gives the assortativity values. The three networks have similar and negative assortativity values.

the others and quantifies how rapidly an effect that generates from that species can spread in the food web (Rocchi et al., 2017).
If a ranking of the nodes is carried out on the basis of their values of abundance, in-degree, out-degree, betweenness and closeness centrality, interesting observations can be made. The rankings for the three webs are shown in Figure 4.26. It should be noted that, in the considered networks, the species with the highest betweenness centrality correspond to omnivores with $r_i > 0$, stressing that these species are the most crucial for the diffusion of indirect effects throughout the whole web. We also realize that the species with high out-degree are the same ones that have high closeness centrality values. These are species topologically close to the others for which a disturbance originating from them spreads quickly throughout the system (note that omnivores with $r_i > 0$ are also included in this case). Finally, it can be seen that vulnerable species are approximatively more abundant than the other species. Undoubtedly what is evident is that the dominant species (the most abundand, i.e. nodes 15, 2 and 33 for network 247, nodes 34, 36 and 30 for network 225 and nodes 42, 19 and 38 for network 230) are always part of the groups with the highest value of closeness centrality. This explains why the scenarios in which the most abundant species are removed upset the architecture of the network and lead to numerous secondary extinctions, even if few species and not entire functional guilds are removed. Indeed, these species, besides being dominant, have a very high closeness centrality value, which makes them fundamental for the integrity of the ecosystem.
The number of species that have betweenness centrality equal to zero (let's call this value B_0), may suggest the degree of competition between species in the ecosystem (Rocchi et al., 2017). In Grassi et al. (2009) it is proved that the betweenness centrality of a node is equal to zero if it belongs to only one complete subgraph of a graph (complete means that all nodes are connected to each other). If B_0 increase, then more species compete with only one particular group of species. In this case we have that species with betweenness centrality equal to zero are herbivores, fungivores and bacterivores, i.e all the species in the first trophic level. These species compete with species in the second trophic level because they are preyed upon by them. So an increase in B_0 suggests a greater competition between species in the first and species in the second trophic level. However at the same time, the species belonging to the second trophic level compete with each other to get hold of the prey that share (mostly in the first trophic level). So an increase in B_0, that is, an increase in the number of species in the first trophic level, also causes a decrease in competition between the species in the second trophic level. Normalizing with respect to the total number of nodes in the network, the fraction of nodes with betweenness centrality equal to zero is 0.85 for network 247, 0.74 for network 225 and 0.72 for network 230. This would indicate that in ecosystems

NETWORK 247				
Abundance	In-degree	Out-degree	Betweenness	Closeness
15	47	0	48	0
2	48	1	49	1
33	49	2	50	2
36	50	3	51	3
49	51	4	52	4
38	52	5	53	5
51	53	13	54	13
5	54	14	55	14
46	55	15	56	15
48	56	31	0	31
56	57	32	1	32
0	58	33	2	33
4	59	34	3	34
32	60	35	4	35
34	61	36	5	36
1	43	37	6	37
14	44	38	7	38
35	45	48	8	48
37	46	49	9	49
53	0	50	10	50
54	1	51	11	51
55	2	52	12	52
13	3	53	13	53
31	4	54	14	54
43	5	55	15	55
44	6	56	16	56
45	7	6	17	43
50	8	7	18	44
52	9	8	19	45
3	10	9	20	46
27	11	10	21	6
41	12	11	22	7
21	13	12	23	8
29	14	16	24	9
39	15	17	25	10
25	16	18	26	11
60	17	19	27	12
61	18	20	28	16
9	19	21	29	17
30	20	22	30	18
10	21	23	31	19
26	22	24	32	20
6	23	25	33	21
7	24	26	34	22
8	25	27	35	23
12	26	28	36	24
18	27	29	37	25
20	28	30	38	26
58	29	39	39	27
42	30	40	40	28
11	31	41	41	29
16	32	42	42	30
17	33	43	43	39
19	34	44	44	40
22	35	45	45	41
23	36	46	46	42
24	37	47	47	47
47	38	57	57	57
57	39	58	58	58
59	40	59	59	59
28	41	60	60	60
40	42	61	61	61

NETWORK 225				
Abundance	In-degree	Out-degree	Betweenness	Closeness
34	52	0	50	0
36	53	1	51	1
30	54	2	52	2
15	50	3	53	3
31	51	4	54	4
14	44	5	41	5
5	45	6	42	6
6	46	7	43	7
29	47	8	44	8
37	48	14	45	14
1	49	15	46	15
4	41	29	47	29
8	42	30	48	30
42	43	31	49	31
50	0	32	0	32
28	1	33	1	33
39	2	34	2	34
0	3	50	3	50
2	4	51	4	51
3	5	9	5	41
7	6	10	6	42
32	7	11	7	43
33	8	12	8	9
41	9	13	9	10
51	10	16	10	11
40	11	17	11	12
38	12	18	12	13
46	13	19	13	16
20	14	20	14	17
54	15	21	15	18
27	16	22	16	19
9	17	23	17	20
11	18	24	18	21
43	19	25	19	22
22	20	26	20	23
23	21	27	21	24
17	22	28	22	25
52	23	36	23	26
48	24	38	24	27
12	25	39	25	28
10	26	40	26	36
13	27	41	27	38
18	28	42	28	39
24	29	43	29	40
26	30	52	30	52
16	31	53	31	53
19	32	54	32	54
21	33	35	33	37
25	34	37	34	35
35	35	44	35	44
44	36	45	36	45
45	37	46	37	46
47	38	47	38	47
49	39	48	39	48
53	40	49	40	49

NETWORK 230				
Abundance	In-degree	Out-degree	Betweenness	Closeness
42	60	0	58	0
19	61	1	59	1
38	62	2	60	2
5	63	3	61	3
35	64	4	62	4
1	58	5	63	5
45	59	6	64	6
2	49	7	49	7
44	50	8	50	8
8	51	9	51	9
40	52	10	52	10
58	53	18	53	18
18	54	19	54	19
37	55	35	55	35
34	56	36	56	36
4	57	37	57	37
7	47	38	48	38
47	48	39	47	39
46	65	40	0	40
0	0	41	1	41
3	1	42	2	42
6	2	11	3	48
9	3	12	4	58
10	4	13	5	59
36	5	20	6	11
39	6	21	7	12
41	7	22	8	13
59	8	23	9	20
28	9	24	10	21
60	10	48	11	22
16	11	58	12	23
13	12	59	13	24
22	13	14	14	47
14	14	15	15	14
29	15	16	16	15
33	16	17	17	16
30	17	25	18	17
56	18	26	19	25
25	19	27	20	26
51	20	28	21	27
32	21	29	22	28
55	22	30	23	29
62	23	31	24	30
12	24	32	25	31
31	25	33	26	32
20	26	34	27	33
24	27	44	28	34
48	28	46	29	44
53	29	47	30	46
11	30	60	31	60
17	31	61	32	61
26	32	62	33	62
43	33	63	34	63
49	34	64	35	64
52	35	43	36	43
61	36	45	37	45
63	37	49	38	49
15	38	50	39	50
21	39	51	40	51
23	40	52	41	52
27	41	53	42	53
50	42	54	43	54
54	43	55	44	55
57	44	56	45	56
64	45	57	46	57
65	46	65	65	65

Figure 4.26: Ranking of the nodes on the basis of their values of abundance, in-degree, out-degree, betweenness and closeness centrality for the three networks. The gradations of color suggest groups of values for the five quantities.

225 and 230 species in the second trophic level are subject to more competition than those in ecosystem 247.

4.3.4 Robustness of the three food webs

The best way to verify what is suggested by the values of the clustering coefficient and of the connectance regarding the robustness of the three networks, is to calculate the value of the robustness of the networks according to the definition provided by Dunne et al. (2002): the robustness value is given by the fraction of nodes that must be removed to induce a total loss of at least 50 % of the species (either by primary extinction and by secondary extinction). The removal or failure of one node is not independent of the others because the activity of each node depends on the activity of its neighboring nodes. As seen in the previous study, cascade failures could be observed in which the failure of a node induces the failure of the nodes connected to it. For this reason it is important to perform the calculations of the robustness of the network, not only from a structural point of view, but simulating the dynamics resulting from the removal of the nodes, as is done in the present study. Using the model previously described, random and targeted attacks were simulated. Random attacks consist of random removal of species from the network, while targeted attacks are aimed at removing species that are considered most important for the integrity of the network.
As specified by Dunne (2006), in the specific case of food webs, the removal of the most interconnected species is not always the best strategy to carry out targeted attacks affecting the integrity of the ecosystem. In particular, Allesina and Bodini (2004) have shown that the most important species for the integrity of the system are the dominant species, that is those that pass energy to other species along the food chain. It is precisely the removal of these species that causes a greater number of secondary extinctions. The dominant species, although probably having a high out-degree value, are not necessarily the ones most interconnected if ingoing links are also considered. For this reason, in this study, the criterion for the removal of species in targeted attacks is the elimination of those nodes with a high closeness centrality value (for the same values of the closeness centrality it has been chosen to remove the species that is most abundant).
I proceeded in the following way: starting from the undisturbed system, the closeness centrality is calculated for all nodes and the one with the highest value is selected and removed. The dynamics of the system and the possible occurrence of secondary extinctions are therefore observed. Once the system has reached a condition of stability, the closeness centrality values are recalculated for all nodes and once again the one with the highest value is selected and removed. This process ends when half of the species have disappeared from the ecosystem (both because of removals and because of secondary extinctions). The robustness values for the

three networks in the case of targeted attacks and in the case of random attacks (averaged over 10 different simulations) together with the alteration index values are shown in Figure 4.27.

From the results obtained, some observations can be made. The first concerns the comparison between networks. Network 247 proves to be the most robust both in the case of targeted attacks and in the case of random attacks, confirming what already suggested by the values of the clustering coefficient and of the connectance; network 225 follows and finally network 230. The second observation concerns a comparison between types of attacks: all three networks are more robust against random attacks rather than targeted attacks. The last consideration concerns the relation between the alteration index and the robustness of the system. The alteration suffered by the ecosystem depends on the robustness of the network. The alteration index, once again, proves to be a good parameter for measuring the disgregation of the system. As expected, in the tests carried out, when robustness is greater, the alteration index is smaller, with the only exception of the case in wich network 247 is subject to targeted attack. Below I try to explain this apparent contradiction.

Figure 4.28 shows the trend of the alteration index, the connectance C, the complexity $c = CS$ and species richness S, as the nodes with the highest closeness centrality are removed for the calculation of the robustness against targeted attacks. We note that connectance and complexity have very similar trends: these decrease much more gradually and ultimately have higher values for network 247 than for the other two networks. The most robust network (web 247) is therefore the one that has higher values of connectance and complexity both at the beginning and at the end of the simulation. From the trend of species richness we can see the moments in which secondary extinctions occurred. Note that the major secondary extinctions occurred earlier in the 247 network than in the other two networks. This explains the evident increase in the alteration index in network 247 which is larger than that recorded for the other two networks: at the time of secondary extinctions, network 247 has a greater number of nodes than webs 225 and 230 and, as a consequence, the number of species that undergo alteration is greater (remember that the alteration index is additive with respect to the abundance variations suffered by the species present in the system). This also explains why the alteration index of networks 225 and 230 undergoes a greater increase at the beginning, when only a small fraction of secondary extinctions occurs, and less when secondary extinctions are more: at the time of the major secondary extinctions, there are fewer species and therefore fewer species undergo an alteration.

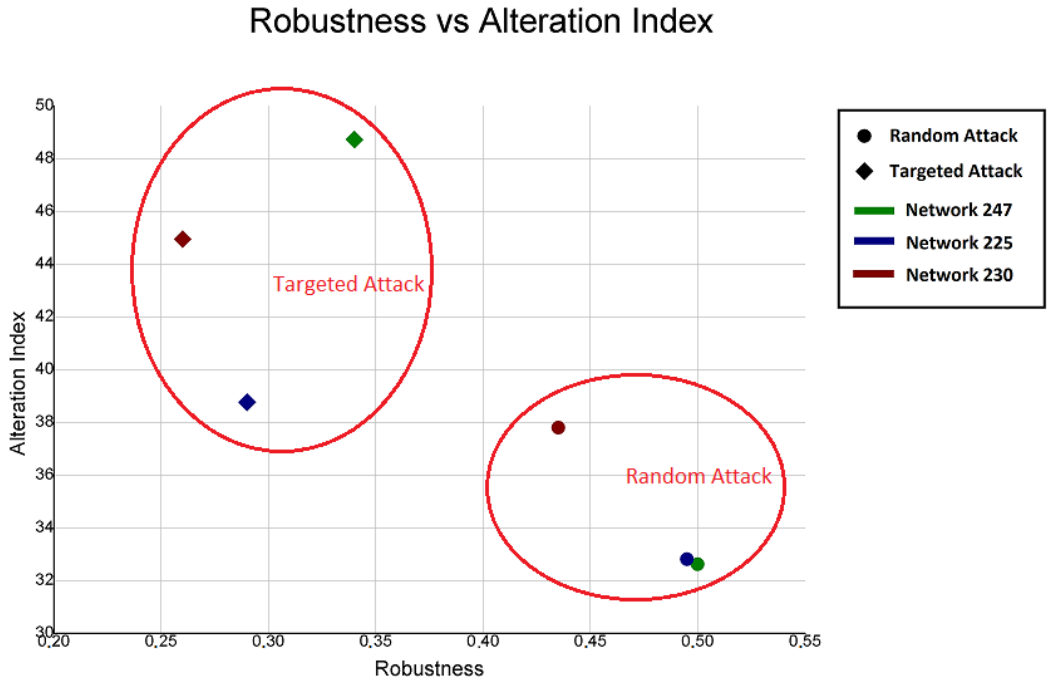

	TARGETED ATTACK	
	ROBUSTNESS	ALTERATION INDEX
NETWORK 247	0.34	48.73
NETWORK 225	0.29	38.76
NETWORK 230	0.26	44.96

	RANDOM ATTACK	
	ROBUSTNESS	ALTERATION INDEX
NETWORK 247	0.50	32.62
NETWORK 225	0.49	32.81
NETWORK 230	0.43	37.80

Figure 4.27: Above are shown the values of the alteration index as a function of the robustness that the three networks have shown if subjected to targeted and random attacks. The tables below show the robustness and the alteration index for the three networks, in the case of targeted attacks and random attacks. The values for random attacks are the average values obtained on 10 tests.

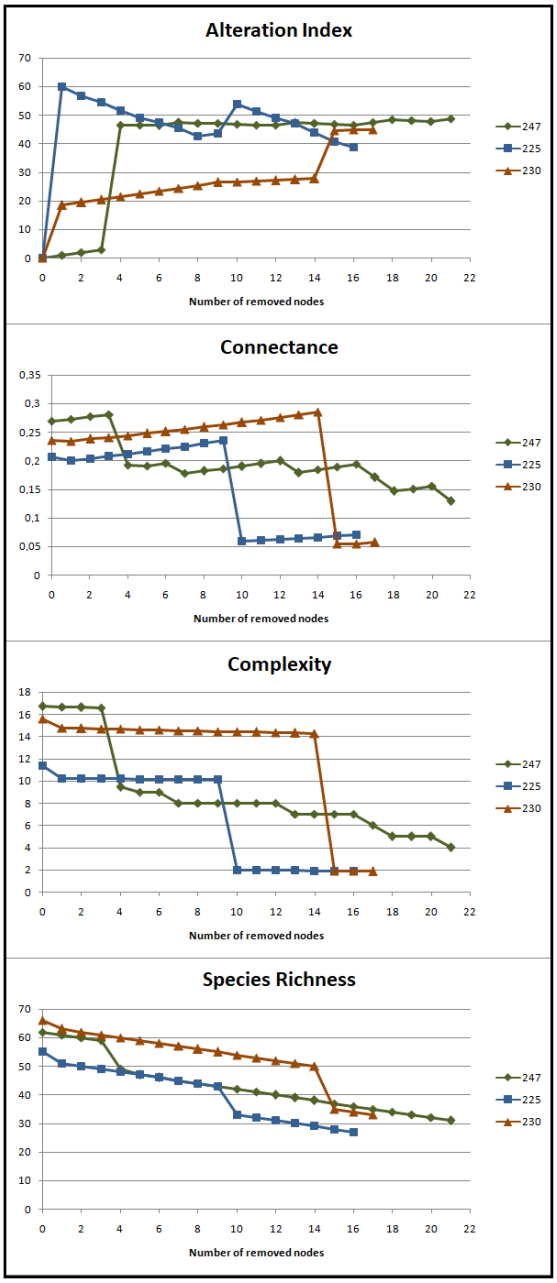

Figure 4.28: Trend of the alteration index, the connectance, the complexity and species richness, as the nodes with the highest closeness centrality are removed, for the three food webs.

4.3.5 Conclusive insights

In this study three soil ecosystems, that differ in the type of management and in the concentration of some elements, have been compared in the attempt to understand if and how anthropogenic action affects soil ecosystems.
With regard to the topology, it has been found that the structure of all three networks is small world. Furthermore, all three networks have a disassortative nature as expected for food webs (Newman (2002, 2003), Stouffer et al. (2005)). Differences were found in the values of the clustering coefficient, of the connectance and of the complexity. These values are greater for network 247 and this suggested a greater robustness of this network than the other two (Dunne et al. (2002)). The calculation of the robustness, through a dynamic model (Conti et al. (2020)), confirmed this hypothesis. It therefore appears that the ecosystem related to the fallowed pastures with low pressure management is more robust than the two ecosystems releted to organic farms subject to middle intensity management. There are also differences between the two sites dedicated to organic agriculture, that could be connected to the different concentration of elements present in the soil and therefore to the anthropic action. The value of the clustering coefficient and the calculation of robustness suggest that network 225 is more robust than network 230, the site with high concentrations of heavy metals in the soil. This result is in contrast with what Dunne et al. (2002) affirmed, about the positive relationship between connectance and robusteness, but remaining available networks may constitute a larger sample on which to test this correspondence. It is quite intuitive to say that the nutrients of the soil and its composition affect the resources available to soil organisms. This affects the type and abundance of organisms present in the soil and therefore the structure of the network from the lowest to the highest trophic levels of the food web (Wall et al. (2015), Clay (2004), Powell (2007)). Despite this, in order to fully ascertain the correlations existing between the robustness of the trophic network and the type of management to which the site is subjected as well as the type of soil composition, further studies would be required in order to shed light on the real impact that this type of management could have on the robustness of soil ecosystems (133 trophic networks, among which are also present conventional, intensive and super-intensive farms, are still available on which to repeat the same analysis conducted on these three networks). If the evidences suggested by this study were to be confirmed, the robustness shown by the networks could be useful for evaluating, from an ecological point of view, the sustainability of the agricultural practices to which the ecosystem is subject.

Conclusion

In my research I dealt with the dilemma between cooperation and competition. As we have seen these two behavioral tendencies can manifest themselves in various subjects and at different levels: cells in our body, individuals in a social group, companies in the market, nations in the world, animals in an ecosystem and so on. One can almost say that every aspect of our life is permeated by this eternal conflict between cooperation and competition. The topic is therefore of crucial importance: understanding the basic concepts of cooperation and competition is fundamental to dissecting the dynamics of all these phenomena. In my own little way, I focused on economic and ecological applications.

In the first study I address the issue of tax evasion, an age-old phenomenon that clearly is related to cooperation and competition. I presented a simple model of tax evasion, which augments a prisoner's dilemma framework with an agent-based design, in order to characterize some elements of collective dynamics when altruism and egoism come to play with regards to the number of taxpayer of a community. Results of simulations show that the model replicates consolidated results of basilar game theory. The average social capital of taxpayers is always lower than the average social capital of evaders: this is the evidence of Nash-dominance of the non-cooperative behavior, that is, non-cooperation is the rational choice from an individual point of view. Nevertheless, the average capital of the collectivity is a positive function of the number of taxpayers. Community with a small fraction of cooperator are disadvantaged. A selfish citizen who uses public goods and services without properly contributing to the related costs causes a severe damage to the socio-economical environment depriving governments of their fiscal resources and reducing well-being of societies. The capital of the collectivity increases only thanks to the contribution of altruistic players. Thus, from the collective point of view, groups with more cooperators are favored compared to groups with few cooperators.
In the second part of the study, the model was enriched by the introduction of the possibility for agents to change their behavior according to imitation and economic satisfaction. New interesting results have been obtained, showing the presence of a

threshold, in the initial percentage of taxpayers, able to ensure an average economic advantage to altruists. As in real systems, the percentage of citizens paying taxes is crucial in sustaining a sufficient quality/quantity of the public good. It has been found that reasonable policy intuitions are devoted to induce a feeling of satisfaction in taxpayers, in order to reduce the temptation to evade, even when the personal economic situation is bad. An educational policy spreading a tax morale is expected to be more effective than a tax amnesty, because it operates in such a way that individuals feel themselves rewarded by institutions. Education can also impact on the number of taxpayers, which has been described as a key factor in determining the average social capital. There is also evidence that the amount of the fine should be far greater than the tax pressure, in order to induce tax payment as a strong economic convenience while an increase in the probability of an audit drastically reduces the value of tax evasion.

In the second study I investigate ecosystems of soil invertebrates through the knowledge of their characteristic trophic web. In this framework, competitiveness is not only found at the level of the trophic web (in the search for resources and in the fight for survival between prey and predator), but, at a different level, comes into play competitiveness between soil organisms and human action that tends to contaminate natural habitats. Human cooperation in this case would consist of seeking eco-sustainable solutions rather than intensive farming methods.
In the first part of the study, I create a model whose dynamics is dictated by an extension of the Lotka-Volterra equations. In particular, I combine the Lotka-Volterra model with the logistic equation in order to take into account intra-specific and inter-specific competition between species in the ecosystem. It has been shown how the removal of some species from the ecosystem, which could reproduce the use of herbicides and pesticides in agricultural activities, can cause secondary extinctions and severe alterations in the architecture of the ecosystem.
In the second part of the study, three soil ecosystems, that differ in the extent of anthropic action to which they are subject, were compared. The study of the structure of the three networks, with the estimate of the clustering coefficient and of the connectance, and the dynamical evaluation of the robustness, by simulating attacks on the ecosystems, clearly show that the ecosystem less subject to anthropic disturbances has a structure that makes it more resistent against perturbations. My study seems to suggest that the robustness of the trophic network is affected by the type of management to which the ecosystem is subject. If this evidence were to be confirmed, in further studies carried out on other networks, the robustness shown by food webs could be considered as an index of sustainability of the type of agriculture to which the ecosystem is subject.
The concept of environmental sustainability has a global meaning, which takes into account social and economic as well as environmental dimensions. It is the

condition of a development capable of ensuring the satisfaction of the needs of the present generation without compromising the possibility of future generations to make their own. A balanced ecosystem is implicitly eco-sustainable. In the case of agriculture, eco-sustainability concerns the use of methods that guarantee the satisfaction of the needs of a growing world population and, at the same time, guarantee a non-destructive exploitation of the soil, so that this availability is guaranteed also in the future. Soil ecosystem is a complex system whose integrity depends on numerous factors including the stability of its trophic web. Since the stability of an ecosystem is closely linked to its robustness, the method proposed here could be useful for evaluating, from an ecological point of view, the sustainability of certain agricultural practices. This would make it possible to identify agricultural methods that are not deleterious for the robustness of the trophic network and, among these, through economic evaluations, choose those that allow the needs of the whole population to be met. Note that this address, as for agriculture, can apply to any type of anthropic disturbance, from cattle breeding to industrial activities. Going to see the impact that these activities have on the robustness of ecosystems, an ecological assessment of the sustainability of these practices can be made.

Acknowledgement

I would like to thank Prof. Alessio E. Biondo for believing in my potential by giving me the opportunity to undertake the path of the PhD, during which I learned the job of the researcher.
Necessary for the success of this venture was Prof. Alessandro Pluchino, to whom my warmest thanks go for accompanying me throughout this journey and for being a guide always careful and helpful.
I would like to thank Professors Christian Mulder and Erminia Conti for giving me the opportunity to do research in a field that is extremely interesting for me, that of ecology. It would be a pleasure for me to continue doing good research with you.
Finally I heartily thank my loving family and Emilio for being there, for all of your support and comfort and for always giving me so many moments of pure serenity.

The bibliography

Albert A., Jeong H., A.L. Barabasi (1999). Diameter of the World-Wide Web. Nature, 401 130

Allesina S., Bodini A. (2004). Who dominates whom in the ecosystem? energy flow bottlenecks and cascading extinction. J. Theor. Biol. 230, 351-358.

Allingham M.G. and Sandmo A. (1972). Income Tax Evasion: A Theoretical Analysis. Journal of Public Economics, vol.1, 323-338.

Alm J. (2012). Measuring, explaining, and controlling tax evasion: lessons from theory, experiments, and eld studies. International Tax and Public Finance, 19 (1), 54–77.

Alm J., McClelland G.H. and Schulze W.D. (1992). Why do people pay taxes? Journal of Public Economics, vol.48, pp.21–38.

Alstadsæter A., Johannesen N. and Zucman G. (2017). Tax Evasion and Inequality. NBER Working Paper No. 23772, September 2017. Invited resubmission: American Economic Review.

Andreoni J., Erard B. and Feinstein J. (1998). Tax compliance. Journal of Economic Literature, 36 (2), 818–860.

Anton A., Geraldi N. R., Lovelock C. E., Apostolaki E. T., Bennett S., Cebrian J., Krause-Jensen D., Marbà N., Martinetto P., Pandolfi J. M., Santana-Garcon J. and Duarte C. M. (2019). Global ecological impacts of marine exotic species. Nature Ecology and Evolution volume 3, pages787–800.

Barabasi Albert-Laszlo (2016). Network Science. Cambridge University Press.

Barabasi A.-L. and Albert R. (1999). Emergence of Scaling in Random Networks.

Science Vol. 286, Issue 5439, pp. 509-512.

Barnosky A. D., Matzke N., Tomiya S., Wogan G. O. U., Swartz B., Quental T. B., Marshall C., McGuire J. L., Lindsey E. L., Maguire K. C., Mersey B. and Ferrer E. A. (2011). Has the Earth's sixth mass extinction already arrived?. Nature volume 471, pages51–57.

Barnosky A.D., Hadly E.A., Bascompte J., Berlow E.L., Brown J.H., Fortelius M., Getz W.M., Harte J., Hastings A., Marquet P.A. et al. (2012). Approaching a state shift in Earth's biosphere. Nature 486: 52-58.

Baumol W. (1952). Welfare Economics and the Theory of the State. Cambridge, Massachusetts: Harvard University Press.

Bazart C., Bonein A., Hokamp S. and Seibold G. (2016). Behavioral economics and tax evasion–calibrating an agent-based econophysics model with experimental tax compliance data. Journal of Tax Administration, vol.2 (1), pp.126–144.

Becker G.S. (1968). Crime and punishment: an economic approach. The Journal of Political Economy, vol.76 (2), pp.169–217.

Bernhardt E.S., Rosi E.J. and Gessner M.O. (2017). Synthetic chemicals as agents of global change. Frontiers Ecol. Environ., 15, 84-90.

Bertotti M.L. and Modanese G. (2014). Micro to macro models for income distribution in the absence and in presence of tax evasion. Applied Mathematics and Computation, vol.224, pp.836–846.

Bertotti, M.L. & Modanese, G. (2016). Microscope Models for the Study of Taxpayer Audit Effects, *arXiv* 1602.08467v1 [q- n.GN] 18 February 2016.

Biondo A.E., Pluchino A., Rapisarda A. and Helbing D. (2013a). Reducing financial avalanches by random investments. Phys. Rev. E 88(6):062814.

Biondo A.E., Pluchino A., Rapisarda A. and Helbing D. (2013b). Are random trading strategies more successful than technical ones. PLoS One 8(7):e68344.

Biondo A.E., Pluchino A. and Rapisarda A. (2013c). The beneficial role of random strategies in social and financial systems. J. Stat. Phys. 151(3-4):607-622.

Biondo A.E., Pluchino A. and Rapisarda A. (2014). Micro and macro benefits of random investments in financial markets. Cont. Phys. 55(4):318-334.

Biondo A.E., Pluchino A. and Rapisarda A. (2015). Modeling financial markets by self-organized criticality. Phys. Rev. E 92(4):042814.

Biondo A.E., Pluchino A. and Rapisarda A. (2017). Contagion dynamics in a multilayer network model of financial markets. Italian Economic Journal, DOI 10.1007/s40797-017-0052-4.

Bloomquist K.M. (2006). A comparison of agent-based models of income tax evasion. Social Science Computer Review, vol.24 (4), pp.411–425.

Bolton G.E., Ockenfels A. (2000). ERC: A theory of equity, reciprocity, and competition. American economic review, vol.90 (1), pp.166-193.

Borrvall C., Ebenman B. and Jonsson T. (2000). Biodiversity lessens the risk of cascading extinction in model food webs. Ecol. Lett., 3, 131-136.

Bourne P.E., Brenner S.E. and Eisen M.B. (2005). A new community journal. PLoS Comput. Biol., 1(1), e4.

Briand F. (1983). Environmental control of foodweb structure. Ecology 64, 395 253-263.

Briand F. and Cohen J. E. (1984). Community FoodWebs Have Scale-Invariant Structure. Nature 398:330-334.

Briand F. and Cohen J.E. (1987). Environmental correlates of food chain length. Science 238, 956-960.

Brose U., Archambault P., Barnes A.D., Bersier L.-F., Boy T., Canning-Clode J. et al. (2019). Predator traits determine food-web architecture across ecosystems. Nature Ecol. Evol., 3, 919-927.

Buehn A. and Schneider F. (2012). Shadow economies around the world: novel insights, accepted knowledge, and new estimates. International Tax and Public Finance, vol.19 (1), pp.139–171.

Callen E. and Shapero D. (1974). A theory of social imitation. Physics Today,

vol. 27(7). DOI: 10.1063/1.3128690

Camacho J., Guimerà R. and Amaral L. A. N. (2002). Robust Patterns in Food Web Structure. Phys. Rev. Lett. 88:228102.

Capraro V. (2013). A model of human cooperation in social dilemmas. PLoS One, vol.8 (8), e72427.

Capraro V., Rand D.G. (2018). Do the Right Thing: Experimental evidence that preferences for moral behavior, rather than equity or efficiency per se, drive human prosociality. Judgment and Decision Making, vol.13 (1), pp.99-111.

Capraro V. and Perc M. (2018). Grand challenges in social physics: In pursuit of moral behavior. Frontiers in Physics, vol.6, p.107

Cattin M. F., Bersier L. F., Banasek-Richter C., Baltensperger M. and Gabriel J-P (2004). Phylogenetic Constraints and Adaptation Explain Food-Web Structure. Nature 427:835-839.

Ceballos G., Ehrlich P.R., Barnosky A.D., García A., Pringle R.M. and Palmer T.M. (2015). Accelerated modern human-induced species losses: Entering the sixth mass extinction. Sci. Advances; 1: e1400253.

Charness G. and Rabin M. (2002). Understanding social preferences with simple tests. The Quarterly Journal of Economics, vol.117 (3), pp.817-869.

Chase J.M. (2000). Are there real differences among aquatic and terrestrial food webs? Trends Ecol. Evol. 15, 408-411.

Cipolla C. M. (2011). The Basic Laws of Human Stupidity. Il Mulino, Bologna.

Clay J. (2004). World agriculture and the environment: A commoditybycommodity guide to impacts and practices. Washington (DC): Island Press.

Clotfelter C.T. (1983). Tax Evasion and Tax Rates: An analysis of individual returns. The Review of Economics and Statistics, vol.65, pp.363-73.

Cohen J.E. (1994). Marine and continental food webs: Three paradoxes?. Phil. Trans. Roy. Soc. Lond. B 343, 57-69.

Cohen J.E. (2004). Mathematics is biology's next microscope, only better; biology is mathematics' next physics, only better. PLoS Biol., 2(12), e439.

Cohen J. E. and Mulder C. (2014). Soil invertebrates, chemistry, weather, human management, and edaphic food webs at 135 sites in the Netherlands: SIZEWEB. Ecology 95:578, http://dx.doi.org/10.1890/13-1337.1.

Cohen J. E. and Newman C. M.(1985). A Stochastic Theory of Community Food Webs: I. Models and Aggregated Data. Proc. Roy. Soc. Lond. B 224:421-448.

Cohen J. E., Briand F. and Newman C. M. (1986). A Stochastic Theory of Community FoodWebs: III. Predicted and Observed Length of Food Chains. Proc. Roy. Soc. Lond. B 228:317-353.

Conti E., Di Mauro L.S., Pluchino A., Mulder C. (2020). Testing for top-down cascading effects in a biomass-driven ecological network of soil invertebrates. Ecology and Evolution doi:10.DOI:10.1002/ece3.6408.

Crane S.E. and Nourzad F. (1987). On the Treatment of Income Tax Rates in Empirical Analysis of Tax Evasion. Kyklos, vol.40, pp.338-348.

D'Agostino G., Scala A., Zlatic V. and Caldarelli G. (2012). Robustness and Assortativity for Diffusion-like Processes in Scale- free Networks. ArXiv:1105.3574v3 [physics.soc-ph] 23 Nov 2012

Dalamagas B. (2011). A Dynamic Approach to Tax Evasion. Public Finance Review, vol.39 (2), pp.309-326.

De Ruiter P.C., Neutel A.-M. and Moore J.C. (1995). Energetics, patterns of interaction strengths, and stability in real ecosystems. Science, 269, 1257-1260.

Di Mauro L. S., Pluchino A., Biondo A. E. (2019). Tax evasion as a contagion game: evidences from an agent-based model. European Physical Journal B, Condensed Matter and Complex Systems (2019) 92: 103

Di Mauro L. S., Mulder C., Conti E. and Pluchino A. (2020). Robustness of soil ecosystems under different regimes of management. arXiv:2005.13414 [q-bio.PE].

Dunne J. A., Williams R. J. and Martinez N. D. (2002). Network Structure and Biodiversity Loss in Food Webs: Robustness Increases with Connectance. Ecol.

Lett. 5:558-567.

Dunne, J.A., Williams, R.J. and Martinez, N.D. (2004). Network structure and robustness of marine food webs. Mar. Ecol. Prog. Ser. 273, 291-302.

Dunne J.A. (2006). The network structure of food webs. In: Ecological Networks: Linking structure to dynamics in food webs (Pascual, M. and Dunne, J.A.,eds.). Oxford: Oxford University Press , pp. 27-86.

Elsenbroich C. and Gilbert N. (2014). Imitation and Social Norms. In: Modelling Norms. Springer, Dordrecht.

Elster J. (1989). Nuts and bolts for the social sciences. Cambridge University Press.

Elton C. S. (1927). Animal Ecology. Sidgwick and Jackson, London.

Elton C. S. (1958). Ecology of Invasions by Animals and Plants. London: Chapman and Hall.

Epstein R.A. (1993). Altruism: Universal and Selective. Social Service Review, vol.67, (3), pp.388-405

Exbrayat J., Liu Y. Y. and Williams M. (2017). Impact of deforestation and climate on the Amazon Basin's above-ground biomass during 1993–2012. Scientific Reports volume 7, Article number: 15615

Faloutsos M., Faloutsos P., Faloutsos C. (1999). On power-law relationships of the Internet topology. Association for Computing Machinery SIGCOMM Computer Communication Review.

Fehr E. and Schmidt K.M., (1999). A theory of fairness, competition, and cooperation. The Quarterly Journal of Economics, vol.114 (3), pp.817-868.

Feld L.P. and Frey B.S. (2007). Tax Compliance as the Result of a Psychological Tax Contract: The Role of Incentives and Responsive Regulation, Law and Policy, doi.org/10.1111/j.1467-9930.2007.00248.x

Fiscus D.A. and Neher D.A. (2002). Distinguishing sensitivity of free living soil nematode genera to physical and chemical disturbances. Ecol. Appl., 12, 565-575.

Flood M.M. (1952). Some Experimental Games. Research Memorandum RM-789. Santa Monica, Calif.: RAND Corporation.

Fortin B., Lacroix G. and Villeval M.C. (2007). Tax evasion and social interactions. Journal of Public Economics, vol.91, pp.2089–2112.

Granovetter M. (1978). Threshold Models of Collective Behavior. American Journal of Sociology, vol. 83(6), pp.1420-1443.

Grassi R., Scapellato R., Stefani S. and Torriero A. (2009). Betweenness centrality: extremal values and structural properties. Networks, Topology and Dynamics. Springer 161-175.

Gross B. and Cardinale B.J. (2005). The functional consequences of random vs. ordered species extinctions. Ecol. Lett., 8, 409-418.

Haldane J. B. S. (1955). Population Genetics. New Biology, 18, pp.34-51.

Hamilton W. D. (1964). The Genetical Evolution of Social Behaviour, i, ii in Journal of Theoretical Biology, 7, pp.1-16, 17-52.

Hardin R. (1995). One for All: The Logic of Group Conflict. Princeton University Press, Princeton, NJ.

Hastings A. (1996). What equilibrium behavior of Lotka-Volterra models does not tell us about food webs. Food Webs: Integration of Patterns and Dynamics, eds. G. A. Polis and K. O. Winemiller , 211-217.

Heckathorn D.D. (1996). The dynamics and dilemmas of collective action. American Sociological Review, vol.61(2), pp.250–277.

Hodzic M., Selman S. and Hadzikadic M. (2016). Complex Ecological System Modeling. Periodicals of Engineering and Natural Sciences, 4 (1).

Hokamp S. (2013). Income tax evasion and public goods provision – theoretical aspects and agent-based simulations. PhD thesis. Brandenburg University of Technology Cottbus.

Hokamp S. and Pickhardt M. (2010). Income tax evasion in a society of hetero-

geneous agents – evidence from an agent-based model. International Economic Journal, 24 (4), 541–553.

Holt R.D. and Polis G.A. (1997). A theoretical framework for intraguild predation. Am. Nat. 149, 745-764.

Hunt H.W. and Wall D.H. (2002). Modelling the effects of loss of soil biodiversity on ecosystem function. Global Change Biol., 8, 33-50.

Hunt H.W., Coleman D.C., Ingham E.R., Ingham R.E., Elliott E.T., Moore J.C. et al. (1987). The detrital food web in a shortgrass prairie. Biol. Fert. Soils 3, 57–68.

Internal Revenue Service (2016). IRS Tax Gap Estimates for Tax Years 2008–2010. https://www.irs.gov/PUP/newsroom/tax gap estimates for 2008 through 2010.pdf (accessed 23 November 2016).

IPBES Intergovernmental Science-Policy Platform on Biodiversity and Ecosystem Services (2019). Report of the Plenary of the Intergovernmental Science-Policy Platform on Biodiversity and Ecosystem Services on the work of its seventh session. IPBES/7/10/Add.1.

Ives A.R., Cardinale B.J. (2004). Food-web interactions govern the resistance of communities after non-random extinctions. Nature, 429, 174-177.

Jackson J.B.C., Kirby M.X., Berger W.H., Bjorndal K.A., Botsford L.W., Bourque B.J., Bradbury R.H., Cooke R., Erlandson J., Estes J.A. et al. (2001). Historical overfishing and the recent collapse of coastal ecosystems. Science; 293: 629-637.

Jeong H., Mason S. P., Barabasi A.-L., Oltvai Z. N. (2001). Lethality and centrality in protein networks. Nature volume 411, pages 41–42.

Jeong H., Tombor B., Albert R., Oltvai Z.N., Barabási A.-L. (2000). The large-scale organization of metabolic networks. Nature 407 (6804):651-4.

Jordán F., Scheuring I. and Vida G., (2002). Species positions and extinction dynamics in simple food webs. J. Theor. Biol. 215, 441-448.

Kirchler E. (2007). The Economic Psychology of Tax Behavior. Cambridge University Press, Cambridge.

Kondoh M. (2005). Linking flexible food web structure to population stability: A theoretical consideration on adaptive food webs. In: De Ruiter, P.C., Wolters, V. and Moore, J.C. (eds.). Dynamic Food Webs – Multispecies assemblages, ecosystem development and environmental change. Theoretical Ecology Series, Academic Press, Burlington, MA, pp. 101-113.

Kratina P., LeCraw R.M., Ingram T. and Anholt B.R. (2012). Stability and persistence of food webs with omnivory: Is there a general pattern?. Ecosphere, 3(6), 50.
La Porta R., Lopez-de-Salanes F ., Shleifer A. and Vishny R. (1999). The Quality of Government. Journal of Law, Economics, and Organization, vol.15 (1), pp. 222–279. doi:10.1093/jleo/15.1.222.

Lawrence D. and Vandecar K. (2015). Effects of tropical deforestation on climate and agriculture. Nature Climate Change volume5, pages27–36

Liljeros F., Edling C. R., Amaral L.A., Stanley H.E. and Aberg Y. (2001). The web of human sexual contacts. Nature 2001 Jun 21;411(6840):907-8.

Lima F.W.S. and Zaklan G. (2008). A multi-agent-based approach to tax morale. International Journal of Modern Physics C: Computational Physics and Physical Computation, vol.19 (12), pp.1797–1808.

Link J. (2002). Does food web theory work for marine ecosystems?. Mar. Ecol. Prog. Ser. 230, 1-9.

Liu X., Pan Q., He M., Liu A. (2019). Promotion of cooperation in evolutionary game dynamics under asymmetric information, Physica A 521, pp.258-266.

Lotka A. J. (1920). Analytical note on certain rhythmic relations in organic systems, Proc. Nat. Acad. 6 , 410-415

MacArthur, R. (1955). Fluctuations of animal populations and a measure of community stability. Ecology 36, 533-536.

Malhi Y., Roberts J. T., Betts R. A., Killeen T. J., Li W. and Nobre C. A. (2008). Climate Change, Deforestation, and the Fate of the Amazon. Science 319, 169 (2008); DOI: 10.1126/science.1146961.

Mancinelli G. and Mulder C. (2015). Detrital dynamics and cascading effects on

supporting ecosystem services. Adv. Ecol. Res., 53, 97-160.

Martinez N. D. (1991). Artifacts or Attributes? Effects of Resolution on the Little Rock Lake Food Web. Ecol. Monogr. 61:367-392.

Martinez N. D. (1992). Constant Connectance in Community FoodWebs. Amer. Natur. 139:1208-1218.

Mäs M., and Opp K.D. (2016) When is ignorance bliss? Disclosing true information and cascades of norm violation in networks. Social Networks, pp.116-129

May R. M. (1973). Stability and Complexity in Model Ecosystems. Princeton, NJ: Princeton University Press.

McCann K., Hastings A. (1997). Re-evaluating the omnivory-stability relationship in food webs. Proc. Roy. Soc. Lond. B 264, 1249-1254.

McDonald R.I. and Crandall C.S. (2015). Social norms and social influence. Current Opinion in Behavioral Sciences, vol.3, pp.147–151.

Milo R., Shen-Orr S., Itzkovitz S., Kashtan N., Chklovskii D. and Alon. U. (2002). Network Motifs: Simple Building Blocks of Complex Networks. Science 298:824-827.

Molloy M. and Reed B. (1995). A critical point for random graphs with a given degree sequence. Random Structures & Algorithms 6, 161-180.

Montoya J. M. and R. V. Solé (2002). Small World Patterns in Food Webs. J. Theor. Biol. 214:405-412.

Moore J.C., De Ruiter P.C. and Hunt H.W. (1993). Influence of productivity on the stability of real and model ecosystems. Science, 261, 906-908.

Moore J.C. and De Ruiter P.C. (2012). Energetic Food Webs: An Analysis of Real and Model Ecosystems. Oxford Series in Ecology and Evolution, Oxford University Press.

Morlon H., White E.P., Etienne R.S., Green .J.L., Ostling A., Alonso D. et al. (2009). Taking species abundance distributions beyond individuals. Ecol. Lett., 12, 488-501.

Mouquet N., Gravel D., Massol F. and Calcagno V. (2013). Extending the concept of keystone species to communities and ecosystems. Ecol. Lett., 16, 1-8.

Mulder C., Boit A., Bonkowski M., De Ruiter P. C., G. Mancinelli G., Van der Heijden M. G. A., Van Wijnen H. J., Vonk J. A. and Rutgers M. (2011). A belowground perspective on Dutch agroecosystems: how soil organisms interact to support ecosystem services. Advances in Ecological Research 44:277–357.

Mulder C., Cohen J.E., Setala H., Bloem J. and Breure A.M. (2005). Bacterial traits, organism mass, and numerical abundance in the detrital soil food web of Dutch agricultural grasslands. Ecol. Lett., 8, 80-90.

Mulder C., De Zwart D., Van Wijnen H.J., Schouten A.J. and Breure A.M. (2003). Observational and simulated evidence of ecological shifts within the soil nematode community of agroecosystems under conventional and organic farming. Funct. Ecol. 17, 516-525.

Mulder C., Den Hollander H.A. and Hendriks A.J. (2008). Aboveground herbivory shapes the biomass distribution and flux of soil invertebrates. PLOS ONE, 3(10), e3573.

Mulder C. and Elser J.J. (2009). Soil acidity, ecological stoichiometry and allometric scaling in grassland food webs. Global Change Biol., 15, 2730-2738.

Mulder C. and Vonk J. A. (2011). Nematode traits and environmental constraints in 200 soil systems: scaling within the 60–6,000 mm body size range. Ecology 92:2004, http://dx.doi.org/10.1890/11-0546.1.

Murakami M., Ishikura S., Kominami D., Shimokawa T. and Murata M. (2017). Robustness and efficiency in interconnected networks with changes in network assortativity. Applied Network Science DOI 10.1007/s41109-017-0025-4 Springer

Myles, G.D. and Naylor, R.A. (1996). A Model of Tax Evasion with Group Conformity and Social Custom. European Journal of Political Economy, vol.12 (1), pp.49-66.

Neher D.A., Wu J., Barbercheck M.E. and Anas O. (2005). Ecosystem type affects interpretation of soil nematode community measures. Applied Soil Ecol., 30, 47-64.

Nicolaides P. (2014). Tax Compliance Social Norms and Institutional Quality: An Evolutionary Theory of Public Good Provision. Taxation Papers 46, Directorate General Taxation and Customs Union, European Commission.

Nash J. F. (1951). Non Cooperative Games. The Annals of Mathematics, Second Series, Vol. 54, No. 2, pp. 286-295.

Neal D. (2019). Introduction to Population Ecology. Cambridge University Press, Cambridge, UK.

Neher D.A., Wu J., Barbercheck M.E. and Anas O. (2005). Ecosystem type affects interpretation of soil nematode community measures. Applied Soil Ecol., 30, 47-64.

Newman M. E. J. (2001). Scientific collaboration networks. Network construction and fundamental results. Physical Review E 64, 016131.

Newman M.E.J. (2002). Assortative mixing in networks. Phys. Rev. Lett. 89, 208701.

Newman M.E.J. (2003). Mixing patterns in networks. Phys. Rev. E 67, 026126.

Nowak M. A. (2006). Five rules for the evolution of cooperation, Science, 314, pp.1560-1563. doi:10.1126/science.1133755.

Nowak M. A. (2011) with Roger Highfield. SuperCooperators: Altruism, Evolution, and Why We Need Each Other to Succeed. Free Press.

Oates L. (2015). Review of recent literature. Journal of Tax Administration, vol.1 (1), pp.141–150.

Panades J. (2004). Tax Evasion and Relative Tax Contribution, Public Finance Review, vol.32 (2), pp.183-195.

Pascual M. and Dunne J.A. (2006). Ecological Networks: Linking Structure to Dynamics in Food Webs. Oxford University Press, Oxford.

Perc M., Szolnoki A. (2010). Coevolutionary games – A mini review. BioSystems, vol.99, pp.109-125.

Perc M., Gómez-Gardeñes J., Szolnoki A., Floría L.M. and Moreno Y. (2013).

Evolutionary dynamics of group interactions on structured populations: A review. Journal of the Royal Society Interface, vol.10, 20120997

Perc M., Jordan J.J., Rand D.G., Wang Z., Boccaletti S., Szolnoki A., (2017). Statistical physics of human cooperation. Physics Reports, vol.687, pp.1-51.

Pickhardt M. and Prinz A. (2014). Behavioral dynamics of tax evasion – a survey. Journal of Economic Psychology, vol.40, pp.1–19.

Pimm S.L., Lawton J.H. (1978). On feeding on more than one trophic level. Nature 275, 542-544.

Pluchino A., Rapisarda A. and Garofalo C. (2010). The Peter principle revisited: A computational study. Physica A: Statistical Mechanics and its Applications, 389(3):467-472.

Pluchino A., Rapisarda A. and Garofalo C. (2011). Efficient promotion strategies in hierarchical organizations. Physica A: Statistical Mechanics and its Applications, 390(20):3496-3511.

Pluchino A., Biondo A. E. and Rapisarda A. (2018). Talent versus Luck: the role of randomness in success and failure. Advances in Complex Systems, Vol.21 No.03n04, 1850014.

Polis G.A., Anderson W.B. and Holt R.D. (1997). Toward an integration of landscape and food web ecology: The dynamics of spatially subsidized food webs. Annu. Rev. Ecol. Syst., 28, 289-316.

Potapov A.M., Brose U., Scheu S. and Tiunov A.V. (2019). Trophic position of consumers and size structure of food webs across aquatic and terrestrial ecosystems. Am. Nat., 194, 823-839.

Poterba J.M. (1987). Tax Evasion and Capital Gains Taxation. American Economic Review, vol.77, pp.234-239.

Poundstone W. (1993). Prisoner's Dilemma. Anchor Books Edition.

Powell, J.R. (2007). Linking soil organisms within food webs to ecosystem functioning and environmental change. Adv. Agr. 96, 307-350.

Power M.E., Tilman D., Estes J.A., Menge B.A., Bond W.J., Mills L.S. et al. (1996). Challenges in the quest for keystones. Bioscience, 46, 609–620.

Rapoport A. (1974). Prisoner's dilemma- Recollections and observations. In Game Theory as a Theory of Conflict Resolution (ed. Rapoport A). Reidel, Dordrecht, The Netherlands, pp. 17–34.

Rocchi M., Scotti M., Micheli F. and Bodini A. (2017). Key species and impact of fishery through food web analysis: A case study from Baja California Sur, Mexico. Journal of Marine Systems 165 (2017) 92–102.

Robbins, L. (1932). An Essay on the Nature and Significance of Economic Science. Macmillan, London.

Simberloff D., Martin J., Genovesi P., Sousa R., Tabacchi E. and Vilà M. (2013). Impacts of biological invasions: what's what and the way forward. Trends in Ecology and Evolution, volume 28, issue 1, p58-66.

Slemrod, J. (2007). Cheating ourselves: the economics of tax evasion. Journal of Economic Perspectives, 21 (1), 25–48.

Slemrod J. and Yitzhaki S. (2002). Tax avoidance, evasion and administration. Handbook of Public Economics, North-Holland, Amsterdam, pp. 1425–1470.

Solé R. V. and Montoya J. M. (2001). Complexity and Fragility in Ecological Networks. Proc. Roy. Soc. Lond. B 268:2039-2045.

Srinivasan T.N. (1973). Tax evasion: a model. Journal of Public Economics, vol.2, pp.339-346.

Stevens J.B. (2018). The Economics Of Collective Choice. Routledge 2018, NY.

Stouffer D. B., Camacho J., Guimerà R., Ng C. A., and Nunes Amaral L. A. (2005). Quantitative Patterns in the Structure of Model and Empirical Food Webs. Ecology 86:1301-1311.

Strona G. and Bradshaw C. J. A. (2018). Co-extinctions annihilate planetary life during extreme environmental change. Scientific Reports volume 8, Article number: 16724.

Sugihara G., Schoenly K., and Trombla A. (1989). Scale Invariance in Food Web Properties. Science 245:48–52.

Tanizawa T. (2012). Structural robustness and transport efficiency of complex networks with degree correlation. arXiv:1209.4897v1 [physics.soc-ph] 21 Sep 2012

Tappin B.M. and Capraro V. (2018). Doing good vs. avoiding bad in prosocial choice: A refined test and extension of the morality preference hypothesis. Journal of Experimental Social Psychology, vol.79, pp.64-70.

Thedchanamoorthy G., Piraveenan M., Kasthuriratna D. and Senanayake U. (2014). Node assortativity in complex networks: An alternative approach. Procedia Computer Science Volume 29, 2014, Pages 2449–2461, Elsevier.

Torgler B. (2002). Speaking to theorists and searching for facts: tax morale and tax compliance in experiments. Journal of Economic Surveys, vol.16, pp.657–683.

Torgler B. and Schneider F. (2009). The impact of tax morale and institutional quality on the shadow economy. Journal of Economic Psychology, vol.30, (2), pp.228-245, doi.org/10.1016/j.joep.2008.08.004.

Traxler C. (2006). Social Norms and Conditional Cooperative Taxpayers. Department of Economics Discussion Paper No. 2006-28. Munich: University of Munich.

Trivers R. L. (1971). The Evolution of Reciprocal Altruism. Quart. Rev. Biol. 46, pp.35-57.

Vale R. (2015). A Model for Tax Evasion with Some Realistic Properties. arXiv:1508.02476 [q-fin.EC]

Verhulst P. F. (1838). Notice sur la loi que la population poursuitdans son accroissement. Correspondance Mathématique et Physique, 10, 113-121.

Volterra V. (1926). Variations and Fluctuations of the Numbers of Individuals in Animal Species Living Together. Reprinted in 1931. In: Chapman, R.N. Animal Ecology. McGraw-Hill, New York.

Volterra V. (1939). The general equations of biological strife in the case of historical actions, Proc. of the Edinburgh Math. Soc. (Series 2) 6 (1) , 4-10

Von Neumann J. (1928). Zur Theorie der Gesellschaftsspiele. Mathematische Annalen 1928b, 100, pp. 295- 320; translated by S. Bargmann as "On the Theory of Games of Strategy," in Contributions to the theory of games. Vol. 4. Eds.: ALBERT TUCKER AND R. DUNCAN LUCE. Princeton: Princeton U. Press, 1959, pp. 13-42.

Von Neumann J., Morgenstern O. (1944). Theory of Games and Economic Behavior. Princeton University Press.

Voss T. (2001). Game-theoretical perspectives on the emergence of social norms. Social Norms (eds Hechter M and Opp KD). Russell Sage Foundation, New York, pp.105–136.

Wall D., Nielsen U. and Six J. (2015). Soil biodiversity and human health. Nature, 528, 69-76.
Watts D. J. and Strogatz S. H. (1998). Collective dynamics of 'small-world' networks. Nature (London) 393, 440.

Wilensky U. (1999). NetLogo. http://ccl.northwestern.edu/netlogo/

Williams R. J. and Martinez N. D. (2000). Simple Rules Yield Complex Food Webs. Nature 404:180-183.

Yaniv G. (2013). Tax Evasion, Conspicuous Consumption and the Income Tax Rate. Public Finance Review, vol.41 (3), pp.302-316

Yeates G.W., Bongers T., De Goede R.G., Freckman D.W. and Georgieva S.S. (1993). Feeding habits in soil nematode families and genera - An outline for soil ecologists. J. Nematol., 25, 315-331.

Yitzhaki S. (1974). A note on Income Tax Evasion: A Theoretical Analysis. Journal of Public Economics, vol.3, 201-202.

Yitzhaki S. (1987). On the excess burden of tax evasion. Public Finance Quaterly, vol.15, pp.123-37.

Zappalà D.A., Pluchino A. and Rapisarda A. (2014). Selective altruism in collective games. Physica A, vol.410, pp.496-512.

Appendix

Networks 225: results for different perturbative scenarios

- **Simulation without interaction between species.** Extinction of all species with $r_i < 0$, i.e. all carnivores and omnivores except species 50 and 51.
- **Simulation with interaction between species.** All species reach their carrying capacity and the ecosystem is in the steady state.
- **Removal of all the herbivorous species.** No significant changes are observed ($AI = 8.59 \times 10^{-8}$).
- **Removal of all the fungivorous species.** No significant changes are observed ($AI = 2.38 \times 10^{-4}$).
- **Removal of all the bacterivorous species.** Extinction of all species with $r_i < 0$ ($AI = 18.21$).
- **Removal of all the herbivorous and fungivorous species.** No significant changes are observed ($AI = 8.59 \times 10^{-8}$).
- **Removal of all the herbivorous and bacterivorous species.** Extinction of all species with $r_i < 0$ ($AI = 15.17$).
- **Removal of all the fungivorous and bacterivorous species.** Extinction of some species with $r_i < 0$. Species 46, 48, 52, 53 and 54 recover after a sharp decrease ($AI = 104.38$).
- **Removal of the most abundant species (bacterivorous 34)** Extinction of carnivores 41, 42 and 43 ($AI = 20.04$).
- **Removal of the two most abundant species (bacterivores 34 and 36).** Extinction of all species with $r_i < 0$ ($AI = 17.88$).

- **Removal of all the carnivorous species.** There is a slight increase in the abundance of species in the first trophic level ($AI = 3.72$).

- **Removal of all the omnivorous species.** There is a slight increase in the abundance of species in the first trophic level ($AI = 1.11$).

- **Removal of all the omnivorous and carnivorous species.** There is a slight increase in the abundance of species in the first trophic level ($AI = 4.62$).

Networks 230: results for different perturbative scenarios

- **Simulation without interaction between species.** Extinction of all species with $r_i < 0$, i.e. all carnivores and omnivores except species 58 and 59.

- **Simulation with interaction between species.** All species reach their carrying capacity and the ecosystem is in the steady state.

- **Removal of all the herbivorous species.** No significant changes are observed ($AI = 1.22 \times 10^{-6}$).

- **Removal of all the fungivorous species.** No significant changes are observed ($AI = 2.08 \times 10^{-4}$).

- **Removal of all the bacterivorous species.** Extinction of all species with $r_i < 0$ ($AI = 20.72$).

- **Removal of all the herbivorous and fungivorous species.** No significant changes are observed ($AI = 1.22 \times 10^{-6}$).

- **Removal of all the herbivorous and bacterivorous species.** Extinction of all species with $r_i < 0$ ($AI = 18.86$).

- **Removal of all the fungivorous and bacterivorous species.** Extinction of species 65, 47 and 48. The other species with $r_i < 0$ recover after a sharp decrease ($AI = 71.03$).

- **Removal of the most abundant species (bacterivorous 42)** Extinction of all species with $r_i < 0$ except species 65 ($AI = 19.83$).

- **Removal of all the carnivorous species.** There is a slight increase in the abundance of species in the first trophic level ($AI = 3.59$).

- **Removal of all the omnivorous species.** There is a slight increase in the abundance of species in the first trophic level ($AI = 2.73$).
- **Removal of all the omnivorous and carnivorous species.** There is a slight increase in the abundance of species in the first trophic level ($AI = 6.22$).

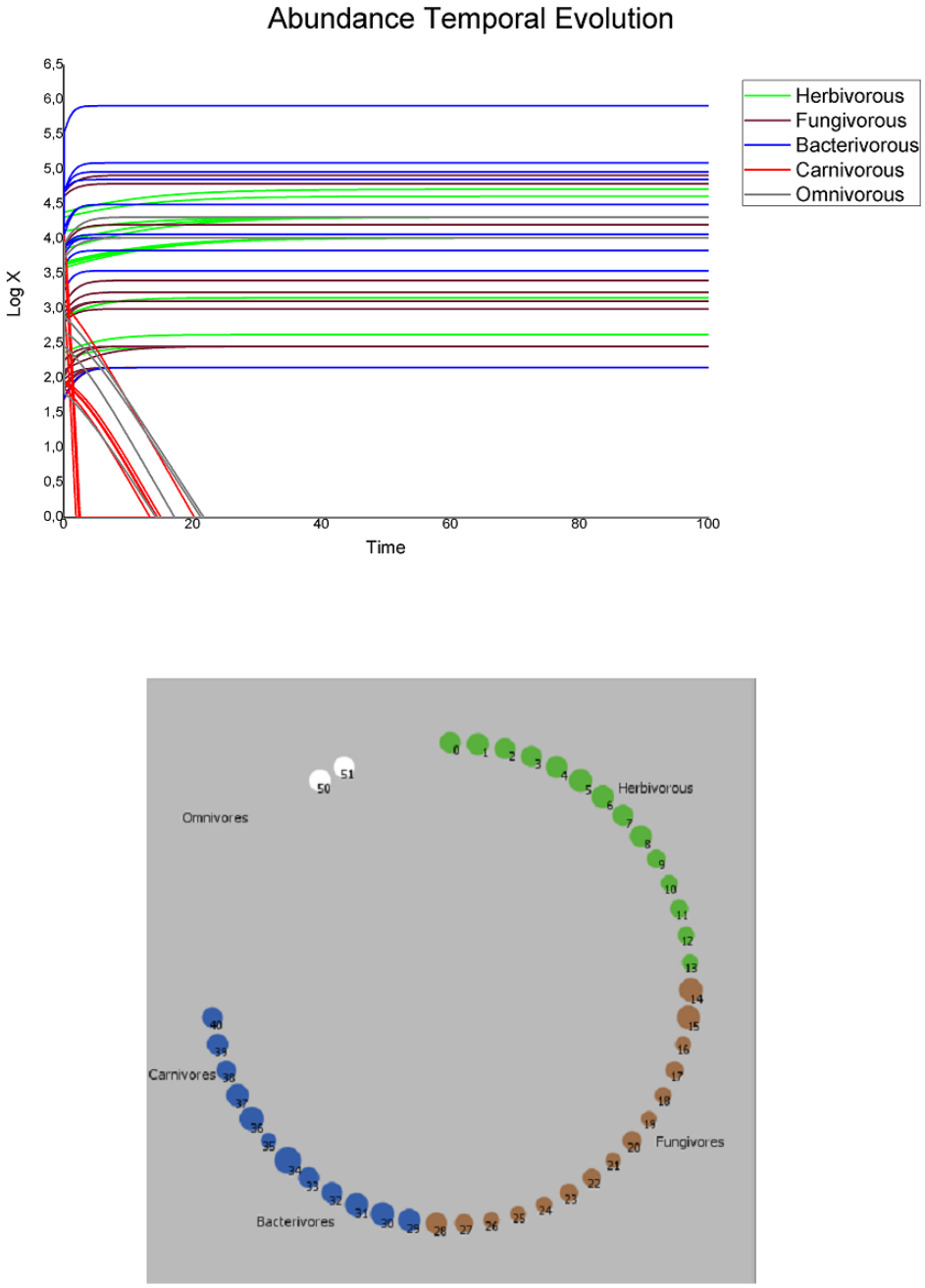

Figure 4.29: **Network 225.** Graphic representation of the simulation results without interaction ($\beta = 0$). Above the temporal evolution of species abundances and below the representation of the trophic web at the end of the simulation.

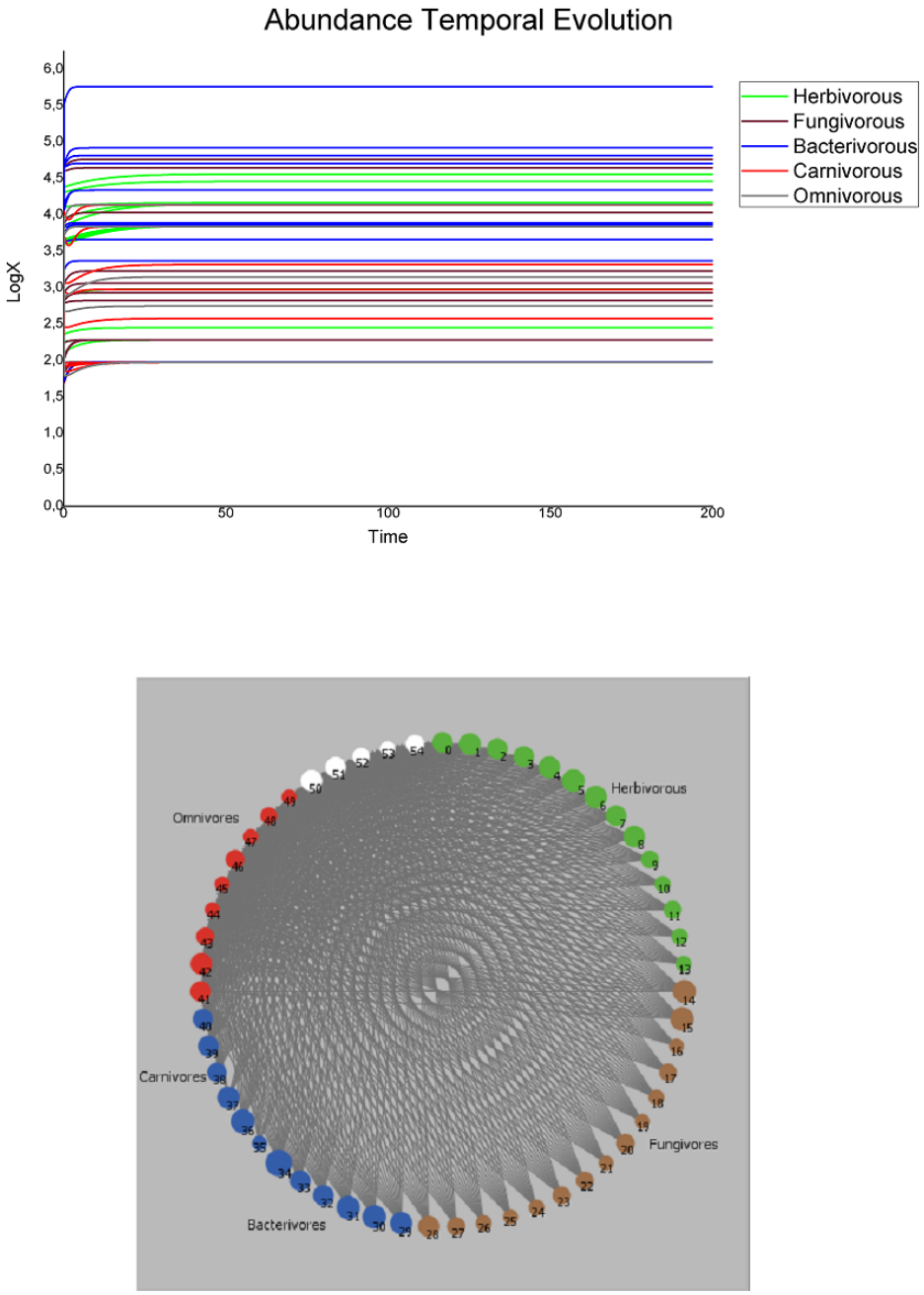

Figure 4.30: **Network 225.** Graphic representation of the simulation results with interaction ($\beta = 1$). Above the temporal evolution of species abundances and below the representation of the trophic web at the end of the simulation.

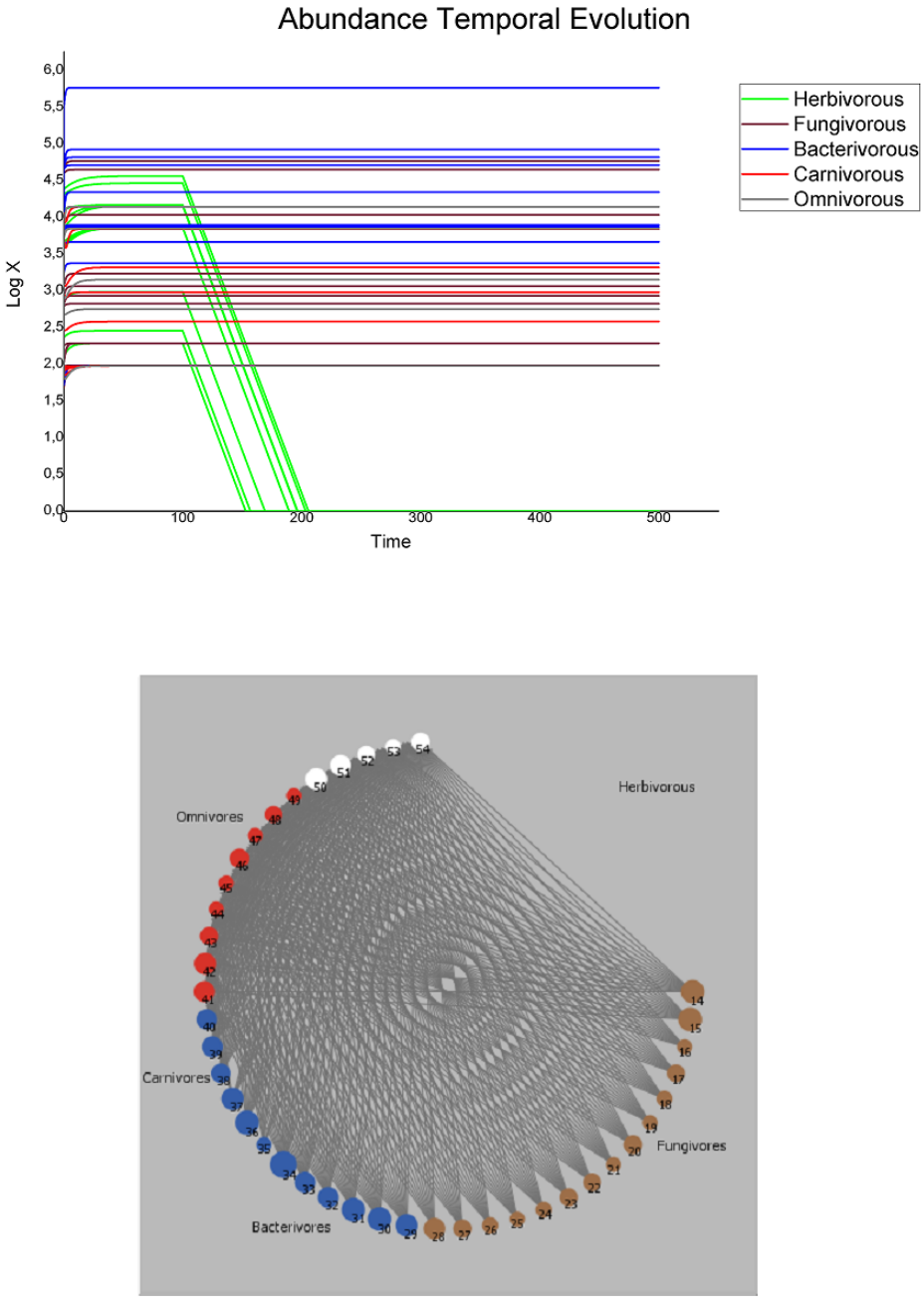

Figure 4.31: **Network 225.** Graphic representation of the simulation results in the case all herbivores are removed from the ecosystem. Above the temporal evolutions of species abundances and below the representations of the trophic web at the end of the simulation.

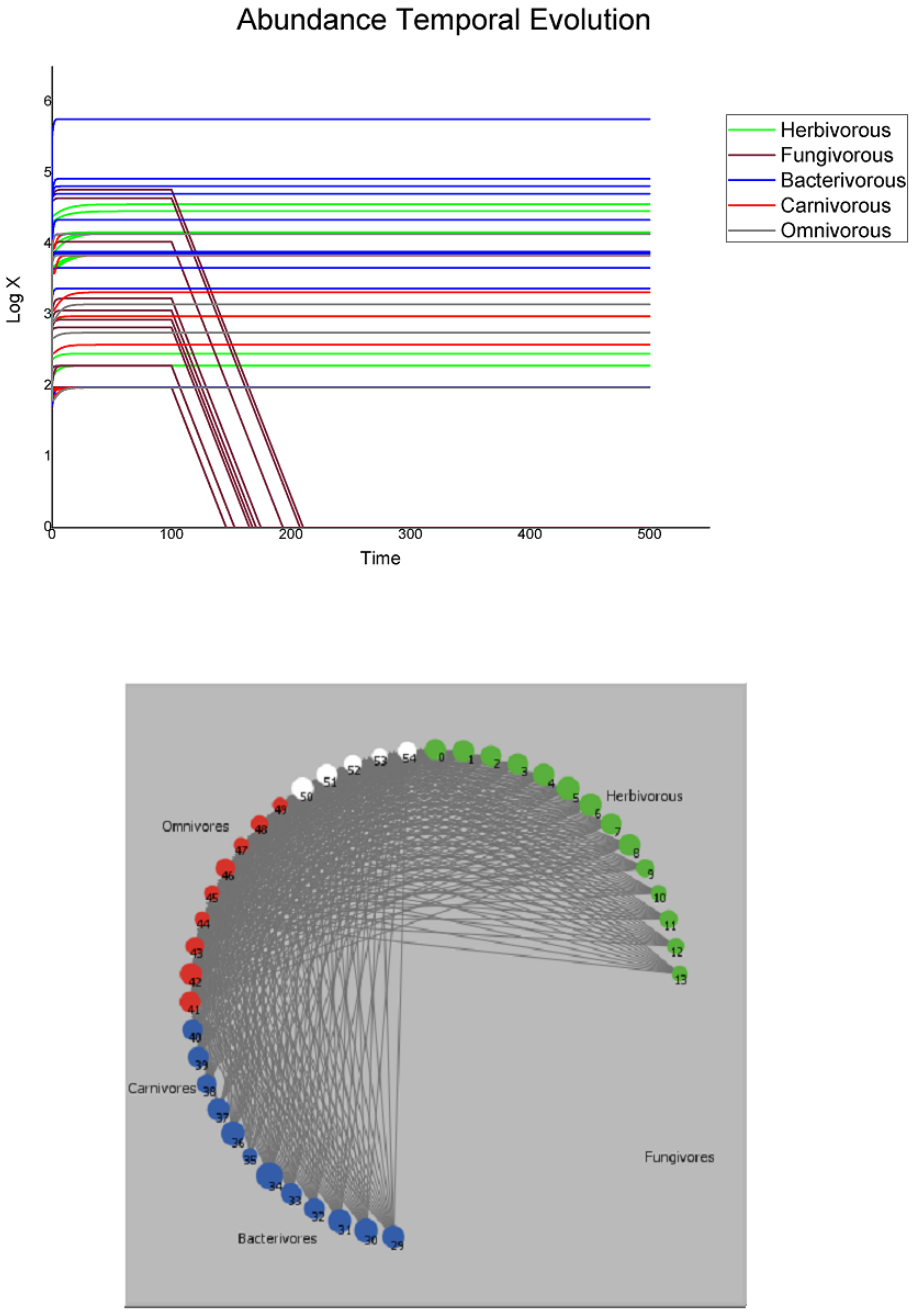

Figure 4.32: **Network 225.** Graphic representation of the simulation results in the case all fungivores are removed from the ecosystem. Above the temporal evolutions of species abundances and below the representations of the trophic web at the end of the simulation.

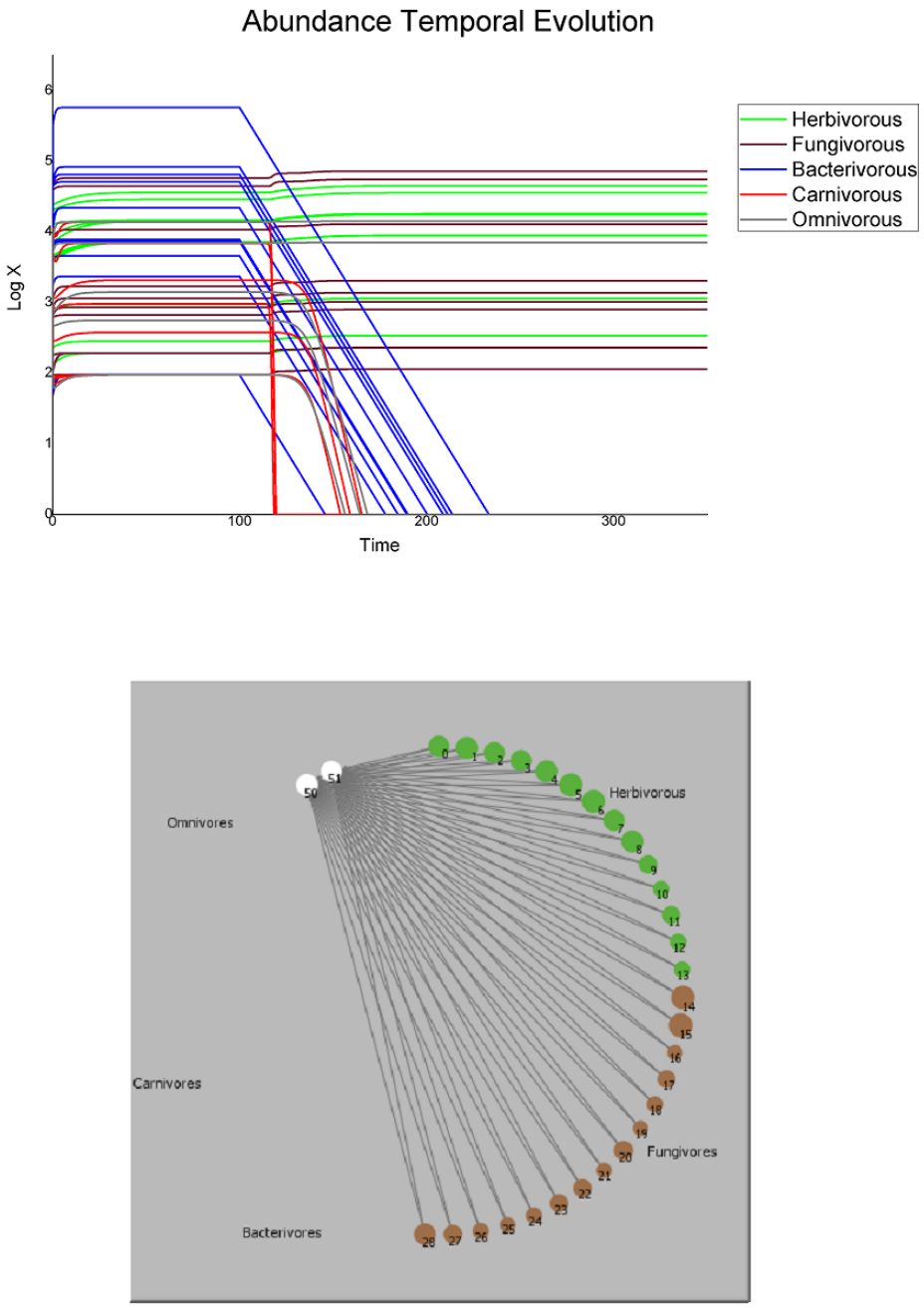

Figure 4.33: **Network 225.** Graphic representation of the simulation results in the case all bacterivores are removed from the ecosystem. Above the temporal evolutions of species abundances and below the representations of the trophic web at the end of the simulation.

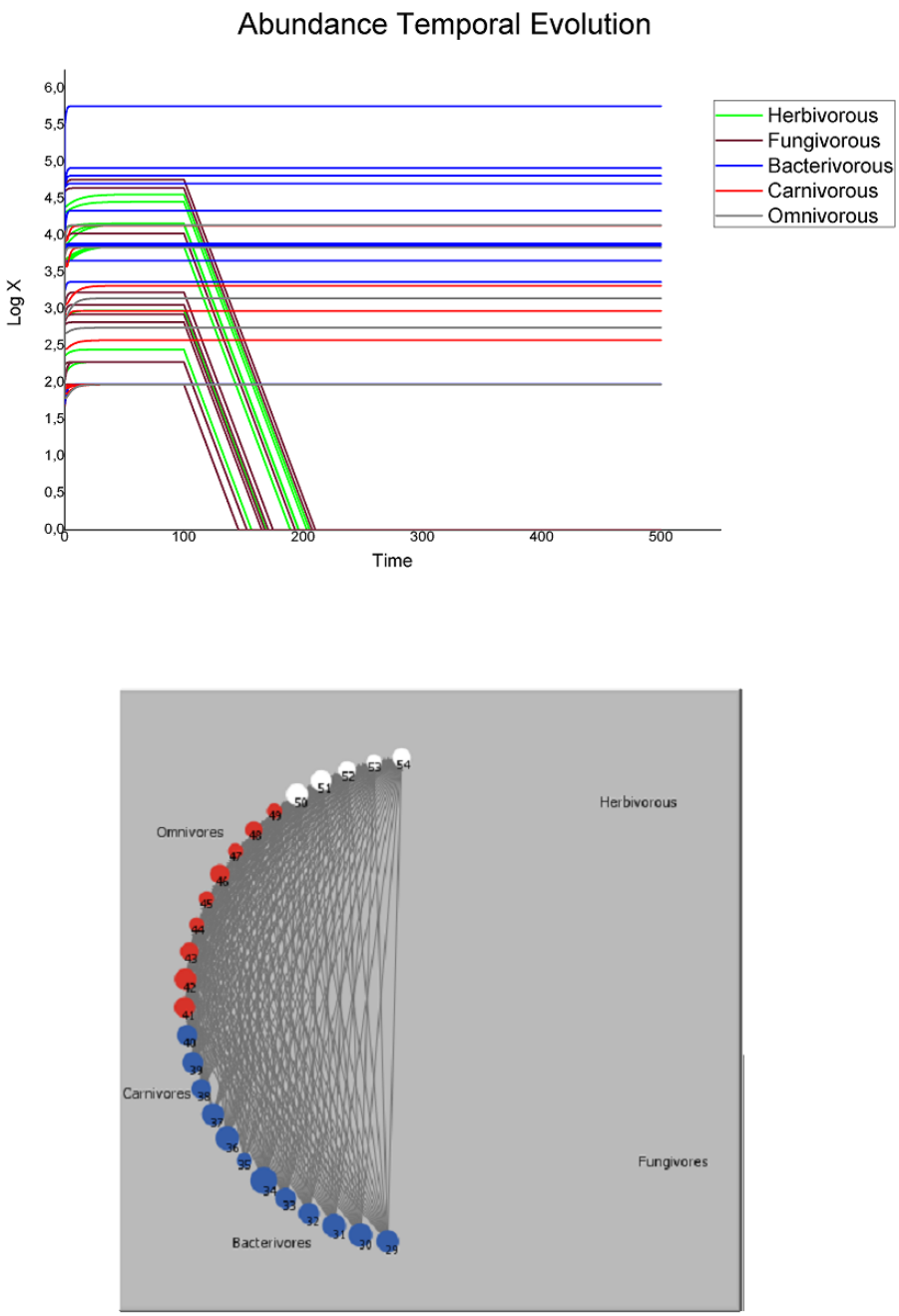

Figure 4.34: **Network 225.** Graphic representations of the simulation results in the case all herbivores and fungivores are removed from the ecosystem. Above the temporal evolutions of species abundances and below the representations of the trophic web at the end of the simulation.

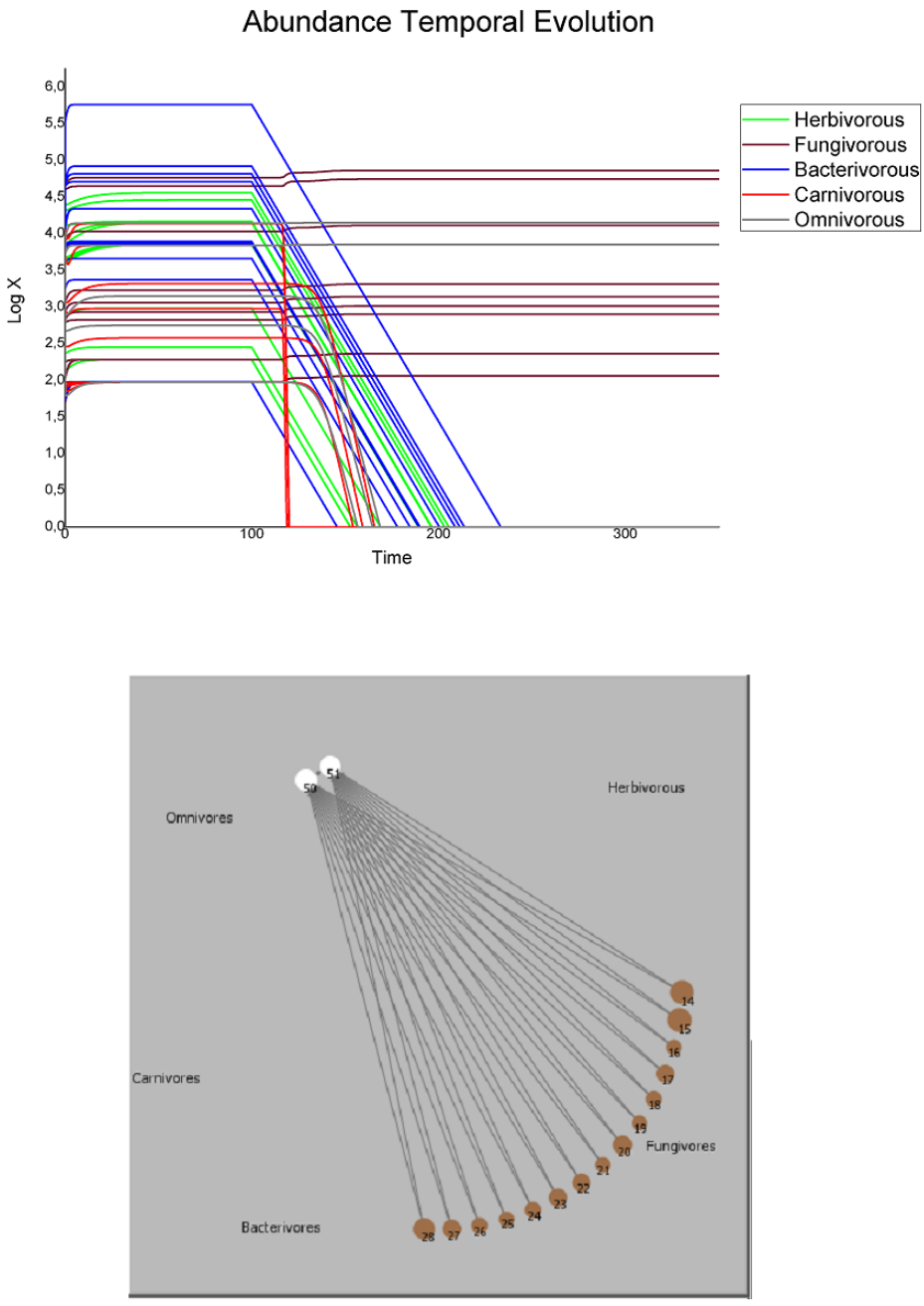

Figure 4.35: **Network 225.** Graphic representations of the simulation results in the case all herbivores and bacterivores are removed from the ecosystem. Above the temporal evolutions of species abundances and below the representations of the trophic web at the end of the simulation.

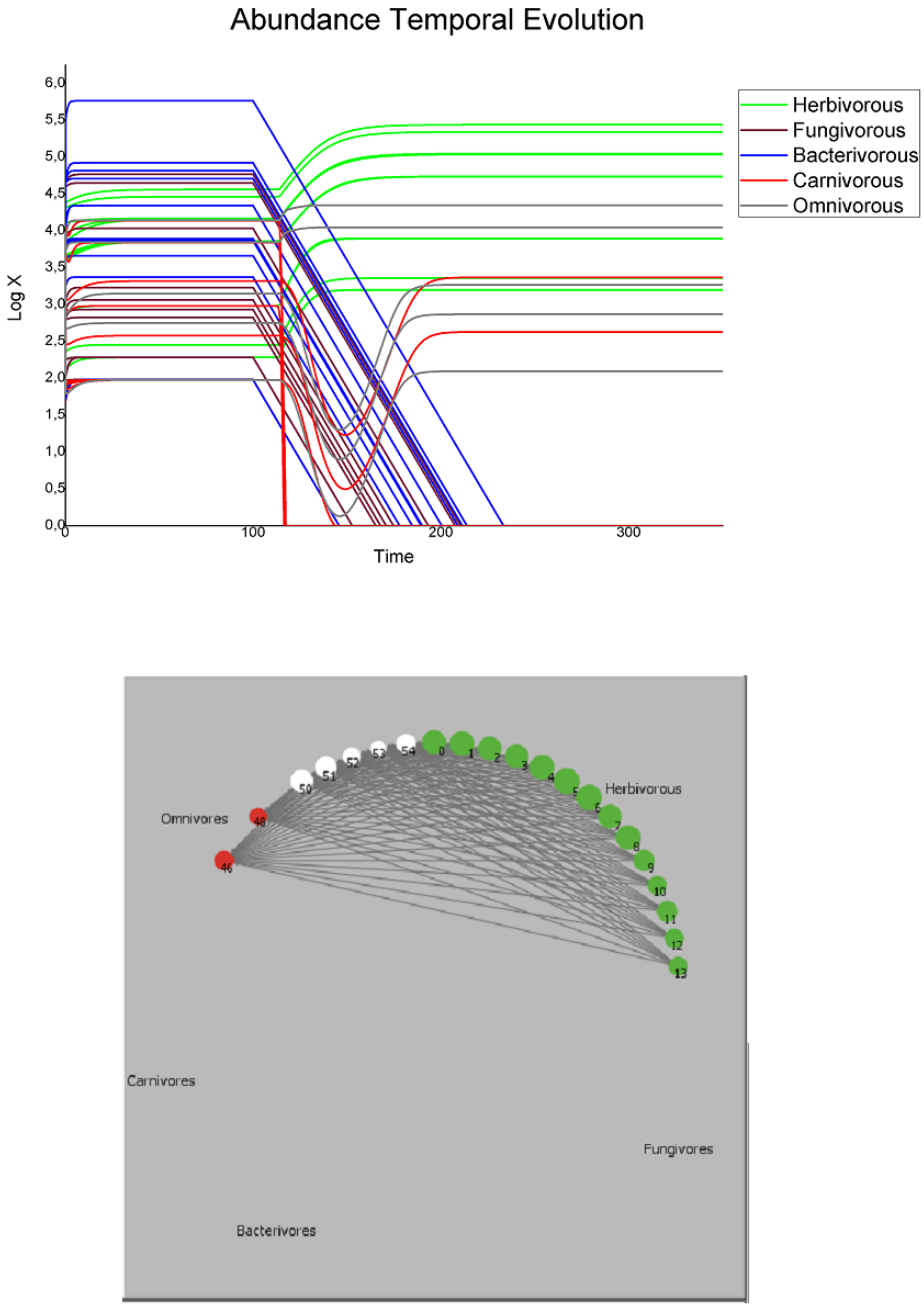

Figure 4.36: **Network 225.** Graphic representations of the simulation results in the case all fungivores and bacterivores are removed from the ecosystem. Above the temporal evolutions of species abundances and below the representations of the trophic web at the end of the simulation.

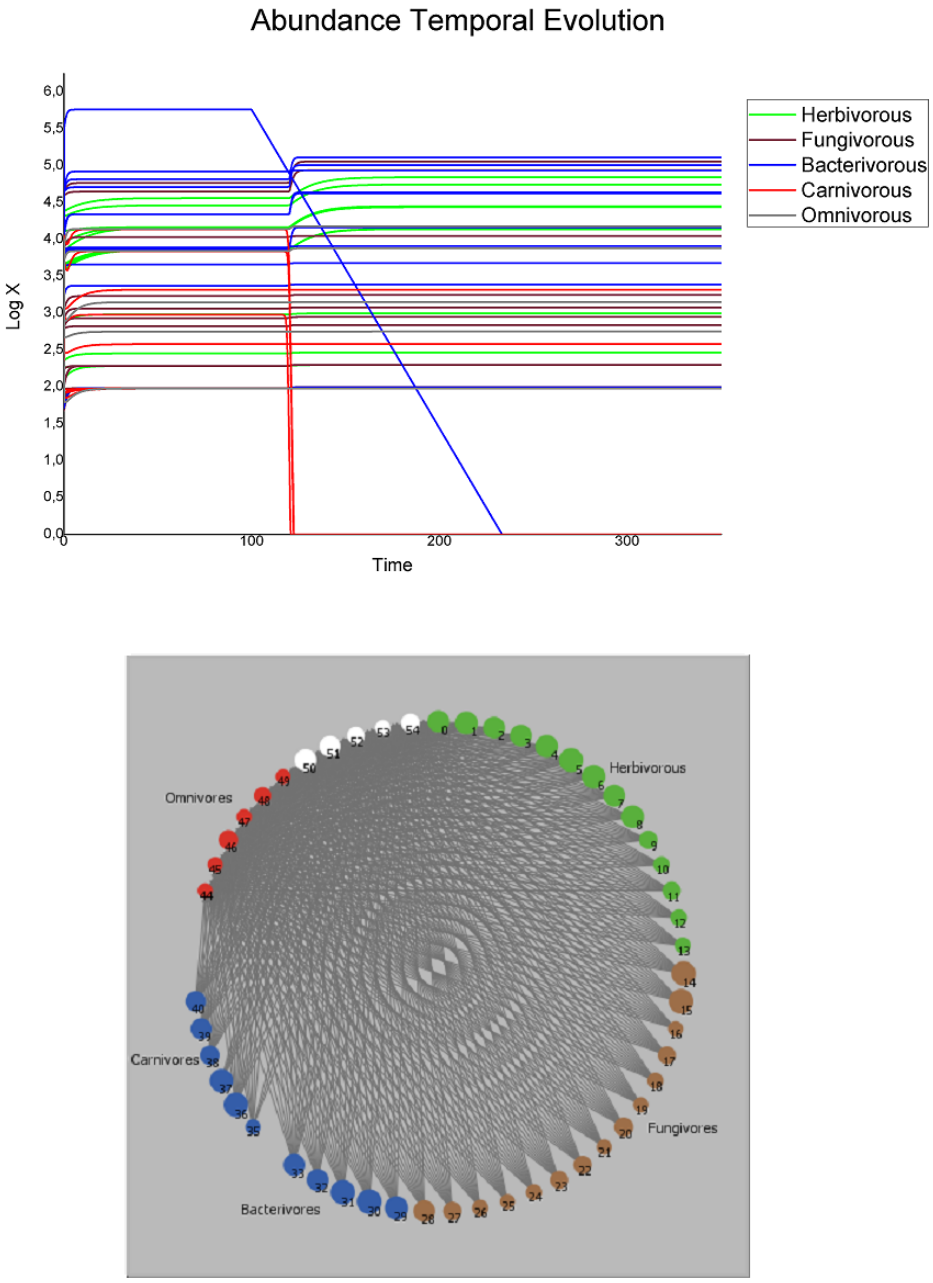

Figure 4.37: **Network 225.** Graphic representation of the simulation results in the case only bacterivores 34 is removed from the ecosystem (see the text for the explanation of these choices). Above the temporal evolutions of species abundances and below the representations of the trophic web at the end of the simulation.

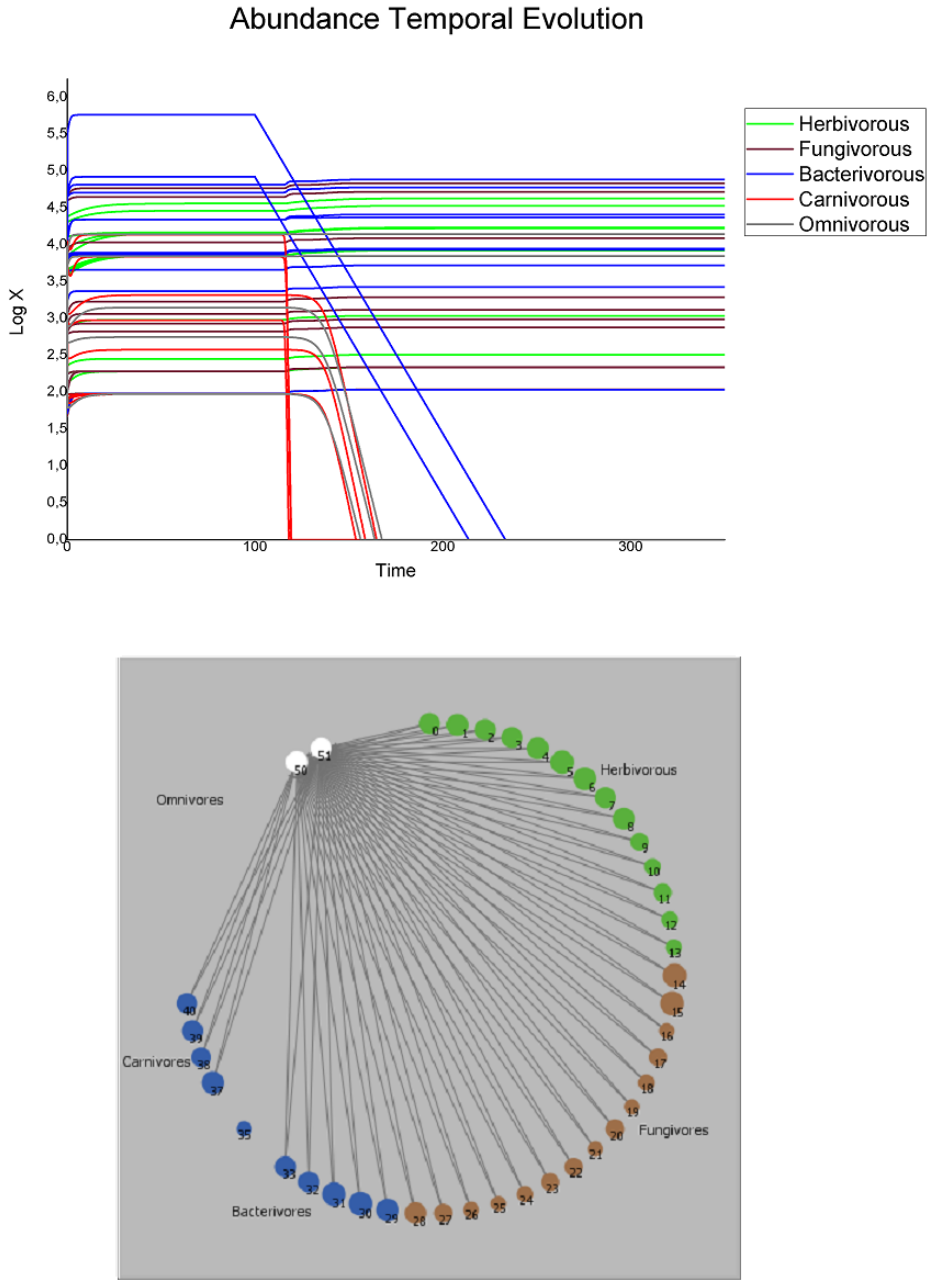

Figure 4.38: **Network 225.** Graphic representation of the simulation results in the case only bacterivores 34 and 36 are removed from the ecosystem (see the text for the explanation of these choices). Above the temporal evolutions of species abundances and below the representations of the trophic web at the end of the simulation.

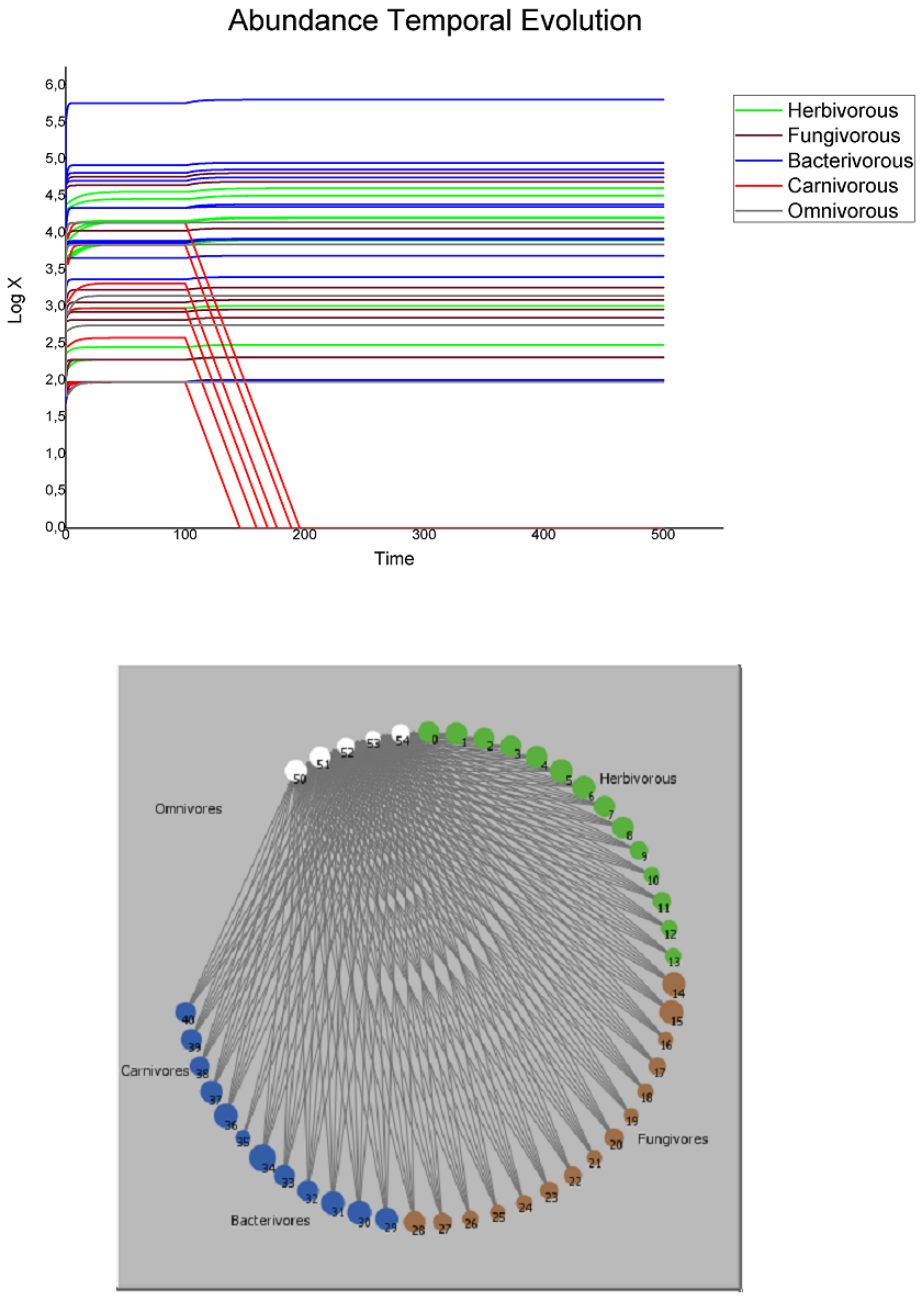

Figure 4.39: **Network 225.** Graphic representation of the simulation results in the case all carnivores are removed from the ecosystem. Above the temporal evolutions of species abundances and below the representations of the trophic web at the end of the simulation.

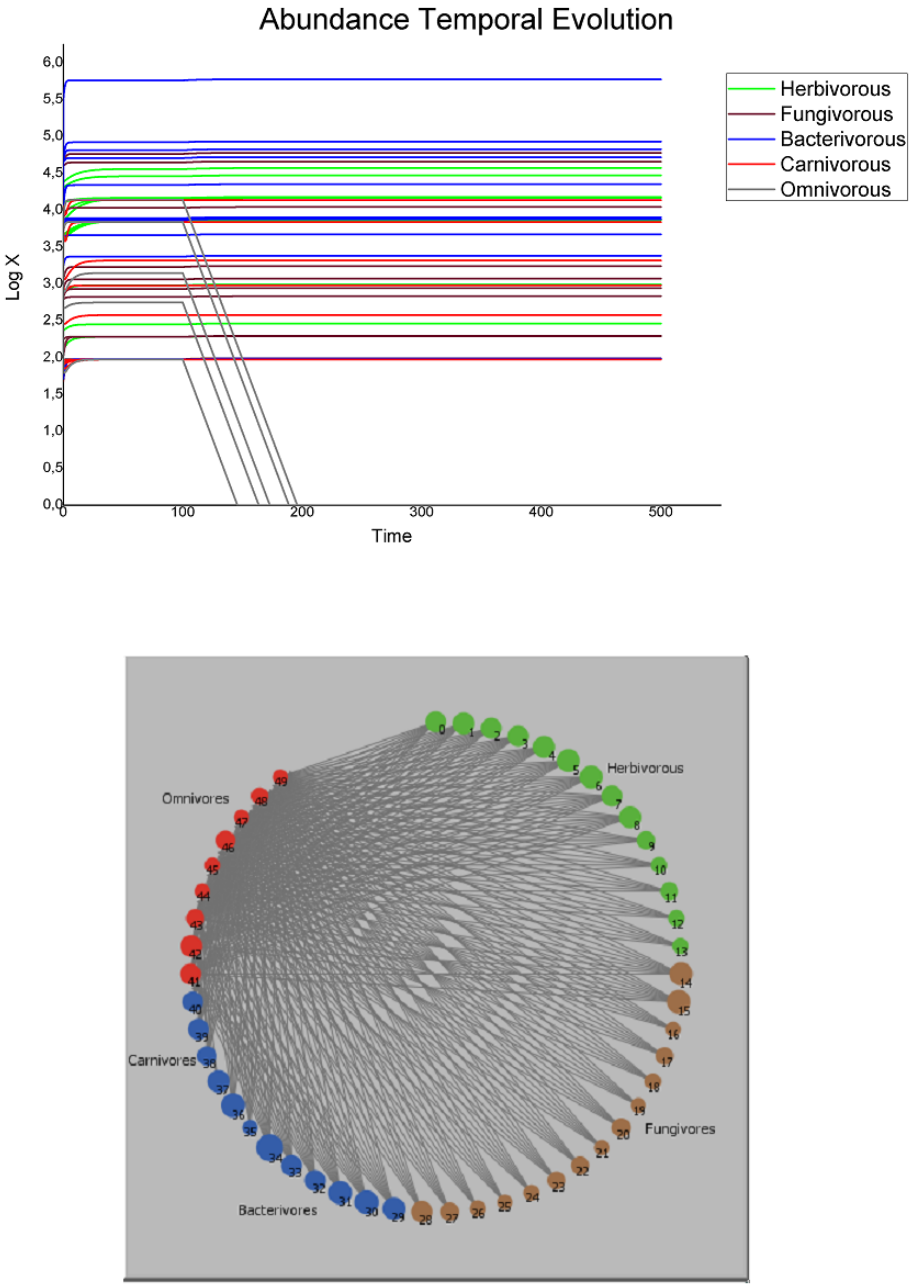

Figure 4.40: **Network 225.** Graphic representation of the simulation results in the case all omnivores are removed from the ecosystem. Above the temporal evolutions of species abundances and below the representations of the trophic web at the end of the simulation.

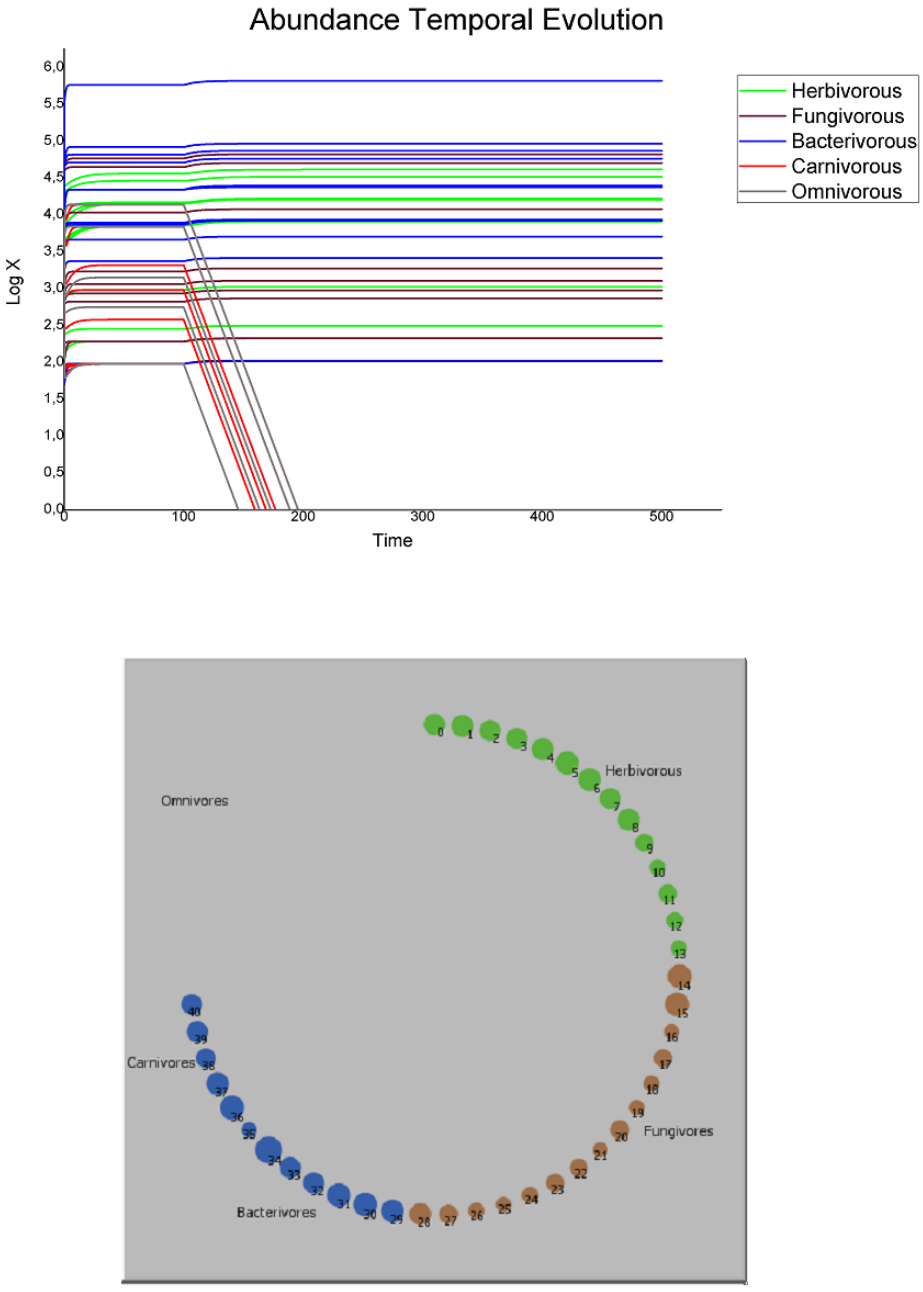

Figure 4.41: **Network 225.** Graphic representation of the simulation results in the case all omnivores and carnivores are removed from the ecosystem. Above the temporal evolutions of species abundances and below the representations of the trophic web at the end of the simulation.

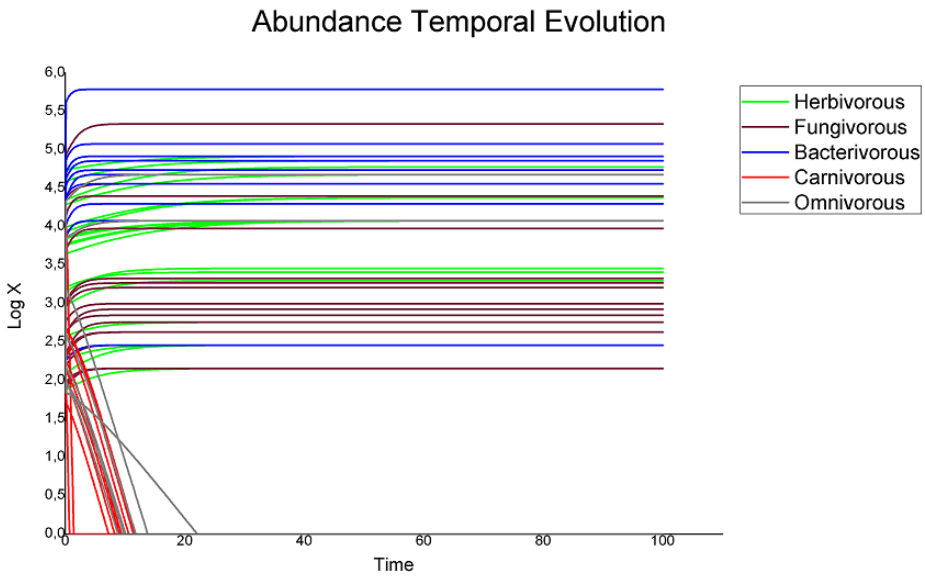

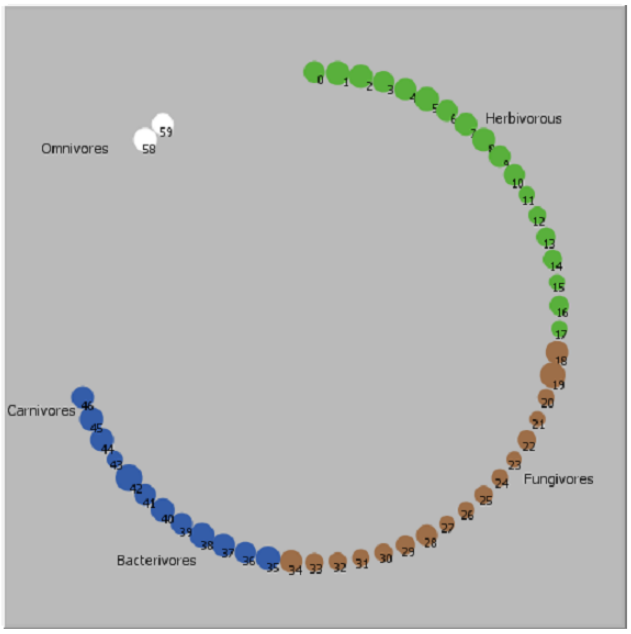

Figure 4.42: **Network 230.** Graphic representation of the simulation results without interaction ($\beta = 0$). Above the temporal evolution of species abundances and below the representation of the trophic web at the end of the simulation.

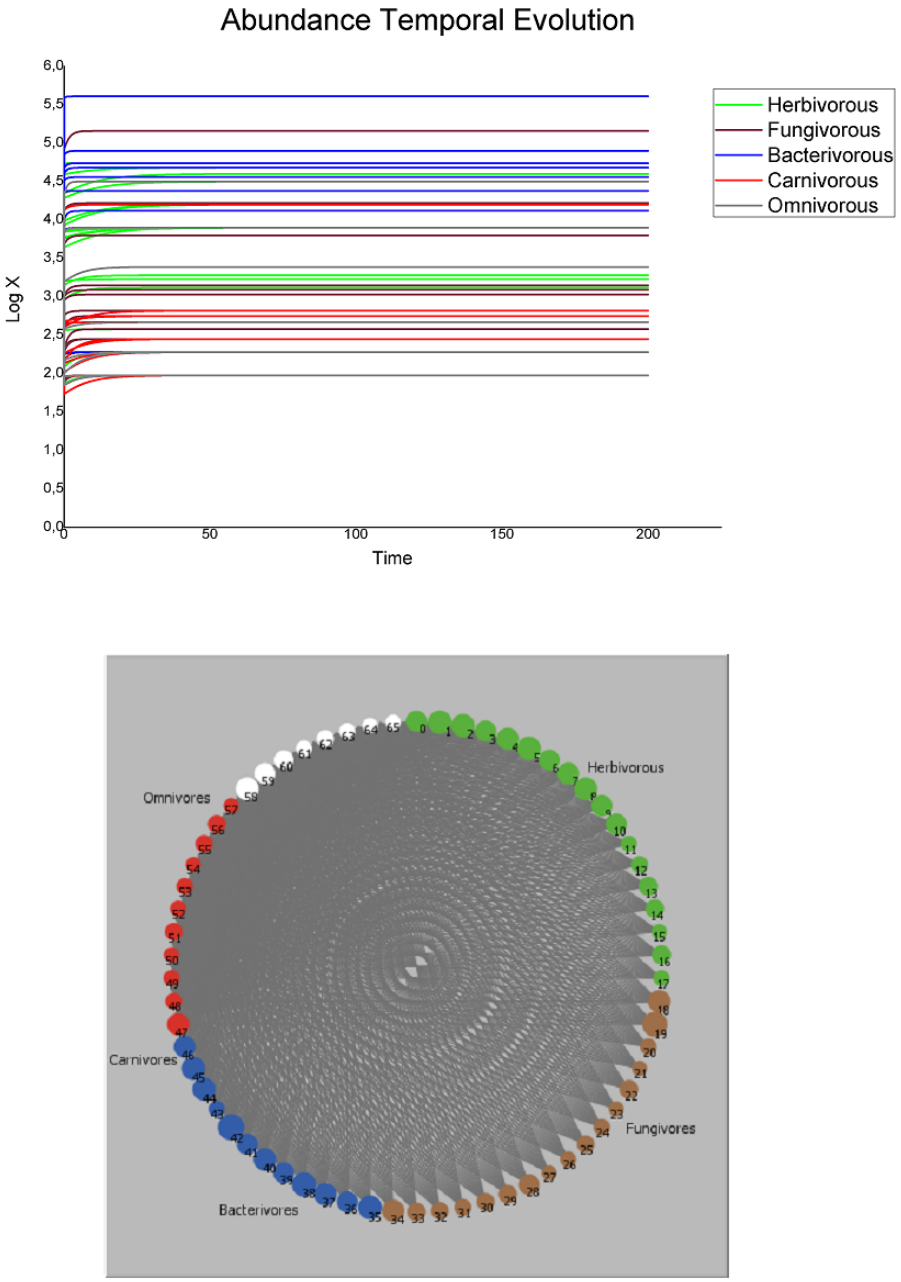

Figure 4.43: **Network 230.** Graphic representation of the simulation results with interaction ($\beta = 1$). Above the temporal evolution of species abundances and below the representation of the trophic web at the end of the simulation.

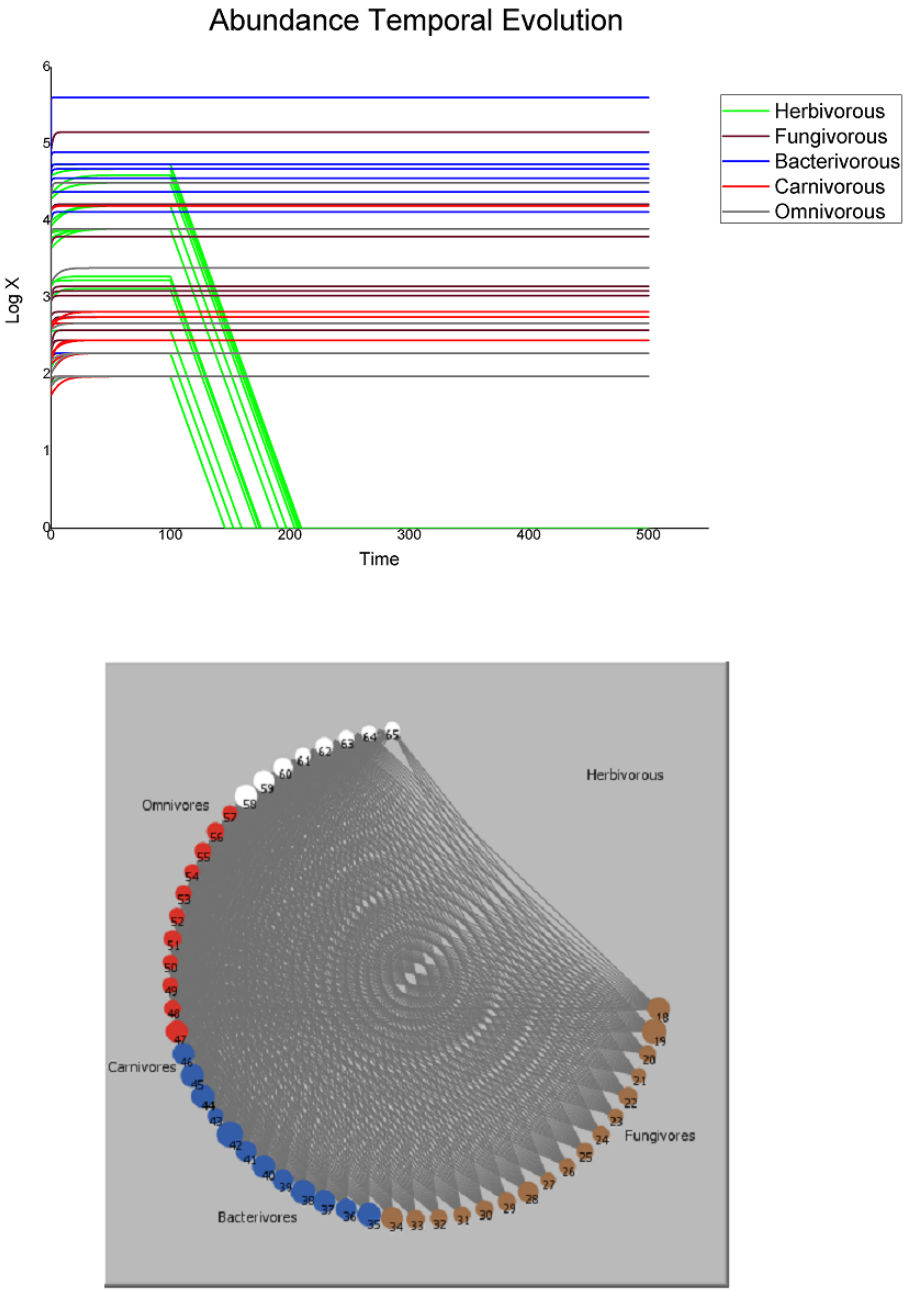

Figure 4.44: **Network 230.** Graphic representation of the simulation results in the case all herbivores are removed from the ecosystem. Above the temporal evolutions of species abundances and below the representations of the trophic web at the end of the simulation.

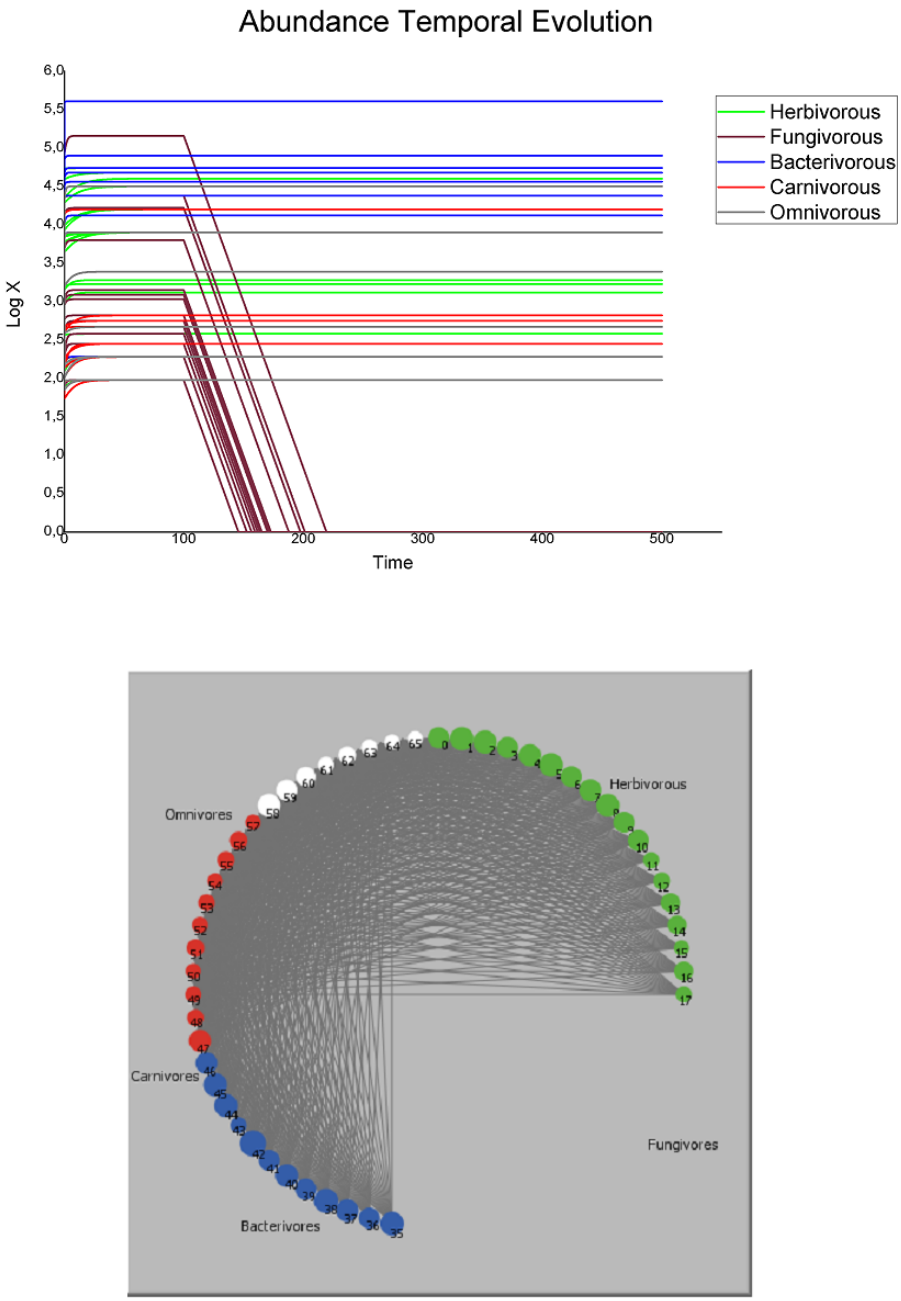

Figure 4.45: **Network 230.** Graphic representation of the simulation results in the case all fungivores are removed from the ecosystem. Above the temporal evolutions of species abundances and below the representations of the trophic web at the end of the simulation.

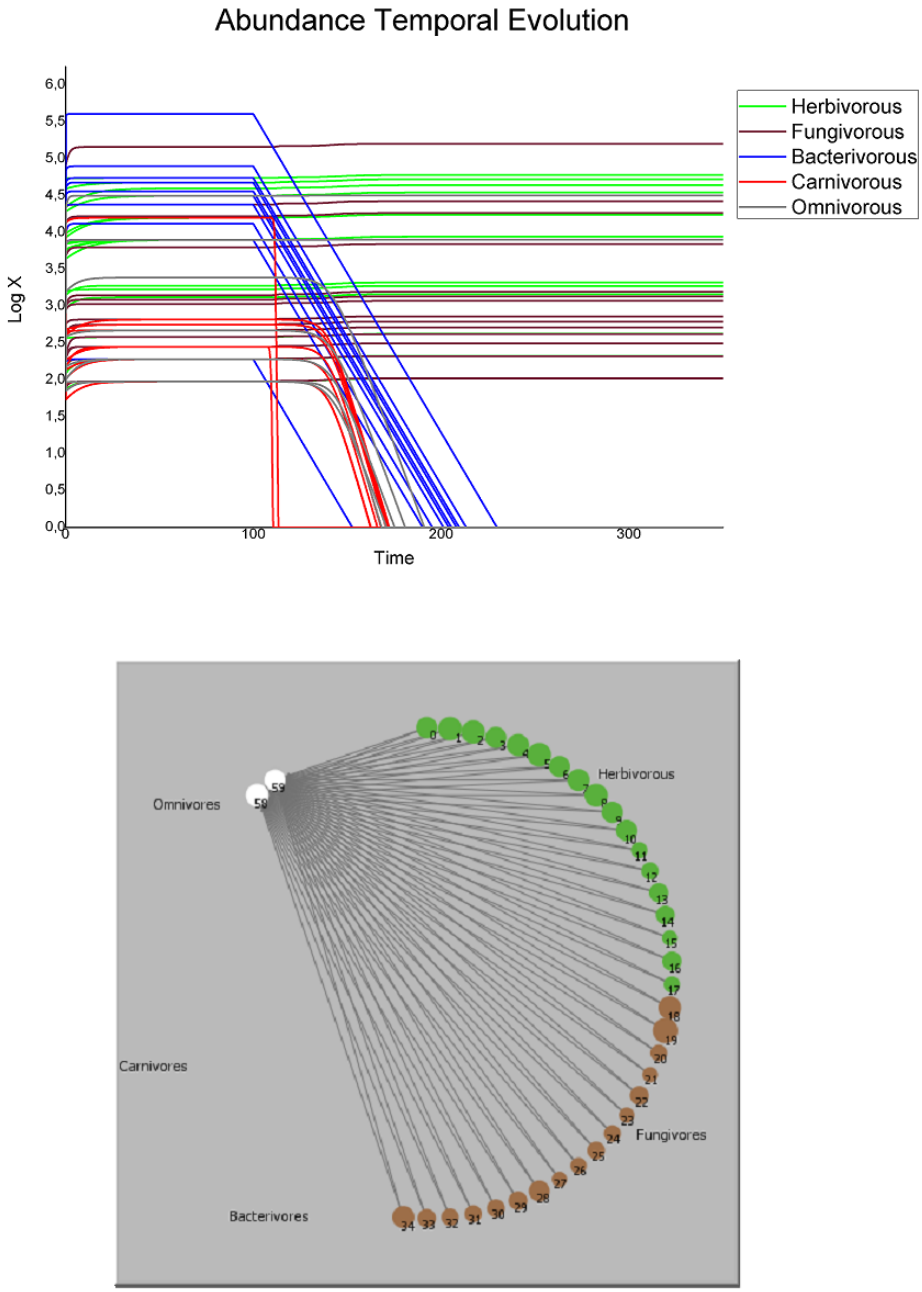

Figure 4.46: **Network 230.** Graphic representation of the simulation results in the case all bacterivores are removed from the ecosystem. Above the temporal evolutions of species abundances and below the representations of the trophic web at the end of the simulation.

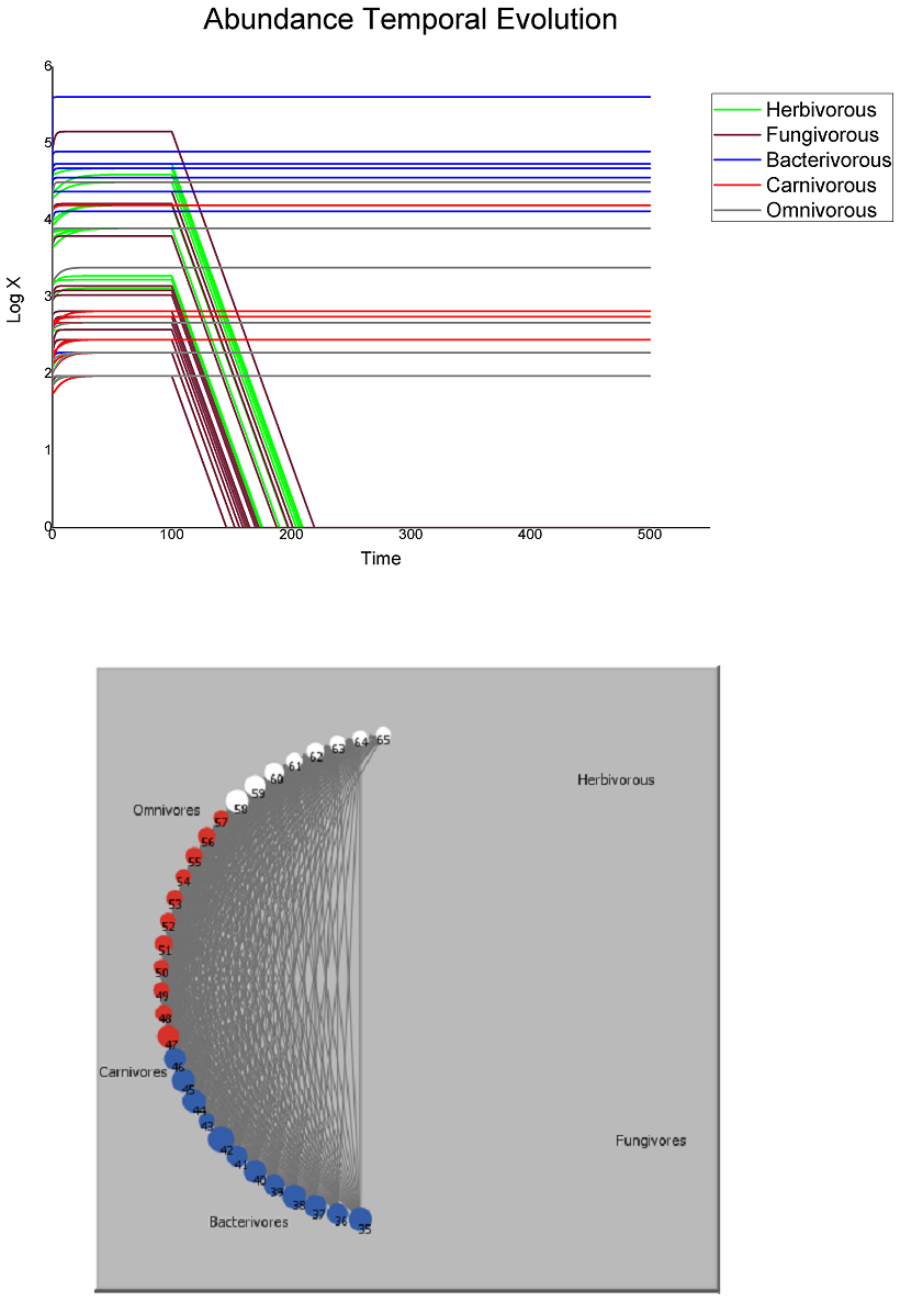

Figure 4.47: **Network 230.** Graphic representations of the simulation results in the case all herbivores and fungivores are removed from the ecosystem. Above the temporal evolutions of species abundances and below the representations of the trophic web at the end of the simulation.

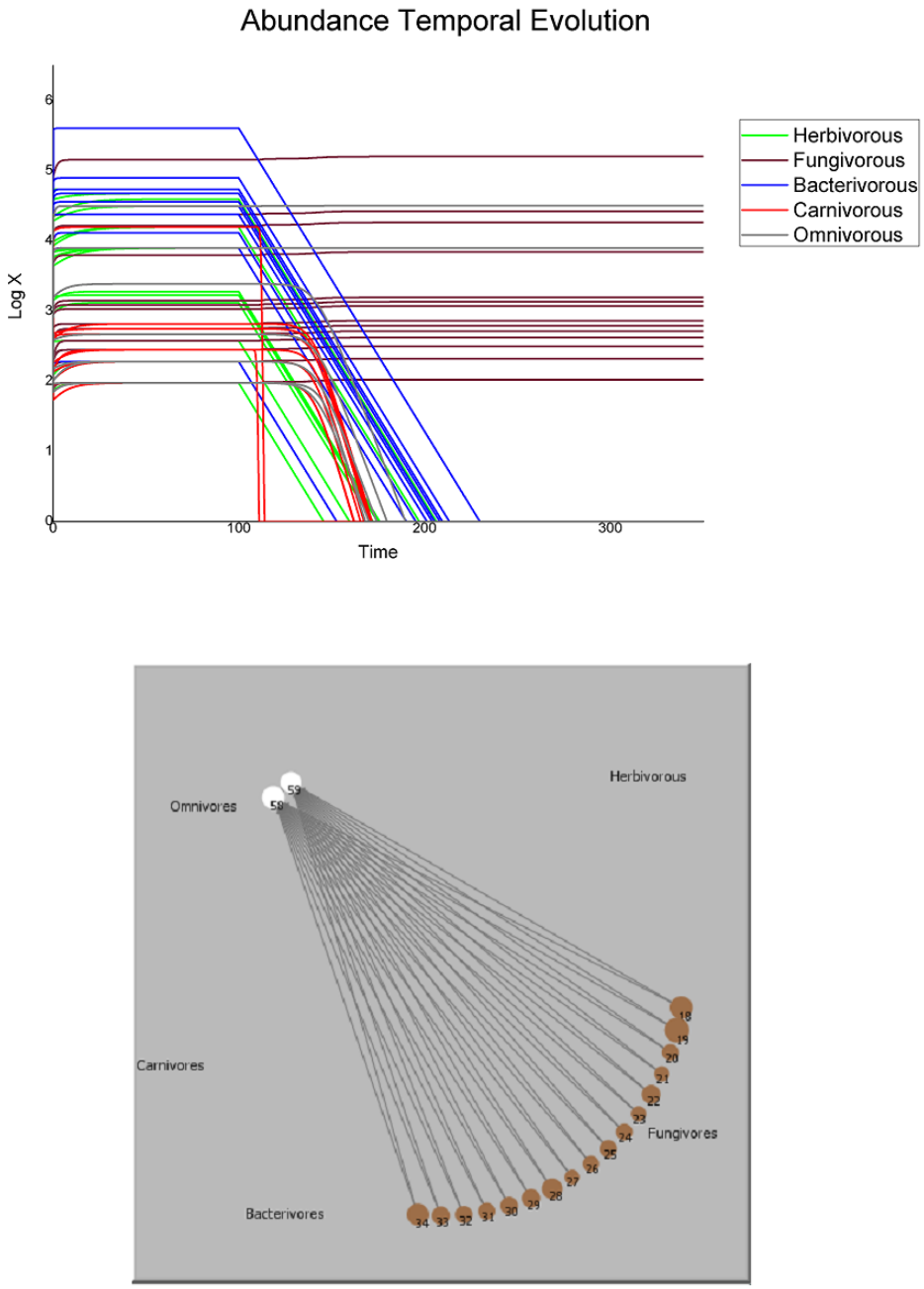

Figure 4.48: **Network 230.** Graphic representations of the simulation results in the case all herbivores and bacterivores are removed from the ecosystem. Above the temporal evolutions of species abundances and below the representations of the trophic web at the end of the simulation.

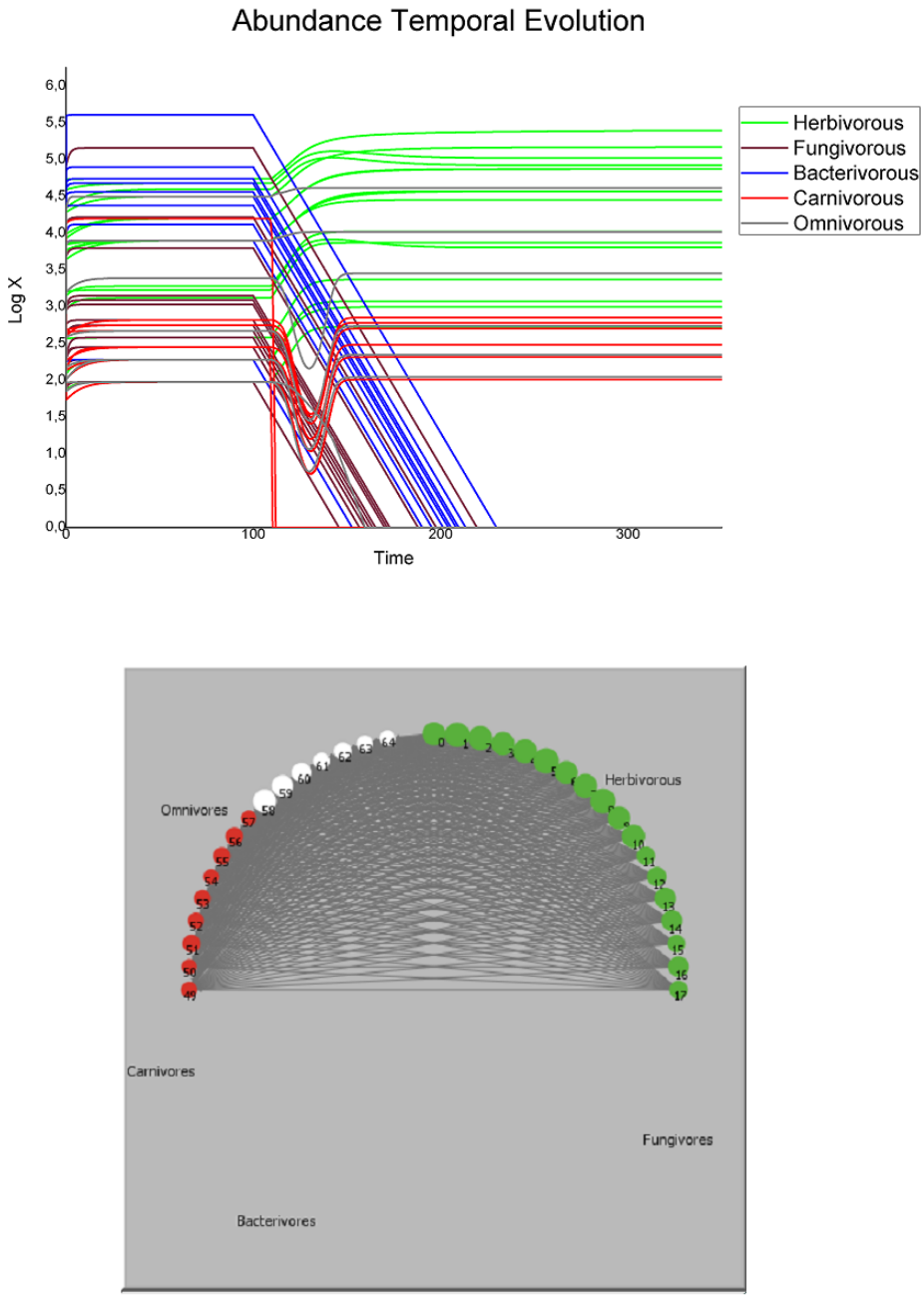

Figure 4.49: **Network 230.** Graphic representations of the simulation results in the case all fungivores and bacterivores are removed from the ecosystem. Above the temporal evolutions of species abundances and below the representations of the trophic web at the end of the simulation.

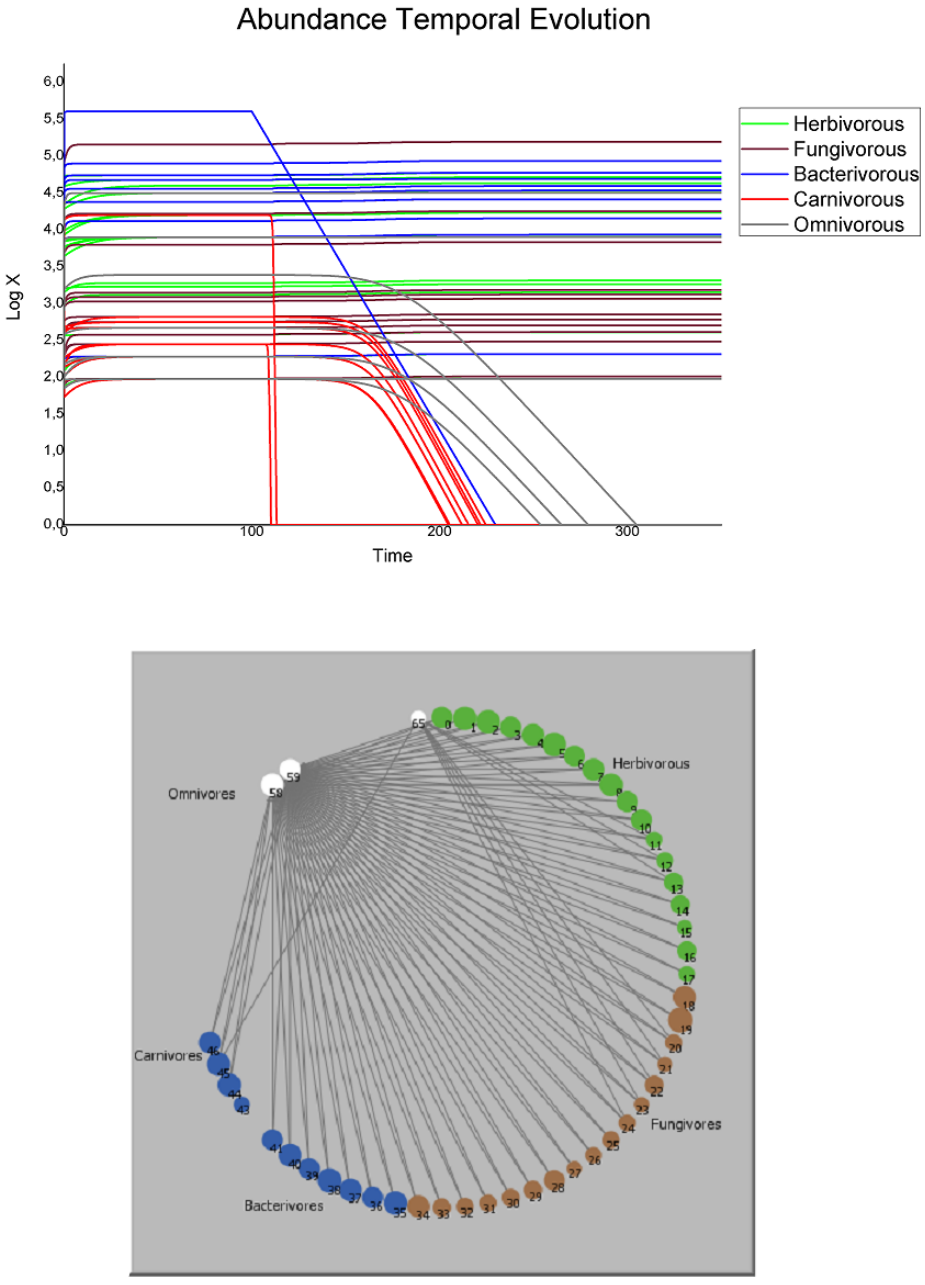

Figure 4.50: **Network 230.** Graphic representation of the simulation results in the case only bacterivores 34 is removed from the ecosystem (see the text for the explanation of these choices). Above the temporal evolutions of species abundances and below the representations of the trophic web at the end of the simulation.

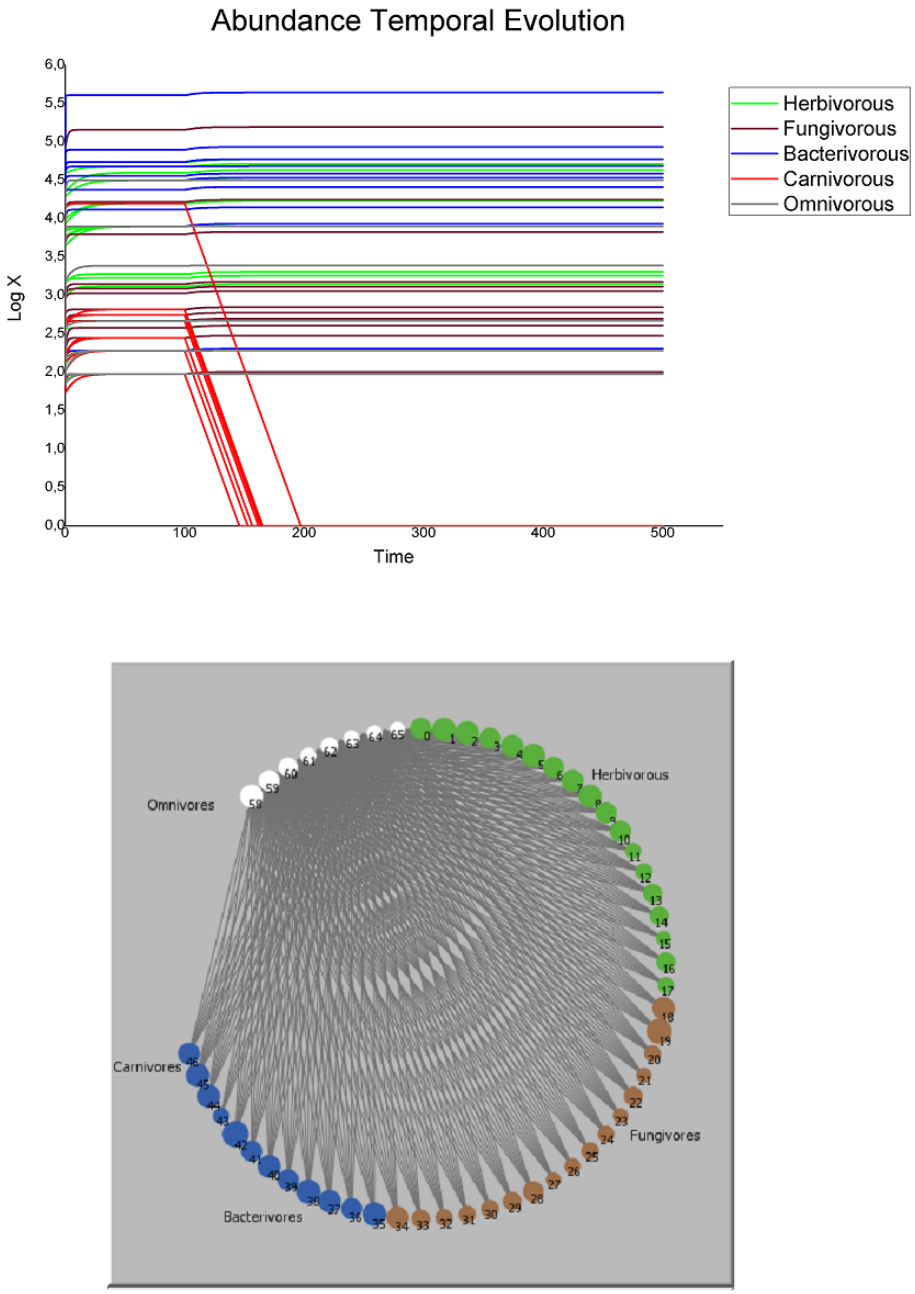

Figure 4.51: **Network 230.** Graphic representation of the simulation results in the case all carnivores are removed from the ecosystem. Above the temporal evolutions of species abundances and below the representations of the trophic web at the end of the simulation.

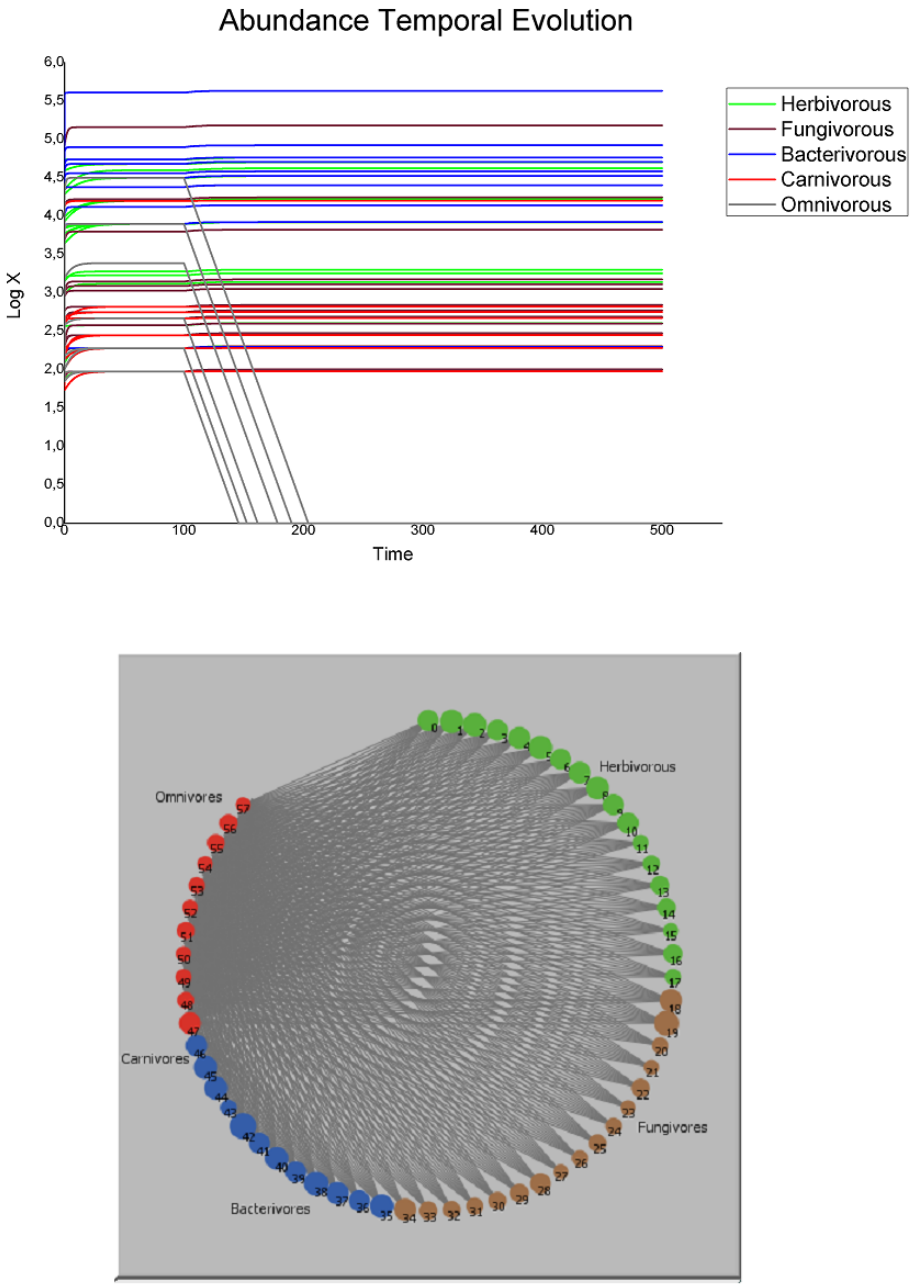

Figure 4.52: **Network 230.** Graphic representation of the simulation results in the case all omnivores are removed from the ecosystem. Above the temporal evolutions of species abundances and below the representations of the trophic web at the end of the simulation.

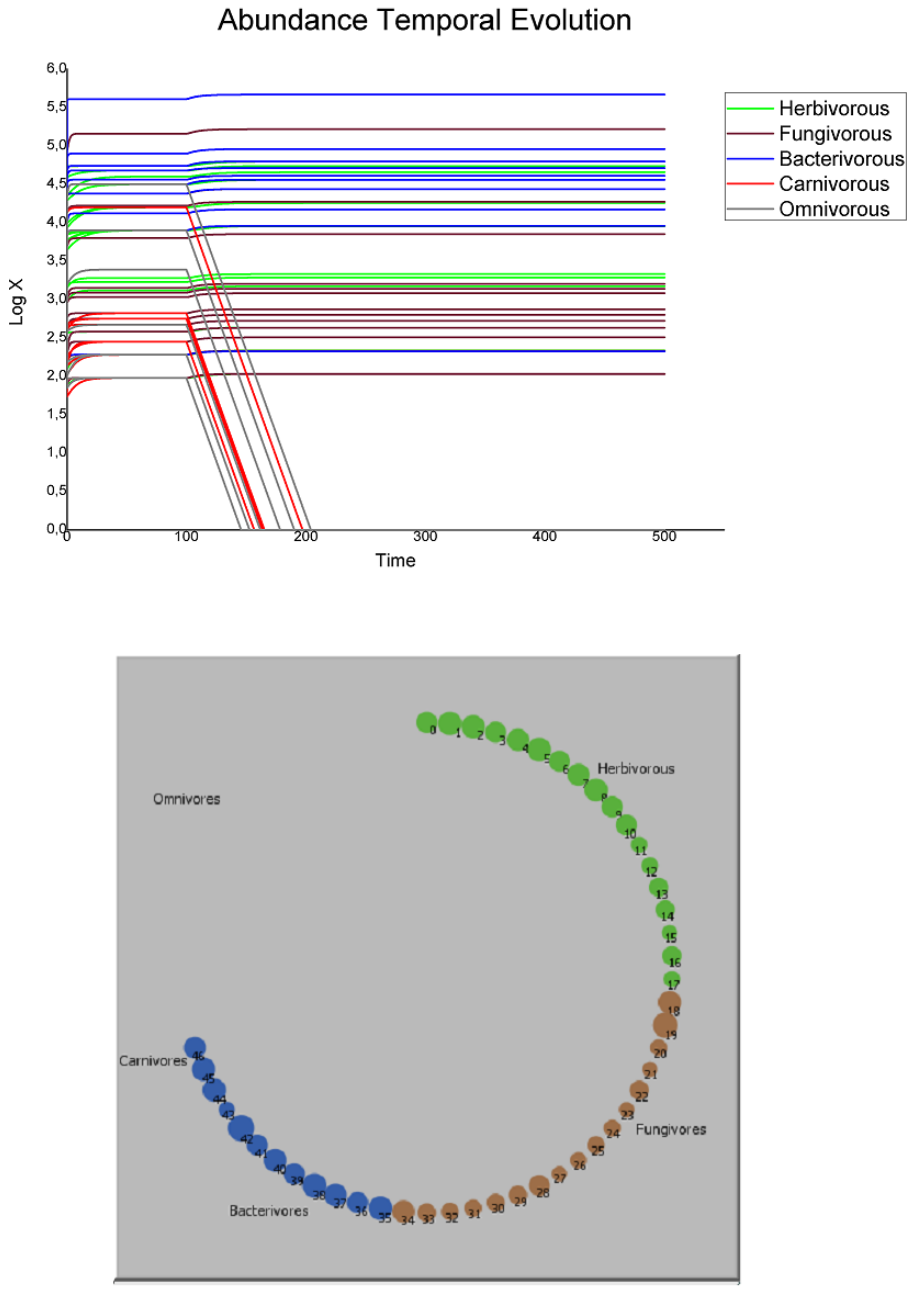

Figure 4.53: **Network 230.** Graphic representation of the simulation results in the case all omnivores and carnivores are removed from the ecosystem. Above the temporal evolutions of species abundances and below the representations of the trophic web at the end of the simulation.